

Actual Trends in Highway and Bridge Engineering

2005

C. Ionescu, F. Paulet-Crainiceanu, R. Andrei, C.C. Comisu

editors



EDITURA SOCIETATII ACADEMICE "MATEI - TEIU BOTEZ"

Iasi, 2005

International Symposium

“Actual Trends in Highway and Bridge Engineering”

Iași, România, December 16, 2005



C. Ionescu, F. Paulet-Crainiceanu, R. Andrei, C.C. Comisu
Editors



EDITURA SOCIETĂȚII ACADEMICE "MATEI-TEIU BOTEZ"
Iași, 2005

**“Actual Trends in Highway and Bridge Engineering”, International Symposium
Iași, România, December 16, 2005**

C. Ionescu, F. Paulet-Crainiceanu, R. Andrei, C.C. Comisu
Editors

Descrierea CIP a Bibliotecii Naționale a României

**Actual trends in highway and bridge engineering 2005 :
International symposium : Iași, 2005** / ed.: Constantin
Ionescu, Fideliu Păuleț-Crăiniceanu, Radu Andrei,
Cristian Comisu. - Iași : Editura Societății Academice
"Matei - Teiu Botez", 2005
Bibliogr.
ISBN 973-7962-76-1

I. Ionescu, Constantin
II. Păuleț-Crăiniceanu, Fideliu
III. Andrei, Radu
IV. Comisu, Cristian Claudiu

625.7(063)
624.21(063)

Table of Contents

1. Ionescu, C., Păuleț-Crăiniceanu, F., Andrei, R., Comisu, C.C. Achievements and performances in Highway and Bridge Engineering	5
2. Oller, S., Barbat, Al.H., Moment-curvature damage bridge piers subjected to horizontal loads	11
3. Dima, Al., Răcănel, I. The strengthening of Străulești Bridge over the Colentina River in Bucharest	38
4. Răcănel, C. The intrinsic characteristics of asphalt mixtures from wearing course	49
5. Gebbeken, N., Baumhauer, A., Ionita, M. Bridge Reconnaissance and Classification System with On-site Wireless Data Acquisition	57
6. Proca, G., Proca, M. Rehabilitation of a railway's section using GPS technology case study	69
7. Oller, S., Barbat, Al.H., Miquel, J. Estudio del comportamiento de los hormigones reforzados con fibras cortas	77
8. Romanescu, C. The use of nondestructive testing methods for bridges foundations conditions determination and implementation of obtained data in bridge management system	101
9. Jantea, C. General buckling of compressed chord of metal truss bottom-way bridges without horizontal bracing	115
10. Ionescu, C., Scînteie, R. Information flow for the determination in time of the bridge behaviour	123
11. Comisu, C.C. Integral abutment bridges	130
12. Roșca, O. ROBOT MILLENIUM - Numerical methods involved in modal analysis	142
13. Rădulescu, Gh.M., Rădulescu, C. Manager systems for the topographic monitoring of bridges, during the execution and for monitoring the time behavior under the action of sunlight and wind	159
14. Ionescu, C. Real and virtual in Bridge Engineering	169

15. Popa, R., Ionescu, C. Considerations on the building of the bridges in Neamț historical area and the rivers Bistrița and Moldova	175
16. Nicuță, A., Ionescu, C. Considerations regarding the evaluation of costs and resources specific to transport infrastructure	187
17. Andrei, R. Transportation research and education in the new millennium	193
18. Tautu, N. Romanian road infrastructure in the frame of sustainable development concept	202
19. Zarojanu, H.Gh., Andrei, R. Considerations on the value of modulus of subgrade reaction	211
20. Zarojanu, H.Gh., Andrei, R. The average thickness of bituminous binder – criterion for the analysis of performance behavior of hot rolled road asphalt pavements	216
21. Vlad, N., Andrei, R. The use of accelerated circular track for performance evaluation and validation of technical specifications for the asphalt mixes stabilized with various fibers, in Romania	220
22. Boboc, V., Iriciuc, C.S., Boboc, A. The use of fly ash and volcanic tuff for the construction of the mixed road pavements	233
23. Andrei, R. The Research Centre for Geotechnics, Foundations and Modern Transportation Engineering Infrastructure «Dimitrie Atanasiu» - CCGEOFIMIT	241
24. Rotaru, A., Răileanu, P., Rotaru, P. How to build on difficult foundation soils in Iasi County area	243

Achievements and performances in Highway and Bridge Engineering

Constantin Ionescu¹, Fideliu Păuleț-Crăiniceanu¹, Radu Andrei² and Cristian Claudiu Comisu²

¹Department of Structural Mechanics, "Gh. Asachi" Technical University, Iasi, 700050, Romania

²Dept. of Transp. Infrastr. & Foundations, "Gh. Asachi" Technical University, Iasi, 700050, Romania

Summary

The symposium "Actual Trends in Highway and Bridge Engineering", held in Iași, România, on December 16, 2005, has already a tradition. The positive feedback from participants to previous symposiums entitled the organizer to continue with such meetings, hoping to provide important help and motivation for in Highway and Bridge Engineering domain.

This paper refers to the achievements and performances highlighted by the papers submitted to this international symposium.

KEYWORDS: Bridge Engineering, Highway Engineering, research, international symposium, Iasi, Romania.

1. INTRODUCTION

This paper refers to the achievements and performances in Highway and Bridge Engineering as they are highlighted by the papers submitted to the International Symposium "Actual Trends in Highway and Bridge Engineering", held in Iași, România, on December 16, 2005 [1].

This symposium has already a tradition. Every December from the last three years, an international symposium on similar topics took place. It was proved that these international meetings were an important platform for researchers to present their work and to exchange knowledge.

Academic staff, young scientists, students, engineers and people involved in practical work from several countries have been between the participants of the above reminded scientific meeting. Their positive feedback entitled the organizer to continue with such meetings, hoping to provide important help and motivation for in Highway and Bridge Engineering domain.

2. HIGHWAY AND BRIDGE ENGINEERING – A FIELD OF HIGH LEVEL OF SCIENTIFIC AND TECHNICAL ACHIEVEMENTS

Damages to bridge piers are the main targets of the paper [2]. The authors, Oller and Barbat, are analyzing the damages caused by horizontal actions (earthquakes) through the moment-curvature models. The main hypothesis is the flexible pier – rigid deck behavior. Dynamic model of the typical bridge is shown and discussed. Then the non-linear analysis of pier is presented and the damage of cross section due to skew bending is studied. The numerical example is performed on the model of the Warth Bridge, Austria and experimental data were also obtained from other researches. Results show very good agreement between the proposed model and experimental data.

In their paper “The strengthening of Străulești Bridge over the Colentina River in Bucharest”, [3], A. Dima and I. Racanel are showing the situation of 80 years old bridge in Romania that had to be rehabilitated. The analyzed bridge was exposed to corrosion, impacts and vibrations of vehicles. Also it was designed and constructed with some deficiencies as: the rivets position located over the maximum allowable distances, the over-passing of the slenderness coefficient for the elements of the truss main girders, the absence of the waterproofing system, the absence of footways. As a consequence the structural safety was questionable. Two strengthening solutions are presented. First consists in: addition of steel sections on upper chords, on diagonals and on posts of the main truss girders; replacement of the diagonals in the midspan panels with new elements having appropriate cross sections; strengthening of the connections between cross girders and main truss girders by increasing the reinforcing plate depth. The second consists in the introduction of steel rods at the bottom part of the cross girders and bottom chords. All the existing construction and execution deficiencies were corrected. A 3D finite element model has been used. Hypothesis and results are presented and analyzed. The final decision for rehabilitation is presented in details. Comparisons before and after strengthening are also shown.

In [4], C. Racanel establishes that for asphalt mixtures the internal friction angle has a constant value according to increase of loading rate and grow up with temperature increase and also that the cohesion increases with the increase of loading rate and decreases with the temperature increase. The paper, “The intrinsic characteristics of asphalt mixtures from wearing course” firstly describes the triaxial testing device and the data that can be obtained with it. Test conditions and materials used in testing are shown. Results are analyzed and graphically presented.

On-site wireless data acquisition is the techniques used by N. Gebbeken, A. Baumhauer and M. Ionita for bridge reconnaissance and classification, [5]. The main task of the researches is to automate as much as possible the bridge

evaluation, which is often a team work and time consumption operation. A project aiming to evaluate the existing infrastructure load bearing capacity is described. A computer program, BRASSCO is developed. The computer program is using measurements for geometry, material properties and reinforcement condition. The data is input through portable devices (laptops, PDAs) and wireless connection. The central server is holding BRASSCO and a GUI is easing the task. Communication protocols and recovery mechanisms are assuring safe and reliable work. For the generated model, various loading scenarios are applied and maximum allowable load are determined. Failure mechanism and weakest points of the structure are shown by the computer program. Then, decisions can easily and fast be generated.

A case study on rehabilitation of a railway's section using GPS technology is the topic treated by G. Proca and M. Proca in their paper [6]. The authors are presenting the objectives of the rehabilitation, the details of the topographical works (verification and rehabilitation of the geodetic network, showing the hardware and software; materialization of stations; measurements; landmarks; coordinate transformation) and the construction work. After all the work have been done, a schedule for construction behavior was set.

In [7], Oller, Barbat and Miguel are using fiber concrete in rehabilitation of structures. A very refined general analysis of composite materials is presented and then short fiber concrete composite materials are introduced. Many compositions are explained. For these types of materials, mathematical modeling is exposed. An application example, with a simple supported concrete girder is shown. The experimental and analytical work proves significant increase in ductility for the element.

C. Romanescu, is proposing non-destructive testing methods for determination of bridges' foundation conditions in order to enhance the bridge management system, [8], mainly dealing with the scouring phenomena. The testing devices (usually very expensive) and severe conditions (limited access, extreme temperatures, dust and dirt) are critically examined. Factors influencing the scouring are carefully investigated and classifications are issued. Methods for non-destructive testing are revealed in deep details. Principles, examples, diagrams, advantages and disadvantages are shown.

A paper on general buckling of compress chord from the bottom-way of metal truss bridges without horizontal bracing is presented by C. Jantea, [9]. In the introduction chapter, a literature review and general principles concerning the topic are shown. Noticing that some Romanian national codes are not treating the problem of the stiffness for a certain type of trusses, the author is investigating the way this characteristic must be obtained.

C. Ionescu and R. Scinteie are dealing with analysis of the procedures for bridges' behavior determination, [10]. The main attention is given to the information flow that should lead to: quick and objective appreciation of the bridge safety state; prevention of the bridge disturbance state; confirmation of calculus hypothesis and the improvement of the bridge design knowledge; beginning of the maintenance works processes for the bridges. 2. Next, the paper is detailing facts about information systems of the operational phase. Diagrams and comments are included. Time-monitoring of the bridge behavior information flow is investigated. Therefore the information system concept related to bridge behavior is stated.

The concept of integral abutment bridges is presented by C.C. Comisu, [11]. The intent of the paper is to enhance the awareness among the engineering community to use integral abutment and jointless bridges in Romania. Advantages of integral bridges are detailed. Also, limitations imposed by integral bridges are revealed. Design of integral abutment, construction procedures and best practice are shown.

O. Rosca, in [12], is treating the problem of numerical methods used in modal analysis by the Robot Millenium computer FEM program, known for its high complexity. The presentation is based on a slides show. Types of analysis, computational parameters, mass modeling, types of inertia matrices and analysis of results are the main parts of the show. Together with the theoretical consideration, the way to use the Robot Millenium's menus is presented.

A system for monitoring bridges for topographic purposes as for time behavior of bridges under sunlight and wind actions is presented by M.T. Rdulescu and C. Radulescu in [13]. Classical and modern topographical methods of monitoring are reviewed in the introduction. Then, the static and dynamic parts of the topographical investigation are shown. Careful analysis of modern techniques, devices and monitoring systems in dynamic regime is undertaken.

Continuing previous work in fundamentals of Bridge Engineering, C. Ionescu is working on what is real and what is "virtual" in this field of engineering, [14]. The complexity of bridge systems is analyzed for the beginning. Two essential facts are pointed, explained, graphically explained: the bridge area complexity (bridge-obstacle-environment interaction) and the bridge. The virtual in Bridge Engineering is mainly made from models and procedure concerning those models linked with the (eventually future) real structure. Also, the concept of "real" in Bridge Engineering is detailed. The conceptual basis and the relation for the interaction Real-Virtual is shown.

R. Popa and C. Ionescu are issuing some considerations regarding construction of bridges located in Neamt area, on Bistrita River and Moldova River, [15]. The main purpose is to make a review based on chronicles, reference literature and on-site observations for the mentioned civil engineering structures. The Neamt historical area is presented. Also, the hydrographic network is shown. For the same

area, Neamt, the road network is analyzed. Notes from old or more recent literature and comments on bridges in Neamt area are enumerated. Explanatory photos and tables with data of bridges are included.

In [16], A. Nicuta and C. Ionescu are dealing with the problem of evaluation of costs and resources needed for specific transport infrastructure, i.e. roads. The problem is very acute in Romania due to high necessity for rehabilitation of existing roads and also because of implementation of European Union's requirements. It is shown that the efficiency in Bridge and Roads Engineering is mainly influenced by construction materials, site organization, technologies, and methods for structural analysis. The construction realization cycle is graphically shown and analyzed. Then the costs evaluation and resources are identified. The global cost is investigated and measures for its optimization are withdrawn.

The paper: “Transportation research and education in the new millennium” [17], is intending to present a comprehensive view and synthesis of transportation research and education, as it exists today and can expect to evolve with the beginning of this new millennium.

[18] is a critical and comprehensive view of the actual poor technical condition of Romanian public road network infrastructure viewed in the concept of durable development. In his significant paper-document: “The Romanian Road Infrastructure in the Concept of Durable Development, the distinguished author and highway specialist Neculai Tautu, the former Director of the Regional Highway Department of Iassy and the actual President of the Moldavian Branch of the Romanian Professional Association for Roads and Bridges is proposing a challenging strategy for the preservation and development of the actual poor national road infrastructure, considered in the context of durable development. At this crucial moment, when our country concentrates its efforts to enter into the European Union, the main objectives of the strategy adopted for the modernization of the road infrastructure has to be undertaken in such a challenging way, in order to meet the requirements adopted by all European countries.

In his papers “Considerations on the Value of Modulus of Subgrade Reaction” [19], and “The Average Thickness of Bituminous Binder-Criterion for analysis of Performance Behavior of Hot Rolled Road asphalt Pavements” [20], Consultant Professor Horia Gh. Zarojanu and his research team from Technical University “Gh. Asachi” of Iasi, is opening new horizons in the field of structural design and performance behaviour of asphalt pavements. The first paper is proposing specific design values for the modulus of subgrade reaction, based on a comprehensive synthesis of the existing correlations between the K value and other deformability characteristics of the subgrade such as CBR value and dynamic elastic modulus E. Specific design values for the modulus subgrade reaction are recommended to be used in the frame of the actual method for structural design of rigid pavements, in our country. In the second paper the average thickness of bituminous binder is

recommended as a sound criterion for the analysis of performance of hot rolled asphalt pavements.

In the series of research dedicated to various asphalt issues Professor Nicolae Vladimir Vlad and his collaborators from Technical University “Gh. Asachi” of Iassy, presents the paper: “The Use of Accelerated Circular Track, for Performance Evaluation and Validation of Technical Specifications for the Asphalt Mixes Stabilized with Fibers, in Romania” [21], describing the research results obtained on the performance of five types of mixes, subjected to intensive accelerating testing, on the accelerated testing facility ALT-LIRA from our University.

In parallel with the above mentioned research, mixed road pavement structures are considered in the paper: “The Use of Fly Ash and Volcanic Tuff for the Construction of the Mixed Road Pavements”, [22], where Professor Vasile Boboc and his research team are presenting their research results obtained on experimental sectors equipped with such mixed pavement structures, investigated on the same ALT facility.

In [23], a short presentation of the newly established Research Centre for Geotechnics, foundations and Modern Transportation Infrastructure Engineering “Dimitrie Athanasiu” – CCGEOFIMIT is done. The Centre is recognized at national level by our Ministry of Education and Research/ CNCISIS. Its Mission Statement, its actual and perspective research objectives are underlined.

In their paper “How to build on difficult foundation soils in Iasi County area” Ancuța Rotaru, Paulică Răileanu and Petru Rotaru are showing a multitude of facts of soil condition in Iasi area, Romania. Also they are proposing solutions for foundations of structures and for soil improvement in this area, where many difficulties could appear.

3. CONCLUSIONS

The papers from “Actual Trends in Highway and Bridge Engineering” International Symposium show a very dynamic and evolutionary research field year by year. Highway and Bridges Engineering is a very vast field of research and applications needed for all the society.

The large spectrum of problems solved and analyzed by researches and the possibility of exchanging expertise are giving the basics for continuing this already traditional international symposium.

References

1. Ionescu, C., Păuleț-Crăiniceanu, F., Andrei, R., Comisu, C.C. (editors), *Actual Trends in Highway and Bridge Engineering 2005*, Editura Societății Academice "Matei-Teiu Botez", Iași, 2005, ISBN 973-7962-76-1.
2. Oller, S., Barbat, Al.H., Moment-curvature damage bridge piers subjected to horizontal loads, *Actual Trends in Highway and Bridge Engineering 2005*, Editura Societății Academice "Matei-Teiu Botez", Iași, 2005, ISBN 973-7962-76-1, pp.11-37.
3. Dima, Al., Răcănel, I., The strengthening of Străulești Bridge over the Colentina River in Bucharest, *idem*, pp.38-48.
4. Răcănel, C., The intrinsic characteristics of asphalt mixtures from wearing course, *idem*, pp.38-48.
5. Gebbeken, N., Baumhauer, A., Ionita, M., Bridge Reconnaissance and Classification System with On-site Wireless Data Acquisition, *idem*, pp.57-68.
6. Proca, G., Proca, M., Rehabilitation of a railway's section using GPS technology case study, *idem*, pp.69-76.
7. Oller, S., Barbat, Al.H., Miquel, J., Estudio del comportamiento de los hormigones reforzados con fibras cortas, *idem*, pp.77-100.
8. Romanescu, C., The use of nondestructive testing methods for bridges foundations conditions determination and implementation of obtained data in bridge management system, *idem*, pp.101-114.
9. Jantea, C., General buckling of compressed chord of metal truss bottom-way bridges without horizontal bracing, *idem*, pp.115-122.
10. Ionescu, C., Scînteie, R., Information flow for the determination in time of the bridge behaviour, *idem*, pp. 123-129.
11. Comisu, C.C., Integral abutment bridges, *idem*, pp.130-141.
12. Roșca, O., ROBOT MILLENIUM - Numerical methods involved in modal analysis, *idem*, pp.142-158.
13. Rădulescu, Gh.M., Rădulescu, C., Manager systems for the topographic monitoring of bridges, during the execution and for monitoring the time behavior under the action of sunlight and wind, *idem*, pp.159-168.
14. Ionescu, C, Real and virtual in Bridge Engineering, *idem*, pp.169-174.
15. Popa, R., Ionescu, C., Considerations on the building of the bridges in Neamț historical area and the rivers Bistrița and Moldova, *idem*, pp.175-186.
16. Nicuță, A., Ionescu, C., Considerations regarding the evaluation of costs and resources specific to transport infrastructure, *idem*, pp.187-192.
17. Andrei, R., Transportation research and education in the new millennium, *idem*, pp.193-201
18. Tautu, N., Romanian road infrastructure in the frame of sustainable development concept, *idem*, pp.202-210
19. Zarojanu, H.Gh., Andrei, R., Considerations on the value of modulus of subgrade reaction, *idem*, pp.211-215
20. Zarojanu, H.Gh., Andrei, R., The average thickness of bituminous binder – criterion for the analysis of performance behavior of hot rolled road asphalt pavements, *idem*, pp.216-219
21. Vlad, N., Andrei, R., The use of accelerated circular track for performance evaluation and validation of technical specifications for the asphalt mixes stabilized with various fibers, in Romania, *idem*, pp.220-232

22. Boboc, V., Iriciuc, C.S., Boboc, A., The use of fly ash and volcanic tuff for the construction of the mixed road pavements, *idem*, pp.233-240
23. Andrei, R., The Research Centre for Geotechnics, Foundations and Modern Transportation Engineering Infrastructure «Dimitrie Atanasiu» - CCGEOFIMIT, *idem*, pp.241-242
24. Rotaru, A., Răileanu, P., Rotaru, P., How to build on difficult foundation soils in Iasi County area, *idem*, pp.243-253

Moment-curvature damage bridge piers subjected to horizontal loads

Sergio Oller and Alex H. Barbat

Escuela de Ingenieros de Caminos Canales y Puertos, Universidad Politécnica de Cataluña, Jordi Girona 1-3, CI, 08034 Barcelona, Spain

Summary

The evaluation of the damage caused by horizontal loads, such as seismic action, to existing bridges has received an important attention in recent years, because it is the first step towards reducing casualties and economic losses. In damage detection and evaluation, the application of simple and reliable models has been prioritized, because they are necessary in further multi-analyses required by Monte Carlo simulations. A simplified moment-curvature damage model, capable of evaluating the expected seismic behaviour of RC highway bridges is proposed in this paper. The damage evaluation model is based on the mechanical modification of the cross sectional inertia of the bridge piers. The model was validated using experimental results obtained at the JRC Ispra for the Warth Bridge of Austria and also FEM analyses performed by other authors for the same bridge.

KEYWORDS: damage estimation, continuum damage mechanics, damage constitutive model and moment curvature model

1. INTRODUCTION

Nowadays, the evaluation of the damage caused by earthquakes in existing bridges received great attention. Numerous researches devoted to the structural damage evaluation have been performed, most of them considering the seismic behavior of buildings. The structural damage in the bridges can be characterized in two ways:

1. In the first way, the structural damage is evaluated at given points of the structure by means of local constitutive models describing the damage accumulation caused by a local micro-structural damage [13, 19, 21, 28].
2. In the second way, the local damage is used for the evaluation of global damage indices, which are scalars depending on some variables (or damage parameters) that characterize the dynamic response of the whole system [1, 2, 24].

This paper proposes a damage evaluation based on structural analysis for RC highway bridges with simple pier bents. This typology of bridges was very used all over Europe during the 1960-1980 periods. The proposed structural model is based

on the hypothesis of the *flexible pier-rigid deck* behaviour of the structure subjected to seismic loads. A flexible pier-rigid deck simplified model was therefore developed, which could be extending after some modification to other typologies of bridges. This model has been chosen after studying the responses correlation between the proposed model and the real structure [9]. Accordingly, the overall seismic behaviour of this bridge typology is decisively influenced by the damage of the piers. Therefore, the study of the damage produced by horizontal loads has been centered on the piers of the bridge [9], while the structural study of the deck has been performed after the structural analysis of the piers, in an uncoupled way. Thus, the maximum damage of the piers under horizontal loads is the principal aim of the proposed structural damage evaluation procedure.

A local damage index, which describes the state of the material at each point of the structure, is the starting point of the proposed method and is based on a constitutive damage law. Details on this constitutive law are given in the Annex of the paper. The global damage of each pier is obtained from the inertia reduction of the cross sections due to the material degradation. The validation of the proposed model was carried out by using the experimental tests on scale models of the piers of the Warth Bridge, Austria, carried out at the Joint Research Center of Ispra, Italy [25] and a FE model developed by R. Faria [8].

The proposed model permits a simple, reliable and efficient structural analysis. Therefore, it is suitable for considering uncertainties in its parameters and for using Monte Carlo simulations with the aim of evaluating the seismic vulnerability of bridges.

2. STRUCTURAL DESCRIPTION OF THE DYNAMIC MODEL

Reinforced concrete highway bridges with simple pier bents have greater redundancy and higher strength in their longitudinal direction; therefore they will undergo greater damage when subjected to transversal seismic actions. The proposed model aims studying the bridge response to horizontal loads acting transversally to the direction of the bridge axis. Experimental studies confirm that the structural system can be modelled simply by piers loaded transversally to the axis of the bridge interconnected at the deck level by means of box girders [9, 23]. Due to the high stiffness of the bridge in longitudinal direction, the structural analysis in this direction is out of the purposes of this work, focusing on the structural study of the pier in transversal direction.

The model has continuous elements with distributed mass for the piers and concentrated mass for the girders. The motion of the n_p piers in transversal direction to the bridge axis is partially restricted by the adjacent girders that are supported by laminated neoprene bearings. Thus, the displacement of piers causes

the distortion of the bearings and the consequent rotation of the adjacent girders. The simplified model shown in Figure 1 is based on the following general hypotheses:

1. The piers are continuous elements with distributed mass and infinite axial stiffness.
2. The girders are perfectly stiff elements concentrating the mass at the top of the piers.
3. The bearings of the girders are equivalent short elements that work to shear, having circular cross section and real dimensions.
4. The soil-structure interaction effect on piers and abutments is considered by means of linear springs that represent the rotational stiffness of the soil.
5. The abutments are perfectly stiff.

Accordingly, the model has as many degrees of freedom as transversal displacements at the top of the piers, that is, n_p degrees of freedom.

In following sections, the traverse stiffness of an isolated pier under non lineal damage effects produced by a horizontal load applied at the deck level will be studied.

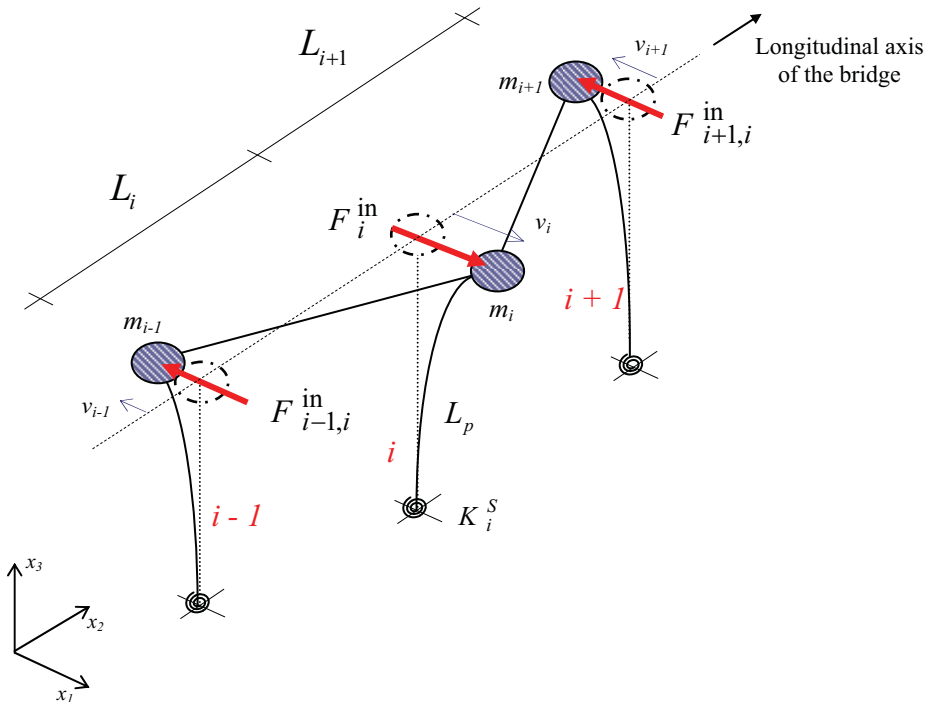


Figure 1. Model for the seismic analysis of the bridge

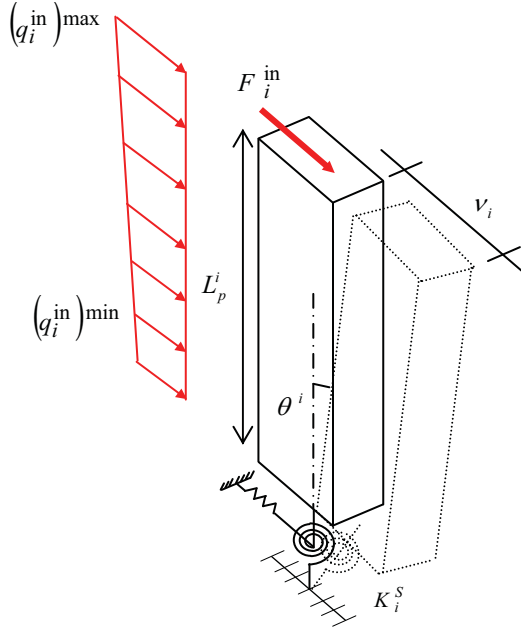


Figure 2. Transversal displacements of pier I considering the soil effect

Transversal behaviour of a single pier

According to the general hypotheses and to Figure 2, the maximum displacement at the top of a pier is

$$v_i = v_\theta^i + v_p^i \quad (1)$$

where

$$v_\theta^i = \theta^i L_p^i = \frac{M_i^{\max}}{K_i^S} \quad (2)$$

is the elastic displacement produced by a rotation at the base of the pier, and

$$v_p^i = \frac{[11(q_i^{\text{in}})^{\max} + 4(q_i^{\text{in}})^{\min}](L_p^i)^4}{120 E_{c_i} I_i} + \frac{F_i^{\text{in}}(L_p^i)^3}{3 E_{c_i} I_i} \quad (3)$$

is the elastic displacement produced by external actions [9]. In equations (2) and (3), θ^i is the rotation due to the soil-structure interaction effect, M_i^{\max} is the maximum bending moment at the base of the pier, K_i^S is the equivalent stiffness of the soil, $(q_i^{\text{in}})^{\max}$ and $(q_i^{\text{in}})^{\min}$ are the maximum and minimum inertial loads by

unit length produced by the horizontal acceleration, F_i^{in} is the total inertial force due to the bridge deck and L_p^i , E_{c_i} and I_i are the length, Young's modulus and the inertia of the reinforced concrete cross section of the pier, respectively.

For the maximum displacement of the pier (for $x_3 = 0$), the bending moment equation is [9]

$$M_i(x_3 = 0) = M_i^{\text{max}} = \frac{\left[2(q_i^{\text{in}})^{\text{max}} + (q_i^{\text{in}})^{\text{min}} \right] (L_p^i)^2}{6} + (F_i^{\text{in}} L_p^i) \quad (4)$$

Substituting equations (2), (3) and (4) into Equation (1), the equivalent internal force at the top of the pier is obtained in function of the maximum displacement v_i of the pier [9].

$$F_i^{\text{in}} = \frac{I}{\left[\frac{L_p^i}{K_i^S} + \frac{(L_p^i)^3}{3 E_{c_i} I_i} \right]} \left[v_i - \frac{\left[2(q_i^{\text{in}})^{\text{max}} + (q_i^{\text{in}})^{\text{min}} \right] (L_p^i)^2}{6 K_i^S} - \frac{\left[11(q_i^{\text{in}})^{\text{max}} + 4(q_i^{\text{in}})^{\text{min}} \right] (L_p^i)^4}{120 E_{c_i} I_i} \right] \quad (5)$$

3. NON-LINEAR ANALYSIS OF THE PIER

When the non-linear behavior of the structural materials is taken into account, the undamped equation of motion for each pier is written as

$$m_i a_i + F_i^{\text{in}} - \Delta F_i^R = 0 \quad (6)$$

where ΔF_i^R is the residual or out-of-balance force. This unbalanced force is due to the fact that the cross-section inertia and Young modulus are not constant during the non linear process and consequently the solution of Equation (6) should be obtained throughout an iterative process using a non-linear Newmark approach [3, 7].

The changes of the pier stiffness and of the internal cross sectional force depend on the damage level reached at each point of the pier whose numerical evaluation is carried out by means of the continuum damage model (see the Annex). In this work, the damage model [19] is used to calculate the local damage index at each point of the structure. Then, by means of a numerical integration of the local damage indices on the cross-section at the base of the piers, the area and the inertia

of the damaged cross section are obtained. Obviously, it is possible to obtain the damage evolution at each cross section of the pier, but the moment-curvature model requires the evaluation of damage only at the most loaded section (base cross section).

To obtain the response and the maximum damage of all the bridge piers using the proposed model, Newmark's non-linear algorithm, summarized in Box 1, is used to solve the equilibrium equation at each time of the process. In this analysis the balance force condition is achieved by eliminating $\Delta \mathbf{F}_i^R$ using a Newton-Raphson process. Indirectly, this process also eliminates the residual bending moment $\Delta \mathbf{M} = \mathbf{M}^0 - \mathbf{M}^{\text{int}}$ included in the residual force array, which is the difference between the maximum elastic external moment, \mathbf{M}^0 , and the pier internal strength capacity moment, \mathbf{M}^{int} . For each step of the non-linear analysis the properties of the system are updated, considering the local degradation of the material caused by the seismic action.

Solution of the dynamic equation of equilibrium

The steps to define the damage in any pier of the bridge are described in boxes 1 and 2. The maximum global damage index of the structure is obtained starting from the cross-sectional damage calculated at the base of the piers for transversal seismic actions. Box 1 shows the numerical procedure to solve the dynamic balance equation (6) using Newmark's non-linear method. As shown previously, the type of bridge under study is modeled by means the piers that behaves like cantilever beams, for which the numerical integration of the damage on the cross section can be simplified, considering in the analysis only the cross-section at the pier base, that is, for $x_3 = 0$. Nevertheless, the procedure could be generalized including when necessary other cross-sections at levels x_3 in the damage integration procedure.

1. **Displacement and velocity prediction at " $t + \Delta t$ ",** starting from null initial conditions

$$\begin{aligned}\ddot{\tilde{\mathbf{U}}}^{t+\Delta t} &= 0 ; \quad \dot{\tilde{\mathbf{U}}}^{t+\Delta t} = \dot{\mathbf{U}}^t + (1-\gamma) \ddot{\mathbf{U}}^t \Delta t ; \\ \tilde{\mathbf{U}}^{t+\Delta t} &= \mathbf{U}^t + \dot{\mathbf{U}}^t \Delta t + \left(\frac{1}{2} - \beta\right) \ddot{\mathbf{U}}^t \Delta t^2 ; \quad {}^i \Delta \mathbf{f}^{t+\Delta t} = \mathbf{F}_i^q\end{aligned}$$

2. **Computation of displacement increment $\Delta \mathbf{U}^{t+\Delta t}$** at instant $t + \Delta t$, starting from the linearized balance equation

$${}^i \Delta \mathbf{f}^{t+\Delta t} = {}^i \mathbf{J}^{t+\Delta t} \Delta \ddot{\mathbf{U}}^{t+\Delta t} ; \quad {}^i \mathbf{J}^{t+\Delta t} = \left[\mathbf{M} \cdot \left(\frac{1}{\beta \Delta t^2} \right) + \mathbf{K} \right]^{t+\Delta t}$$

3. **Displacement and velocity correction**

$${}^{i+1}\ddot{\mathbf{U}}^{t+\Delta t} = \left(\frac{1}{\beta \Delta t^2} \right) {}^{i+1}\Delta \ddot{\mathbf{U}}^{t+\Delta t}; \quad {}^{i+1}\dot{\mathbf{U}}^{t+\Delta t} = \dot{\tilde{\mathbf{U}}}^{t+\Delta t} + \left(\frac{\gamma}{\beta \Delta t} \right) {}^{i+1}\Delta \mathbf{U}^{t+\Delta t}; \quad {}^{i+1}\mathbf{U}^{t+\Delta t} = \tilde{\mathbf{U}}^{t+\Delta t} + {}^{i+1}\Delta \mathbf{U}^{t+\Delta t}$$

4. **Loop over k bridge piers.** The damage constitutive equation are computed at each pier k and at each cross section (see next section and Box 2 for more details)

4a. Computation of the generalized forces (predictor) and the elastic curvatures and axial strain at each cross section x_3 , using the

displacement ${}^{i+1}\mathbf{U}^{t+\Delta t}$ at the top of pier k

$$M_1^0(x_3) = \frac{(L_p^k - x_3)}{\left(\frac{(L_p^k)^2}{K_k^S} + \frac{(L_p^k)^3}{3E_{ck}^0(I_k(0))_{11}} \right)} {}^{i+1}[v_2(L_p^k)]_k^{t+\Delta t}; \quad M_2^0(x_3) = \frac{(L_p^k - x_3)}{\left(\frac{(L_p^k)^2}{K_k^S} + \frac{(L_p^k)^3}{3E_{ck}^0(I_k(0))_{22}} \right)} {}^{i+1}[v_1(L_p^k)]_k^{t+\Delta t}$$

$$N^0(x_3) = N^{ap}; \quad [\hat{\sigma}^0(x_3)]_k = \begin{Bmatrix} N^0(x_3) \\ M_1^0(x_3) \\ M_2^0(x_3) \end{Bmatrix}; \quad [{}^{i+1}\mathbf{U}^{t+\Delta t}(x_3)]_k = \begin{Bmatrix} [u(x_3)]_k^{t+\Delta t} \\ [v_1(x_3)]_k^{t+\Delta t} \\ [v_2(x_3)]_k^{t+\Delta t} \end{Bmatrix}$$

4b. Computation of the residual flexural moment

For the first load step : $[\mathbf{J}(x_3)]_k \equiv [\mathbf{J}^0(x_3)]_k; \quad [\hat{\sigma}^{\text{int}}(x_3)]_k = \mathbf{0}$

$$[\Delta \hat{\sigma}(x_3)]_k = [\hat{\sigma}^0(x_3) - \hat{\sigma}^{\text{int}}(x_3)]_k \stackrel{\text{Unbalanced equivalent force}}{=} [\Delta \mathbf{f}^{t+\Delta t}(x_3)]_k = \begin{Bmatrix} {}^{i+1}\Delta N^{t+\Delta t}(x_3) \\ {}^{i+1}\Delta M_1^{t+\Delta t}(x_3) / L_p^k \\ {}^{i+1}\Delta M_2^{t+\Delta t}(x_3) / L_p^k \end{Bmatrix}_k$$

4c. Balance equation verification on the clamped cross section

$$\|\Delta \hat{\sigma}(0)\| \stackrel{?}{=} \begin{cases} 0 & \Rightarrow \text{go to EXIT} \\ \neq 0 & \Rightarrow \text{Continue} \end{cases}$$

4d. Computation of the incremental generalized strains and theirs current value

$$\begin{aligned} [{}^{n+1}\Delta \hat{\epsilon}^{t+\Delta t}(0)]_k &= -[{}^n\mathbf{J}^{n+1}(0)]_k^{-1} [{}^n\Delta \hat{\sigma}^{t+\Delta t}(0)]_k \\ [{}^{n+1}\hat{\epsilon}^{t+\Delta t}(0)]_k &= [{}^n\hat{\epsilon}^{t+\Delta t}(0)]_k + [{}^{n+1}\Delta \hat{\epsilon}^{t+\Delta t}(0)]_k \end{aligned}$$

4e. Damaged inertia computation at the base cross section of pier k (see Box 2)

5. **Back to point 4b** followed by the minimization of generalized unbalanced force equation.
6. **Calculate the displacement at each point x_3 of the pier and EXIT.**

$$\begin{aligned}
 \left[{}^{i+1}\mathbf{U}^{t+\Delta t}(x_3) \right]_k &= \begin{Bmatrix} \left[\mathbf{u}(x_3) \right]_k \\ \left[\mathbf{v}_1(x_3) \right]_k \\ \left[\mathbf{v}_2(x_3) \right]_k \end{Bmatrix}^{t+\Delta t} = \begin{Bmatrix} \left[\mathbf{u}(x_3 - \Delta x_3) \right]_k \\ \left[\mathbf{v}_1(x_3 - \Delta x_3) \right]_k \\ \left[\mathbf{v}_2(x_3 - \Delta x_3) \right]_k \end{Bmatrix}^{t+\Delta t} - \begin{Bmatrix} \left[\varepsilon^N(x_3 - \Delta x_3) \right]_k \cdot \Delta x_3 \\ \left[\varphi_2(x_3 - \Delta x_3) \right]_k \cdot \Delta x_3 \\ \left[\varphi_1(x_3 - \Delta x_3) \right]_k \cdot \Delta x_3 \end{Bmatrix}^{t+\Delta t} + \begin{Bmatrix} 0 \\ \frac{\left[\chi_2(x_3 - \Delta x_3) \right]_k}{2} \cdot \Delta x_3^2 \\ \frac{\left[\chi_1(x_3 - \Delta x_3) \right]_k}{2} \cdot \Delta x_3^2 \end{Bmatrix}^{t+\Delta t} \\
 \begin{Bmatrix} \left[\varphi_1(x_3) \right]_k \\ \left[\varphi_2(x_3) \right]_k \end{Bmatrix}^{t+\Delta t} &= \begin{Bmatrix} \left[\varphi_1(x_3 - \Delta x_3) \right]_k \\ \left[\varphi_2(x_3 - \Delta x_3) \right]_k \end{Bmatrix}^{t+\Delta t} + \begin{Bmatrix} \left[\chi_1(x_3 - \Delta x_3) \right]_k \cdot \Delta x_3 \\ \left[\chi_2(x_3 - \Delta x_3) \right]_k \cdot \Delta x_3 \end{Bmatrix}^{t+\Delta t}
 \end{aligned}$$

7. **Back to point 2** after the damage evaluation over all the piers and balance equation over the complete bridge $\| \Delta \mathbf{F}^{t+\Delta t} \| \rightarrow 0$ verification.

8. **New time increment and dynamic load application over all the bridge.** Back to point 1.

Box 1. Solution of the non-linear equilibrium equation applied for the bridge using Newmark's method

4. STUDY OF THE DAMAGED CROSS SECTION FOR SKEW BENDING

Theoretical aspects

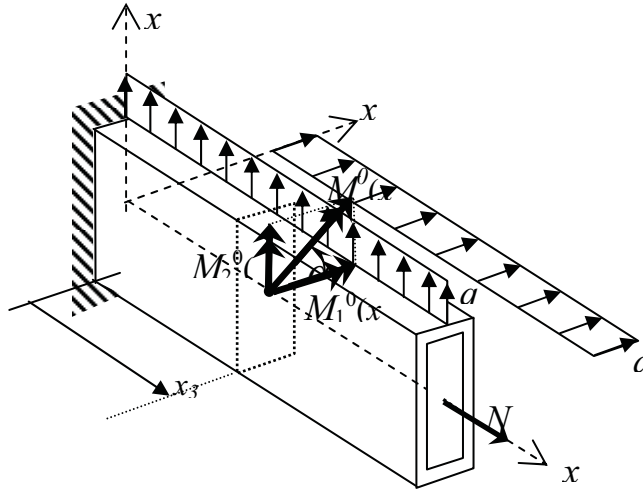


Figure 3. Bridge pier represented as a cantilever Bernoulli beam

In order to define the inertia and the bending moment of the damaged base cross section of a pier required by the solution of the non linear equation (6) –see Box

1–, the isotropic damage model [19] has been applied (see Annex). In this section, the way of computing the local damage and its contribution to the cross sectional damage of a pier is described for Bernoulli beams subjected to skew bending. For this purpose, the damaged cantilever beam under skew bending of Figure 3 is considered.

The external loads produce the following generalized forces in a cross section located at a distance x_3

$$\hat{\sigma}^0(x_3) = \begin{Bmatrix} N^0(x_3) \\ M_1^0(x_3) \\ M_2^0(x_3) \end{Bmatrix} = \begin{Bmatrix} N^0(x_3) \\ M^0(x_3) \cdot \cos \alpha \\ M^0(x_3) \cdot \sin \alpha \end{Bmatrix} \quad (7)$$

The following strain and curvature of the Bernoulli beam, due to the elastic bending moment of Equation (7), will be taken as the predictor variables of the algorithm

$$\begin{aligned} \varepsilon^N(x_3) &= \frac{du(x_3)}{dx_3} = \frac{N(x_3)}{E^0 A^0} \\ \chi_1(x_3) &= -\frac{d^2 v_2(x_3)}{dx_3^2} = \frac{M_1^0(x_3)}{E^0 I_{11}^0} \\ \chi_2(x_3) &= -\frac{d^2 v_1(x_3)}{dx_3^2} = \frac{M_2^0(x_3)}{E^0 I_{22}^0} \end{aligned} \quad (8)$$

being E^0 the initial undamaged elasticity module, A^0 the initial area of the undamaged cross section and I_{ii}^0 the initial inertia of the undamaged of cross section regarding the principal reference system for $x_i \ \forall i = 1, 2$.

Considering the Bernoulli beam basic hypotheses, the following expressions for the strain and stress fields are obtained, Equation (9).

All the previous descriptions have been made for a linear elastic skew axial-bending problem. Thus, the material has limitless capacity to resist the applied loads as expressed in Equation (9). This threshold is not possible to be reached for a real material, because its strength is limited to c^{\max} , as it can be seen in Equation (A.8) of the Annex. Therefore, the initial generalized internal forces $\hat{\sigma}^0(x_3)$ produced by the external loads $\mathbf{F}^0(x_3)$ is initially unbalanced with the generalized internal stresses $\hat{\sigma}(x_3)$, producing unbalanced residual generalized internal forces $\Delta\hat{\sigma}(x_3)$. These residual stresses should be zero due to the equilibrium

condition and this state is reached by increasing the curvature $\Delta\chi(x_3)$ and axial strain $\Delta\varepsilon^N(x_3)$ of the beam.

$$\left\{ \begin{aligned} \varepsilon(x_1, x_2, x_3) &= \varepsilon^N(x_3) + \chi_1(x_3) \cdot x_2 + \chi_2(x_3) \cdot x_1 = \frac{N^0(x_3)}{E^0 A^0} + \frac{M_1^0(x_3)}{E^0 I_{11}^0} x_2 + \frac{M_2^0(x_3)}{E^0 I_{22}^0} x_1 \\ &= \begin{Bmatrix} 1 & x_2 & x_1 \end{Bmatrix} \cdot \begin{bmatrix} E^0 A^0 & 0 & 0 \\ 0 & E^0 I_{11}^0 & 0 \\ 0 & 0 & E^0 I_{22}^0 \end{bmatrix}^{-1} \cdot \begin{Bmatrix} N^0(x_3) \\ M_1^0(x_3) \\ M_2^0(x_3) \end{Bmatrix} \\ \sigma(x_1, x_2, x_3) &= E^0 \cdot \varepsilon(x_1, x_2, x_3) = \frac{N^0(x_3)}{A^0} + \frac{M_1^0(x_3)}{I_{11}^0} x_2 + \frac{M_2^0(x_3)}{I_{22}^0} x_1 \\ &= \begin{Bmatrix} 1 & x_2 & x_1 \end{Bmatrix} \cdot \begin{bmatrix} A^0 & 0 & 0 \\ 0 & I_{11}^0 & 0 \\ 0 & 0 & I_{22}^0 \end{bmatrix}^{-1} \cdot \begin{Bmatrix} N^0(x_3) \\ M_1^0(x_3) \\ M_2^0(x_3) \end{Bmatrix} \\ &= \mathbf{x}^T \cdot [\mathbf{J}^0]^{-1} \cdot \hat{\boldsymbol{\sigma}}^0(x_3) \end{aligned} \right. \quad (9)$$

This procedure is iterative and starts with the linearization of the following unbalanced equilibrium equation at each cross section of the beam:

$$\Delta\hat{\boldsymbol{\sigma}}(x_3) = [\hat{\boldsymbol{\sigma}}^0(x_3) - \hat{\boldsymbol{\sigma}}^{\text{int}}(x_3)] \rightarrow \mathbf{0}$$

$$\begin{Bmatrix} \Delta N(x_3) \\ \Delta M_1(x_3) \\ \Delta M_2(x_3) \end{Bmatrix} = \begin{Bmatrix} N^0(x_3) \\ M_1^0(x_3) \\ M_2^0(x_3) \end{Bmatrix} - \begin{Bmatrix} \int_A \sigma(x_1, x_2, x_3) \cdot dA \\ \int_A \sigma(x_1, x_2, x_3) \cdot x_2 dA \\ \int_A \sigma(x_1, x_2, x_3) \cdot x_1 dA \end{Bmatrix} \rightarrow \mathbf{0} \quad (10)$$

where the stress at each point of the cross section is obtained by using the constitutive damage model briefly described by the following equations:

$$\sigma(x_1, x_2, x_3) = E(x_1, x_2, x_3) \cdot \varepsilon(x_1, x_2, x_3) = E(x_1, x_2, x_3) \cdot [\varepsilon^N(x_3) + \chi_1(x_3) \cdot x_2 + \chi_2(x_3) \cdot x_1]$$

with: $E(x_1, x_2, x_3) = f(x_1, x_2, x_3) \cdot E^0$

(11)

According to the Annex, the evolution of the local damage internal variable at each point of each cross section of the Bernoulli beam, obtained from the local damage

constitutive model, is $f(x_1, x_2, x_3) = (1 - d(x_1, x_2, x_3)) = \frac{c^{\max}}{c} e^{A \left(1 - \frac{c(d)}{c^{\max}}\right)}$, with

$0 \leq c^{\max} \leq c$. The values c^{\max} and c are the maximum and current tension strength at each point of the solid, A is a parameter depending of the fracture energy and $E(x_1, x_2, x_3) = f(x_1, x_2, x_3) \cdot E^0$ is the damaged elastic module. Substituting this expression in Equation (10), the residual forces become

$$\begin{aligned} \begin{Bmatrix} \Delta N(x_3) \\ \Delta M_1(x_3) \\ \Delta M_2(x_3) \end{Bmatrix} &= \begin{Bmatrix} N^0(x_3) \\ M_1^0(x_3) \\ M_2^0(x_3) \end{Bmatrix} - \begin{Bmatrix} E^0 \cdot \int_A f(x_1, x_2, x_3) \cdot (\varepsilon^N(x_3) + \chi_1(x_3) \cdot x_2 + \chi_2(x_3) \cdot x_1) dA \\ E^0 \cdot \int_A f(x_1, x_2, x_3) \cdot (\varepsilon^N(x_3) \cdot x_2 + \chi_1(x_3) \cdot x_2^2 + \chi_2(x_3) \cdot x_1 \cdot x_2) dA \\ E^0 \cdot \int_A f(x_1, x_2, x_3) \cdot (\varepsilon^N(x_3) \cdot x_1 + \chi_1(x_3) \cdot x_2 \cdot x_1 + \chi_2(x_3) \cdot x_1^2) dA \end{Bmatrix} \\ \begin{Bmatrix} \Delta N(x_3) \\ \Delta M_1(x_3) \\ \Delta M_2(x_3) \end{Bmatrix} &= \begin{Bmatrix} N^0(x_3) \\ M_1^0(x_3) \\ M_2^0(x_3) \end{Bmatrix} - \begin{Bmatrix} E^0 \cdot (\varepsilon^N(x_3) \cdot A(x_3) + \chi_1(x_3) \cdot m_1(x_3) + \chi_2(x_3) \cdot m_2(x_3)) \\ E^0 \cdot (\varepsilon^N(x_3) \cdot m_1(x_3) + \chi_1(x_3) \cdot I_{11}(x_3) + \chi_2(x_3) \cdot I_{12}(x_3)) \\ E^0 \cdot (\varepsilon^N(x_3) \cdot m_2(x_3) + \chi_1(x_3) \cdot I_{21}(x_3) + \chi_2(x_3) \cdot I_{22}(x_3)) \end{Bmatrix} \\ \begin{Bmatrix} \Delta N(x_3) \\ \Delta M_1(x_3) \\ \Delta M_2(x_3) \end{Bmatrix} &= \begin{Bmatrix} N^0(x_3) \\ M_1^0(x_3) \\ M_2^0(x_3) \end{Bmatrix} - E^0 \cdot \begin{bmatrix} A(x_3) & m_1(x_3) & m_2(x_3) \\ m_1(x_3) & I_{11}(x_3) & I_{12}(x_3) \\ m_2(x_3) & I_{21}(x_3) & I_{22}(x_3) \end{bmatrix} \begin{Bmatrix} \varepsilon^N(x_3) \\ \chi_1(x_3) \\ \chi_2(x_3) \end{Bmatrix} \end{aligned} \quad (12)$$

$$\Delta \hat{\sigma}(x_3) = \hat{\sigma}^0(x_3) - E^0 \cdot [\mathbf{J}] \cdot \hat{\varepsilon}(x_3)$$

In this equation, $A(x_3) = \int_A f(x_1, x_2, x_3) \cdot dA$ is the damaged cross section, $m_i(x_3) = \int_A f(x_1, x_2, x_3) \cdot x_j dA$ are the moment of the damaged area respecting the x_i centroidal principal axes (initially, for undamaged cross section, it is equal to zero), $I_{ii}(x_3) = \int_A f(x_1, x_2, x_3) \cdot x_j^2 dA$ are the damaged inertia corresponding to the same principal axes x_i and $I_{ij}(x_3) = \int_A f(x_1, x_2, x_3) \cdot (x_j \cdot x_i) dA$ are the damaged inertia products regarding to the same principal axes ($x_i \ x_j$). Notice that the principal inertia axes at certain time instant of the process can change their position in a next instant due to the damage of the cross section of the beam; consequently the damaged inertia products related to the changed axes can be not equal to zero.

Numerical evaluation of the inertia of the damaged cross-section

Due to the difficulties in performing a closed integration of the nonlinear equation (12) using the non-linear damage function defined by Equation (11), the inertia tensor and the area of the damaged cross section is calculated by means of a numerical algorithm (see Box 2). It is important to note that the selected integration algorithm requires to consider that one of the points at which the function to be integrated is located is on the border of the cross section, allowing to capture appropriately the evolution of the damage.

When the cross section of the pier to be analyzed has a rectangular shape, the described procedure is applied directly. However, if the piers have a box shape, the inertia of the damaged cross section is obtained by dividing the element into four subsections, as shown in Figure 4. For each subsection, the damaged area, $A(x_3)_{(j)}$, is

$$A(x_3)_{(j)} = \int_{A_{(j)}} f(x_1, x_2, x_3) dA \quad (13)$$

and the distance between the neutral axes of each sub cross section and the global neutral axis of the complete cross section is calculated. The global inertia of the damaged cross section, $\mathbf{I}_T(x_3)_{(j)}$, is then defined by

$$\begin{aligned} \mathbf{I}_T(x_3)_{(j)} &= \sum_{j=1}^4 \mathbf{I}_{(j)} + A(x_3)_{(j)} \cdot \mathbf{X}^2_{(j)} = \\ &= \sum_{j=1}^4 \left\{ \begin{bmatrix} \int_{A_{(j)}} f(x_1, x_2, x_3) \cdot x_2^2 dA & \int_{A_{(j)}} f(x_1, x_2, x_3) \cdot x_2 \cdot x_1 dA \\ \int_{A_{(j)}} f(x_1, x_2, x_3) \cdot x_1 \cdot x_2 dA & \int_{A_{(j)}} f(x_1, x_2, x_3) \cdot x_1^2 dA \end{bmatrix} + (14) \right. \\ &\quad \left. + \left[\int_{A_{(j)}} f(x_1, x_2, x_3) dA \right] \cdot \begin{bmatrix} X_{2(j)}^2 & X_{2(j)} X_{1(j)} \\ X_{1(j)} X_{2(j)} & X_{1(j)}^2 \end{bmatrix} \right\} \end{aligned}$$

where $\mathbf{I}_{(j)}$ is the damaged inertia of subsection j , evaluated by means of Equation (14), $A_{(j)}$ is the damaged area of the subsection j and $\mathbf{X}^2_{(j)}$ are the distances between the neutral axis of the subsections and the global neutral axis of the whole cross-section, which depend on the damage at the cross section. In the equations (13) and (14), the numerical integration has been carried out following its classical form

$$\begin{aligned} A(x_3)_{(j)} &= \int_{A_{(j)}} f(x_1, x_2, x_3) \cdot dA = J_{acob} \cdot \left[\sum_{p=1}^n \sum_{q=1}^n w_p \cdot w_q [f(\xi_1, \xi_2, x_3)] \right]_{(j)} \\ m_i(x_3)_{(j)} &= \int_{A_{(j)}} f(x_1, x_2, x_3) \cdot x_j dA = J_{acob} \cdot \left[\sum_{p=1}^n \sum_{q=1}^n w_p \cdot w_q [f(\xi_1, \xi_2, x_3) \cdot \xi_j] \right]_{(j)} \\ I_{ii}(x_3)_{(j)} &= \int_{A_{(j)}} f(x_1, x_2, x_3) \cdot x_j^2 dA = J_{acob} \cdot \left[\sum_{p=1}^n \sum_{q=1}^n w_p \cdot w_q [f(\xi_1, \xi_2, x_3) \cdot \xi_j^2] \right]_{(j)} \\ I_{ij}(x_3)_{(j)} &= \int_{A_{(j)}} f(x_1, x_2, x_3) \cdot x_j \cdot x_i dA = J_{acob} \cdot \left[\sum_{p=1}^n \sum_{q=1}^n w_p \cdot w_q [f(\xi_1, \xi_2, x_3) \cdot \xi_j \cdot \xi_i] \right]_{(j)} \end{aligned} \quad (15)$$

where J_{acob} is the determinant of the gradient of the strains, w_p and w_q are the numerical weight coefficients, ξ_1 and ξ_2 are the isoparametric normalized coordinates and n is the order of the quadrature of the numerical integration (see Zienkiewicz and Taylor [28]). Particularly, when damage occurs due to the external load, the position of the neutral axis of each subsection is modified according to the area of the subsection that is damaged. This modification must be reflected in the calculation of the distances to the global neutral axis of each subsection. Thus, to obtain each $\mathbf{X}^2_{(j)}$, it is necessary to know the coordinates $X_{1(j)}$ and $X_{2(j)}$ for each subsection, which are evaluated in a general form by means of the following equations:

$$X_{1(j)} = \left[\frac{\int_{A_{(j)}} x_1 f(x_1, x_2, x_3) dA}{\int_{A_{(j)}} f(x_1, x_2, x_3) dA} \right] ; \quad X_{2(j)} = \left[\frac{\int_{A_{(j)}} x_2 f(x_1, x_2, x_3) dA}{\int_{A_{(j)}} f(x_1, x_2, x_3) dA} \right] \quad (16)$$

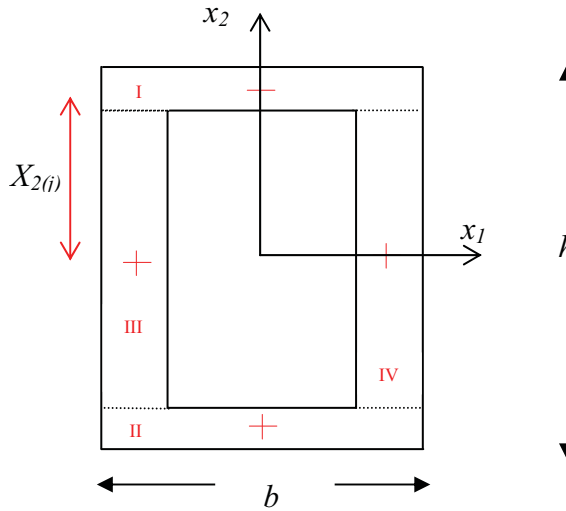


Figure 4. Subsections of a box cross section

Linearization of the unbalanced equilibrium equation

Linearizing Equation (10) and using the Newton-Raphson procedure, the cross section equilibrium equation is solved by successive iterations, increasing the curvature and axial strain of the pier in the corresponding cross section. For this purpose, the generalized strains (axial strain and bending moment) at increment

$(n+1)$ and instant $(t + \Delta t)$ is written by means of Taylor series, truncated at its first term, and then forced to zero

$$\begin{aligned}
 \mathbf{0} &= {}^{n+1} \Delta \hat{\boldsymbol{\sigma}}^{t+\Delta t}(x_3) \cong {}^n \Delta \hat{\boldsymbol{\sigma}}^{t+\Delta t}(x_3) + \frac{\partial [{}^n \Delta \hat{\boldsymbol{\sigma}}^{t+\Delta t}(x_3)]}{\partial \hat{\boldsymbol{\epsilon}}} \cdot {}^{n+1} \Delta \hat{\boldsymbol{\epsilon}}^{t+\Delta t}(x_3) + \dots \\
 \Rightarrow {}^{n+1} \Delta \hat{\boldsymbol{\epsilon}}^{t+\Delta t}(x_3) &= -[{}^n \mathbf{J}^{n+1}]^{-1} {}^n \Delta \hat{\boldsymbol{\sigma}}^{t+\Delta t}(x_3) \Rightarrow {}^{n+1} \hat{\boldsymbol{\epsilon}}^{t+\Delta t}(x_3) = {}^n \hat{\boldsymbol{\epsilon}}^{t+\Delta t}(x_3) + {}^{n+1} \Delta \hat{\boldsymbol{\epsilon}}^{t+\Delta t}(x_3) \\
 {}^{n+1} \Delta \boldsymbol{\sigma}^{t+\Delta t}(x_1, x_2, x_3) &= E^0(x_1, x_2, x_3) \cdot {}^{n+1} \mathbf{x}^T \cdot \Delta \hat{\boldsymbol{\epsilon}}^{t+\Delta t}(x_3) \Rightarrow {}^{n+1} \boldsymbol{\sigma}^{t+\Delta t} = {}^n \boldsymbol{\sigma}^{t+\Delta t} + {}^{n+1} \Delta \boldsymbol{\sigma}^{t+\Delta t}
 \end{aligned} \tag{17}$$

being

$${}^n \mathbf{J}^{n+1} = \frac{\partial [{}^n \Delta \hat{\boldsymbol{\sigma}}^{t+\Delta t}(x_3)]}{\partial \hat{\boldsymbol{\epsilon}}} = E^0 \cdot \begin{bmatrix} A(x_3) & m_1(x_3) & m_2(x_3) \\ m_1(x_3) & I_{11}(x_3) & I_{12}(x_3) \\ m_2(x_3) & I_{21}(x_3) & I_{22}(x_3) \end{bmatrix}$$

the Jacobian matrix.

For each time increment in which the predictor moment produces an unbalanced load increment greater than an adopted tolerance (equations 17 and 18), the procedure considers an increment of the curvature in order to obtain a corrector of generalized stresses which permits to reach the equilibrium state. The used convergence criterion states that the stable response is obtained for the cross section if

$$\sqrt{\frac{\sum_i \Delta \hat{\boldsymbol{\sigma}}_i^2}{\sum_i (\hat{\boldsymbol{\sigma}}_i^0)^2}} \leq TOL \tag{18}$$

where TOL is the tolerance adopted ($TOL \rightarrow 0$).

1. Loop over the time $t + \Delta t$
2. Loop over the cross section position x_3
3. Compute the elastic generalized stresses –predictor– for each cross section.
4. Compute the residual generalized internal stresses

For the first load step : $\mathbf{J}(x_3) \equiv \mathbf{J}^0(x_3)$; $\hat{\boldsymbol{\sigma}}^{\text{int}}(x_3) = \mathbf{0}$

$$\Delta \hat{\boldsymbol{\sigma}}(x_3) = [\hat{\boldsymbol{\sigma}}^0(x_3) - \hat{\boldsymbol{\sigma}}^{\text{int}}(x_3)]$$

5. Balance equation verification on x_3 cross section :

$$\|\Delta \hat{\boldsymbol{\sigma}}(x_3)\| = \begin{cases} 0 & \Rightarrow \text{go to EXIT} \\ \neq 0 & \Rightarrow \text{Continue} \end{cases}$$

6. Starting loop over Newton-Raphson $n^{\text{iteration}}$ process. Incremental generalized strain computation and obtaining of its current value:

$${}^{n+1}\Delta\hat{\mathbf{e}}^{t+\Delta t}(x_3) = -\left[{}^n\mathbf{J}^{n+1}(x_3)\right]^{-1} {}^n\Delta\hat{\mathbf{e}}^{t+\Delta t}(x_3)$$

$${}^{n+1}\hat{\mathbf{e}}^{t+\Delta t}(x_3) = {}^n\hat{\mathbf{e}}^{t+\Delta t}(x_3) + {}^{n+1}\Delta\hat{\mathbf{e}}^{t+\Delta t}(x_3)$$

7. Damaged inertia computation at each x_3 cross section of pier k , using the continuum damage model showed in Box A-1 of the Annex:

$${}^{n+1}[\sigma^0]^{t+\Delta t}(x_1, x_2, x_3) = E^0 \cdot {}^{n+1}\mathbf{x}^T \cdot {}^n\hat{\mathbf{e}}^{t+\Delta t}(x_3)$$

$$f(\sigma^0) - {}^n[c(f)]^{t+\Delta t} \begin{cases} \leq 0 & \text{Maintain the inertia value and go to (**)} \\ > & \text{The process of damage continues (*)} \end{cases}$$

$$(*) \quad {}^{n+1}[f(x_1, x_2, x_3)]^{t+\Delta t} = \frac{c^{\max}}{c} e^{A\left(1 - \frac{c(d)}{c^{\max}}\right)} \quad \text{with} \quad 0 \leq c^{\max} \leq c$$

$${}^n\mathbf{J}^{t+\Delta t}(x_3) = \begin{bmatrix} \int_A f(x_1, x_2, x_3) \cdot dA & \int_A f(x_1, x_2, x_3) \cdot (x_2) dA & \int_A f(x_1, x_2, x_3) \cdot (x_1) dA \\ \int_A f(x_1, x_2, x_3) \cdot (x_2) dA & \int_A f(x_1, x_2, x_3) \cdot x_2^2 dA & \int_A f(x_1, x_2, x_3) \cdot (x_2 \cdot x_1) dA \\ \int_A f(x_1, x_2, x_3) \cdot (x_1) dA & \int_A f(x_1, x_2, x_3) \cdot (x_1 \cdot x_2) dA & \int_A f(x_1, x_2, x_3) \cdot x_1^2 dA \end{bmatrix}^{t+\Delta t}$$

$$(**) \quad \hat{\mathbf{e}}^{\text{int}}(x_3) = E^0 \cdot {}^n\mathbf{J}^{t+\Delta t}(x_3) \cdot {}^{n+1}\hat{\mathbf{e}}^{t+\Delta t}(x_3)$$

$${}^{n+1}\sigma^{t+\Delta t}(x_1, x_2, x_3) = E^0(x_1, x_2, x_3) \cdot {}^{n+1}\mathbf{x}^T \cdot {}^n\hat{\mathbf{e}}^{t+\Delta t}(x_3)$$

8. Back to point 4

9. EXIT

Box 2. Algorithm for the cross sectional damage integration

5. NUMERICAL EXAMPLE FOR THE WARTH BRIDGE, AUSTRIA

General description of Warth Bridge

The Warth Bridge is located 63 km far from Vienna, Austria, was built 30 years ago and has two spans of the deck of 62.0 m and five of 67.0 m, with a total length of 459.0 m. The seven spans of the bridge give rise to six piers with heights of 31.0 m, 39.0 m, 37.0 m, 36.0 m, 30.0 m and 17.6 m, as it can be observed in Figure 5.

The geometrical and mechanical properties of the Warth bridge structure were obtained from the original design drawings [25]. Thus, the simple compression strength of the concrete is $f_{cu}^- = 45.0$ MPa for girders and $f_{cu}^- = 43.0$ MPa for piers. The weight density and Poisson modulus of the concrete are $\gamma = 24.0$ kN/m³ and $\nu = 0.2$, respectively. In order to consider the weight of the non-structural components, the value of the weight density of the girders was increased to a value of $\gamma = 28.0$ kN/m³. For the reinforcement bars,

$\gamma = 78.5 \text{ kN/m}^3$, $\nu = 0.3$ and $E_s = 2.0 \times 10^5 \text{ MPa}$ were considered. The elastic modulus of the reinforced concrete, E_c , was obtained using the Mixing Theory [10, 23] which allows calculating the properties of the elements composed of more than one material.

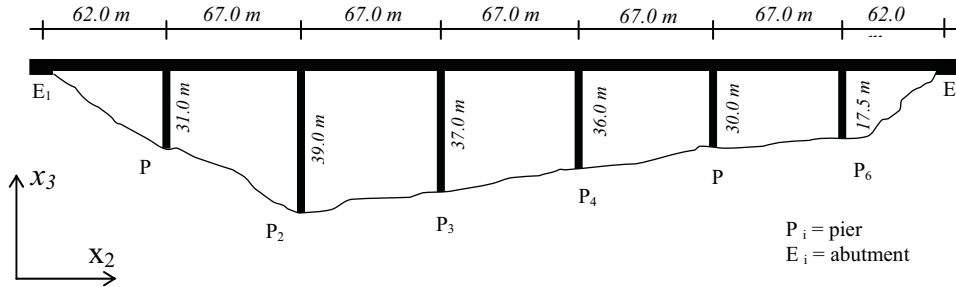


Figure 5. Elevation of the Warth Bridge, Austria

Quasi static pier response of the Warth Bridge

In this work, the numerical simulation of the quasi static structural behavior of shorter pier of the Warth Bridge is given (identified as P6 in the Figure 5). This pier was studied experimentally in the JCR Ispra Laboratory, Italy [25] and numerically, using a finite elements approach, by Faria et al. [8]. The top of this 5.75 m high pier has been subjected to a horizontal quasi static load. The seismic behavior of the pier has been evaluated using the described Bernoulli beam formulation extended to the non linear case of Kachanov damage [18, 12]. That is, without using the finite element approach, it has been introduced within the frame of the classical theory of Bernoulli a non linear continuum damage model. This formulation allows the evaluation of the structural behavior in the non linear field with a very low computational cost and results comparable with those obtained experimentally and also by means of the finite elements approach are obtained. This model leads to a good, low computational cost, non linear solution required by the evaluation of the seismic vulnerability of the bridge, what implies multiple structural dynamic response calculations. The objective of the structural solution developed in this paper is not only a good prediction of the load-displacement relationship, but also a good evaluation of the cross-sectional damage.

Properties of the materials

The mechanical properties of the reinforced concrete bridge pier are calculated using the mixing theory [4, 23], which combines the mechanical behavior of the concrete and steel. The behavior of the concrete is represented by means of a damage model described in the Annex and the behavior of the steel is represented

by means of a anisotropic perfect elasto-plastic model [20]. This combination of the concrete and steel behaviors given by the mixing theory, permits considering a plastic-degradable behavior without softening at each point of the composite material

$$\sigma(d, \epsilon^p) = k_c \sigma_c(d) + k_s \sigma_s(\epsilon^p) = k_c [(1-d)(C_0)_c : \epsilon] + k_s [(C_0)_s : (\epsilon - \epsilon_s^p)] \quad (19)$$

being: $\sigma, \sigma_c(d), \sigma_s(\epsilon^p)$, the stresses in the composite material, in the damaged concrete and in the plastic steel, respectively. $(C_0)_c$ and $(C_0)_s$ are, respectively, the initial constitutive tensors in the concrete and steel while $k_c = A_c(d) / [A_c(d) + A_s]$ and $k_s = A_s / [A_c(d) + A_s]$ are the relative areas corresponding to each material of the cross section of the pier. The characteristics of the used materials are given in Table 1.

Table1. Properties of the materials compounding the reinforced concrete

Mechanical properties	Steel	Concrete
Young's modulus	$E_s = 200,00 \text{ GPa}$	$E_c = 33,50 \text{ GPa}$
Compression strength at the elastic limit	$f_{sy}^- = 545,00 \text{ MPa}$	$f_{cy}^- = 20,00 \text{ MPa}$
Maximum compression strength	$f_{su}^- = 600,00 \text{ MPa}$	$f_{cu}^- = 43,00 \text{ MPa}$
Tension strength at the elastic limit	$f_{sy}^+ = 545,00 \text{ MPa}$	$f_{cy}^+ = 3,10 \text{ MPa}$
Maximum tension strength	$f_{su}^+ = 600,00 \text{ MPa}$	$f_{cy}^+ = 3,10 \text{ MPa}$
Fracture energy	$(G_f)_s = 12.000,00 \text{ MN} / \text{m}$	$(G_f)_c = 1,20 \text{ MN} / \text{m}$

The initial values at the clamped cross section, corresponding to the initial, non damaged state, are the following:

$$\begin{aligned} (A_c)_0 = 0,6579 \text{ m}^2, (A_s)_0 = 76,77 \times 10^{-4} \text{ m}^2 &\Rightarrow \begin{cases} (k_c)_0 = 0,9884 \\ (k_s)_0 = 0,011533 \end{cases} \\ (E)_0 = (k_c)_0 (E_c)_0 + (k_s)_0 E_s &= 35,418 \text{ MPa} \\ \left. \begin{aligned} (f_y^+)_0 &= (k_c)_0 (f_{cy}^+)_0 + (k_s)_0 (f_{sy}^+)_0 = 9,984 \text{ MPa} \\ (f_y^-)_0 &= (k_c)_0 (f_{cy}^-)_0 + (k_s)_0 (f_{sy}^-)_0 = 49,421 \text{ MPa} \end{aligned} \right\} n_r = \frac{(f_y^-)_0}{(f_y^+)_0} &= 4,95 \end{aligned} \quad (20)$$

Geometry and boundary conditions

Figure 6 shows the geometric characteristics and boundary condition for pier P6.

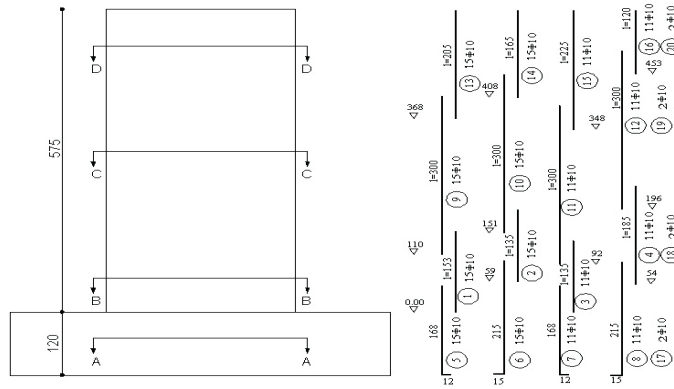


Figure 6. Geometry and reinforcement description of pier P6 belonging to Warth Bridge [25]

The pier is considered perfectly clamped to the foundation and the following sequence of loads is applied at its top end:

1. A compressional axial load of 3820,00 kN
2. Once applied this load, three horizontal displacements are applied sequentially
 - 1) $-0,026m \leq u_h \leq +0,026m$
 - 2) $-0,055m \leq u_h \leq +0,055m$
 - 3) $-0,1m \leq u_h \leq +0,1m$

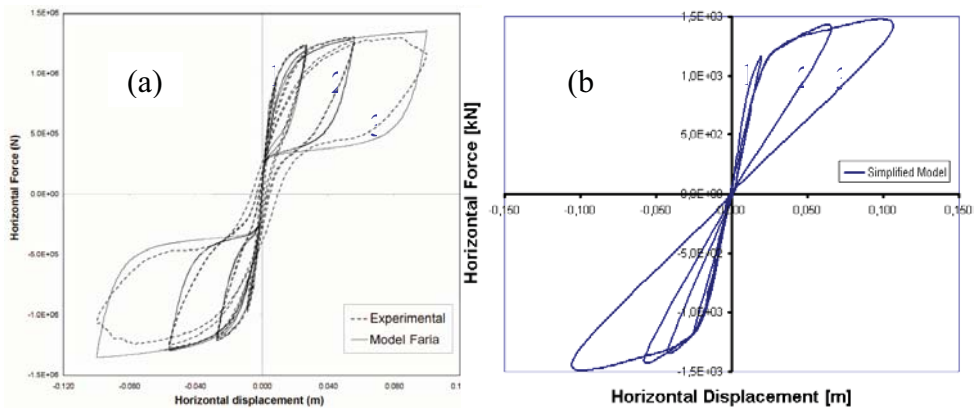


Figure 7. Load-displacement behavior in the pier for the load sequences 1, 2 and 3. a) Experimental results [25] and numeric results [8]. b) Results obtained in the present work

These cycles of displacements introduce degradation on the clamped cross section of the pier and the numerical results obtained in this paper (Figure 7.b.) are

compared with those obtained by Faria et al. [8] and in the JCR Ispra laboratory [25] (see Figure 7.a).

From the results obtained in the present work by using the damage model and the described structural approach, a good solution is obtained in many cases. In spite of the simplicity of the model, the results, in their general features, reach similar values than those obtained experimentally and numerically through FEM models with two internal damage variables (damage variable for compression and tension). Nevertheless, the most important aspect is the very low computational cost that encourages to its application in solving multiple analysis problems like Monte Carlo simulations [11]. The most important differences between the two graphics of Figure 7 can be observed in the unloading branch, because in this case the recovery of the material properties during the change of the sign of the load is evaluated using a simple constitutive model with a single damage index. In Figure 8 the top pier displacement is represented at the end of the load sequence 1 and then, in the same figure, the deformed pier is drawn at the end of the last load sequence 3. In this last case the damaged cross section is localized near the foundation of the pier, while the rest of cross-sections of the pier turns to its initial un-damaged state (rotation of rigid solid around the kneecap (Figure 8)).

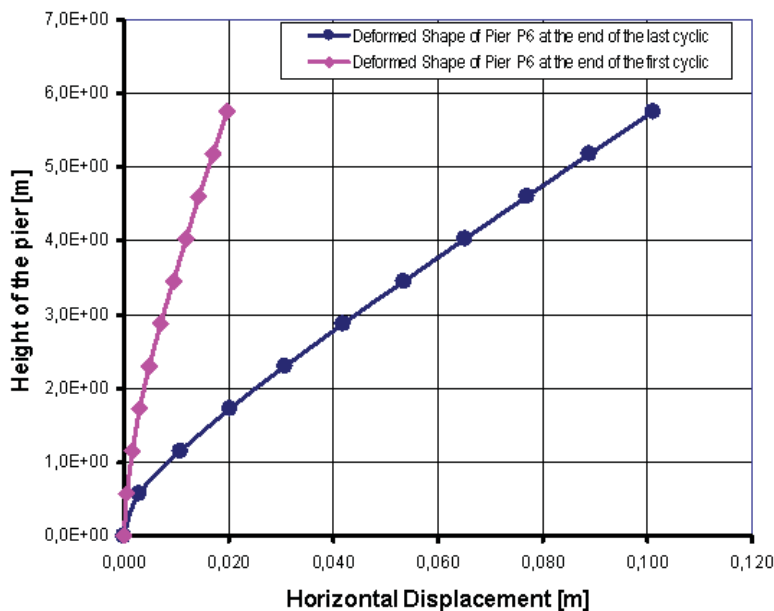


Figure 8. Displacement of the pier P6 at the end of the first load cycle and at the end of the last load cycle

The degradation of the cross-section is shown in Figure 9. Figure 9a shows the moment-curvature evolution, and Figure 9b shows the evolution of the damage index in function of the curvature. It can be seen in this figure that the level of damage at the end of the process is near to one.

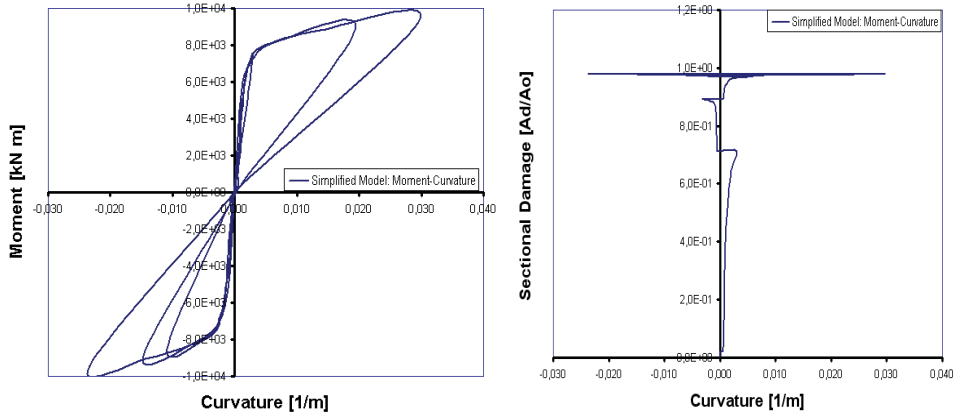


Figure 9. a) Moment-curvature evolution. b) Evolution of the cross-sectional damage depending on the curvature level

6. SUMMARY AND CONCLUSIONS

A model of evaluation of the damage caused by a horizontal action in the piers of RC bridges with single pier bents is developed in this work. For this structure, the proposed model considers only one degree of freedom for each pier, namely the transversal displacements at their top.

The damage in a pier due to the seismic action is defined by using an isotropic damage model based on the Continuum Damage Mechanics. The damage is obtained in terms of the inertia of the damaged cross section at the base of each bridge pier is obtained. The proposed simplified model was verified using experimental and FEM results.

The simplified non-linear analysis performed with the proposed model gives satisfactory results similar to those of the laboratory test and the FEM results. On the basis of these results it is concluded that the proposed model suitably describes the maximum damages of the piers of RC bridges, and that it is a low-cost computer tool, ideal for the multi-analysis processes required by the evaluation of seismic vulnerability.

A future research objective is to develop a model for the complete bridge, using the developed pier model as an element of the structural model.

Acknowledgments

This research was partially supported by European Commission Environmental program RTD Project ENV4-CT-97-0574 “Advanced Methods for Assessing the Seismic Vulnerability of Bridges (VAB)”, by the Spanish Government (Ministerio de Educación y Ciencia), project REN2002-03365/RIES “Development and application of advanced approaches for the evaluation of the seismic vulnerability and risk of structures (EVASIS)” and project BIA2003-08700-C03-02 “Numerical simulation of the seismic behaviour of structures with energy dissipation devices”. This support is gratefully acknowledged.

References

1. R. Aguiar and A. H. Barbat, “*Daño sísmico en estructuras de hormigón armado*”. Universidad Politécnica del Ejército, Quito, Ecuador., 1997.
2. S. Arman and M. Grigoriu, *Markov model for local and global damage indexes in seismic analysis*, NCEER-94-0003, National Center for Earthquake Engineering Research, 1994.
3. H. Barbat, S. Oller, E. Oñate and A. Hanganu, “Viscous Damage Model for Timoshenko Beam Structures”. *International Journal of Solids and Structures*, Vol.34, No.30, pp. 3953-3976. 1997.
4. E. Car, S. Oller and E. Oñate, “An anisotropic elastoplastic constitutive model for large strain analysis of fiber reinforced composite materials”. *Computer Methods in Applied Mechanics and Engineering*, Vol. 185, No. 2-4, 245-277, 2000.
5. J. Chaboche, “Continuum damage mechanics part I. General Concepts”. *Journal of Applied Mechanics*, 55, 59-64, 1988.
6. J. Chaboche, “Continuum damage mechanics part II. Damage Growth”. *Journal of Applied Mechanics*, 55, 65-72, 1988.
7. R. W. Clough and J. Penzien, *Dynamics of Structures*. McGraw-Hill, 1992.
8. R. Faria, N. Vila Pouca and R. Delgado, “Simulation of the cyclic behaviour of r/c rectangular hollow section bridge piers via a detailed numerical model”. *Journal of Earthquake Engineering*, Vol. 8, No. 5, 725-748, 2004.
9. C. Gómez-Soberón, S. Oller and A. Barbat, *Seismic vulnerability of bridges using simple models*. *Monographs of Seismic Engineering*, Monograph series in Earthquake Engineering, CIMNE IS-47, International Center of Numerical Methods in Engineering, Barcelona, Spain, 2002.
10. D. Hull, “*Materiales compuestos*”, Reverté Editorial, Spain, 1987.
11. J. E. Hurtado and A. H. Barbat, “Monte Carlo techniques in computational stochastic mechanics”. *Archives of Computational Methods in Engineering*, Vol. 5, No.1, 3-30, 1998.
12. L. M. Kachanov, “Time of rupture process under creep conditions”. *Izvestia Akademii Nauk; Otd Tech Nauk*, 8 26-31, 1958, .
13. J. Lemaitre “*A course on damage mechanics*”, 2nd edition, Springer, 1992.
14. J. Lemaitre and J. L. Chaboche “Aspects phénoménologiques de la rupture par endommagement”. *Journal of Applied Mechanics*, 2, 317-365, 1978.
15. J. Lubliner, J. Oliver, S. Oller and E. Oñate, “A plastic damage model for non linear analysis of concrete”. *Int. Solids and Structures*, Vol. 25, No. 3, pp. 299-326, 1989.

16. B. Luccioni and S. Oller, "A directional damage model", *Computer Methods in Applied Mechanics and Engineering*, Vol. 192, No. 9-10, 1119-1145, 2003.
17. B. Luccioni, S. Oller and R. Danesi, "Coupled plastic-damaged model". *Computer Methods in Applied Mechanics and Engineering*, Vol. 129, No. 1-2, 81-89, 1996.
18. G. A. Maugin, *The thermomechanics of plasticity and fracture*. Cambridge University Press, 1992.
19. J. Oliver, M. Cervera, S. Oller and J. Lubliner, "Isotropic damage models and smeared crack analysis of concrete". *Second International Conference on Computer Aided Analysis and Design of Concrete Structures*, 2, 945-958, Austria, 1990.
20. S. Oller, E. Car and J. Lubliner, "Definition of a general implicit orthotropic yield criterion". *Computer Methods in Applied Mechanics and Engineering*, Vol. 192, No. 7-8, 895-912, 2003.
21. S. Oller, B. Luccioni and A. Barbat, "Un método de evaluación del daño sísmico de estructuras de hormigón armado". *Revista Internacional de Métodos Numéricos para el Cálculo y Diseño en Ingeniería*, 12(2), 215-238, 1996.
22. S. Oller, A. H. Barbat, E. Oñate and A. Hanganu, "A damage model for the seismic analysis of buildings structures". *10th World Conference on Earthquake Engineering*. 2593-2598, 1992.
23. S. Oller, E. Oñate, J. Miquel and S. Botello, "A plastic damage constitutive model for composite material". *International Journal of Solids and Structures*, Vol.33, No.17, pp. 2501-2518, 1996.
24. Y. J. Park and A. H. Ang, "Mechanistic seismic damage model for reinforced concrete". *Journal of Structural Engineering*, 111(4), 722-739, 1985.
- A. Pinto, J. Molina and G. Tsionis, *Cyclic Test on a Large Scale Model of an Existing Short Bridge Pier (Warth Bridge-Pier A70)*. EUR Report, Joint Research Centre, ISIS, Ispra, Italy.
25. J. Simo and J. Ju, "Strain and stress based continuum damage models – I Formulation". *Int. J. Solids Structures*, 23, 821-840, 1987.
26. J. Simo and J. Ju, "Strain and stress based continuum damage models – II Computational aspects". *Int. J. Solids Structures*, 23, 841-869, 1987.
27. O. Zienkiewicz and R. Taylor, *The Finite Element Method*. Fourth edition, Volume 1 and 2, McGraw-Hill, 1988.

Annex: Continuum Constitutive Damage Law

Introduction to isotropic damage model

This annex contains a brief review of the isotropic continuum damage model at a point of a structure [19], which is used in the paper to formulate the damage of the cross section of a bridge pier. The damage at a point of a continuous solid is defined as the degradation of the stiffness and strength due to the decrease of the effective area [11]. The continuum theory of the damage was formulated by Kachanov [12] in the creep behavior context, but later on it has been reformulated and accepted as a valid alternative to simulate the rate independent behavior of several materials [4-6, 14-17, 26, 27].

Formulation of isotropic damage model

Degradation of the material properties happens due to the presence and growth of small cracks and voids inside the structure of the material. This phenomenon can be simulated by means of the continuum mechanics taking into account a scalar or tensorial internal damage variable. This internal variable of damage measures the level of degradation of the material in a point and its evaluation is based on the

transformation of the real stresses in other effective stresses. For the simple isotropic damage used here, the relationship between the real and the effective stress is described using an isotropic damage variable d

$$\boldsymbol{\sigma}_0 = \frac{\boldsymbol{\sigma}}{(1-d)} \quad (\text{A.1})$$

In this equation, d is the internal variable of damage; $\boldsymbol{\sigma}$ it is the Cauchy stress tensor and $\boldsymbol{\sigma}_0$ is the effective stress tensor, evaluated in the “no-damaged” space. This internal variable represents the loss of stiffness level in a point of the material and its upper and lower limits are given by

$$0 \leq d \leq 1 \quad (\text{A.2})$$

The upper limit ($d=1$) represents the maximum damage in a point and the lower limit ($d=0$) represents a non damaged point.

Helmholtz free energy and constitutive equation

The Helmholtz [18] free energy for the isotropic damage model is given by the expression

$$\begin{aligned} \Psi &= \Psi(\boldsymbol{\epsilon}; p_i) \quad \text{with} \quad p_i = \{d\} \\ \Psi &= \Psi(\boldsymbol{\epsilon}; d) = (1-d) \Psi_0(\boldsymbol{\epsilon}) \end{aligned} \quad (\text{A.3})$$

The elastic part of the free energy, in the small strain case, can be written in the following quadratic form:

$$\Psi_0(\boldsymbol{\epsilon}) = \frac{1}{2} \boldsymbol{\epsilon} : \mathbf{C}_0 : \boldsymbol{\epsilon} \quad (\text{A.4})$$

where \mathbf{C}_0 is the elastic undamaged constitutive tensor. The mechanical part of the dissipation, for uncoupled thermal problem, can be written by using the Clausius-Plank inequality [18]

$$\Xi = \left(\boldsymbol{\sigma} - \frac{\partial \Psi}{\partial \boldsymbol{\epsilon}} \right) : \dot{\boldsymbol{\epsilon}} - \frac{\partial \Psi}{\partial d} \dot{d} \geq 0 \quad (\text{A.5})$$

Applying the Coleman method (see Maugin [18]) to the dissipative power (Equation A.5) the following constitutive equation and dissipative inequality are obtained for each point of the material

$$\boldsymbol{\sigma} = \frac{\partial \Psi}{\partial \boldsymbol{\epsilon}} = (1-d) \frac{\partial \Psi_0}{\partial \boldsymbol{\epsilon}} = (1-d) \mathbf{C}_0 : \boldsymbol{\epsilon} \quad (\text{A.6})$$

$$\Xi = \Psi_0 \dot{d} \geq 0 \quad (\text{A.7})$$

Fundamentals of the constitutive damage model

Damage threshold criterion

This approach defines the beginning of the non linear behavior in each point of the solid and it can be defined using the Plasticity Theory

$$F(\boldsymbol{\sigma}_0; \mathbf{q}) = f(\boldsymbol{\sigma}_0) - c(d) \leq 0, \quad \text{with} \quad \mathbf{q} \equiv \{d\} \quad (\text{A.8})$$

where $f(\boldsymbol{\sigma}_0)$ is a scalar function of the stress tensor $\boldsymbol{\sigma}_0 = \mathbf{C}_0 : \boldsymbol{\varepsilon}$ and $c(d)$ is the strength threshold of damage. The initial value of damage is set up on $c(d^0) = c^{max} = \sigma^{max}$ and represents the uniaxial strength at crushing state. The damage process begins when $f(\boldsymbol{\sigma}_0)$ is greater than $c^{max} = \sigma^{max}$. Equation (A.8) can be written in a more general form throughout the following equivalent expression:

$$\bar{F}(\boldsymbol{\sigma}_0; \mathbf{q}) = G[f(\boldsymbol{\sigma}_0)] - G[c(d)] \leq 0, \quad \text{with} \quad \mathbf{q} \equiv \{d\} \quad (\text{A.9})$$

where $G[\chi]$ is a monotonic scalar function, invertible and positive with positives derivative.

Evolution law for the internal damage variable

The evolution law for the internal damage variable can be written in the following general from:

$$\dot{d} = \dot{\mu} \frac{\partial \bar{F}(\boldsymbol{\sigma}_0; \mathbf{q})}{\partial [f(\boldsymbol{\sigma}_0)]} \equiv \dot{\mu} \frac{\partial G[f(\boldsymbol{\sigma}_0)]}{\partial [f(\boldsymbol{\sigma}_0)]} \quad (\text{A.10})$$

where μ is a non negative scalar value named damage consistency parameter, whose definition is close to the plastic consistency parameter λ . As in the Plasticity Theory, the evaluation of this parameter is made using the Ilyushin [18] consistency condition. From this condition, and from the properties of $G[\chi]$, the following function is obtained:

$$\bar{F}(\boldsymbol{\sigma}_0; \mathbf{q}) = 0 \Rightarrow G[f(\boldsymbol{\sigma}_0)] = G[c(d)] \Rightarrow f(\boldsymbol{\sigma}_0) = c(d) \Rightarrow \frac{\partial G[f(\boldsymbol{\sigma}_0)]}{\partial f(\boldsymbol{\sigma}_0)} = \frac{\partial G[c(d)]}{\partial c(d)} \quad (\text{A.11})$$

and, from here, the permanency condition is deduced:

$$\dot{\bar{F}}(\boldsymbol{\sigma}_0; \mathbf{q}) = 0 \Rightarrow \frac{\partial G[f(\boldsymbol{\sigma}_0)]}{\partial f(\boldsymbol{\sigma}_0)} \dot{f}(\boldsymbol{\sigma}_0) - \frac{\partial G[c(d)]}{\partial c(d)} \dot{c}(d) = 0 \Rightarrow \dot{f}(\boldsymbol{\sigma}_0) = \dot{c}(d) \quad (\text{A.12})$$

Observing the rate of the threshold damage function $\partial G[f(\boldsymbol{\sigma}_0)] / \partial t = \dot{G}[f(\boldsymbol{\sigma}_0)]$ (Equation A.12) and comparing with the evolution law of the internal variable \dot{d} (Equation A.10), the following expression for the damage consistency parameter is obtained:

$$\left. \begin{aligned} \dot{G}[f(\boldsymbol{\sigma}_0)] &= \frac{\partial G[f(\boldsymbol{\sigma}_0)]}{\partial f(\boldsymbol{\sigma}_0)} \dot{f}(\boldsymbol{\sigma}_0) \\ \dot{d} &= \dot{\mu} \frac{\partial G[f(\boldsymbol{\sigma}_0)]}{\partial [f(\boldsymbol{\sigma}_0)]} \end{aligned} \right\} \Rightarrow \begin{aligned} \dot{d} &\equiv \dot{G}[f(\boldsymbol{\sigma}_0)] \Rightarrow \dot{\mu} \equiv \dot{f}(\boldsymbol{\sigma}_0) = \dot{c}(d) = \\ &= \frac{\partial f(\boldsymbol{\sigma}_0)}{\partial \boldsymbol{\sigma}_0} : \dot{\boldsymbol{\sigma}}_0 = \frac{\partial f(\boldsymbol{\sigma}_0)}{\partial \boldsymbol{\sigma}_0} : \mathbf{C}_0 : \dot{\boldsymbol{\epsilon}} \end{aligned} \quad (\text{A.13})$$

Time integration over the rate of internal damage variable (Equation A.13) gives the following explicit expression for the damage evaluation in each point of the solid:

$$d = \int \dot{d} \, dt = \int \dot{G}[f(\boldsymbol{\sigma}_0)] \, dt = G[f(\boldsymbol{\sigma}_0)] \quad (\text{A.14})$$

Substituting Equation (A.14) in (A.5), the following expression for the rate of the mechanical dissipation at each damaged point is established

$$\Xi = \Psi_0 \dot{G}[f(\boldsymbol{\sigma}_0)] = \Psi_0 \frac{\partial G[f(\boldsymbol{\sigma}_0)]}{\partial f(\boldsymbol{\sigma}_0)} \frac{\partial f(\boldsymbol{\sigma}_0)}{\partial \boldsymbol{\sigma}_0} : \mathbf{C}_0 : \dot{\boldsymbol{\epsilon}} \quad (\text{A.15})$$

The current value for the damage threshold c can be written, at time $s = t$, as

$$c = \max \left\{ c^{\max}, \max \left\{ f(\boldsymbol{\sigma}_0) \right|_s \right\} \right\} \quad \forall \quad 0 \leq s \leq t \quad (\text{A.16})$$

Particular expression used for the damage threshold criterion

There are several ways to define the damage threshold criterion. In this work, the exponential of reference [19] for concrete structures is used. The scalar function $G[\chi]$ (Equation A.11) is here defined in function of the *unit normalized dissipation variable* κ as [15]

$$\dot{\kappa} = K(\boldsymbol{\sigma}_0) \cdot \Xi_m = \left[\frac{r(\boldsymbol{\sigma}_0)}{g_f} + \frac{1-r(\boldsymbol{\sigma}_0)}{g_c} \right] \cdot \Xi_m \Rightarrow 0 \leq \left[\kappa = \int_t \dot{\kappa} \, dt \right] \leq 1 \quad (\text{A.17})$$

where $\Xi_m = \Psi_0 \dot{d}$ is the damage dissipation and $r(\boldsymbol{\sigma}) = \sum_{\mathbf{I}=1}^3 \langle \sigma_{\mathbf{I}} \rangle / \sum_{\mathbf{I}=1}^3 |\sigma_{\mathbf{I}}|$ a scalar function to define the sign of the stress state at each point and at each time

instant of the damage process, being $\langle x \rangle = 0,5 [x + |x|]$ the McAully function. The variables g_f and g_c are the maximum values for the tension-compression dissipation at each point, respectively [15]. By this way, the damage dissipation will be always normalized to the maximum consumed energy during the mechanical process.

Using κ as an auxiliary variable, it is now possible to evaluate the damage function $G[\chi]$ in the following form [19]:

$$d = G[c(\kappa)] = 1 - \frac{c^{\max}}{c(\kappa)} e^{A \left(1 - \frac{c(\kappa)}{c^{\max}} \right)} \quad \text{with} \quad 0 \leq c^{\max} \leq c(d) \quad (\text{A.18})$$

but, under the damage condition $f(\sigma_0) \equiv c(\kappa)$. This equation can be also written as

$$G[f(\sigma_0)] = 1 - \frac{f^0(\sigma_0)}{f(\sigma_0)} e^{A \left(1 - \frac{f(\sigma_0)}{f^0(\sigma_0)} \right)} \quad \text{with} \quad f^0(\sigma_0) = c^{\max}$$

where $A = \left[g_f / (f^0(\sigma_0))^2 - 0.5 \right]^{-1}$ is a parameter depending on the fracture energy dissipation g_f [19]. The value $f^0(\sigma_0) = c^{\max}$ is obtained from the agreement with the first damage threshold, when the condition $G[f^0(\sigma_0)] - G[c^{\max}] = 0$ is reached and $G[f^0(\sigma_0)] = G[c^{\max}] \equiv 0$ shows the damage integration algorithm for each single point of the structure.

1. Compute the elastic prediction stress and the internal variable at current time " $t + \Delta t$ ", and equilibrium iteration " i ", ,

$$[\sigma_0]^{t+\Delta t} = C_0 : [\epsilon]^{t+\Delta t}$$

$$^i[d]^{t+\Delta t} ; \tau = ^i[G[f(\sigma_0)]]^{t+\Delta t}$$

$$\tau^0 = ^i[G[f^0(\sigma_0)]]^{t+\Delta t}$$

2. Damage threshold checking:

- a. If: $\tau - \tau^{\max} \leq 0$

$$\text{Then } \left\{ \begin{array}{l} ^i[\sigma]^{t+\Delta t} = [\sigma_0]^{t+\Delta t} \\ ^i[d]^{t+\Delta t} ; \tau^{\max} = \tau \end{array} \right\} \text{ and go to the EXIT}$$

- b. If: $\tau - \tau^{\max} > 0$

Then start with the damage constitutive integration

3. Integration of the damage constitutive equation,

$$\tau^{\max} = \tau$$

$$^i[d]^{t+\Delta t} = 1 - \left[\frac{\tau^0}{\tau} e^{A \left(1 - \frac{\tau}{\tau^0} \right)} \right]^{t+\Delta t}$$

4. Stress and tangent constitutive tensor actualization.

$$^i[\boldsymbol{\sigma}]^{t+\Delta t} = (1 - ^i[d]^{t+\Delta t}) [\boldsymbol{\sigma}_0]^{t+\Delta t}$$

$$^i[\mathbf{C}_T]^{t+\Delta t} = \left[(1 - d) \mathbf{C}_0 - \frac{\partial G[f(\boldsymbol{\sigma}_0)]}{\partial [f(\boldsymbol{\sigma}_0)]} [\mathbf{C}_0 : \boldsymbol{\epsilon}] \otimes \left[\frac{\partial f(\mathbf{C}_0 : \boldsymbol{\epsilon})}{\partial \boldsymbol{\epsilon}} \right] \right]^{t+\Delta t}$$

5. EXIT

Box A1. Integration of the continuum damage equation at each structural point with exponential softening

Stress function particularization

Simo and Ju stress function [26, 27] is used in the paper

$$\tau = f(\boldsymbol{\sigma}_0) = \sqrt{2 \Psi_0(\boldsymbol{\epsilon})} = \sqrt{\boldsymbol{\epsilon} : \mathbf{C}_0 : \boldsymbol{\epsilon}} \quad (\text{A.19})$$

Taking into account this function, parameter A used in Equation (A.18) can be written as

$$A = \frac{1}{\frac{g_f}{(f^0(\boldsymbol{\sigma}_0))^2} - \frac{1}{2}} \quad (\text{A.20})$$

where g_f represents the maximum of the fracture energy to be dissipated at each point of the solid and $f^0(\boldsymbol{\sigma}_0)$ is the value given by the threshold equation for the first damage threshold.

The strengthening of Străulești Bridge over the Colentina River in Bucharest

Alexandru Dima and Ionuț Răcănel

Bridges Department, Technical University of Civil Engineering, Bucharest, Romania

Abstract

The roadway bridge STRĂULEȘTI erected in 1924 is placed over the Colentina River, on the North-West ring road of Bucharest city, on the Aeroportului Street. The bridge superstructure consists in a simply supported semi-through steel riveted bridge deck, having the span $L=30.70$ m and the substructure consists in two concrete abutments with the back and retaining walls executed in brick masonry.

The important damages of the deck caused by the corrosion, vehicle impacts etc. during 80 years of service, but also the construction or execution deficiencies (the rivets position over the maximum allowable distances, the over passing of the slenderness coefficient for the elements of the truss main girders, the absence of the waterproofing system, the absence of footways) affect the structural safety and require the urgent strengthening of the bridge, so that it will correspond to the local traffic conditions, with high capacity heavy trucks.

In this paper, two strengthening solutions are presented. The first, the direct solution, consists in the addition of steel sections on upper chords, on diagonals and on posts of the main truss girders, in replacement of the diagonals in the midspan panels with new elements having appropriate cross sections and in strengthening of the connections between cross girders and main truss girders by increasing the reinforcing plate depth. The second one, the indirect solution, consists in the introduction of steel rods at the bottom part of the cross girders and bottom chords. In the same time, all the existing construction and execution deficiencies were corrected; the existing roadway deck was replaced by a new concrete slab which forms with the stringer a composite structure. The slab has a one side footway and also a guiding guardrail in order to avoid the impact of the elements of the main truss girders by vehicles, so that the deck correspond to the actual norms and to the Class “E” of vehicles..

The design of the strengthening elements and the checks by calculation on the strengthened deck are performed using the sectional stresses values established using 3D finite element models, the loading hypotheses being correlated with the strengthening stages.

KEYWORDS: bridge, riveted steel deck, strengthening, tensioning rods.

1. INTRODUCTION

The main truss girders of the bridge are with 10 panels of 3.07 m length each, have the upper and bottom chords executed with riveted cross section with a single plate forming the web. The diagonals are descending (in tension) and consist in cross sections formed by two near webs which are fixed at the joints with rivets on both sides of chord webs, excepting those diagonals in the midspan panels, where they are disposed in “X” system. The ascending diagonals in these panels have the cross section built with only one web, which is fixed at the joints using two cover-plates. In figure 1 a general view of the analyzed bridge is presented.



Figure 1 General view of the bridge

The upper chords of the main truss girders were recently strengthened by welding on their entire length with angles having the vertical wing coming from top to bottom, with respect to the horizontal edges of the upper chords (Fig. 3).



Figure 2 Deck structure

The bridge deck has a width of 5.0 m and consists in a simple concrete slab poured over Zores profiles. The grillage girders are formed by 6 continuous stringers from

I30 laminated profiles, which are disposed over the cross girders, these assembled as plate girders using rivets (Fig. 2). The connections between cross girders and main truss girders is made through reinforcing plates in the joints at bottom part of the main truss girders, where also posts are present. (Fig.4).



Figure 3 Detail of the existing strengthening at the upper chords

The current posts of the main truss girders have the cross section built up with 4 angles (L80×80×8) joined together at the superior ends through the chord webs and across the bridge through the cross girder reinforcing plates respectively. Along the posts there are also washers.

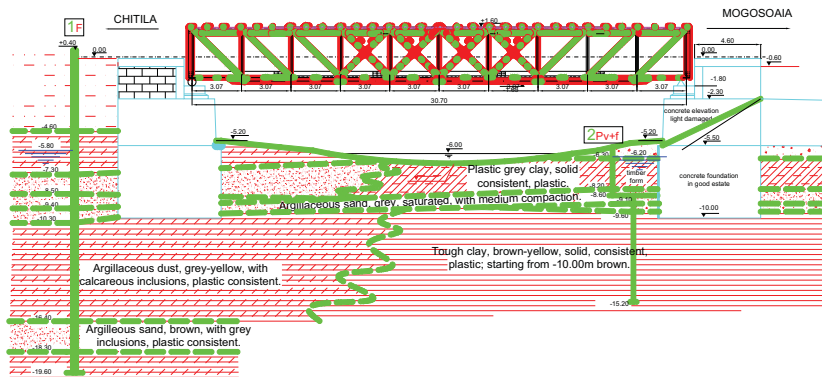
The bottom wind bracing system is performed in “X” system over two panels, the beams being angles placed below the level of the bottom chords flanges.

The footways are placed inside the bridge cross section and they are made as wood floor, at the present all the wood deals are missing.

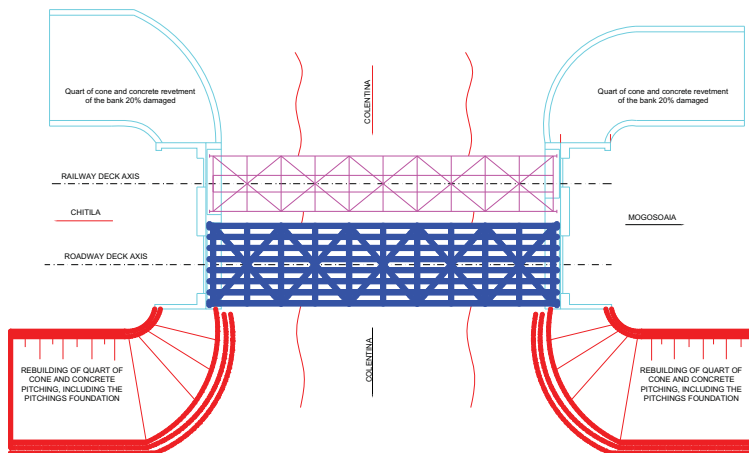
A bridge elevation together with the main dimensions is presented in figure 5.



Figure 4. Detail of the connection cross girders-main girders



a)



b)

Figure 5 General scheme of the bridge a) Elevation b) Plan view

2. DAMAGES AND DEFICIENCIES OF THE BRIDGE DECK

The deck has the following damages, faults and construction deficiencies:

- The existing strengthening at the upper chords, performed with welded angles, do not respect the strengthening construction requirements for riveted steel bridges. Cross section variations, upper chord vibrations and inappropriate quality of the welding seams have lead to the local broken of the angles;

- The deck has generalized corrosion processes between steel pieces, caused by the absence of maintenance, but also because of the rivets disposition at distances over the maximum allowable values;
- The “butterfly” angles of the main truss girders posts are connected with rivets disposed at large distances and they need reinforcements on their entire length, over the cross girders in order to ensure the stability of the compressed flange against lateral buckling phenomenon;
- The diagonals structure don’t ensure the slenderness coefficient in transverse direction and it is necessary their strengthening by adding some angles or by replacing the existing angles with laminated profiles having the same width as the existing steel plates of the diagonal. The existing riveted connections of the diagonals are unsymmetrical with respect to the element axis and the diagonals steel plates have multiple local deformations;
- The cross girders and the stringers have generalized corrosion processes on all visible surfaces, with the reduction of the cross section of those structural elements (Fig. 2);
- The footways are inside the bridge cross section and they don’t have floor on their entire length, the footway spaces on both sides being free, unmarked and without guardrail in order to separate the footway and roadway zones.

3. STRUCTURE MODELING. HYPOTHESES FOR ANALYSES

3.1 *Finite element models types*

According to the strengthening requirements two 3D finite element models are built:

- a finite element model for the existing structure (Fig. 6.a), in order to obtain the sectional stresses coming from permanent loads resulted after the demolition of the existing deck and to establish the structural elements to be strengthened
- another finite element model of the strengthened structure (Fig 6.b) (with new reinforced concrete deck, having a roadway width of 4.00 m and one side footway), finalized in successive stages, till the verification criteria for all strengthened elements and their connections are fulfilled for class E of vehicles.

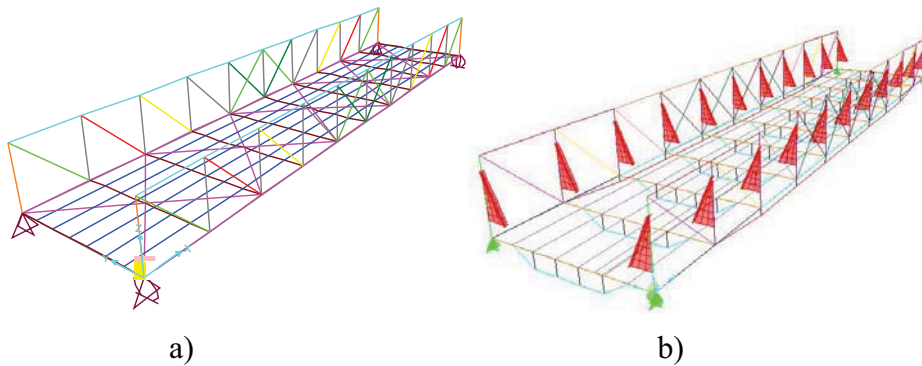


Figure 6. a) Finite element model for existing structure; b) Finite element model for strengthened structure

The bridge structure was modelled in three dimensions using straight frame elements with two joints, according to the geometrical formation of the bridge deck and also using finite elements with four joints having a shell and membrane behaviour in order to model the reinforcing plates at the connections between cross girders and truss main girders. For the model of the strengthened deck it have been introduced, according to the strengthening stages, steel rods at the cross girders bottom flanges and bellow the bottom chords respectively. In the same time, all the cross section changes resulted after the strengthening processes of upper chords and diagonals were operated. The steel rods were connected to the cross girder and bottom chord joints using fictive frames. The restraints of connection joints between each steel rod and the strengthened structural element were imposed so that in rods only axial forces appear.

3.2 Calculation hypotheses

The deck will be strengthened on the site, in following stages:

- the demolition of the of the road concrete deck, including the Zores profiles
- the strengthening of the steel structure
- introduction of the timber form and pouring in this form of the concrete slab over the existing stringers
- the execution of waterproofing system, of the road layers and of the guiding guardrail.

The considered calculation hypotheses correspond to the strengthening stages as following:

Hypothesis 1

Sectional stresses coming from the self weight of the existing steel structure, unstrengthened, determined using the finite element model for the existing structure (without roadway deck);

Hypothesis 2

Sectional stresses resulted from the weight of the strengthening material, determined using the finite element model of the existing structure (without roadway deck);

Hypothesis 3

Sectional stresses from the weight of the green concrete for the new deck determined with the finite element model of the strengthened structure;

Hypothesis 4

Sectional stresses from the loading with A30 vehicles, determined using the finite element model of the strengthened structure;

Hypothesis 5

Sectional stresses from the loading with V80 vehicles, determined using the finite element model of the strengthened structure.

4. ADOPTED STRENGTHENING SOLUTIONS

Following the analysis of deficiencies and damages, but also of the results of the calculations according to the hypotheses presented above, the rehabilitation and strengthening solutions presented in figures 7,8 and 9 were adopted.

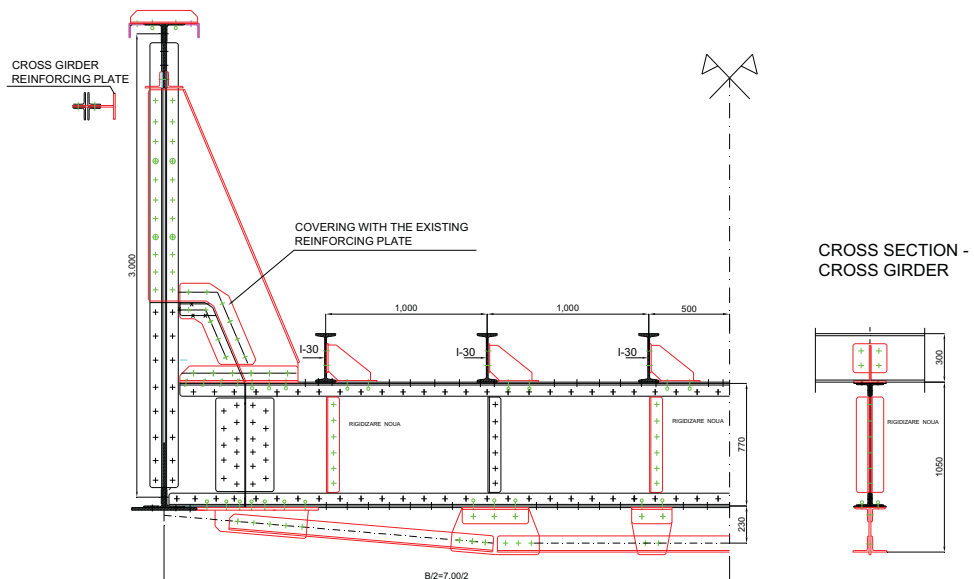


Figure 7 Cross section through the strengthened deck

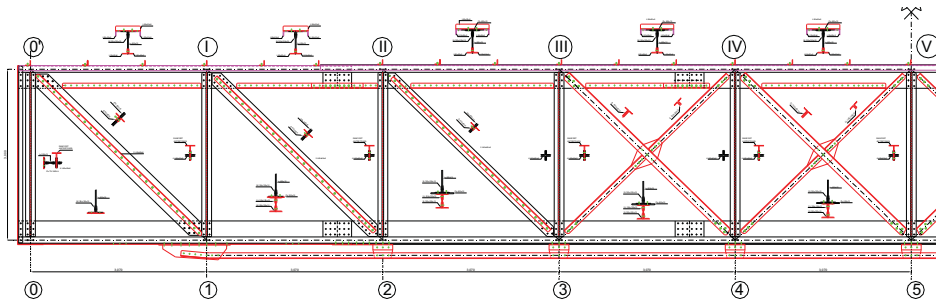


Figure 8 Elevation of the strengthened deck

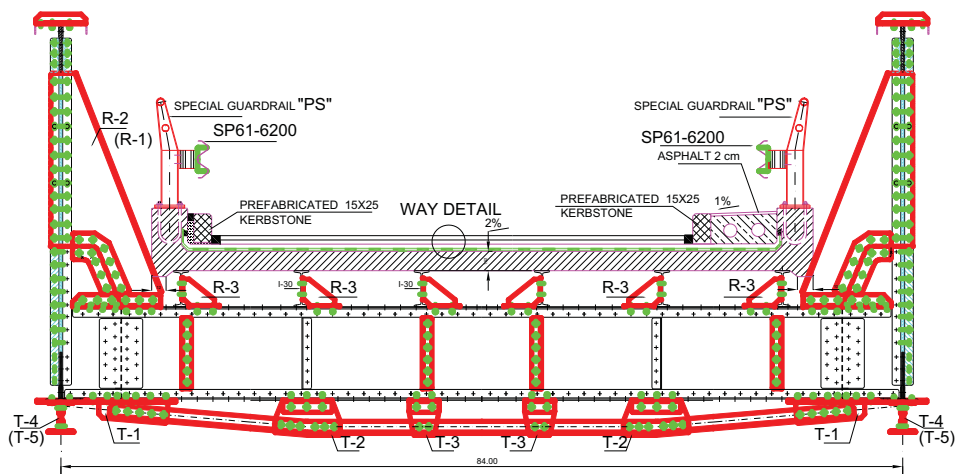


Figure 9 Cross section through the strengthened bridge

- DIRECT STRENGTHENING WITH RIVETED ANGLES OF THE STRUCTURAL ELEMENTS
 1. The main trusses upper chords (with riveted angles at the bottom part of the upper chords web)
 2. Diagonals in panels 0-1-2-3 (and symmetrical) with angles disposed over the existing steel plates of the cross section
 3. The posts (through introduction of new reinforcing plates and filling plates between the angles forming the post).
- INDIRECT STRENGTHENING BY INTRODUCING STEEL RODS FOR THE FOLLOWING STRUCTURAL ELEMENTS
 1. Bottom chords (with untensioned steel rods)
 2. Cross girders (with pretensioned steel rods at the bottom chord, the tensioning force being 10 tf).

- INTRODUCTION OF SOME REINFORCEMENT OR LOCAL STRENGTHENING
 1. By adding riveted transverse angles over the main truss girders upper chord, in order to fix the welded angles from the previous strengthening operation of the deck
 2. Supplementary steel reinforcing plates at the connections between cross girders and main truss girders, to avoid the lateral buckling of the compressed upper chord
 3. The strengthening of the cross girders web through completion with new riveted stiffeners disposed between the existing stiffeners, below each stringer
 4. The reinforcement of the connections between stringers and cross girders.
- ELIMINATION OF SOME EXECUTION DEFICIENCIES
 1. Elimination of diagonals which are impossible to strength in the central panels 3-4-5 and also of the symmetrical diagonals. Introduction of some new diagonals
 2. Correction of the existing rivets positions by introducing new rivets in the zones where the distances overcomes the allowable limits
 3. The demolition of the damaged Zores profiles
 4. Increasing of the upper chords stiffness (with riveted angles at the bottom part of the upper chords web)
 5. Introduction of filling plates between the closed plates forming the cross section of posts and diagonals
 6. Replacement of damaged rivets
 7. Rust cleaning of steel pieces and painting of the deck after the strengthening process
 8. Execution of a new reinforced concrete slab which form with the stringers a composite section, foreseen with lateral guiding guardrail in order to protect the main truss girders against collisions (the width of the roadway is 4.00 m and a one side footway).

5. CONCLUSIONS AND RESULTS

In Table 1, the slenderness coefficient values for the structural elements of the existing structure λ_{ex} (unstrengthened) and of the structural elements of the strengthened structure respectively λ_{cons} are presented, for comparison.

In Tables 2 and 3, the stresses values for the unstrengthened structure, resulted from the loading with A30 vehicles and V80 vehicles respectively, are presented.

Table 1. Slenderness coefficients

Element type	Element length, [m]	Buckling length, [m]	Slenderness coefficient, existing structure, λ_{ex}	Slenderness coefficient, strengthened structure, λ	Allowable slenderness coefficient, λ_a
Bottom chord 4-5	3.7	3.33	44.18	43.82	150
Upper chord IV-V	3.7	3.33	29.96	28.20	100
Diagonal 0'-1	4.3	3.87	228.32	140.01	150
Diagonal I-2	4.3	3.87	220.64	133.17	150
Diagonal II-3	4.3	3.87	481.94	125.53	150
Diagonal III-4	4.3	3.87	481.34	101.90	150
Diagonal IV-5	4.3	3.87	481.34	125.73	150
Final post	3	2.7	76.68	74.88	120
Current post	3	2.7	72.50	72.50	120

Following the strength checks, it is observed that it is necessary to tension the steel rods at the cross girder bottom flange, using a tensioning force of 10 tf and to change the cross sections of the diagonals 0'-1, I-2 (by increasing the dimensions for the angles used for strengthening) and of the current posts respectively (by considering in the checks of a medium cross section of the reinforcing plate).

The steel rods disposed below the bottom chord of the main girders were not tensioned, because the analyses shown that they don't bring a important amount into the bearing capacity of the deck.

Table 2. Values of the stresses (strengthened structure, convoy A30)

Element type	Calculated maximum stress, [N/mm ²]	Allowable stress, [N/mm ²]
Bottom chord 4-5	107.73	152.25
Upper chord IV-V	98.60	145
Diagonal 0'-1	132.57	152.25
Diagonal I-2	131.65	152.25
Diagonal II-3	110.33	152.25
Diagonal III-4	56.31	152.25
Diagonal IV-5	43.90	152.25
Diagonal 4-V	49.75	145
Cross girder	111.40	152.25
Final post	76.44	145
Current post	167.81	145

The new values of the stresses, resulted from strength checks of the deck, are presented, for the structural elements for which the conditions were not previously satisfied (in Table 3) in Table 4.

Table 3. Values of the stresses (strengthened structure, convoy V80)

Element type	Calculated maximum stress, [N/mm ²]	Allowable stress, [N/mm ²]
Bottom chord 4-5	135.80	152.25
Upper chord IV-V	134.82	145
Diagonal 0'-1	156.94	152.25
Diagonal I-2	163.68	152.25
Diagonal II-3	145.90	152.25
Diagonal III-4	87.57	152.25
Diagonal IV-5	67.43	152.25
Diagonal 4-V	80.89	145
Cross girder	197.12	168
Final post	100.65	145
Current post	248.75	145

Table 4. Stresses values after pretensioning of the steel rods (strengthened structure, convoy V80)

Element type	Calculated maximum stress, [N/mm ²]	Allowable stress, [N/mm ²]
Diagonal 0'-1	142.28	152.25
Diagonal I-2	157.74	152.25
Cross girder	118.37	168
Current post	84.24	145

References

1. Coleș, V., Georgescu, D. *Montarea construcțiilor metalice*, Editura Tehnică, 1965
2. ***, *Aspecte actuale din domeniul podurilor metalice*, Al III-lea seminar de poduri "Direcții actuale în calculul și proiectarea podurilor", Editura Mirton Timișoara, 1998
3. ***, *Aspecte actuale din domeniul podurilor metalice*, Al IV-lea seminar de poduri "Direcții actuale în calculul și proiectarea podurilor", Editura Mirton Timișoara, 1999
4. ***, Documentație consolidare pod Străulești peste râul Colentina, Decembrie 2005

The intrinsic characteristics of asphalt mixtures from wearing course

Carmen Răcănel

Department of Roads and Railways, Technical University of Civil Engineering, Bucharest, Romania

Summary

The static triaxial test provides data useful to determination of several physical and mechanical characteristics of asphalt mixtures like internal friction angle and cohesion in material structure.

The knowledge of them is very important to obtain the information concerning to stability in structure, so to verification of asphalt mixture quality.

This paper presents the results obtained on several asphalt mixture from wearing course according to test temperature and loading rate.

The conclusions are the following:

- The internal friction angle has a constant value according to increase of loading rate and grow up with temperature increase;*
- Cohesion increase with the increase of loading rate and decrease with the temperature increase.*

KEYWORDS: asphalt mixture, fiber, internal friction angle, cohesion

1. INTRODUCTION

Using the triaxial apparatus it can be determined the deformation by shearing of an asphalt mixture cylindrical sample. The main stresses for the triaxial compression are $\sigma_1 > \sigma_2 > \sigma_3$.

The static triaxial test is used to determine many physical-mechanical characteristics of asphalt mixtures:

- The internal friction angle and cohesion in material structure;
- The tangent modulus in origin – the elasticity modulus;
- The secant modulus, that gives emphasis to the viscoelastic character of material;
- The reversible modulus, that shows the visco-elasto-plastic recovery of material.

As a result of all this determinations it can be obtained some information concerning to the stability in structure of asphalt mixture under the external loading.

The test is achieved in two ways:

- the test with constant deviator ($\sigma_1 - \sigma_3$), that give information on asphalt mixture creep and can take from 20 - 30 minutes to some hours, depending on material nature;
- The fracture test, when $\sigma_3 = \text{constant}$, but the vertical load increases continuously, with constant rate, until sample collapse, the vertical deformation recording during this time.

From the graphs of MOHR circles (Figure 1) it can be determined the intrinsic characteristics of material: internal friction angle, φ and cohesion, c .

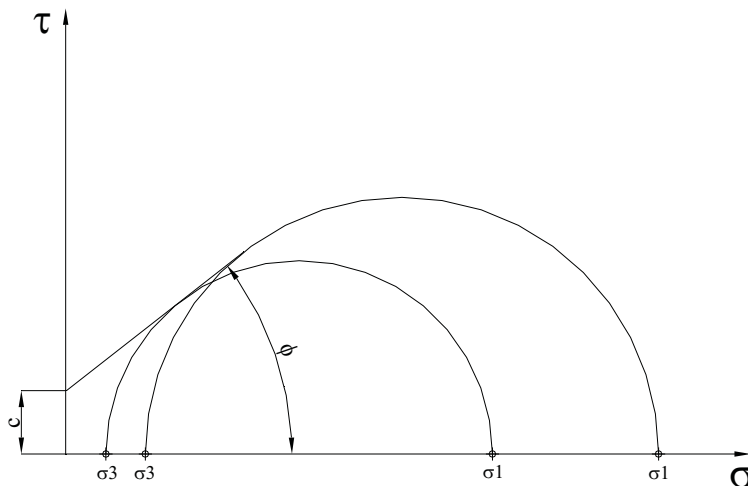


Figure 1. The intrinsic characteristics of asphalt mixture by static triaxial test

It is necessary the fracture test for at least two samples with variable lateral pressure σ_3 to obtain the intrinsic characteristics of asphalt mixture. The obtained common tangent to MOHR circles, determines the internal friction angle, φ by its inclination according to the horizontally, and by the ordinate in origin, the cohesion, c .

Because of the rheological strong character of asphalt mixture it can gives emphasis to the cohesion and internal friction angle variation according to test rate and temperature by triaxial test.

2. THE USED MATERIALS AND RECIPES. THE TEST CONDITIONS

This study was carried out in Roads Laboratory of Faculty of Railways, Roads and Bridges on two types of asphalt mixtures: a classic asphalt mixture BA16 type and an asphalt mixture with fiber MASF16 type.

The aggregates used to preparing the asphalt mixture were Chileni and the filler, Basarabi. It was used two types of bitumen: one of import, ESSO D 50/70 (noted by A) and another of Romanian, Suplacu de Barcău D 60/80 (noted by B). The fiber from MASF16 mixture was Viatop 80 plus. The asphalt mixtures recipes are presented in Table 1.

Table 1. The recipes of the used asphalt mixtures

Mixture	% Crashed rock			% Filler	% Fiber by mixture	% Bitumen by mixture
	8/16	4/8	0/4			
BA16	35	20	40	5	-	5.6
MASF16	60	18	12	10	0.66	6.43

The experimental tests on asphalt mixtures using triaxial apparatus were lead at fracture, maintaining the $\sigma_3 = \text{constant}$.

The asphalt mixture samples used for triaxial test are cylindrical samples with 70 mm in diameter and 140 mm in height, compacted to press at a 234 daN/cm² compaction pressure, leading to densities between 2.28 and 2.33 g/cm³.

The static triaxial test at which subjected the cylindrical samples of asphalt mixture, was performed in the following conditions:

- variable temperature of 3°C, 23°C and 40°C;
- variable loading rate of 0.46mm/min., 4.95mm/min., 12.5mm/min. and 50mm/min.;
- two lateral confining pressure, σ_3 : 2 daN/cm² and 4 daN/cm².

3. THE RESULTS OF LABORATORY TESTS

Following the performing of triaxial test on the asphalt mixture samples, corresponding to Table 1, by maintaining constant the lateral confining stress, σ_3 during the test, were obtained the vertical stresses at fracture, σ_1 .

By mean of graphic construction of MOHR circle were established the intrinsic characteristics of studied asphalt mixtures for three test temperatures and four loading rates.

On the basis of intrinsic characteristics values of studied asphalt mixtures it could draw the graphics with the variation of cohesion and internal friction angle according to loading rate and temperature for the two types of asphalt mixtures.

The cohesion is determined by the mineral aggregate – binder interaction, by the binder viscosity, by the thickness of binder film, by the specific surface of aggregate and by the resistance gave by the coarse aggregate wedging. Higher binder viscosity stronger aggregate – binder interaction and higher cohesion. The interaction increase with the specific surface and the wedging depends on chippings shape and size.

The cohesion decrease with the increase of binder percent because of the film thickness of binder.

The cohesion versus loading rate for the classic asphalt mixtures with A bitumen, BA16-A and B bitumen, BA16-B and for the asphalt mixtures with fiber with B bitumen, MASF16-B at 23°C temperature, are shown in the graphics from Figure 2.

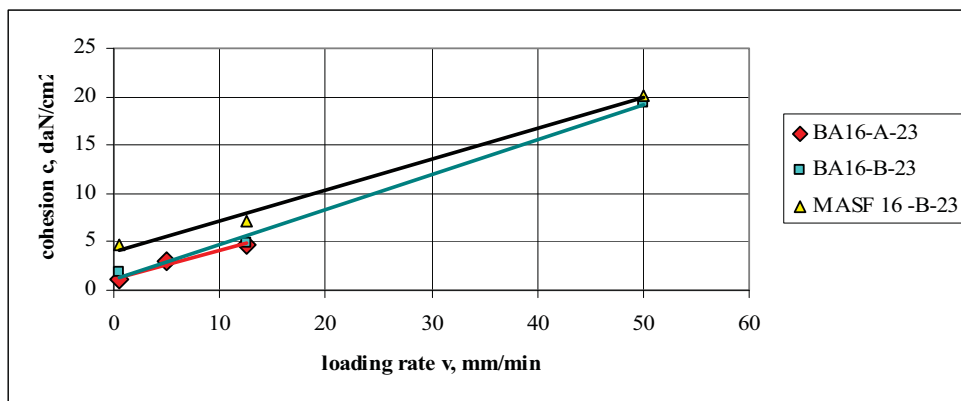


Figure 2. Cohesion versus loading rate at 23°C

The cohesion versus temperature for the classic asphalt mixtures with A bitumen, BA16-A and B bitumen, BA16-B at 0.46 mm/min. loading rate, for the classic asphalt mixtures with B bitumen, BA16-B and the asphalt mixtures with fiber with B bitumen, MASF16-B at a 12.5 mm/min. loading rate and for the classic asphalt mixtures with B bitumen, BA16-B at a 50 mm/min. loading rate, are shown in graphics from Figure 3.

The internal friction angle is the second intrinsic characteristic of asphalt mixtures and is in good connection with the cohesion.

The decrease of cohesion comes with an increase of internal friction angle. In this case, the resistance to traction will decrease, being directly proportional with cohesion and inversely proportional with internal friction angle.

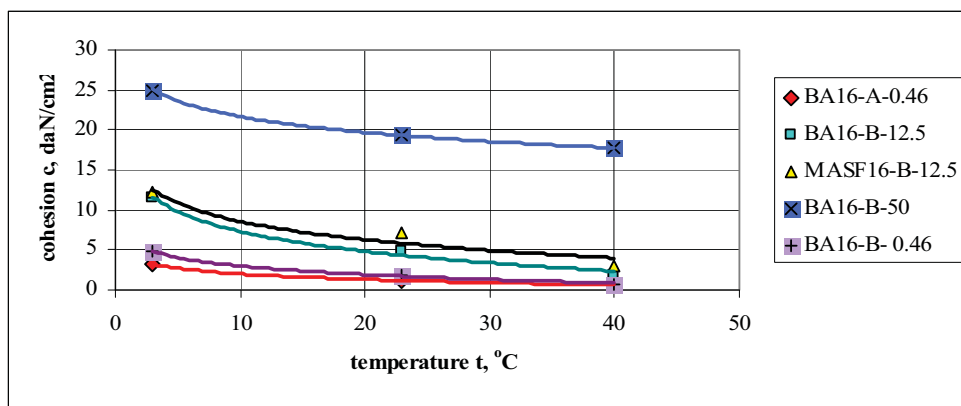


Figure 3. Cohesion versus temperature

The internal friction angle versus loading rate for the classic asphalt mixtures with A bitumen, BA16-A and B bitumen, BA16-B and the asphalt mixtures with fiber with B bitumen, MASF16-B at 23°C temperature, are shown in the graphs from Figure 4.

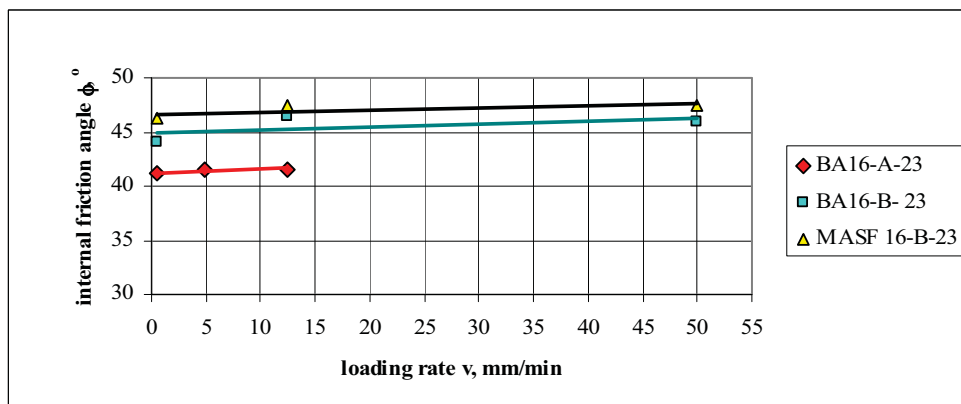


Figure 4. Internal friction angle versus loading rate at 23°C

The internal friction angle versus temperature for the classic asphalt mixtures with A bitumen, BA16-A and B bitumen, BA16-B at 0.46 mm/min. loading rate and for the classic asphalt mixtures with B bitumen, BA16-B and the asphalt mixtures with fiber with B bitumen, MASF16-B at a 12.5 mm/min. loading rate, are shown in the graphics from Figure 5.

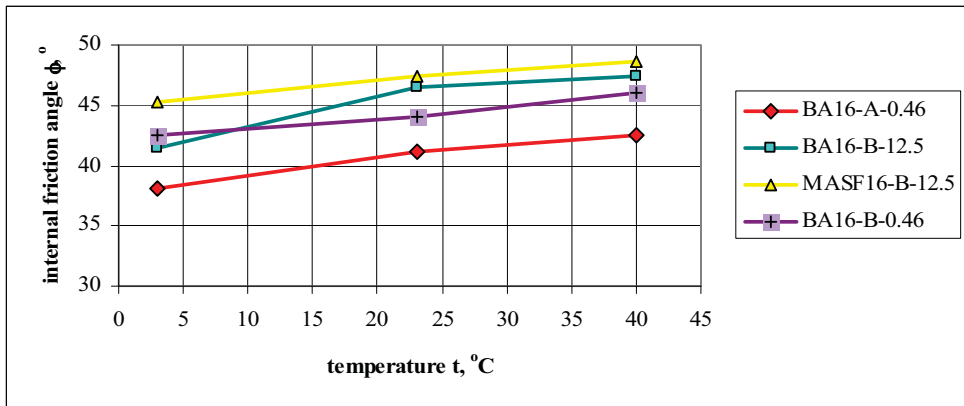


Figure 5. Internal friction angle versus temperature

4. CONCLUSIONS

From this experimental study the following conclusions can be drawn:

- The cohesion value is influenced by the loading rate respective an increase of loading rate lead to a linear increase of cohesion for all of the mixture and bitumen type;
- The slope of cohesion-rate straight line is interpreted like a viscosity of an asphalt mixture;
- The equation of correlation straight line of cohesion versus loading rate for 23°C temperature is the following (Equations 1, 2 and 3):

- for BA16-A-23:

$$y = 0.2859 \cdot x + 1.2731 \quad R^2 = 0.9744 \quad (1)$$

- for BA16-B-23:

$$y = 0.3616 \cdot x + 1.1385 \quad R^2 = 0.9939 \quad (2)$$

- for MASF16-B-23:

$$y = 0.3169 \cdot x + 4.8007 \quad R^2 = 0.9935 \quad (3)$$

where y is cohesion

x – loading rate

Consequently, for any loading rate, for classic and with fiber asphalt mixture with A and B bitumen, compacted to press and tested at 23°C temperature, BA16-A-23, BA16-B-23, MASF16-B-23, can be determined the values of cohesion, using a correlation equation of linear type.

- For the above presented loading rate the cohesion is correlated with temperature according to a logarithmic Equation (4):

$$y = A \ln x + B \quad (4)$$

where y is cohesion

x - temperature

A and B – material constants, with the values presented in Table 2.

Table 2 Material constants and correlation coefficient for equation 4

Mixture	A	B	R ²
BA16-A-0.46	-0.9987	4.3135	0.9998
BA16-B-0.46	-1.526	6.5076	0.9928
BA16-B-12.5	-3.5759	15.546	0.9908
MAF16-B-12.5	-3.292	16.149	0.9249
BA16-B-50	-2.8166	28.15	0.9945

Consequently, for any test temperature, for classic and with fiber asphalt mixture with A and B bitumen, compacted to press and tested to 0.46 mm/min, 12.5 mm/min. and 50 mm/min. loading rate, BA16-A-0.46, BA16-B-0.46, BA16-B-12.5, BA16-B-50, MASF16-B-12.5, can be determined the values of cohesion using a logarithmic correlation equation.

- At the same time with the temperature increase the binder viscosity decrease what has a considerable decrease of cohesion as a effect; the cohesion being minimum, the asphalt mixture become plastic and the shear resistance is minimum; consequently, slips and undulates appear. This is the cause for decrease of cohesion value according to temperature increase, shown in Figure 3.
- By studying the graphs form Figures 4 and 5 it can say that the internal friction angle is almost constant with respect to loading rate variations and increase with temperature increase;
- The correlation of internal friction angle with temperature for asphalt mixtures presented in Figure 5 is made by a II grade equation:

$$y = A \cdot x^2 + B \cdot x + C \quad (5)$$

where γ is internal friction angle

x - temperature

A, B and C – material constants, according to Table 3

Table 3 Material constants and correlation coefficient for equation 5

Mixture	A	B	C	R ²
BA16-A-0.46	-0.002	0.2068	37.4181	1
BA16-B-0.46	0.001	0.0528	42.368	1
BA16-B-12.5	-0.0054	0.391	40.308	1
MASF16-B-12.5	-0.0011	0.1364	44.816	1

Consequently, for any test temperature, for classic and with fiber asphalt mixture with A and B bitumen, compacted to press and tested to 0.46 mm/min. and 12.5 mm/min. loading rate, BA16-A-0.46, BA16-B-0.46, BA16-B-12.5, MASF16-B-12.5, can be determined the values of internal friction angle using a correlation equation of II grade polynomial type.

References

1. Dallas, N.L, Hisham, A.Y. *Improved ACP Mixture Design: Development and Verification*, Research report 1170-1F, Texas Transportation Institute, 1992.
2. Jercan, S., Romanescu, C., Dicu, M. *Construcția drumurilor – Incercări de laborator*, Ed.I.C.B. Eurohot, București, 1992. (in Romanian)
3. Răcănel, C. *Efectele din fluaj și oboseală asupra comportării mixturilor asfaltice*, Teză de Doctorat, București 2002. (in Romanian)
4. SR 174-1/2002, *Îmbrăcăminți bituminoase cilindrate executate la cald*.

Bridge Reconnaissance and Classification System with On-site Wireless Data Acquisition

Prof.-Univ. Dr.-Ing. Norbert Gebbeken, Dipl.-Ing. Andreas Baumhauer,
Dipl.-Ing. Mihai Ionita

*Institute of Engineering Mechanics and Structural Mechanics, University of German Armed Forces,
Neubiberg, 85577, Germany, www.unibw-baustatik.de*

Summary

Some civil engineering tasks such as bridge evaluation are large, time consuming operations (depending on the bridge type and conditions from less than an hour to several hours). They usually require team work in order to obtain the necessary data in the shortest time frame possible. In order to make team work efficient, specific communication tools need to be employed. Therefore, most steps of the evaluation process should be automatized to the highest extent. The opportunity to obtain a result directly on-site is vital in certain situations (e.g. catastrophes, military operations area and remote location lacking established long range communications).

A typical situation this paper takes into account, is that of a bridge located in a remote area with no communication connectivity infrastructure in place (mobile phone coverage, Internet access, etc.), needing to be evaluated with respect to the (residual) load bearing capacity. A computer model of the aforementioned bridge has to be constructed in order to use it as input for the analysis program. In case that no construction plans are available, the computer model has to be constructed from data obtained during reconnaissance. Up to now, data had to be sent to an engineering office for carrying out the structural analysis. The reason is the lack of qualified personnel and tools (devices, software) that can perform this on-site.

The focus of this paper is exploring possible improvements in the data processing, computer model generation as well as model analysis, using only the equipment and manpower present at the bridge location. An ongoing project at the University of the German Armed Forces includes the development of a software tool for on site determination of the residual load-bearing capacity of existing bridges. It is also suited for bridges for which no building documents are available. The goal is the prediction of the admissible military load class within a short timeframe. This timeframe includes data acquisition (e.g. material properties, geometry), numerical modelling of the finite element structure and numerical simulation which is performed using the finite element method (FEM). The goal is achieved by automatization of structural modelling and analysis, implementation of quality management systems for input data and by an easy to use graphical user interface.

KEYWORDS: bridge, assessment, reconnaissance, software, load-bearing capacity

1 INTRODUCTION

Bridges and buildings are designed for given standardized load combinations, according to national and/or international standards. These load combinations consider an estimation of future traffic development. Due to changes in vehicle standardization and traffic density or in construction state (deterioration), it is sometimes necessary to re-examine the behaviour of the structure under these new conditions.

Re-examination is also necessary in some extraordinary situations, when no plans are available or the time spent is critical. We consider as an example, operations such as peacekeeping missions.

A computer analysis model is used to perform the re-examination. Due to the improvements of modern computers, larger and more detailed models can be generated and computed with the FEM. Instead of superposing results of partial simulations, complete structures can be simulated at once within an acceptable time. Thus, the cost efficiency of the designing process can be increased.

However, the most time-consuming parts of performing numerical simulations with FEM remain: data input in a computer, creation of the analysis model and verification.

Modern computer networking technology is used for establishing a consistent data flow in order to take advantage of:

- portable measurement and computer devices
- parallel distributed work.

2 OVERVIEW OF THE PROJECT „BRIDGE CLASSIFICATION“

Within the framework of peacekeeping operations of the German Armed Forces one relevant task of the Army Corps of Engineers (Pioniertruppe) is to evaluate the existing infrastructure in the operational area. Load bearing capacity of bridges (damaged or intact) is especially important in order to ensure the safety and traffic ability of routes.

For this, a methodology is being developed to allow an on site determination of the (residual) load bearing capacity of existing bridges. Provided that no building documents of the bridges are available, this methodology includes the reconnaissance of the bridges, their structural modelling and structural calculations. Input parameters are necessarily the geometry, material properties as well as boundary conditions.

This paper underlines the aspects of the computer program, named BRIDGE ASSESSMENT CODE (“BRASSCO”), which is under development, for performing the numerical simulations necessary for predicting the admissible load.

The software is designed in such a way that the user is released from almost every work that can be automatized and done by the computer. This includes the assembling and checking of incoming data and the automatic determination of the load bearing capacity of the bridge under investigation.

The data gathering interface will be presented in the following section. Later on, a brief overview will be given, concerning the automatic structural modelling and numerical simulations.

3 (DISTRIBUTED) DATA-GATHERING INTERFACE

This section deals with acquiring data from the measurement devices and feeding it to the computer model.

3.1 Measurement devices

Devices currently used (within this project) for bridge reconnaissance:

- tools for measuring geometry (ruler, tachymeter, laser distance gauge),
- tools for probing material properties (Schmidt hammer, Steel hardness gauge) and
- tools for checking the reinforcement, when not exposed due to damage (Ferro scanner).

3.2 Tools for data input and processing

The equipment comprises of two sets of devices. First a general purpose computer (laptop needed due to increased mobility) for model generation and analysis. This acts as server for interlinking all other devices. Second, Pocket PCs for data input, distributed to the team doing the measurements (optional). The main characteristic of the data input equipment is ultra-portability. Touch-sensitive displays replace the keyboard and mouse input and the dimensions of the equipment are reduced. Presence of a wireless network card is required.

3.3 Equipment array and setup

The computer (laptop) with the analysis software (BRASSCO) is considered the central node (team leader computer). The ultra-portable devices (team member computers) communicate with the central node.

3.3.1 Console setup

The data input for the console setup is provided via a graphical user interface, part of the software responsible for the analysis. This interface is designed to be as easy to use as possible. Double-check mechanisms are in place in order to make sure a consistent data model is created. There are maximal and minimal plausible value checks for geometrical parameters, concrete and steel strength, number of reinforcement bars, etc. Additional visual effects are provided for the elements in the graphical user interface to signal incoming data, which is then assembled and transformed into a scaled 3D model. This makes it easy for the team leader to keep an overview over the incoming information (fig. 1, box changes from red to green, later blue, following successive modifications).

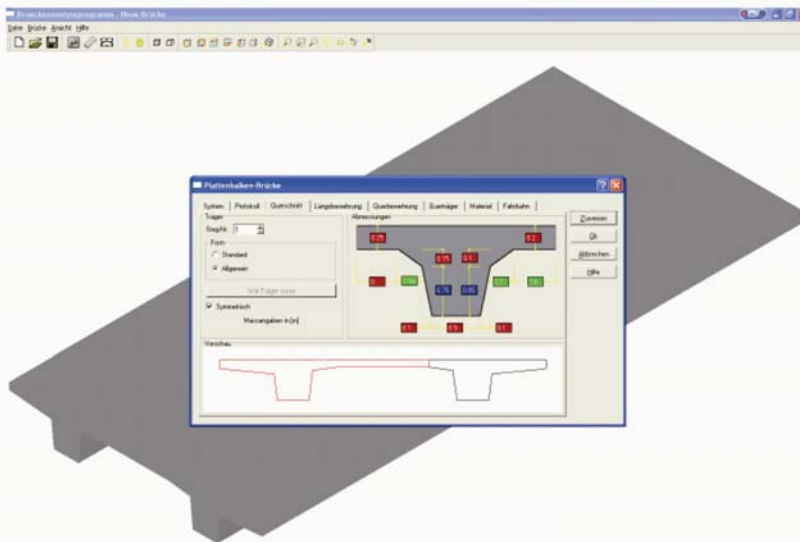


Fig. 1: Graphical user interface in BRASSCO

3.3.2 Wireless local area network setup

By this setup the use of ultra-portable devices is added to the data input scheme. The devices (team member computers) are communicating with the central node, within an "ADHOC" type network (i.e. without any additional equipment).

Communications consists of requests sent by the team leader. The team members have the task of measuring the requested element(s) and send back the corresponding values. Encryption of the data transfer can be activated when needed. The collection of data from different team members in parallel is made possible as values, once entered on Pocket PC, are automatically transmitted to the computer of the team leader. Advantages that come with this setup comprise of

protection for the team leader computer which can remain in the car, not exposed to the elements as well as an easier to use system, able to be adapt to various situations (rain, extreme temperatures, etc.).

3.3.2.1 The client software on the team member computers



Fig 2a: Tree structure (reinforcement branch) Fig 2b: Image for cross-section element

The client software is easy to operate using touch screen technology. The requests are grouped in a tree structure, by the bridge element they belong to (figure 2a) with images that are associated to some elements (figure 2b) for easier identification. This layout maximizes the efficiency, by optimal use of the available display space.

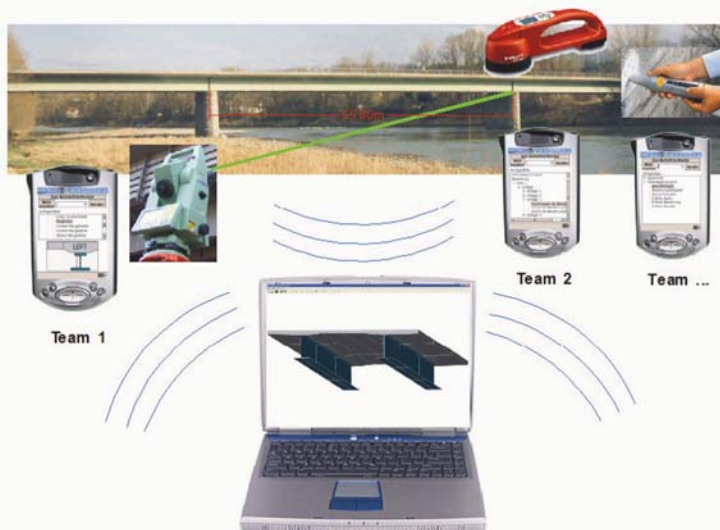


Fig 3: Setup of devices

3.3.2.2 Range limitations

All information exchange is piped through the team leader computer in order to provide the best possible range of communication. The wireless devices determine the maximum range limitation (in open spaces typically more than 150 meters without additional antennas, using current test equipment).

The communication protocol does not require a permanent connection between devices. In case an obstacle reflects or absorbs the radio waves and therefore breaks the connection, it will be automatically re-established. The user is not required to intervene; he has only to monitor the status of the connection, which is displayed on the screen.

3.3.2.3 Communication protocol and recovery mechanism

Upon starting BRASSCO on the team leader computer, a listening socket is established waiting for the team member computers to “log in”. Starting the client application on a team member computer, a connection to the listening socket on the team leader computer is established, consisting of both a message queue and request queue (requests are sent from the team leader to the members consisting of a description of what element needs to be measured).

The queues on the server are constantly being updated and connection attempted with the stations addressed by the requests. On connection failure (e.g. station out of range) the request will remain in the queue and connection will be attempted again later. The team leader can monitor which of the team member computers are within range, and which measurements have already been received.

A recovery mechanism is in place for the team member computers, in order to provide enough continuity for in-field operation.

3.3.3 Multiple reconnaissance teams

Beside the console and wireless setup mentioned above, an extension is being developed for new deployment scenarios. It involves more reconnaissance teams performing the data gathering without generating the model, but still benefiting from a consistent data flow. The need was recognized during field tests in Kosovo, given the difference in the level of technical equipment and human expertise necessary for reconnaissance on the one hand and computer analysis on the other.

3.4 Field tests

The devices and computer program mentioned before have been field tested in several occasions. The experience gained from these tests allowed for successive improvements of the whole system. It has also shown the procedure to be applicable in the theater of operations.

4 AUTOMATIC PERFORMING OF ANALYSIS

The developed software tool is not used to design bridges. It is used to investigate existing structures. For this, two use cases are implemented.

First, the user can choose typical loading scenarios, e.g. according to the STANAG 2021², within the graphical user interface. The software tool creates all necessary load combinations and super-positions automatically. Performing the verification for all components of the structure the grade of utilization can be determined, and, thus, a decision can be made, whether a vehicle is allowed to pass the bridge or not.

Second, the maximum admissible load of a given bridge in terms of military load classes (MLC) can be calculated. For this, four loading scenarios are available:

- One way traffic of tracked vehicles
- Two way traffic of tracked vehicles
- One way traffic of wheeled vehicles
- Two way traffic of wheeled vehicles

For both use cases, modeling and analysis is treated as a “black box”.

4.1 Data Model

The data model consists of the geometrical information, the material properties and rule based algorithms for creating the structural model. The geometrical information is stored using the BREP (boundary representation). No data condensation occurs.

Thus, the data model can be connected directly to the flow of information, coming in via the distributed data-gathering interface. All information gathered during reconnaissance are preserved, to be used later on for various discretisations.

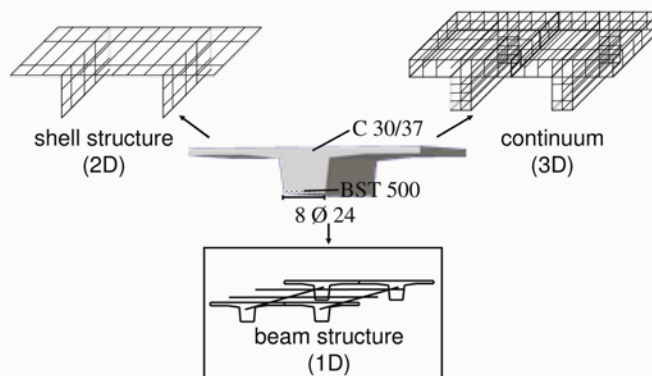


Fig 4: Processing of model

The following section will explain the implemented transformation algorithm for creating a finite element model consisting of beam elements, out of the 3D model.

Approximating the mechanical properties of a bridge with one-dimensional beam elements is on the one hand sufficiently accurate for predicting the behaviour of most bridges and on the other hand reduces the calculation time needed for the simulation.

4.2 Creating the 3d structural model with 1d beam elements

The process of creating the structural model of the bridge consists of two steps.

In the first step, the 3D model is converted into a meta-model, reflecting the topology of the resulting beam structure.

In the second step, beam elements are created on basis of this meta-model and assembled to the finite element model of the bridge.

Creating the meta-model of a bridge depends on the construction type. However, for further treatment of the generated meta-model, the same mechanism can be used. The main task of this mechanism is to condense the 3D information of a component to the one-dimensional centroidal axis and corresponding cross-sections.



Fig 5: Model transformation

The mechanical parameters (EI, EA, GA, GI) of a volume are described in the principal coordinate system of its cross-sections. These cross-sections are determined by the fact that their ideal centre of gravity is a point on the centroidal axis and their normal vector is parallel to the tangent vector of the neutral fibre in that point. This determines the origin and one axis of the principal coordinate system. Rotating around this axis with the angle α until the moments of inertia (I_η , I_ζ) are extreme, leads to the principal coordinate system.

$$\frac{dI_\eta(\alpha)}{d\alpha} = 0 \quad \text{resp.} \quad \frac{dI_\zeta(\alpha)}{d\alpha} = 0 \quad \Leftrightarrow \quad \alpha = \alpha_0 \pm n \cdot \frac{\pi}{2}; \quad n \in \mathbb{N}_0$$

For arbitrary volumes, the determination of the coordinate system of a cross-section decomposes in two steps: In the first step, the centroidal axis has to be determined. In the second step, the cross-sections and their principal coordinate systems are calculated.

The centroidal axis is determined as described above. In addition to pure geometrical algorithms⁴ arbitrary composite components with multiple materials can be treated with this algorithm.

The plane for a cross-section is found analogously to the principle axis by minimizing the area of the cross-section. The angles α and β correspond to the two remaining axis and determine the rotation to find the plane with the minimum area.

$$\frac{\partial A(\beta, \gamma)}{\partial \beta \partial \gamma} = 0 \Leftrightarrow \beta = \beta_0 \pm n \cdot \frac{\pi}{2} \wedge \gamma = \gamma_0 \pm n \cdot \frac{\pi}{2}; n \in N_0$$

In prismatic bodies ($l \gg b, h$) with sufficient distance to the boundaries, this plane determines a cross-section. Within this cross-section, the principal axis can be determined. The calculated centroids of the cross-sections found, will be interpolated through a B-Spline. The B-Spline is determined by the points of support (centroids) and through the normal vector of the sections. Thus, the amount of necessary cuts can be minimized for a sufficiently accurate approximation of the neutral fibre.

Using linear beam elements, within a finite element structure, the original curve has to be approximated by a polygon of the straight elements. The number of elements is determined by the grade of approximation. This grade is controlled by the maximum allowable distance of the approximating polygon from the original curve.

Assembling the created beams according to the meta-model, the finite element structure approximating the bridge is created and the distribution of the internal force variables can be calculated.

4.3 Determination of the admissible load

The determination of the admissible load of an existing bridge means finding the greatest load still satisfying the equation:

$$S_d \leq R_d$$

where S_d is the design value of internal variables/stresses due to action and R_d the design value of the structural resistance.

The load patterns for wheeled vehicles according to STANAG 2021² have discontinuous changes in the topology, i.e. number and distances of axes.

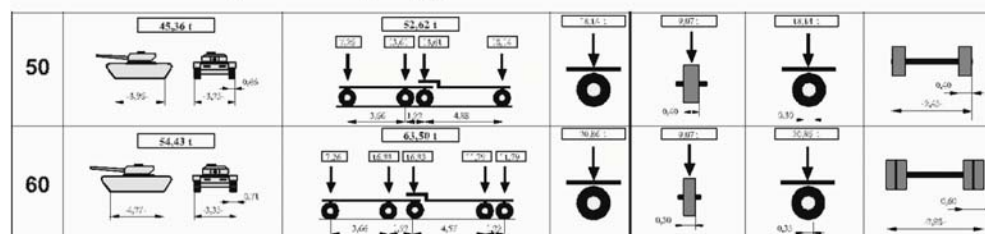


Fig 6: Chart out of STANAG 2021

Examining all loading scenarios described at the beginning of the current section, up to 64 crossings have to be calculated. This number can be reduced using an iterative algorithm with a linear estimation of the next step, thus decreasing the time needed for calculations. Let U_G be the maximum grade of utilization due to permanent loads and U_{curr} the maximum grade of utilization due to the current load (traffic and permanent loads) then

$$\alpha = \frac{1 - U_G}{U_{curr} - U_G}$$

is an estimation of the increase factor. Multiplying the MLC_{curr} (current MLC) with this increase factor leads to the MLC_{new} of the next step. The iteration is stopped if the rounded MLC_{new} equals MLC_{curr} .

$$MLC_{new} \approx \alpha \cdot MLC_{curr}$$

On the one hand, the linear estimation reduces the amount of load cases, but, on the other hand, it makes it necessary to determine the maximum grade of utilization for each load case. This is done using a regula-falsi iteration, finding a factor β , for which a given stress resultant $S\{N, T_z, M_y, T_y, M_z, M_T\}$ satisfies the equation $\beta \cdot S = S_{max}$, where S_{max} is a point on the failure surface $g(N, T_z, M_y, T_y, M_z, M_T)$.

Inversion of the minimum β of all beams and corresponding cross-sections, leads to the maximum utilisation $U_{curr} = 1/\beta_{min}$. Especially for nonlinear material properties (e.g. concrete) and large systems, the calculation of β can become relatively time consuming. Therefore, as long as a new S remains within the hyper-cube created by S'_{max} (hatched area in image) the utilisation is approximated by the minimum distance of S to the boundaries of the hyper-cube. Only if S lies outside the hyper-cube a new S'_{max} and thus a new β is determined. The new hyper-cube then replaces the old one.

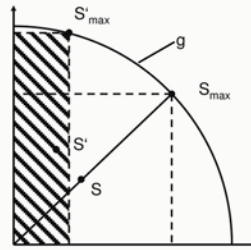


Fig 7: 2D space of internal variable

Therefore, all stored grades of utilization are a lower boundary of the actual utilization. For a proper estimation of the MLC_{new} the actual utilization has to be determined. Starting with the beam with the highest degree of utilization, the actual

factor β (and α respectively), is calculated. Within a cycle, we search for the highest utilization, taking the new factor into account. The result is the MLC_{new} .

4.4 Results



Fig 8: Output of final result (MLC)

Besides displaying the load-bearing capacity of the supporting structure, in terms of MLC or tons, additional information about the condition of the bridge is available. A message is posted to inform the user about the weakest structural element of the bridge and the failure mechanism. For damaged bridges, this information is useful for strategies to repair and/or retrofit.

5 OUTLOOK

The main field of further development is now the assessment of damaged bridges.

In order to determine the (residual) load bearing capacity of damaged or deteriorated bridges, the numerical model, on which the analysis is performed, has to be enlarged. Information is kept structured in two layers. In the first layer the reconnaissance data, assembled in the 3D model and in the second one the rules for the algorithm responsible for creating the numerical model. For this, a structure independent damage model will be implemented. In order to keep the direct data flow from the measurement devices to the data model, the fuzzy set theory is used as an approach for directly incorporating uncertainties of damages. This allows not only implementing a damage model only based on measurable parameters, but furthermore the description of the state of a bridge within human language.

6 CONCLUSIONS

The described application for (re-)examination of existing bridges involves a two-layer architecture. The top layer (data model) is connected to the graphical user interface, processing the data input. The bottom layer (structural modeling) consists of a rule base for transforming the data model in order to perform numerical simulations. A well-defined connection is established between the top and bottom layer. Separating the incoming data flow (and data model) from the analysis model allows enlarging and/or refining the analysis model, by independently adjusting the rule basis. Furthermore, it allows an easy handling of the software program because input data directly corresponds to the measurement devices. Additionally a quality management system ensures consistency of incoming data for the model build-up. Due to this easy handling, field tests have shown an increase in reliability and efficiency using the software tool.

7 REFERENCES

- [1] European Committee for Standardization: ENV 1991-3, Brussels, 1995.
- [2] Stanag 2021, Edition 6.
- [3] Normenausschuß Bauwesen (NABau) im DIN Deutsches Institut für Normung e.V.: DIN 1072, Beuth Verlag GmbH, Berlin 1985.
- [4] P. Veron and J-C. Léon (2001). Using Polyhedral Models to Automatically Sketch Idealized Geometry for Structural Analysis, *Engineering with Computers* 17: 373-385, Springer-Verlag, London Limited

8 ACKNOWLEDGEMENTS

This project was initiated by the development department at the German Army Corps of Engineers (Pioniertruppe). Currently, the BWB (Bundesamt für Wehrtechnik und Beschaffung) supports the work. This support is gratefully acknowledged.

Rehabilitation of a railway's section using GPS technology case study

Proca Gabriela¹ and Proca Mihaela²

¹Technical University “Gh. Asachi”, Iasi, Romania

²S.C. VIO-TOP S.R.L., Bucuresti, Romania

Summary

This paper introduces some aspects concerning topographically works developed on Romanian railways' embankments in order to rehabilitate its.

Are presented constructional and topographically works done on the IV'th corridor Pan European. Related with related precision, rapidity and efficiency was used GPS technologies.

Thus, for constructional works abandoned after 1990 year on section Vâlcea-Valcele was remarked even the stability loss in the same time with bridges 'punctually wastes. The rehabilitation's project had enclosed geotechnical and geologic experiments, leveling up activities on railways areas with a following up character.

On this occasion the geodetic network using GPS technologies was rehabilitated.

1. INTRODUCTION

The section mentioned in this paper is a variant for the existent route, but shorter. The railway was designed to be circulated with 160 km/h. Constructional works were leaved after 1990; more than 45% of art works and understructure being executed.

But how the understructure was not protected in time; thus can be observed: sliding embankments, plants and trees on line platform and the joined embankments, even on current way, (Photo.1).

Breaking off all constructional and protective works, and without a program to protect its, the railways' areas were destroyed by an accelerate degradation generated by water's action.

2. REHABILITATION'S PHASES

2.1 Objectives

In order to rehabilitate and to finish the mentioned railway section were analyzed and adopted new solutions having in view the real situation, on terrain. Were proposed the following phases:

- The complete inventory of unstable terrains in the railway areas;
- The inventory of existing geodetically network;
- A land surveying fly in order to do photogrametrically observations;
- Designing new constructional works and monitoring of all works to be executed.



Photo 1 Embankment's Sliding

2.2 Engineering Topographically Works

Engineering Topographically Works were: verifying on area the geodetically network and rehabilitating it using a GPS technology; leveling up the railway's route, designing crossing profiles of railways and the longitudinal profiles on line's axis.

a. Verifying and Rehabilitating Geodetically Network

The operations specified to this phase consisted in a precise determination of the spatial coordinates X, Y, Z for an amount of 66 points materialized in the ground along the railway segment using GPS technology. In order to use these points also in the photogram-metric process, they have been pre-marked using a square of 50 x 50 cm.

The technical potential engaged in work were:

- **Equipment:** for the surveying campaign there were used 8 complete systems JAVAD-Topcon GPS, L1/L2 + GLONASS, with extra options which have contributed to ensure the quality and safety of the data. In order to ensure the precision of measurements, the GPS equipment has been mounted only on tripods and centered using an optical plummet eyepiece. For some first order points of the National Geodetic Network there have been used pillar plates.

- **Software:**

- PINNACLE package, used for GPS measurements processing (basic calculus, processing the geodetic network, specific report's generation, etc.) software produced of GPS manufacturer company JAVAD;

- GPS Tools package, and INTERGIS software product, containing options to solve the coordinates' problem.

b. Materialization of stations

The RGS materialization was executed as stipulated in Technical Norms. Thus, on the field, were materialized 56 stations using FENO 10 x 10 types of benchmarks with anchor implantation up to 50 cm depth and 10 stations using concrete benchmarks of the existing network. There, have been executed reconnaissances for the new benchmarks. For the benchmark installation, there has been taken into consideration the visibility between the pairs of benchmarks, that they would be placed as much as possible in uncovered, stable zones. The benchmarks have been signalized with 50-60 cm squares

c. Verifying Existing Network. Measurements

For *measurements* and verifying operations was used a GPS technology, respectively 8 equipments.

The survey schedule was the following:

- The measurements campaign for the fix stations and for the junction stations with the National Geodetic Network;

- The measurements campaign for the determination the new stations, based on the measurements of the fixed ones. The measurement method was GPS static surveying. For the RGS junction with geodetic network used at the railways' construction, were identified 2 old stations included in the GPS network.

The big volume of data acquired in GPS measurements campaign had imposed to elaborate a processing strategy (11 steps of data processing)

According to precision of coordinates' values, can be indicated individual errors of RGS less than 1...2 cm.

For *data processing* works had used Pinnacle software, other than the standard method (Static Method), also the Stop&Go, Rapid Static and Cinematic Methods. It can be processed any data combination simple or double frequency, GPS or GLONASS. The simultaneous processing with the least squares method data allows rather short period of occupation and reduces the cycle slips influence as those ones (the cycle slips) are spotted rapidly. For each processing session the software was configured himself using the optimal parameters.

The network compensation module is extremely versatile and automated. Was selected, the compensation in two steps. In the first step, the compensation's vectors can be eliminated or re-pondered. In order to detect and to control the results of compensation were introduced special statistical tests. The second step was in constraining the network on the local control stations. This last, can be used as fixes or as stations having a certain weight in the network's constraint.

Having in view the verifications' results can be mentioned the following:

- The benchmarks B13, B44, B45, L48, L49, L50, TB5, B46, L47, TB2, B50, B51, B52, B53, B54, B57, B58, B59, B60 were in admissible tolerances;
- The benchmarks B1, B2, B4, B5, B6, B7, B8, B9, B10, B11, B14, B15, B16, L51, TB3, TB6, TB4, B18B, B19B, B17, B49, B18, B19, B55, VV1a, VV1b, VV2a, VV2b, VV3a, VV3b were not in tolerance area, being necessary to establish the new coordinates;

c. The benchmarks B12, B21B, B20B, B48, B47, TB1, B56, non -existing on terrains and /or aren't usefully being destroyed. The marks' location is shown in Figure 1.

d. Coordinates transformation was accomplished using GPS Tools software developed by INTERGIS. The coordinated inventory was shown the 1D and 3D coordinate transformation that had lead to obtaining the RGS stations coordinates in the National Geodetic System Stereo 1970 and Black Sea for the heights.

Verifications' conclusions were materialized in following proposals:

1- Re- marking and doubling a number of 18 benchmarks because of their location in the influence area of constructional works, or an initial faulty position. Were named the following points: B1, B2, B5, B11, B12, B17, B45, B48, B47, TB1, B56, B20B, L46, TB4, TB3, L48, L49 and VV3a.

2. New 12 supplementary benchmarks in the following locations:

- Between the pear of points B1-B2 and B3-B4,
- Between the pear of points B15-B16 and tunnel 1;

- Between the pair of points L48-L49 and L50-L51,
- Between the pair of points: B44-B45, VV3a-VV3b, VV2a-VV2b, VV1a-VV1b.

As result of network verification on the analyzed section on the 4th Pan European Corridor, in order to rehabilitate it, were necessary to plant new 30 concrete benchmarks with metallic anchored head, to replace the destroyed existing marks, to redoubling those benchmarks placed in non-stable terrains and to plant supplementary new benchmarks for leveling up works.

The topographical leveling up plan realized on section Km157+421.96-Km 57+564.26 is showing in Figure 2. Supplementary topographically works were done in order to establish; the final route of railway, tunnels, bridges and over bridges, inferior under passages, areas corresponding to rivers, having in view the existing railways in the area as over passages, additional constructional works, etc.

4. CONSTRUCTIONAL WORKS

All constructional works were realized using topographically plans and techniques, after the rehabilitation of geodetic network. The rehabilitation's works for the analyzed railway section are those typically for railways' construction. Were included supplementary works, like: at embankments (repairing the geometry in horizontal plan, in long - plan and cross- plan); reinforcement of understructure, execution of remaining bridges, over bridges and the corrections of rivers' beds, tunnels (repairing the existing works); super-structure: repairing and to continue the constructional works designed.

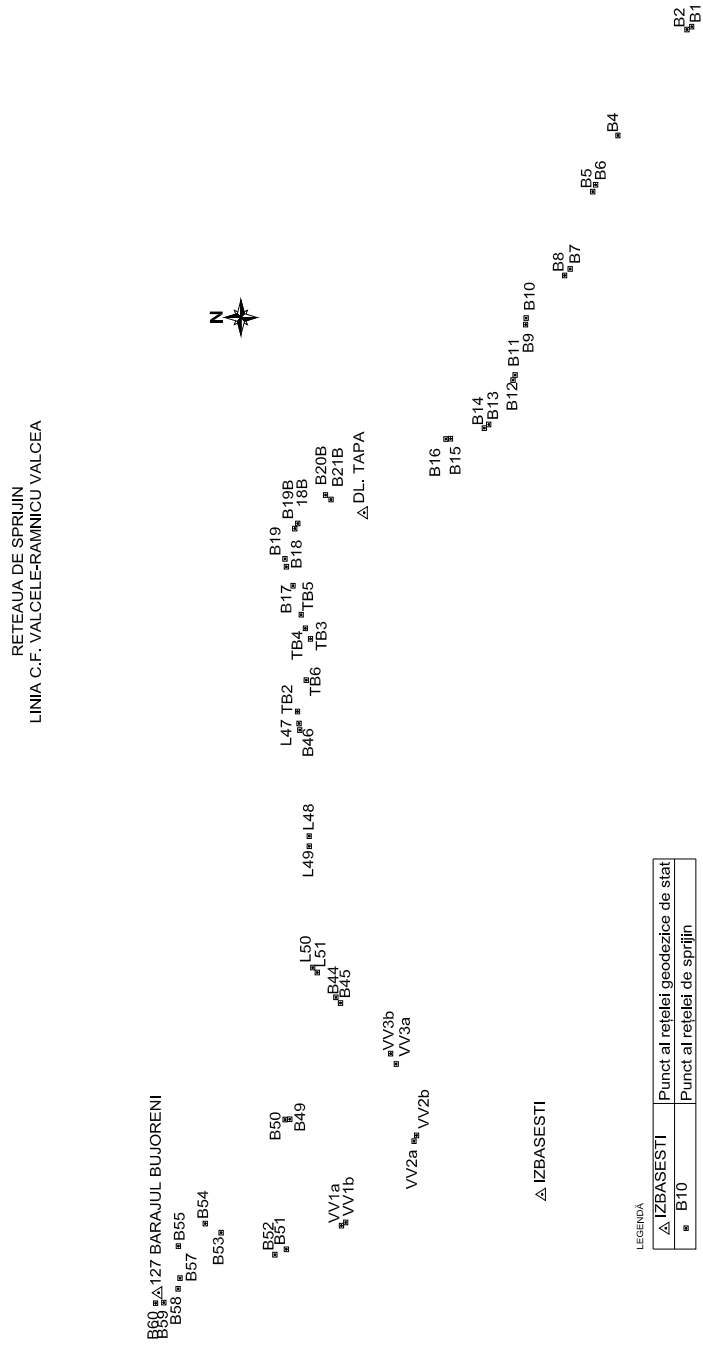
After finalizing all works, is necessary to impose a serious schedule in order to follow the comportment of constructions and terrains in entire railways' constructed area. Can be used fixed signs for the characteristically sections of constructional works to be executed, according the Romanian regulations in this domain.

5. CONCLUSIONS

The technical solution to rehabilitate the railway section had in view: complex studies on the real situation available on terrain; topographically plans for constructional works, rehabilitation of National geodetic Network, particularly the local network and a serious schedule to follow the comportment of constructed areas and buildings.

References:

1. Păunescu, M, Pop, V., şa, *Geotehnică şi Fundaţi* EDP, Bucureşti, 1982.
2. Proca, G., *Construcţii*, Ed. Matrix Rom Bucureşti, 2002.
3. Proca, Mihaela, *Reţele de sprijin şi de trasare pentru căi ferate şi lucrări de artă*, Referat Doctorat, UT Iaşi, 2005.
4. * * *, Caiet de sarcini, reabilitare tronson CF Vâlcea- Vâlcele, ISPCF, Bucureşti.



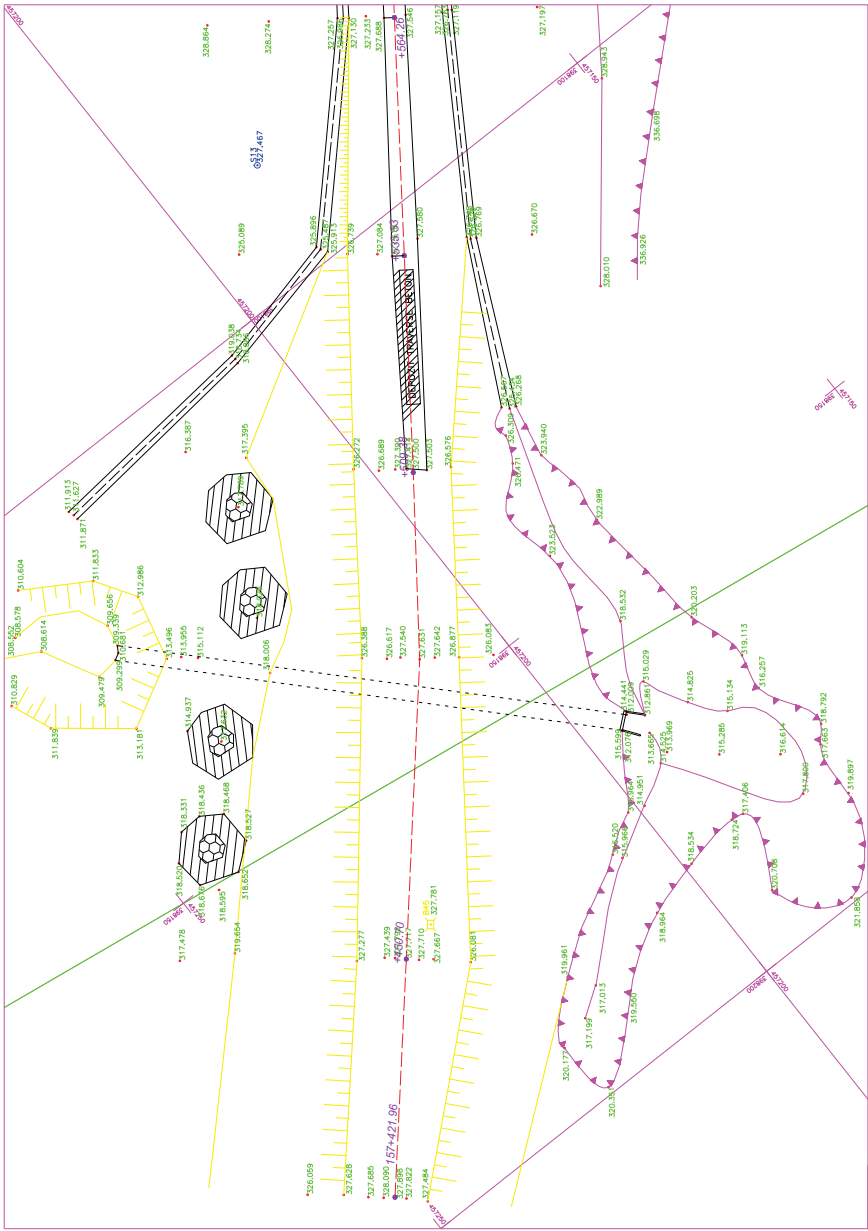


Figure 2 Situation Plan KM 157 + 421.96 – KM 57 + 564.2

Estudio del comportamiento de los hormigones reforzados con fibras cortas

Sergio Oller, Alex H. Barbat and Juan Miquel

Departamento de Resistencia de Materiales, ETSECCPB, Universidad Politécnica de Cataluña

Resumen

En este trabajo se presenta un acercamiento al estudio del comportamiento de los hormigones reforzados con fibras cortas. Se establece una formulación basada en una modificación de la teoría de mezclas clásica para determinar sus parámetros mecánicos a partir de las características de los materiales componentes (hormigón-fibras cortas). También se muestran resultados numéricos obtenidos mediante el método de los elementos finitos y se comentan las posibilidades de un método analítico simplificado para el estudio de su comportamiento.

El desarrollo del trabajo trata sobre el comportamiento del hormigón reforzado con fibras y las características que justifican su utilización. Se estudia el equilibrio interno y mecanismo de transmisión de tensiones entre el hormigón y las fibras cortas y la formulación general del problema e inserción dentro de la técnica de los elementos finitos. Se hace un breve comentario sobre el tratamiento simplificado del comportamiento de los hormigones reforzados con fibras cortas y se presenta un ejemplo de comprobación.

Summary

An approach for the short fibers reinforced concrete behavior is presented in this work. A formulation based on a modification of the classical mixing theory to obtain the composite mechanical properties starting from the single compounding characteristics (concrete-short fibers) is developed. Numerical results obtained by means of the finite element method are also shown and the possibilities of using a simplified analytical method in the study of the short fibers reinforced concrete are commented.

The development of the work studies the behavior of the concrete reinforced with short fibers and the characteristics that justify its use. It studies the internal balance and the stress transmission mechanism between the concrete and the short fibers as well as the general formulation of the problem and its insertion within the frame of the finite element technique. A brief comment is made on the simplified treatment of the behavior of the concrete reinforced with short fibers and a validation example is presented.

1. CLASIFICACIÓN DE LOS MATERIALES COMPUESTOS

Es muy difícil definir un material compuesto dada sus cualidades, composición, propiedades, forma de fabricación, etc. Por esta razón hay distintas maneras de clasificar los materiales compuestos y con seguridad cada uno de ella acertaría en la forma de hacerlo. En este caso, y para ser coherente con el posterior desarrollo del trabajo, se presenta la siguiente clasificación:

1.1 Clasificación según su topología

Entre las posibles clasificaciones, está aquella que se basa en su configuración topológica, es decir en como son y como se distribuyen los componentes: materiales de matriz compuesta (hormigón), materiales de matriz compuesta con fibras cortas y/o largas (hormigón reforzado con fibras), materiales laminados y también una combinación de cada uno de estos tipos enunciados.

1.2 Clasificación según sus componentes

Los materiales compuestos pueden también clasificarse según el tipo y forma en que están constituidos:

- **Fibrosos:** Compuestos por fibras continuas cortas o largas, en una dos o tres direcciones, o bien distribuidas en forma aleatoria aglutinados por una matriz. A su vez esta matriz puede estar formada por dos o más materiales (caso de hormigones reforzados con fibras).
- **Particulados:** Formados por partículas que puntualmente trabajan aglutinadas por una matriz.
- **Laminares:** Compuestos por capas o constituyentes laminares con características de resistencia en magnitud y dirección diferentes.
- **Hojuelados:** Compuestos por hojuelas planas inmersas en una matriz.
- **Relleno esqueleto:** formado por un esqueleto relleno por otro material.

Los más utilizados son los fibrosos, en los cuales las fibras asumen el papel de resistir las acciones mecánicas y la matriz sirve como aglutinante y protector del medio ambiente. La resistencia mecánica de las fibras es del orden de 25 a 50 veces mayor que la matriz. En el caso del hormigón a tracción esta relación es del orden de 100 veces. Esto provoca un comportamiento fuertemente anisótropo.

Al aplicar una carga en un material compuesto se producen en su interior esfuerzos y para lograr una buena transmisión de estos entre fibra y matriz se estudia la longitud y adherencia de este refuerzo.

La función de la matriz (hormigón) es la de repartir y transmitir las cargas a las fibras. En el caso de laminados compuestos las propiedades de resistencia al corte son muy importantes. La matriz cumple la función de asegurar la continuidad de

desplazamientos entre láminas en todo el espesor de la estratificación e influye en el modo de rotura.

1.3 Clasificación estructural

Desde el punto de vista del estudio del comportamiento mecánico, los materiales compuestos pueden clasificarse según su

- **Estructura básica.** En este caso se considera en la clasificación la estructura a nivel de las simples moléculas o mallas cristalinas,
- **Estructura microscópica.** Se tiene en cuenta para la clasificación la interacción fibra-matriz, su influencia en la distribución de tensiones y la aparición de fallas, discontinuidades o fisuras bajo condiciones de cargas elementales,
- **Estructura macroscópica.** Se considera en la clasificación al material compuesto desde un punto de vista macroscópico, como una combinación de sustancias diferentes, que contribuyen al estado de equilibrio del conjunto.

En este trabajo se presentará un estudio estructural desde el punto de vista macroscópico, considerando las siguientes hipótesis:

- Las fibras se distribuyen uniformemente en la matriz,
- Existe perfecta adherencia entre la matriz y el refuerzo, pudiéndose considerar el deslizamiento relativo entre ambos mediante la incorporación de la teoría de la plasticidad en la interface de la matriz-fibra,
- La matriz no contiene vacíos ni defectos,
- No existen tensiones residuales en el material compuesto provenientes de posibles defectos en la fabricación. Sin embargo, es posible incluirlos como condiciones iniciales.

Una extensa descripción sobre los tipos de materiales compuestos y de componentes, formas de fabricación y aplicaciones industriales, puede consultarse en [1] y [2].

2. INTRODUCCIÓN LOS COMPUESTOS REFORZADOS CON FIBRAS

La utilización de nuevos materiales compuestos en el diseño de las estructuras se ha visto incrementada notablemente en los últimos años. Esta tendencia se debe a la posibilidad de diseñar el material con ciertas propiedades especiales que mejoren las cualidades de comportamiento de las estructuras.

Las mayores dificultades que se encuentran en la utilización de estos nuevos materiales radican en la falta de tecnología apropiada para garantizar su correcto

funcionamiento. Esta situación ocurre en los materiales con fibras largas de matrices de hormigón o epoxy. Hay también una cierta incertidumbre en cuanto a la durabilidad de los refuerzos cortos y largos y sobre todo, actualmente hay un problema serio en conseguir una evaluación estructural fiable, pues son materiales cuya no linealidad se manifiesta desde que comienzan los micro-movimientos entre fibra y matriz, situación que ocurre a cargas bajas.

Particularmente, se define el hormigón con fibras como aquel material compuesto por cemento árido y agua, más la adición de fibras cortas discontinuas y/o fibras largas continuas.

La distribución de estas fibras en el hormigón es aleatoria, pero se busca una homogeneidad que confiera una cierta isotropía al conjunto. Para conseguir esto se hade realizar una mezcla evitando tanto la segregación de los áridos como la concentración o preservando una dada orientación dominante en las fibras.

Las fibras para hormigones pueden ser de acero, de vidrio, de asbesto, cerámicas o de algún material plástico. Las fibras confieren al hormigón propiedades muy diversas, pero entre las cualidades mecánicas más importante que aporta al comportamiento del material compuesto se puede sintetizar en:

- a. Las fibras cortas dan al material compuesto mayor ductilidad, aunque no aumenta la resistencia del conjunto,
- b. Las fibras largas dan al material compuesto mayor resistencia, sin muestras de aumento de ductilidad.

De estas dos ideas surge que el hormigón con fibras cortas y largas se transforma en un buen material estructural, transformándose en un material de cualidades destacables frente a otros materiales tradicionales.

Entre las fibras más utilizadas en hormigones puede citarse:

- a. **Fibras de asbesto:** Se han utilizado en la década de los '60 y '70, desarrollándose patentes comerciales como "Uralita". Proporcionan gran ductilidad al conjunto y mejoran sus propiedades mecánicas, pero en los últimos años se ha dejado de utilizar porque su manipulación produce alteraciones fisiológicas en el cuerpo humano. Este material es muy dúctil, tiene una resistencia a tracción entre 500 y 1000 MPa y su módulo de elasticidad es similar al del acero. Su utilización dentro del hormigón es muy buena, porque suelen acomodarse en forma paralela una a otra fibra dejándose envolver por la pasta de cemento, evitando enmarañarse y así perder efectividad.
- b. **Fibras de Vidrio:** Resultan de un filtrado del vidrio a través de una malla metálica. El diámetro depende de esta malla, de la temperatura del vidrio y de la velocidad de estiramiento. La colocación en el hormigón puede realizarse luego de constituir un tejido uni, bi o tridimensional. Hay fibras con buenas propiedades mecánicas y

aislantes de bajo medio y alto costo y suelen ser muy resistentes a los medios agresivos. Su primera incorporación en el mundo de los materiales compuestos data del 1950, cuando se intentó sustituir el acero mediante tendones de fibra de vidrio, puesto que su resistencia es del orden de los 2000 MPa y el módulo de elasticidad de 70 GPa. El mayor problema en la utilización de las fibras de vidrio surgió a nivel tecnológico por las dificultades de anclaje que estas tienen [3].

- c. **Fibras Plásticas:** Se caracteriza por su bajo peso específico y bajo coste. Sus características mecánicas son más modesta que las del grupo anterior, pues su resistencia alcanza escasamente los 500 MPa con un módulo de elasticidad de 10 GPa. Este tipo de fibras admite endurecimientos y aumento de resistencia por plasticidad en frío, mediante retorcido y/o estirado. Entre sus cualidades está su inalterabilidad frente a agentes agresivos junto a su bajo coste y peso. También puede tratarse como ventaja su trabajabilidad durante la fabricación del hormigón.

Tabla 1. Valor orientativo de la resistencia a tracción de algunos materiales

Tipo de Material	Material	Resistencia [MPa]	Tenacidad [MPa m ^{1/2}]
Metálico	Aluminio LM27	153	–
Metálico	Hierro Fundido	265	15-50
Metálico	Acero Templado EN32	590	30-100
Cerámico Puro	Al ₂ O ₃ (Alúmina)	200-2000	5
Cerámico Puro	SiC (Carburo de Silicio – Fibras de Carbono)	300-3000	3
Cerámico Puro	Si ₃ N ₄ (Nitruro de Silicio)	350-3500	6
Cerámico Puro	ZrO ₂ (Oxido de Zirconio – Zirconia)	500-5000	9

- d. **Fibras Cerámicas:** Un grupo de materiales que ha comenzado a ser muy atractivo en la conformación de compuestos, son los denominados cerámicos de altas prestaciones o también cerámicas finas o nuevas cerámicas. Estos materiales se componen principalmente de Óxidos de Aluminio, Zirconio, Silicio, Berilio, Titanio, Magnesio, etc.; de Nitruros de Silicio, Boro, Aluminio, etc.; y de Carburos de Silicio (fibra de carbono) y Boro. Estos nuevos materiales tienen una gran

potencialidad para ser utilizados en distintas formas, solos o formando parte de un compuesto. Tiene cualidades como alta tenacidad a la fractura, alta resistencia mecánica, la capacidad de soportar altas temperaturas y resistir la oxidación.

- e. **Fibras Metálicas:** Es un tipo de fibras cortas muy utilizado en el hormigón. Su resistencia es del orden de 2 a 3 GPa y su modulo elástico de 210 GPa. Uno de los problemas más serios es su falta de adherencia con el hormigón, situación que se pone de manifiesto en ensayos a tracción y flexión. Esta situación, que en menor medida ocurre en otras fibras, hace que su capacidad de participación en el material compuesto está limitado a su posibilidad de transferir esfuerzos, más que a su resistencia nominal. En algunos casos se suele dar a las fibras cortas forma de grapas, ayudando así al anclaje de las mismas en el hormigón.

3. REPRESENTACIÓN DEL COMPORTAMIENTO DE UN COMPUESTO REFORZADO CON FIBRAS CORTAS

3.1 Introducción

Los materiales compuestos están formados por diferentes tipos de sustancias inorgánicas u orgánicas. Su estado de equilibrio atómico depende de distintos tipos de ligaduras interatómicas, dando lugar a materiales amorfos o cristalinos.

Las características mecánicas de los materiales compuestos dependen de sus propiedades intrínsecas: estructura macroscópica, tipo de ligadura, estructura cristalina, etc. También influyen en el comportamiento de estos materiales sus propiedades extrínsecas: características del proceso de fabricación, tamaño de micro-poros y defectos y distribución de los mismos, microfisuras, estados tensionales iniciales, etc. Desde el punto de vista de la simulación del comportamiento constitutivo sólo se puede aportar una contribución en estudios que conduzcan a mejorar las propiedades extrínsecas del compuesto.

Cada una de las sustancias componentes que integran el compuesto condicionan con su propia ley constitutiva el comportamiento del conjunto en función de la proporción del volumen en que participan y de su distribución morfológica dentro del compuesto.

Existen diversas teorías que permiten simular el comportamiento constitutivo de los materiales compuestos (ver una síntesis de ellos en [4], [5]), una de ellas es la “Teoría de Mezclas” [6], que se considera adecuada para la simulación del comportamiento de materiales compuestos en régimen lineal y con ciertas modificaciones permite representar el comportamiento no lineal del material. Por otro lado, esta teoría, en su forma clásica, establece que los materiales

componentes, que coexisten en un punto del sólido deben tener la misma deformación (componentes participando en paralelo). Esta hipótesis plantea una fuerte limitación en la utilización de esta teoría para la predicción del comportamiento de los materiales compuestos. Para solucionar este problema, se debe reformular la teoría clásica a partir de una ecuación de compatibilidad que se adapte al comportamiento del compuesto (componentes participando en serie-paralelo).

El tratamiento de la anisotropía de los materiales componentes [7,8], abre de una manera muy amplia la posibilidad de tratamiento de distintos materiales compuestos de matriz reforzada con fibras.

La teoría de mezclas clásica fue estudiada inicialmente por [6] en el año 1960 y a su vez estos estudios establecieron las bases de otros trabajos posteriores [9-13]. La teoría que aquí se presenta es más general que la clásica y representa el comportamiento constitutivo de un material compuesto por “*n-fases*” altamente anisótropas y sin la limitación exigida por la clásica ecuación de compatibilidad de la teoría original, permitiendo que la relación de comportamiento entre las sustancias componentes pueda ser en serie o en paralelo.

La teoría de mezclas podría entenderse como un “gestor de los modelos constitutivos” de cada componente del compuesto, permitiendo considerar la interacción entre las distintas leyes de comportamiento de las diversas fases de un compuesto. Esta técnica de combinación de comportamientos, o de sustancias en este caso particular, permite que cada una de ellas conserve su ley constitutiva original, isótropa o anisótropa, lineal o no-lineal, y a la vez condicione el comportamiento global del conjunto o compuesto.

Como ya se ha mencionado, la forma clásica de la teoría de mezclas es sólo adecuada para simular el comportamiento mecánico de ciertos materiales compuestos, cuyos componentes responden en paralelo (con igual deformación y sin movimientos relativos entre ellos). Materiales que responden a este perfil son aquellos constituidos de matrices con refuerzo de fibras largas alineadas con la acción de la carga. Para otra orientación de la carga u otros tipos de materiales compuestos, como son los tejidos cuyas fibras tienen diversas orientaciones entre sí, es necesario realizar modificaciones en la teoría clásica.

3.2 Teoría de mezclas clásica

La teoría de mezclas clásica de sustancias básicas se basa en la mecánica del sólido continuo local y se considera adecuada para explicar el comportamiento de un punto de un sólido compuesto. Se basa en el principio de interacción de entre las sustancias que componen el material compuesto, suponiendo las siguientes hipótesis básicas:

- i. En cada volumen infinitesimal de un compuesto participan un conjunto de sustancias componentes;
- ii. Cada componente contribuye en el comportamiento del compuesto en la misma proporción que su participación volumétrica;
- iii. Todos los componentes poseen la misma deformación –ecuación de cierre o compatibilidad–;
- iv. El volumen ocupado por cada componente es mucho menor que el volumen total del compuesto.

La segunda de las hipótesis implica una distribución homogénea de todas las sustancias en cada punto del compuesto. La interacción entre las diferentes sustancias componentes, cada una con su respectiva ley constitutiva, determina el comportamiento del material compuesto y depende básicamente del porcentaje en volumen ocupado por cada componente y de su distribución en el compuesto. Esto permite combinar materiales con comportamientos diferenciados (elástico, elasto-plástico, etc.), donde cada uno de ellos presenta un comportamiento evolutivo gobernado por su propia ley.

La tercera hipótesis establece que en ausencia de difusión atómica* se cumple la siguiente condición de compatibilidad bajo la hipótesis de pequeñas deformaciones para cada una de las fases del material compuesto:

$$\varepsilon_{ij} = (\varepsilon_{ij})_1 = (\varepsilon_{ij})_2 = \dots = (\varepsilon_{ij})_n \quad (1)$$

donde ε_{ij} y $(\varepsilon_{ij})_n$ representan respectivamente las deformaciones del material compuesto y de la componente i -ésima de dicho material compuesto.

El factor de ponderación o coeficiente de participación volumétrica k_c permite considerar la contribución de cada fase y se obtiene considerando la participación volumétrica de cada una de los materiales componentes respecto del volumen total

$$k_c = \frac{dV_c}{dV_0} \Rightarrow \sum_{c=1}^n k_c = 1 \quad (2)$$

donde V_c representa el volumen del componente c -ésimo del material y V_0 es el volumen total del material compuesto.

* **Nota:** Los fenómenos de difusión atómica se producen a temperaturas cercanas al punto de fusión. En los análisis se considera una temperatura inferior a la correspondiente al punto de fusión.

La ecuación constitutiva deriva de un planteo termodinámico consistente y tiene la siguiente forma

$$\sigma_{ij} = C_{ijkl}^S \varepsilon_{kl}^e = \sum_{c=1}^n k_c (\sigma_{ij})_c = \sum_{c=1}^n k_c (C_{ijkl}^S)_c (\varepsilon_{kl}^e)_c \quad (3)$$

Siendo σ_{ij} la tensión en el material compuesto, $(\sigma_{ij})_c$ la tensión en cada componente (fibra/matriz) C_{ijkl}^S el tensor constitutivo del compuesto, $(C_{ijkl}^S)_c$ el tensor constitutivo de cada material componente y $(\varepsilon_{kl}^e)_c = \varepsilon_{kl} - (\varepsilon_{kl}^p)_c - (\varepsilon_{kl}^\theta)_c$ la deformación elástica de cada material componente. En esta última $(\varepsilon_{kl}^e)_c$, $(\varepsilon_{kl}^p)_c$ y $(\varepsilon_{kl}^\theta)_c$ representan las cuotas de deformación elástica, plástica y de origen térmico.

De las ecuaciones anteriores surge que el tensor constitutivo del compuesto adquiere la forma

$$C_{ijkl}^\sigma = \sum_{c=1}^n k_c (C_{ijkl}^\sigma)_c \quad (4)$$

La teoría de mezclas clásica, la cual se parte de la hipótesis de que el campo de deformaciones es el mismo para todos los componentes del compuesto, es rigurosamente válida sólo si se aplica a materiales cuyos componentes trabajan en paralelo.

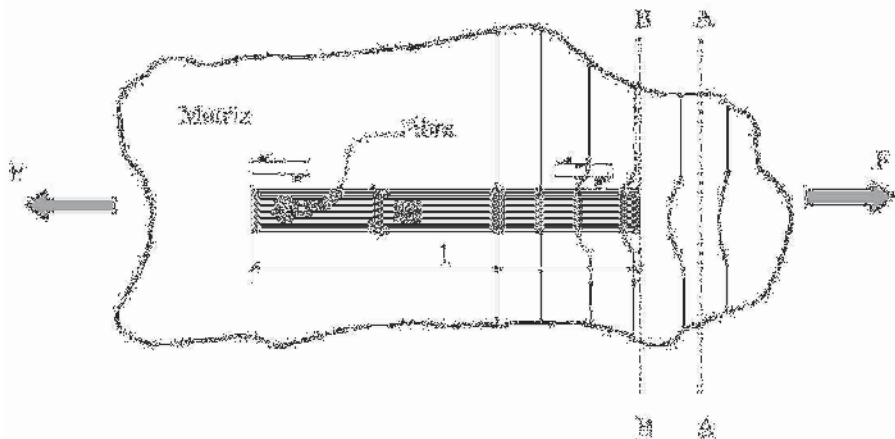


Figura 1. Deformación alrededor de una fibra discontinua embebida en una matriz sometida a tracción

Estos materiales se caracterizan por que su estado tensional resulta ser la suma de las tensiones de cada componente, ponderadas de forma proporcional al volumen que ocupa cada fase respecto del total –ejemplo: matriz con fibras largas, hormigón armado, etc.–.

En el caso de matrices con refuerzo de corta longitud no resulta válida la hipótesis de igualdad entre las deformaciones de todos los componentes. Para solucionar este inconveniente existen dos alternativas: definir otra ecuación de cierre, ecuación (1), que permita simular adecuadamente los fenómenos que se producen en el material, o realizar una corrección en las propiedades de cada componente y mantener la hipótesis de igualdad deformaciones en cada uno de los componentes del compuesto, expresión que se utilizará en este trabajo y se explicará más adelante.

3.3 Teoría de mezclas para refuerzo de poca longitud

La formulación de la teoría de mezclas clásica está orientada a un material de matriz reforzada con fibras largas, y a medida que la relación de aspecto* de la fibra disminuye, la condición de compatibilidad fibra-matriz deja de cumplirse. Así, al acortarse la longitud de la fibra el efecto de deslizamiento se hace más significativo y disminuye la capacidad de transmisión de esfuerzos entre fibra y matriz y la “eficacia” de la contribución de las fibras en la rigidez del material compuesto disminuye.

La Figura 1 muestra la deformación de la matriz circundante a una fibra discontinua embebida en la misma y sometida a una carga de tracción paralela a la fibra.

En un material compuesto con refuerzo de fibras largas, se tiene el mismo estado de deformaciones para la matriz y las fibras. Por otro lado, la tensión a lo largo del refuerzo no varía salvo en la zona de los extremos, donde se verifica que la deformación de la misma es menor respecto a la de la matriz. En el caso de refuerzos de corta longitud embebidos en una matriz este fenómeno juega un papel fundamental en la determinación de las propiedades mecánicas del compuesto.

Este fenómeno puede explicarse teniendo en cuenta la Figura 1. En la misma, en la sección *AA* la deformación del conjunto se debe sólo a la deformación de la matriz. En la sección *BB*, justo en el extremo de la fibra, evidencias experimentales muestran que la transferencia de esfuerzos de la matriz hacia la fibra es gradual, con esfuerzo nulo en la punta y con un aumento gradual de la tensión a lo largo de

* NOTA: Se define como relación de aspecto al cociente $l/2r$ donde l y r son la longitud y el radio de una fibra corta respectivamente.

la fibra hasta el punto en el cual las deformaciones de matriz y fibra son iguales. De acuerdo con esto, la zona central de una fibra presenta el máximo valor de tensión axial. Se define como *longitud de transferencia* l_c a la longitud de refuerzo necesaria para garantizar la compatibilidad fibra-matriz y la transferencia de los esfuerzos desde la matriz hacia la fibra. Cualquier refuerzo cuya longitud sea inferior a esta magnitud, no participa plenamente en los mecanismos de transferencia de esfuerzo [14].

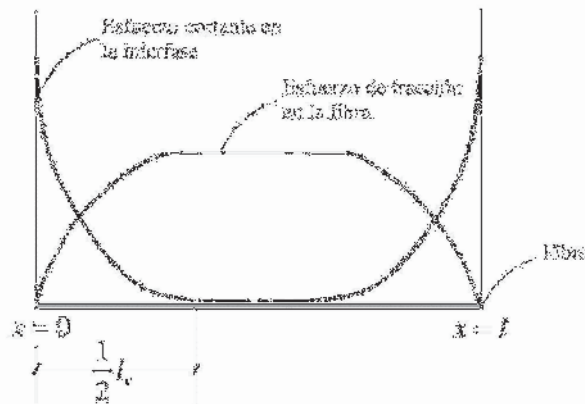


Figura 2. Distribución de esfuerzos axiales en la fibra y cortantes en la interfaces fibra-matriz

En la Figura 2 se muestra la distribución de esfuerzos en una fibra de refuerzo. La tensión tangencial es máxima en los extremos de las fibras y resulta casi nulo en la zona central. En la misma Figura se observa que en los extremos de las fibras la tensión axial cae a cero, resultando un esfuerzo medio en la fibra de longitud l menor que en una fibra continua sometida a las mismas cargas externas. La “eficacia” del refuerzo disminuye en la medida en que lo hace la longitud de la fibra debido a que no toda la fibra puede trabajar a la máxima tensión. Por lo tanto, en los materiales compuestos reforzados con fibras cortas es necesario que la longitud l de la fibra sea superior a la longitud crítica de transferencia l_c con el objetivo de que las mismas sean aprovechadas a su máxima capacidad.

Debido a estos fenómenos locales, los materiales compuestos reforzados con fibras cortas no cumplen exactamente con la condición de compatibilidad expresada en la

(1), debido a las diferentes deformaciones que se presentan entre la matriz y las fibras. Por ello, a los fines de representar el comportamiento constitutivo de estos materiales, es necesario el planteo de otra ecuación de cierre de deformaciones [7], o mantener la clásica teoría de mezclas, manteniendo la hipótesis de igualdad de deformaciones en todos los componentes, y realizar una corrección en las propiedades de cada componente [15].

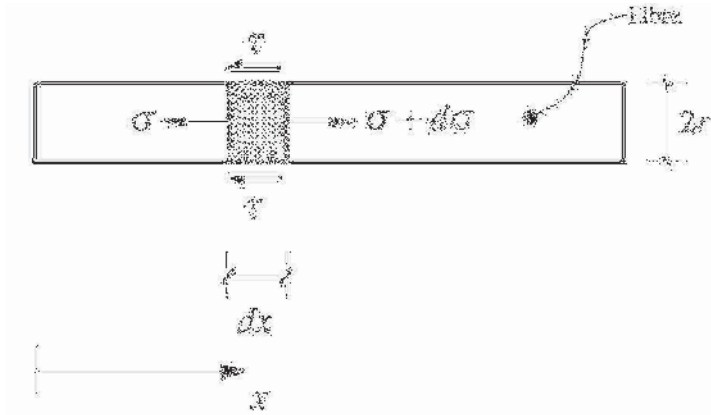


Figura 3. Esfuerzos en los extremos de fibras

Distribución de tensión axial en la fibra

A los fines de determinar una expresión analítica de la distribución de tensiones en una fibra es necesario considerar el equilibrio en la zona de transferencia de tensiones (ver Figura 3). El equilibrio de la fibra en la dirección longitudinal x está dado por la siguiente ecuación

$$\sigma_f \pi r^2 + 2 \tau \pi r dx = (\sigma_f + d\sigma_f) \pi r^2 \quad \Rightarrow \quad \frac{\partial \sigma_f}{\partial x} = \frac{2 \tau}{r} \quad (5)$$

O en términos de fuerzas,

$$\frac{\partial P_f}{\partial x} = 2 \tau \pi r \quad (6)$$

donde σ_f es la tensión en la fibra en la dirección x , $d\sigma_f$ es el incremento de la tensión en la fibra en $x+dx$ y τ es la tensión tangencial en la interface fibra-matriz. La tensión tangencial τ se produce debido a las deformaciones diferenciadas entre fibra y matriz y por lo tanto depende de la diferencia entre los campos de desplazamientos de fibra y matriz. El equilibrio entre matriz y fibra corta puede describirse mediante la siguiente ecuación diferencial sobre el eje longitudinal de la fibra resulta [14].

$$\frac{\partial^2 P_f}{\partial x^2} = H \left[\frac{P_f}{C_f^\sigma A_f} - E_m \right] \quad (7)$$

donde P_f es la fuerza máxima de interacción entre el refuerzo y la matriz, H una constante que depende de la distribución topológica de las fibras, C_f^σ el módulo de Young del refuerzo, A_f la sección transversal media del refuerzo y E_m es la deformación longitudinal en la matriz. La solución de la ecuación diferencial (7) permite obtener la siguiente fuerza en la fibra,

$$P_f = C_1 \sinh(\beta x) + C_2 \cosh(\beta x) + C_f^\sigma A_f E_m \quad (8)$$

siendo C_1 y C_2 las constantes que resultan de las condiciones de contorno $P_f = 0$ en $x = 0$ y $x = l$; β es un coeficiente dado por la siguiente expression

$$\beta = \sqrt{\frac{H}{C_f A_f}} = \sqrt{\frac{G_c}{C_f^\sigma A_f} \frac{2\pi}{\ln\left(\frac{r'}{r}\right)}} \quad (9)$$

En la cual G_c es el módulo elástico transversal del compuesto y r' la distancia media entre las fibras de refuerzo (ver Figura 4).

Una vez obtenidas las constantes de integración, la ecuación de la tensión resulta

$$\sigma_f(x) = C_f^\sigma E_m \left[1 - \frac{\cosh\left(\beta\left(\frac{l}{2} - x\right)\right)}{\cosh\left(\beta\frac{l}{2}\right)} \right] \quad \forall \quad 0 \leq x \leq \frac{l}{2} \quad (10)$$

Esta ecuación establece la distribución de tensiones axiales a lo largo de la fibra. Esta distribución se muestra esquemáticamente en la Figura 2. En la zona central del refuerzo no existe un valor de tensión constante, pero si el refuerzo es lo suficientemente largo se puede admitir la hipótesis de que $\sigma_f \cong C_f^\sigma E_m$. El valor de tensión máximo se produce en $x = l/2$ y está dado por

$$(\sigma_f)_{\max} = \sigma_f(x = \frac{l}{2}) = C_f^\sigma E_m \left[1 - \frac{1}{\cosh\left(\beta\frac{l}{2}\right)} \right] \quad (11)$$

Distribución de tensión tangencial en la interface

La distribución de tensión tangencial en la zona de interface se obtiene haciendo el equilibrio en la fibra entre tensiones axiales y adherencia con la matriz. Para ello, teniendo en cuenta la ecuación (5) y (10), resulta

$$\tau_f(x) = \frac{C_f Er \beta}{2} \frac{\sinh\left(\beta\left(\frac{l}{2} - x\right)\right)}{\cosh\left(\beta\frac{l}{2}\right)} \quad (12)$$

Esta última ecuación establece la función de distribución de tensiones tangenciales en la interface fibra-matriz. Esta distribución se muestra esquemáticamente en la Figura 2. El valor de la tensión cortante es nulo en la zona central de la fibra y coincidente con el máximo de la tensión axial. En esta zona no existen deformaciones diferenciadas entre fibra y matriz lo cual explica el valor nulo de las tensiones tangenciales. La máxima tensión tangencial se verifica en el extremo de la fibra y está dada por:

$$(\tau_f)_{\max} = \tau_f\left(x = \frac{l}{2}\right) = \frac{C_f^\sigma Er \beta}{2} \tanh\left(\frac{\beta l}{2}\right) \quad (13)$$

Una forma de incorporar la contribución del refuerzo en fibras cortas a la teoría de mezclas es a través de la tensión media a lo largo de la fibra, esto es

$$\bar{\sigma}_f = \frac{1}{l} \int_0^l \sigma_f(x) dx = C_f^\sigma \left[1 - \frac{\tanh\left(\beta\frac{l}{2}\right)}{\left(\beta\frac{l}{2}\right)} \right] E_m = \tilde{C}_f^\sigma E_m \quad (14)$$

siendo \tilde{C}_f^σ el módulo de Young medio del refuerzo o módulo homogeneizado. La ecuación (14) muestra que el módulo de Young de un refuerzo de fibras es función de la longitud de las mismas y de otros parámetros geométricos. En el caso de fibras largas el módulo elástico promedio tiende al valor del módulo de Young del refuerzo, en tanto en este caso se ve fuertemente afectado por las cualidades para transferir las tensiones que tiene la interface matriz-refuerzo.

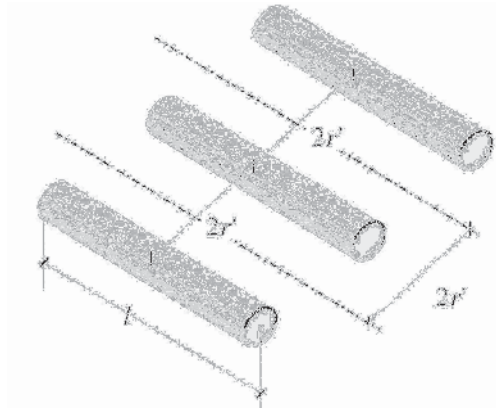


Figura 4. Relación de aspecto que se considera en el refuerzo

La definición de un módulo de Young promedio del refuerzo, de magnitud inferior al real, explica que la participación de este aporta unas características mecánicas al compuesto que no sólo dependen de las propiedades intrínsecas del mismo, sino también de las propiedades del conjunto matriz-refuerzo. En esta situación las propiedades de la interface entre los componentes son determinantes en la forma de participación de los mismos. Esto significa que las propiedades mecánicas de un punto del sólido no sólo dependen de si mismas, sino del conjunto matriz-refuerzo.

Modelo constitutivo para fibras cortas

La matriz de un material compuesto reforzado con fibras de corta longitud suele estar sometido a tensiones superiores a aquellas constituidas con fibras largas. En general, las propiedades mecánicas del material compuesto con fibras cortas son inferiores que los compuestos con refuerzo continuo*.

El concepto de homogeneización que se describe en la sección anterior puede extenderse a "3-D" mediante la simplificación de admitir una distribución isótropa del cambio de propiedades, resultando el siguiente tensor constitutivo aproximado para la fibra corta,

$$\tilde{\mathbf{C}}_f^S = \mathbf{C}_f^S \left[1 - \frac{\tanh\left(\beta \frac{l}{2}\right)}{\left(\beta \frac{l}{2}\right)} \right] \quad (15)$$

donde el tensor constitutivo del refuerzo en la configuraciones referencial \mathbf{C}_f^S es ortótropo. De esta manera la formulación que se presenta permite tener en cuenta la pérdida de efectividad del refuerzo en la respuesta debido a su escasa longitud que impide una total transferencia de los esfuerzos desde la matriz.

Considerando el tensor constitutivo de la fibra corta, definido en la ecuación (15), se obtiene la ley constitutiva de la fibra, afectada de sus condiciones de contorno,

$$\boldsymbol{\sigma} = \underbrace{\left[1 - \frac{\tanh\left(\beta \frac{l}{2}\right)}{\left(\beta \frac{l}{2}\right)} \right]}_{\zeta} \cdot \mathbf{C}_f^S : \boldsymbol{\varepsilon}^e = \tilde{\mathbf{C}}_f^S : \boldsymbol{\varepsilon}^e \quad (16)$$

* NOTA: Se entiende por refuerzo continuo a aquel que presenta una longitud mayor a la necesaria para transmitir los esfuerzos desde la matriz hacia el refuerzo

El factor ς representa la corrección de las propiedades mecánicas del material debido a la presencia de un refuerzo de corta longitud dentro del material compuesto.

3.4 Ecuación del compuesto – Propiedades de conjunto del material compuesto

En el caso de materiales compuestos reforzados con fibras cortas se debe modificar la ecuación de compatibilidad (1) o hacer una corrección en las propiedades de cada componente manteniendo la ecuación de cierre de la teoría de mezclas clásica (Car *et al.* (1998) [16]). Este último método conduce a una formulación más simple que es la que se mostrará a continuación.

La eficacia de la participación del refuerzo de fibras cortas es menor que la del de fibras largas, por lo tanto se deduce que las propiedades mecánicas de los materiales compuestos reforzados con fibras cortas no son mejores que aquellos reforzados con fibras largas. La expresión del tensor constitutivo del material compuesto dado en la ecuación (4) en pequeñas deformaciones se generaliza en la siguiente forma para el caso de refuerzos de cortas longitud.

$$\mathbf{C}_{ijkl}^S = \underbrace{\sum_{c_m=1}^{n_m} k_{c_m} (\mathbf{C}_{ijkl}^S)_{c_m}}_{\text{Componentes de la matriz}} + \underbrace{\sum_{c_r=1}^{n_r} k_{c_r} \varsigma_{c_r} (\mathbf{C}_{ijkl}^S)_{c_r}}_{\text{Componentes del refuerzo}} \quad (17)$$

En las definiciones anteriores n_m es el número de materiales componentes que constituyen la matriz del compuesto y n_r es el número de materiales componentes que constituyen la fase del refuerzo. En el caso de refuerzos continuos el factor ς_{c_r} tiende a la unidad y hace que la expresión para fibras cortas coincida con la de fibras largas.

La ecuación de la tensión en el material compuesto queda definida como

$$\sigma_{ij} = \underbrace{\sum_{c_m=1}^{n_m} k_{c_m} (\mathbf{C}_{ijkl}^S)_{c_m} (\varepsilon_{kl}^e)_{c_m}}_{\text{Componentes de la matriz}} + \underbrace{\sum_{c_r=1}^{n_r} k_{c_r} \varsigma_{c_r} (\mathbf{C}_{ijkl}^S)_{c_r} (\varepsilon_{kl}^e)_{c_r}}_{\text{Componentes del refuerzo}} \quad (18)$$

3.5 Deslizamiento fibra-matriz

Entre las causas del comportamiento no-lineal de los materiales compuestos reforzados con fibras largas y más aun aquellos con fibras cortas, está el fenómeno de formación de grietas en la matriz, acompañada del deslizamiento o movimiento relativo entre fibra y matriz. Este fenómeno se conoce en la literatura en inglés como "*debonding*" y se caracteriza porque el agrietamiento de la matriz y el deslizamiento relativo entre fibra y matriz. Esta pérdida de adherencia se

manifiesta como una pérdida de rigidez del material compuesto e induce a movimientos que pueden representarse en forma de deformaciones inelásticas, o no-recuperables, entre la fibra y la matriz. El fenómeno antes mencionado se designará en este trabajo con las siglas "DFM" (Deslizamiento Fibra-Matriz).

El proceso de apertura de fisuras en la matriz ocurre a niveles de tensiones que resultan significativamente menores que el nivel tensional necesario para producir la rotura de las fibras. La rotura de la matriz ocurre a valores bajos de tensión y está usualmente alineado con la dirección de las tensiones principales, produciendo una disminución en la rigidez e induciendo deformaciones inelásticas y ciclos de histéresis [17,18].

Los materiales compuestos sometidos a estados tensionales en los cuales se ha producido el fenómeno “DFM” no cumplen con la condición cinemática impuesta por la teoría de mezclas de sustancias básicas. Este fenómeno tiene como consecuencia directa la limitación de la matriz, para transferir esfuerzos a la fibra. Esto es, la fibra no es capaz de aumentar su estado tensional por causas atribuibles a la adherencia limitada que existe en la zona de interface fibra-matriz.

La incorporación de éste fenómeno en el modelo constitutivo mencionado en los apartados previos se basa en la idea de que el proceso de transferencia de cargas de matriz a fibra varía en el momento en que la matriz sufre deformaciones plásticas. El movimiento relativo entre fibra y matriz puede representarse en mecánica de medios continuos a través de una deformación inelástica irre recuperable en la fibra. La determinación del inicio de este fenómeno se realiza mediante una condición umbral máxima de resistencia que compara la tensión efectiva en un punto con la resistencia de la fibra.

Dada la forma en que participa la fibra dentro del compuesto y el mecanismo de transmisión de tensiones entre fibra y matriz, la determinación de su máxima resistencia o resistencia real y su capacidad de colaboración depende de su propia resistencia nominal $(f^{\sigma})_{\text{fib}}^N$, o resistencia de la fibra en condiciones aisladas, de la resistencia nominal de la matriz $(f^{\sigma})_{\text{mat}}^N$ y de la resistencia nominal de la interface fibra-matriz $(f^{\tau})_{\text{fib-mat}}^N$, o capacidad de transferencia de tensiones desde la matriz a la fibra.

Desde otro punto de vista, se puede decir que la fibra participa dentro del compuesto en función de su propia resistencia y de la capacidad de transferencia de esfuerzo de la interfaz fibra-matriz, por lo tanto su resistencia está influenciada por el medio que la contiene y podría decirse que su tratamiento constitutivo implica una formulación no-local. Se define entonces la resistencia de una fibra contenida en una matriz como:

$$(f^\sigma)_{\text{fib}} = \min \left[(f^\sigma)_{\text{fib}}^N, (f^\sigma)_{\text{mat}}^N, \left[\frac{(f^\tau)_{\text{fib-mat}}^N \cdot 2\pi r_f}{A_f} \right] \right] \quad (19)$$

en la que r_f representa el radio de la fibra y A_f es el área de la sección transversal del la fibra. A partir de la ecuación (19) se deducen los siguientes casos límites:

- Si la matriz es más resistente que la fibra y la adherencia fibra-matriz es perfecta, la capacidad de participación de la fibra queda limitada por su propia resistencia nominal $(f^\sigma)_{\text{fib}} \equiv (f^\sigma)_{\text{fib}}^N$.
- Si se produce un fallo en la matriz por microfisuras, etc., en tanto la fibra se mantiene en régimen lineal, la resistencia de la fibra queda limitada por la resistencia de la matriz, pues se rompe el “mecanismo” de transferencia de tensión entre fibra y matriz y no se podría transferir más tensión que la permitida por el medio que contiene la fibra $(f^\sigma)_{\text{fib}} \equiv (f^\sigma)_{\text{mat}}^N$.
- Si el fallo se produce en la interface fibra-matriz, la resistencia de la fibra queda limitada por la de la interface
$$(f^\sigma)_{\text{fib}} \equiv \frac{2 \cdot (f^\tau)_{\text{fib-mat}}^N \cdot 2\pi r_f}{A_f} = \frac{2 \cdot (f^\tau)_{\text{fib-mat}}^N}{r_f}.$$

En la mayoría de los materiales compuestos se verifica que el agrietamiento por tensiones tangenciales en la interfaz se produce antes que la rotura de las fibras y se observa una separación masiva entre fibra y matriz y por lo tanto la resistencia de la fibra queda limitada por la capacidad de la interfaz de transmitir esfuerzos.

La aparición de fenómenos plásticos en la matriz de un material compuesto sometido a un estado de cargas monótono creciente impide la transferencia de los esfuerzos desde la matriz hacia las fibras dando lugar a la aparición de deformaciones irreversibles por deslizamiento de la fase de refuerzo respecto de la matriz. A partir de este momento la transferencia de cargas de fibras a matriz no es nula debido a la presencia de fenómenos de fricción entre ambas fases del material compuesto. Por lo tanto, las fibras aumentan su estado tensional según un módulo elástico diferente del inicial.

4. EJEMPLO DE APLICACIÓN

A continuación se realiza una comparación de los resultados obtenidos en laboratorio [19] de una viga constituida de hormigón reforzado con fibras cortas de acero –DRAMIX–, con los que resultan de aplicar el modelo mencionado en este artículo a una discretización por elementos finitos de dicha viga.

4.1 Detalles del ensayo y la viga

El material compuesto utilizado en el ensayo de laboratorio es un hormigón de alta resistencia con humo de sílice reforzado con fibras cortas de acero en diferentes fracciones de volumen (0.0%, 0.5% y 1.0%).

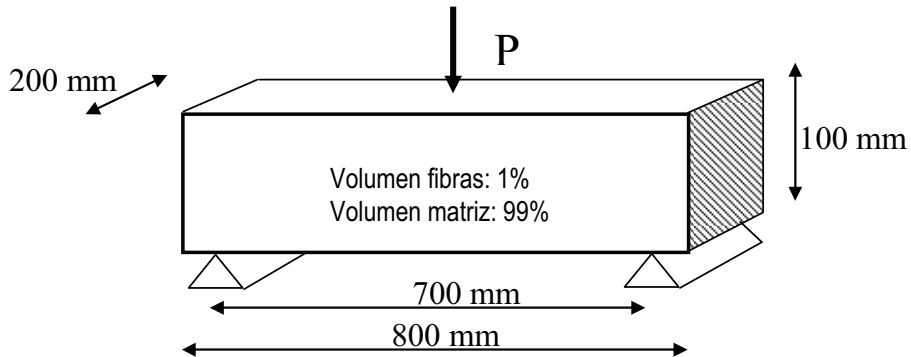


Figura 5. Características geométricas de la viga del ensayo

Tabla 2. Características mecánicas de los materiales componentes

Propiedad	Matriz	Fibras (real)	Fibras (modificado)
Módulo de Young	50000 MPa	210000 MPa	190000 Mpa
Coefficiente de Poisson	0,17	0,25	0,25
Resistencia umbral a tracción	8,27 Mpa	1150 Mpa	277 Mpa
Resistencia umbral a compresión	82,7 Mpa	1150 Mpa	277 Mpa
Módulo de endurecimiento	Ablandamiento	0	0
Material simulado	Mohr-Coulomb, $\phi=30^\circ$	von-Mises	von.Mises
Energía de fractura	25 KN/m	3×10^6 KN/m	7.2×10^5
Energía de aplastamiento	2500 KN/m	3×10^6 KN/m	7.2×10^5

Los materiales componentes del hormigón fueron cemento I 55-A (ASTM tipo III, CEN clase I 52.5), arena silícea (0-5 mm), arcilla (5-12 mm) y humo de sílice (ELKEM grado 920D). También se añadió súper plastificante GRACE Darcem 195 en la proporción de 25.4 litros/m³ de hormigón (súper plastificante seco/cemento = 1.5% en peso).

Los valores medio de la resistencia a compresión $f_c = 86.4 \text{ MPa} (\pm 2.76\%)$, $f_c = 88.3 \text{ MPa} (\pm 2.82\%)$ y $f_c = 92.47 \text{ MPa} (\pm 5.39\%)$ para el 0.0%, 0.5% y 1.0% en volumen de fibra, respectivamente. Las fibras cortas fueron de acero tipo DRAMIX ZC30, con un límite elástico de 1150 MPa, 30 mm de longitud y 0.5 mm de diámetro. Las vigas se construyeron en moldes de madera laminada, con el plano de carga vertical, echando el hormigón en dos capas compactadas por vibración. Los ensayos se realizaron aplicando una carga de 1MN en un Instron 8505, bajo control de desplazamiento en el punto de aplicación de la carga Figura 5.

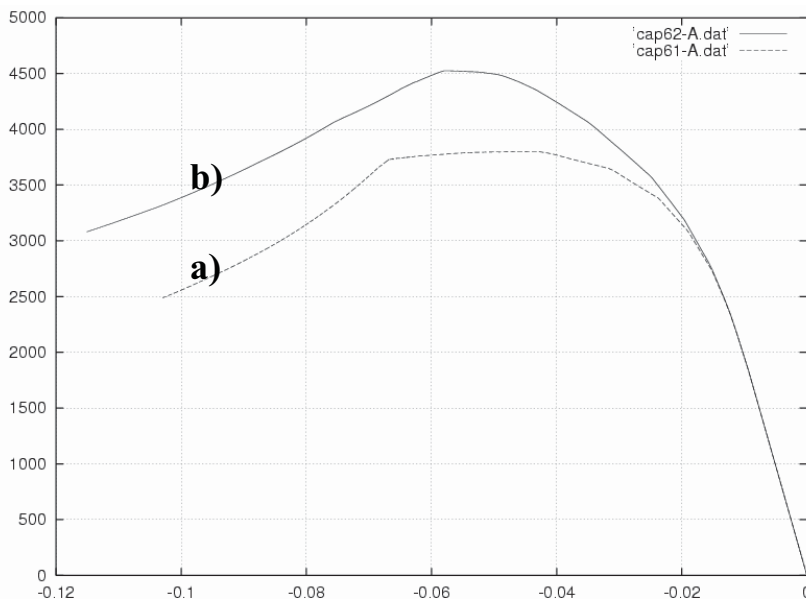


Figura 6. Respuesta numérica Carga [x10=N]– Desplazamiento [x10 =mm]: a) Hormigón (100%). b) Hormigón (99%)+ Fibra corta (0,5%-00)+ Fibra corta (0,5%-900)

El problema por elementos finitos ha sido resuelto con 80 elementos de tensión plana con 4 nodos y dos grados de libertad por nodo, bajo la hipótesis de tensión cuasi-estática. A este modelo numérico se le ha incorporado el modelo constitutivo mencionado en apartados previos, considerando los siguientes tres casos:

- a- Hormigón 100%,
- b- Hormigón 99% + Fibras cortas metálicas 0.5% orientadas a 0° +
Fibras cortas metálicas 0.5% orientadas a 90° ,
- c- Hormigón 99% + Fibras cortas metálicas 0.3% orientadas a 0° +
Fibras cortas metálicas 0.7% orientadas a 90° ,

En las figuras que a continuación se muestran, puede verse la influencia de la ductilidad que añaden estas fibras cortas al hormigón simple. También puede verse la comparación de estos resultados numéricos con los experimentales.

En la Figura 6 puede verse la comparación entre la respuesta numérica de un hormigón simple y un hormigón con un 1% de fibras cortas, de las cuales la mitad de ellas está orientada según el eje longitudinal de las fibras (0°) y la otra mitad transversal a dicho eje (90°).

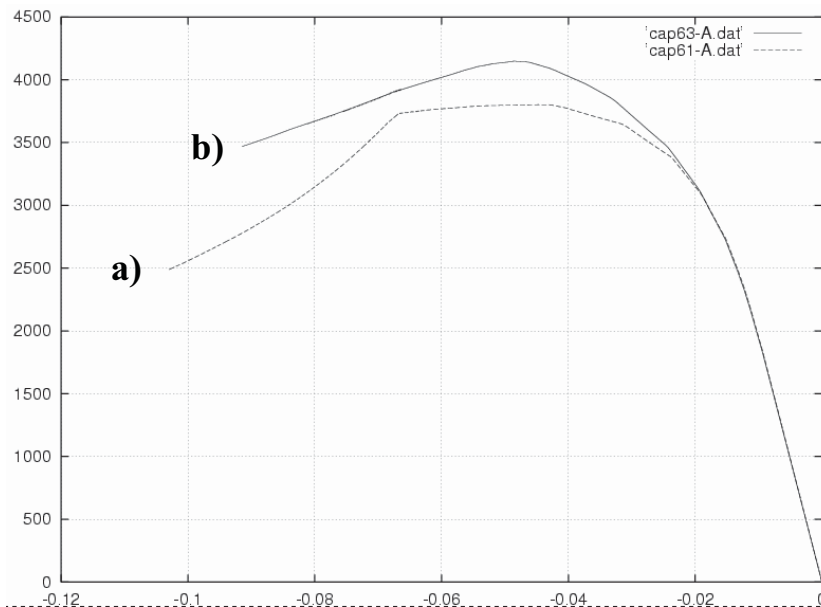


Figura 7. Respuesta numérica Carga [x10=N]– Desplazamiento [x10=mm]: a) Hormigón (100%). b) Hormigón (99%)+ Fibra corta (0,3%-00)+ Fibra corta (0,7%-900)

Como puede verse en la Figura 7, la sola disminución de la proporción de fibras en la dirección longitudinal a 0° (de 0,5% a 0,3%), se produce una disminución de la carga máxima o carga de pico de 4500 N a 4200 N. Esta situación el material sea muy sensible a la orientación de dichas fibras.

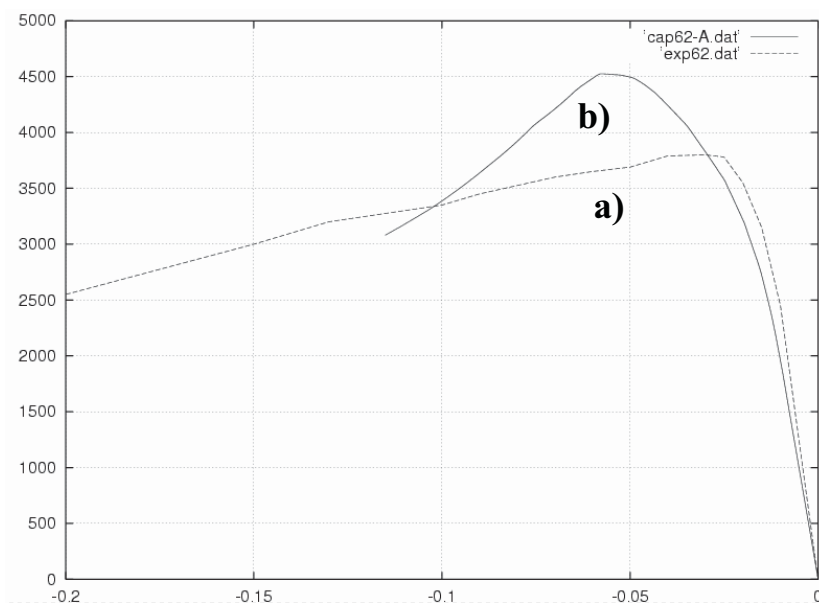


Figura 8. Respuesta numérica Carga [x10=N]– Desplazamiento [x10 =mm]: a) Experimental. b) Hormigón (99%)+ Fibra corta (0,5%-00)+ Fibra corta (0,5%-900)

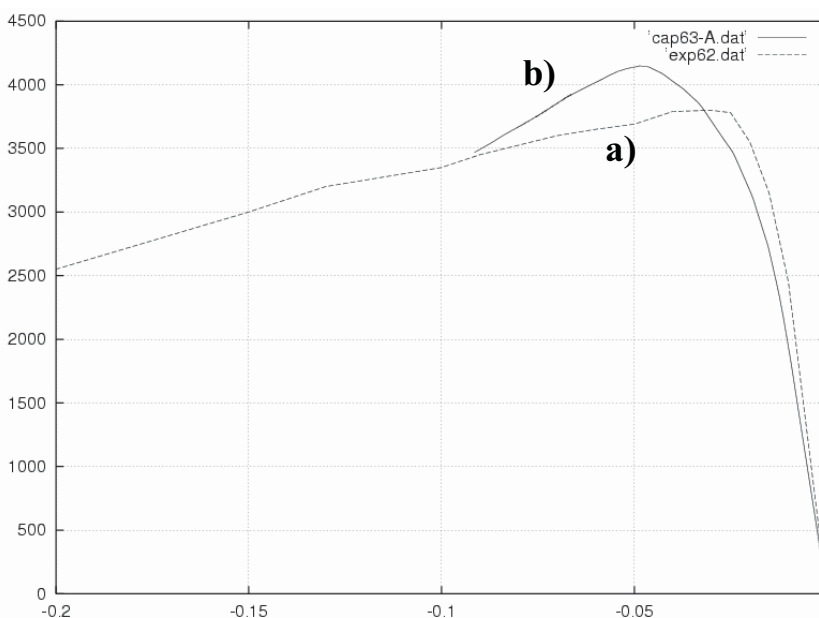


Figura 9 – Respuesta numérica Carga [x10=N]– Desplazamiento [x10 =mm]: a) Experimental. b) Hormigón (99%)+ Fibra corta (0,3%-00)+ Fibra corta (0,7%-900)

La Figura 8, muestra la comparación entre la respuesta numérica y experimental. En ella puede verse una diferencia en el nivel de la carga de pico que puede soportar la viga y se considera que esto se debe al problema de deslizamiento fibra matriz, del que no hay datos suficientes para ajustar el modelo.

La Figura 9, muestra también la comparación entre la respuesta numérica y experimental. En ella nuevamente puede verse una diferencia en el nivel de la carga de pico que puede soportar la viga y se considera que esto se debe al problema de deslizamiento fibra matriz, del que no hay datos suficientes para ajustar el modelo. A diferencia de la Figura 8, aquí puede verse que la diferencia entre la carga de pico entre la respuesta experimental y numérica es menor.

5. CONCLUSIONES

De todo esto surge como conclusión que la incorporación de fibras cortas en el hormigón mejora notablemente su ductilidad y por lo tanto se convierte en un material con mejores cualidades para su utilización estructural. Además, el cálculo y diseño de estructuras con este material es posible tratarlo en forma simplificada si se admite el cambio de las propiedades reales del material por otras que serían las denominadas propiedades efectivas. Esto permitiría utilizar estas nuevas propiedades dentro del esquema de cálculo simplificado tradicional que se realiza en el hormigón. No obstante esta simplificación, cabe decir que si se quiere estudiar el material en rotura es necesario incursionar la solución del mismo a través de las también denominadas propiedades equivalentes, pero prestando especial atención a los efectos no lineales del deslizamiento fibra matriz mediante la utilización del modelo constitutivo previamente presentado, dentro de la técnica de los elementos finitos.

Agradecimientos

Los autores agradecen a la DGICYT por la financiación concedida a través del contrato MAT2000-0741-C02-02 y al Ministerio de Fomento por el proyecto de investigación concedido en el área de la construcción civil.

Referencias

1. Miravete A. (2000). *Materiales Compuestos. Vol. 1 y Vol. 2*. Director de la obra: Antonio Miravete
2. Car E. (2000). *Modelo constitutivo continuo para el estudio del comportamiento mecánico de los materiales compuestos*. Tesis Doctoral, Universidad Politécnica de Cataluña
3. Paez A. (1979). *Hormigones fibrosos*. Universidad de Santander, Escuela de Ingenieros de Caminos Canales y Puertos
4. Car E. (2000). *Modelo constitutivo continuo para el estudio del comportamiento mecánico de los materiales compuestos*. PhD thesis, Universidad Politécnica de Cataluña. Barcelona, España

5. Zalamea F. (2000). *Tratamiento numérico de materiales compuestos mediante la teoría de homogeneización*. PhD thesis, Universidad Politécnica de Cataluña. Barcelona, España
6. Trusdell, C. y Toupin, R. (1960). *The classical Field Theories*. Handbuch der Physik III/I. Springer Verlag, Berlin
7. Oller S., Botello S., Miquel J. y Oñate E. (1995). "An anisotropic elastoplastic model based on an isotropic formulation". *Engineering Computation*, 12 (3), pp. 245-262
8. Car E., Oller S., Oñate E. (2001). "A large strain plasticity model for anisotropic materials — Composite material application". *International Journal of Plasticity*, 17, pp. 1437-1463
9. Green A. and Naghdi P. (1965). "A dynamical theory of interacting continua". *Journal of Engineering Science*, 3 3-231
10. Ortiz M. and Popov E. (1982). "A physical model for the inelasticity of concrete". *Proc. Roy. Soc. London*, A383, 101-125
11. Ortiz M. and Popov E. (1982). "Plain concrete as a composite material". *Mechanics of Materials*, 1, 139-150
12. Oller S., Oñate E., Miquel J., and Botello S. (1996). "A plastic damage constitutive model for composite materials". *Int. J. Solids and Structures*, 33 (17), 2501-2518
13. Oller S., Oñate E. (1996). "A Hygro-Thermo-Mechanical constitutive model for multiphase composite materials". *Int. J. Solids and Structures*. Vol.33, (20-22), 3179-3186
14. Jayatilaka, A. (1979). *Fracture of engineering brittle materials*. Applied Science Publishers
15. Car, E., Oller, S., & Oñate, E. (1997). "Un modelo constitutivo elasto-plástico acoplado con daño mecánico e higrométrico. Aplicación a pavimentos flexibles". U. de Brasilia (Ed.), *XVIII CILAMCE Congresso Ibero Latino-Americano de Métodos Computacionais Em Engenharia* (pp. 2100 - 2108). Brasilia
16. Car, E., Oller, S., & Oñate, E. (1998). "Un modelo constitutivo elasto plástico acoplado con daño mecánico e higrométrico. Aplicación a pavimentos flexibles". *Rev. Int. de Ingeniería de Estructuras*, 3(1), 19 – 37
17. Beyerley D. and Spearing S. M. and Zok F. W. and Evans A. G. (1992). "Damage, degradation and failure in a unidirectional ceramic-matrix composite". *J. Am. Ceram. Soc.*, 75, pp. 2719-2725
18. Pryce A. W. and Smith P. A. (1992). "Modelling of the stress/strain behavior of unidirectional ceramic matrix composite laminates". *J. Mater. Sci.*, 27, pp. 2695-2704
19. Saldivar H., Gettu R. and Aguado A. (1997). *Test on high strength fiber reinforced concrete beams*. Dpto. De Ingeniería de la Construcción, ETSECCPB-UPC

**THE USE OF NONDESTRUCTIVE TESTING METHODS FOR BRIDGES
FOUNDATIONS CONDITION DETERMINATION AND IMPLEMENTATION OF
OBTAINED DATA IN BRIDGE MANAGEMENT SYSTEM**

Cristina ROMANESCU, dipl. eng *

ABSTRACT

Scouring is one of the main reasons for bridges collapse. It is an important phenomenon that takes place around the bridge piers and lead to foundation material erosion and movements and/or rotations of the infrastructure. This degradation usually appears when the flow volumes are high, in spring or autumn or when the precipitations levels are high. Thus understanding the phenomena and having methods to measure it may allow bridge administrators to take action at a proper time.

This paper presents the processes that lead to scouring of bridge foundations and various methods for determination of levels of river beds around the piers.

BMS and nondestructive investigations

A key factor in development of bridges lifetime increasing strategies in the limits of strong budgetary restrictions is an efficient bridge management system (BMS).

BMS gives guidelines to road administrators both in repair and rehabilitation activities having minimal costs and traffic safety activities using an optimal funds allocation for maintenance and rehabilitation.

An essential component of the bridge management system is monitoring of time evolution of condition of bridges within the patrimony. All elements that directly affect road bridges performances, including foundation, infrastructure, superstructure and carriageway must be surveyed. At this moment, the surveying of bridges condition is based almost entirely on the visual inspection. That's the reason for subjectivity of bridge management system input data.

Nondestructive evaluation represents a instrument that is not often used on bridges but can eliminate a big amount of errors of input data. The reduced use of nondestructive testing of bridges has a obvious motivation.

* Head of Bridge Division, Centre for Technical Road Studies and IT, National Company for Highways and National Roads, Romania

One of the most important is the lack of understanding of how the nondestructive testings (NDT) are crossing by the needs of bridge administrator and the interference between NDT and BMS the need of bridge engineers training in correct interpretation of NDT results. The high costs of equipments is another strong reason.

Applying NDT methods, as the Schmidt hammer or ultrasonic impulse methods are time consuming for wide surfaces of the structure and are costly. Those methods are used in generally in crisis situations such as fissures or even cracks appeared in bridge elements subjected to critical conditions.

The development of BMS all around the world led to a increase of importance given to systematic applying of NDT for bridge condition establishment.

An raising attention is given to necessary equipments that must be practical, viable and easy to use for NDT in severe conditions of in field working. Usually it includes limited accessibility, extreme temperatures, dust and dirt.

Scouring is the main cause of destruction of over water bridges. The flow of water in the immediate vicinity of infrastructures leads to two effects: foundation material erosion and movements and/or rotations of piers and abutments.

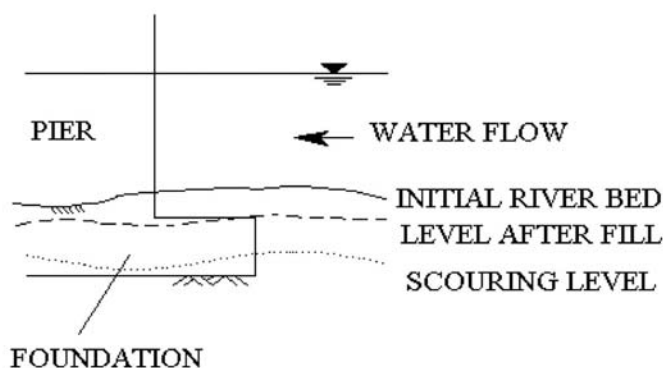


Fig. 1 Scour mechanism

These effects have as a final result the destruction of the construction due to supplemental solicitation of the bridge structure. In order to understand the scouring process is essential the determination of seasonal variations of water depth and erosion and deposal modalities evaluation next to existing or projected bridges piers.

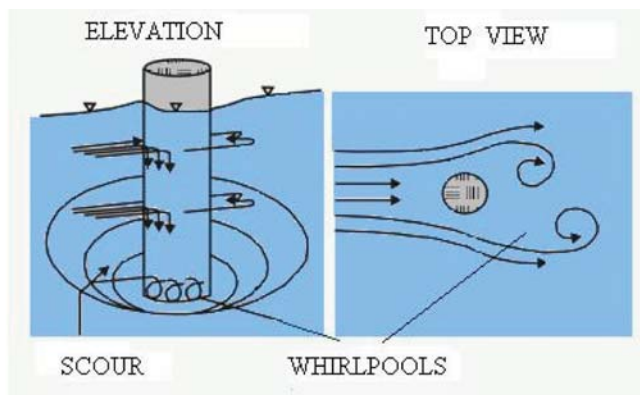


Fig. 2 Scouring mechanism

When the local scouring process is known the remedial actions are efficient and have optimal costs. Unfortunately the scouring phenomenon usually takes place when the flow volumes are high, thus making information about the depth of scouring difficult and dangerous to obtain. More, the scouring characteristics are often continuously modified during top flow volumes, making direct measurement of the maximal scouring after these events to be almost impossible.

The erosion of the river bed material in the bridge area is a result of natural flow processes, especially of seasonal variations of speed and depth of water. The depth of maximal scouring is usually estimated taking into account that the scouring depth is proportional to the increase of water level. The scouring is also influenced by the bridge elements as piers, abutments, embankments or even superstructure.

As is well-known, scouring can be divided into three categories: general scour, contraction scouring and local scouring.

General scour

This is a long time process that takes place on the ins and outs of the river. This process has as result scouring, respectively material deposal on the sides of the river and implicit variations of water depth. General scour leads to abutments degradations if effective protection actions are not taken (as protective works for riverbed and banks and construction of abutment foundations under the deepest scouring depth).

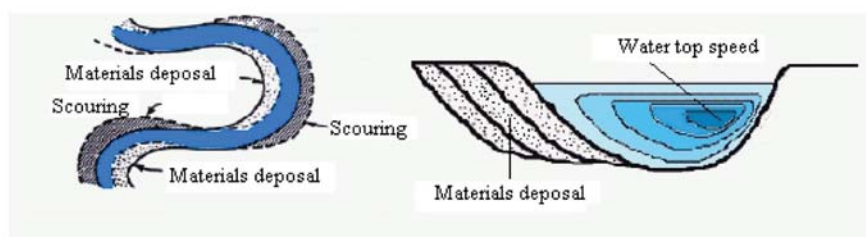


Fig. 3 General scour

Contraction scour

The narrowing of the channel in the bridge area leads to growth of water speed and increased erosion. A solution would be the widening of the channel or to insure under the bridge a channel of same width as the adjacent channel.

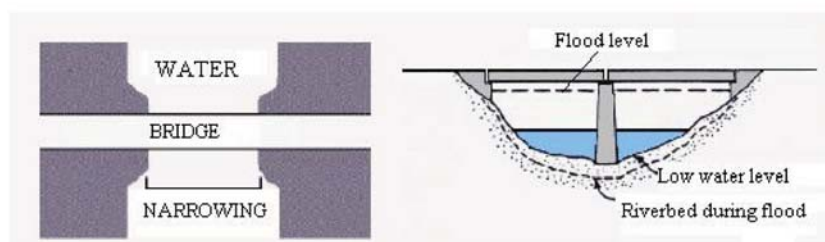


Fig. 4 Contraction scour

Local scour

In this process, obstruction of the river by the bridge piers leads to narrowing of the channel in transversal section, which conducts to growth of flow speed and increase of erosion during floods.

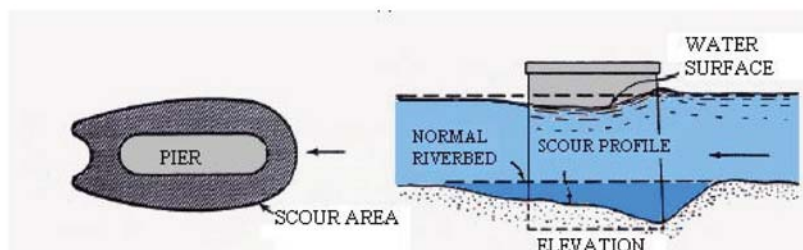


Fig. 5 Local scour

The whirls that appears around the piers produces material removing from the base of foundation, thus weakening the structure. The importance of scouring depends on the configuration and obliquity of the pier, on the channel narrowing and deposal volumes around the bridge.

Local scour implies material disposal around immersed structures as piers, abutments, wings and embankments. Therefore, this scour type has the greatest impact on the bridge integrity.

In order to estimate the condition of existing foundations of piers and abutments is necessary the use of nondestructive evaluation.

At this moment, measuring the depth of water and and/or scour characteristics for bridges is done using several nondestructive testing methods. Those are: Time Domain Reflectometry (TDR), Parallel Seismic method (PS), Ground Penetrating Radar method (GPR) Continuous Seismic Reflection Profiling method (CSP), Echo Sounders or Fathometer method (ES). Each of the equipments has advantages and disadvantages.

Time Domain Reflectometry Method (TDR)

In this method, electromagnetic waves are traveling through a cable to the ground and the reflected energy is recorded by TDR equipment. Any impedance modification, as the one given by the cable ends or degradations and its imperfections will produce a quantity of energy that will be reflected to TDR equipment where will be on screen. Foundation movements lead to local deformations of the cable thus generating variations of the electric stream. Knowing the wave speed it is possible then to calculate the distance. I.e., movement of rotation of the foundation will produce local shearing of the cable in the foundation-soil contact area.

The cable can be configured in two ways: two cables between two central conductors or a coaxial cable.

For this method is essential the configuration and placement of the cable. Monitoring begins when errors due to cables are known, the other reflections that reach the TDR device indicating the depth of scour or movements of the piers during floods.

Measurements done for bridge founded on swamp soil showed that maximal scour during floods appear on the upstream area of foundations. The advance of scour and soil erosion

exposes foundations leading to important movements of the pier. Therefore optimal placement of the TDR cables should be done in the upstream section of foundations. It is very important that the system should operate during the periods with high flow volumes, when there is the biggest possibility to have movements of foundations and piers determined by scour.

Although the bridge abutments may be less affected by scour, in some circumstances it is necessary to monitor them for detection of eventual displacements. The abutments may be inspected using the same system to detect small movements (around 2 mm), that may constitute a warning for progressive displacements that may affect the bridge stability.

The most used of possible installation of cables is the one where the cable has the upper end on or under the deck, then continues on the pier through a protective pipe, then through a hole in foundation down to the sole of the foundation. The inferior end will be buried on the soil to measure relative displacements between foundation and soil.

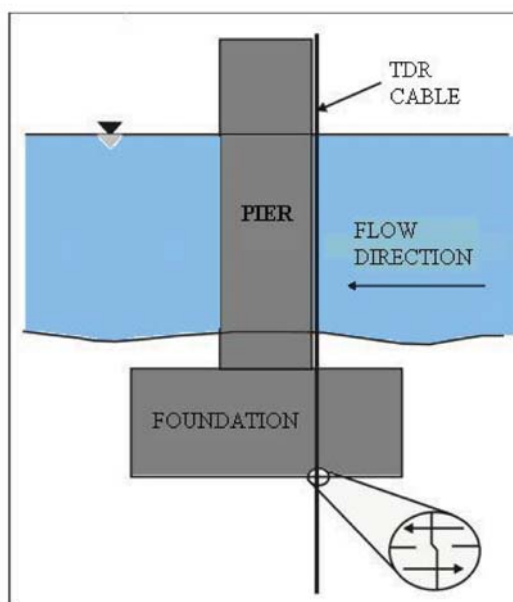


Fig. 6 TDR method

Measurements can be done in emplacement but also remote using telecommunication lines (phone, optical cables, etc.).

The number and disposal of installed TDR cables depends on various factors, such as: scour type, the hazard of structure collapse, installment and monitoring costs, etc. It is

recommendable that for new bridges the TDR monitoring system to be implemented from the execution stage.

The TDR system presents the advantage that it is robust and can face severe condition during floods and earthquakes. As disadvantages one may mention the difficulty of installment and signal accuracy loss proportional to the increase of cable length.

This method may be used both for bridge scour detection and displacement monitoring of abutments and piers during floods.

The TDR method is relatively new but it has a great potential in scour determination.

Parallel Seismic method (PS)

The Parallel Seismic method (PS) is used for determination of foundation depth and may be used for measuring the scour area after floods.

This method may be applied for concrete, wood, masonry or metal foundations.

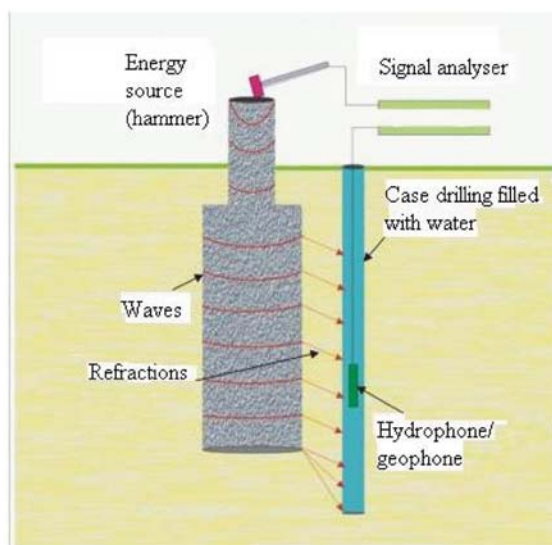


Fig. 7 PS method

The foundation, if it is accessible or an area of the structure that makes common body with it will be hit by a hammer. In a drilling having a diameter of 5 to 10 cm at a distance of maximum 150 cm of foundation is inserted an hydrophone or a geophone. The depth of drilling must overpass the supposed depth of the foundation. In the case of using the hydrophone in the drilling must be inserted a protective pipe with a lid to the end and is filled with water. In the case of a geophone the drilling will be filled with gravel to avoid the break-down of the walls during the test. The hydrophone, respectively geophone receivers will measure both the time needed by the shock wave created by the hammer to travel through the structure and the amplitude of the wave.

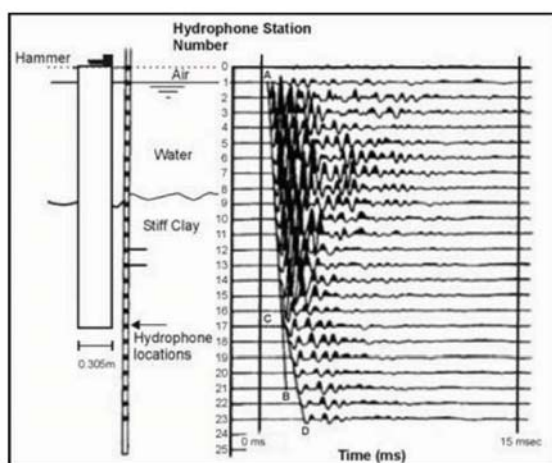


Fig. 8 Result of the PS method

This method has the advantage that it can be used where the upper part of foundation is not accessible or where the piers are very high and thin. As disadvantage one may mention the necessity of a drilling near by pier to make measurements.

GPR method

The GPR method uses a electromagnetic wave produced by a transducer antenna that is send through the soil. Every time the wave “hits” an object that has psychical dimensions big enough and is characterized by electromagnetic properties different of the soil, a partial reflection appears and is recorded by the same transducer antenna shifted along the profile. Inthis way a *radar-gram* is obtained, generated based on delay time and amplitude of reflected recorded waves.

For scour study, the antenna must be placed on or immediately under water. The transducer produces electromagnetic pulsatory waves (frequency between 25 and 1500 MHz) to a fixed time and distance.

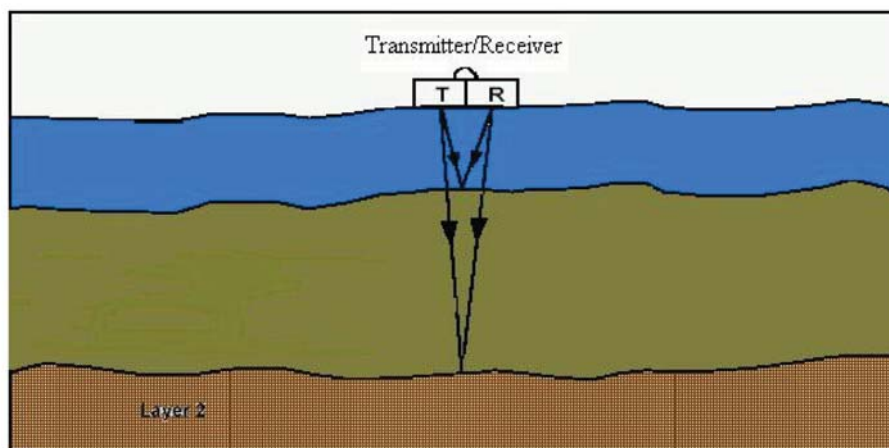


Fig. 9 GPR method

The frequency of the wave, the nature of soil layers, (conductivity and dielectric constant), dimension and depth of geologic structures determines the amplitude and shape of the reflected wave and the way it can be observed on the *radar-gram*. Generally, the best results can be obtained for dried soils and hidden structures as cavities and foundations. The GPR method is the only geophysical method that permits obtaining satisfactory results when the interior of constructions is investigated or when investigated space is covered by other construction types.

For scour evaluation this method may give a clear and continuous view of riverbed and inferior layers, including scour characteristics.

The estimated speed of electromagnetic wave can be used to transform the time – depth diagram to a profile of riverbed. Those speeds depend on the quantity of particles in suspension on the investigation area.

Data given by GPR may be used without any previous processing. Nevertheless, some steps are required to improve the information quality:

1. Distance normalization
2. Horizontal scaling

3. Frequency filtration on vertical
4. Horizontal filtration
5. Speed corrections
6. Subsequent obtained data processing
7. Amplifying

These steps are increasing the interpretation possibilities of profiles given by GPR by removal of eventual measurement errors (ex: mistaken reflections, noise, etc.) and improval of amplitude on major interest areas.

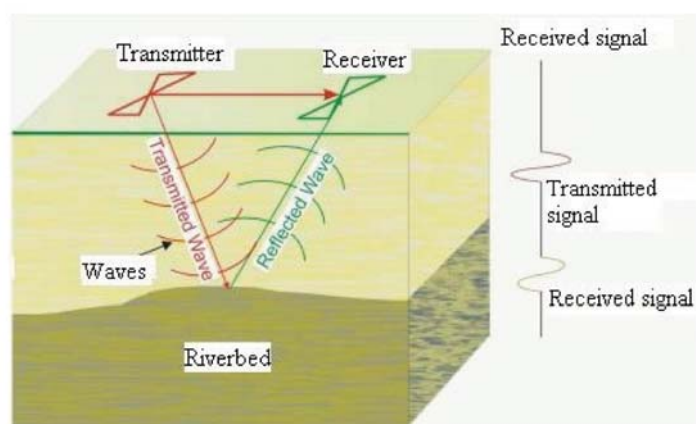


Fig. 10 GPR principle

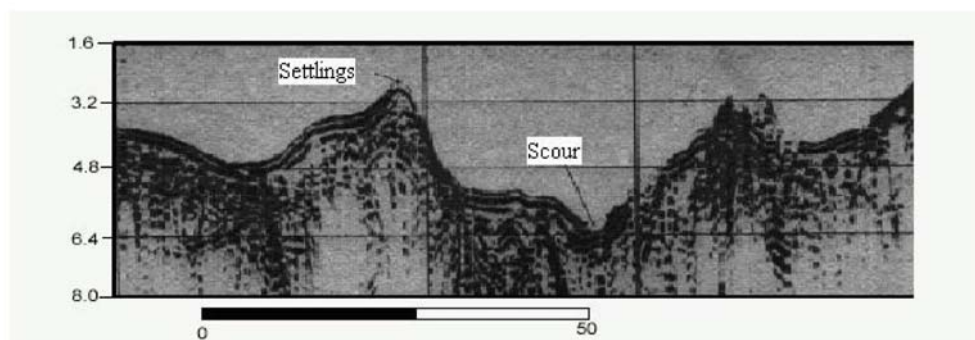


Fig. 11 Radargram obtained using the GPR method

The GPR method has the following advantages:

- The used antenna can be easily and fast moved according to necessities;

- The device can be used remotely of antenna, thus not endangering it or the personnel;
- The device may give a profile of the precise riverbed and other geological layers image (depths until 9 m).

Disadvantages of the GPR system:

- Data may be affected by unwanted noise such as multiple reflections or piers echos
- It is sometimes necessary to ulterior analyze data for soils having big slopes
- GPR is a efficient device for depths smaller than 9 m;
- GPR cannot be used in salty waters.

CSP method

This method consists in transmission of acoustic waves through a transducer located on water surface. These waves passes through the water column and a part of its are reflected on the riverbed, another part is further transmitted to the inferior later.

At the interface between two geological layers or at the level water – riverbed acoustic

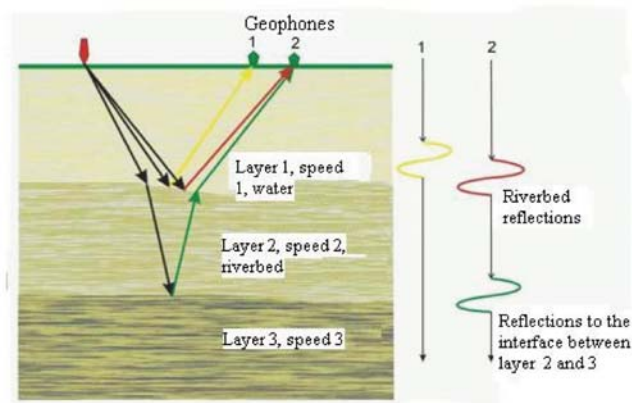


Fig. 12 The CSP method

impedance modifications appear. The quantity of reflected energy coming from a interface is determined by its own reflection coefficient that depends on the acoustic impedance of the materials of the two adjacent layers. Acoustic impedance is the multiply of material density and

the speed of sound through this material. The reflected waves are captured by several geophones that record these waves, then processed and assembled as a amplitude – time diagram.

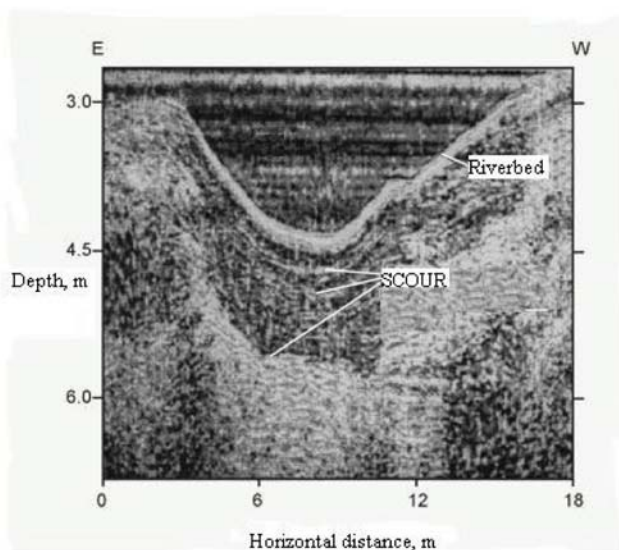


Fig. 13 Diagram depth – horizontal distance

The transducer that transmits the acoustic waves can be situated under the water level. In this case the energy source, situated in a boat that has a constant speed, pulses automatically at a fixed time intervals. One or more hydrophones records received data. The waves traverses the water column and the layer beneath the riverbed and are reflected with a impedance delay, first reflected waves being the ones send back by the riverbed.

The frequency of the acoustic signal determines the maximal penetration depth and the resolution. It can be fixed or variable.

In the data acquiring process some interference may appear due to echoes or multiple reflections at the interface between water and the riverbed, being relatively big if the riverbed is made out of river stone.

This method should be used for big depths rivers to reduce reflections caused by riverbed.

For bridge scour evaluation this method can give scouring characteristics through a continuous picture of the riverbed and layers beneath the riverbed.

As a disadvantage one can mention the difficulty of data interpretation due to multiple interferences and reverberations given by the interface between water – riverbed.

ES method

Generally this method is used to determine the depth of the water, but can be used to detect scours.

The method consists in a repeated transmission of acoustic waves through the water and recording the time needed to cover the distance between the riverbed and the water surface. The device processes these data and shows a diagram of the profile of riverbed. The bandwidth of the used signal is small, around 200 kHz. On that reason this device gives precise information about the water depth and very small amount of information about the geological layers of the riverbed. Using a low frequency (i.e. 20 kHz) permits detection of reflections given by the scour.

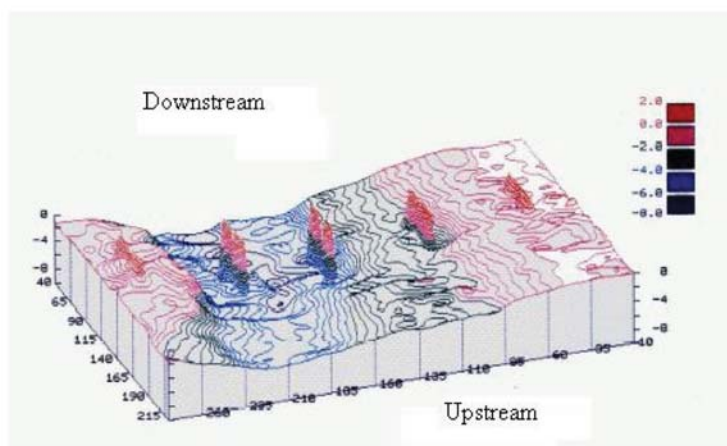


Fig. 14 The result for fathometer method: 3D view a of riverbed

Monitoring using the fathometer is done using a boat that has a low speed. Usually, the antenna is mounted on a side of the boat and is inserted in water. Data acquiring is done automatically by a recording device and can be visualized on the monitor.

During the data recording there is the possibility to mark the position of monitored elements.

The fathometers has the disadvantage of reduced penetration depth of the signal at the time of frequency increase and implicitly of received data accuracy regarding geological layers.

Conclusions

During the floods the riverbed material around the bridge piers is continuously removed. This process can compromise the structural integrity of bridges and in extreme cases may lead even to collapse. Therefore it is essential to be known the scour processes and its stage.

Investigations regarding scour has a obvious preventive character, thus constituting a efficient both economic and social way to administrate the bridge patrimony. The costs of appeared scour mitigation actions are a lot smaller than the ones generated by the eventually replacement of the bridge and user costs and that's why it is recommendable to have permanent investigation activities, mostly on important rivers.

Nondestructive investigations are a integrant part of the BMS, as shown at the beginning of this paper. Obtained date greatly contributes to bridge condition evaluation, having a important role in their behavior prediction establishment.

Taking into account actual preoccupations to constitute a more complete and accurate database for bridges nondestructive investigations regarding scouring become a implicit activity that must be constantly done in Romania.

General buckling of compressed chord of metal truss bottom-way bridges without horizontal bracing

Constantin Jantea

“Gh. Asachi” Technical University Iași, 700050, România

Abstract

The paper presents the calculus of rigidity at lateral displacement of the transverse semi-frames of the metal bridge superstructures with braced girders by considering the influence of all the truss members that form nodes at the level of the compressed girder flange and which constitute elastic supports that resist the lateral buckling of the flange.

KEYWORDS: chord buckling, transverse semi-frames, semi-frames rigidity.

1. INTRODUCTION

In the case of superstructures of metal- truss bottom-way bridges, without upper bracing, the bars of the upper flange of the main girders are joined in nodes that are not allowed to move in the girder plane and can only do it only when normal to the girder plane. Consequently, if the buckling of the compressed flange is analyzed when normal on the girder plane, this can be considered a continuous, compressed beam, elastically supported at the side of the nodes made by the trusses of the girders (stanchions and diagonals), and the buckling strength depends on the stiffness of these supports.

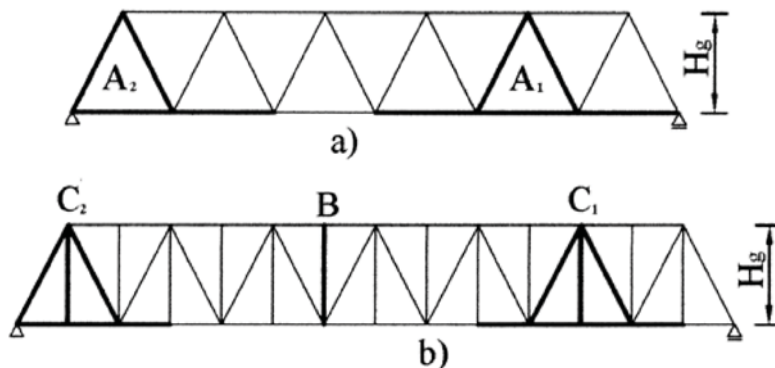


Fig. 1 Truss girders used in bridges

$$H = \frac{E}{\frac{h_o^2 b_a}{2I_a} + \frac{h_o^3}{3EI_m}} \quad (1)$$

E – elasticity modulus of steel;

h_o – height measured from the compressed flange centroid to the cross girder section centroid;

b_a – distance between the braced girders axes;

I_a, I_m – inertia moment of the cross girder and stanchions, respectively.

When the transverse semi-frame is provided with reinforcements in the 2nd term of the denominator in relation (1), h_o is replaced by h_v , the height measured from the centroid of the compressed flange to that of the reinforcement.

EUROCODE 3 provides, in addition to SR 1911 – 98 the calculus of type A semi-frames rigidity, according to the relation:

$$H = \frac{A + B - 2D}{AB - D^2} EI \quad (2)$$

with:

$$A = \frac{H_g^2 I}{n_s} + \frac{l_{ds}^3 \cdot I}{3I_{ds}} + \frac{a_s^2 \cdot l_t}{3}$$

$$B = \frac{H_g^2 I}{n_d} + \frac{l_{dd}^3 \cdot I}{3I_{dd}} + \frac{a_d^2 \cdot l_t}{3}$$

$$D = \frac{l}{6} a_s a_d l_t$$

$$n_s = \frac{2}{b_a} I_{as} + \frac{G \cdot I_{ts}}{E \cdot l_{ts}}$$

$$n_d = \frac{2}{b_a} I_{ad} + \frac{G \cdot I_{td}}{E \cdot l_{td}}$$

Where the terms have the meaning (see Fig. 2 A1):

I – inertia moment of panel flange section under investigation in relation to the axis situated in the girder plane;

I_{ds}, I_{dd} – inertia moment of diagonal section from the left of the panel and its right, respectively, in relation to the axis situated in the girder plane;

I_{as} , I_{ad} – inertia moment of the cross girder section from the left of the panel and the right of it, respectively;

I_{ts} , I_{td} – torsional rigidity of the flange on the left side of the panel and on its right, respectively.

2. MEASUREMENT OF STIFFNESS IN TYPE C TRANSVERSE SEMI-FRAMES

As the two Codes do not analyse the rigidity of a type C truss semi frame (combination of A and B types members), in what follows we will try to determine them, measuring, first of all, the flexibility δ of such a truss semi-frame. The type C semi-frame is analysed in the two variants, current semi-frame (C1) and end semi-frame (C2). The analysis enables us to determine what happens if we do not take into account the contribution of diagonals and stanchions of the truss semi-frames in the increase of rigidity by comparison with the rigidity of type B truss semi-frames and type A ones, respectively.

In order to determine the displacement δ of the C1 semi-frame (Fig. 2), we will consider it as being loaded by two horizontal loadings $H = 1$ – the real loading state – to be followed by a horizontal loading $P = 1$ in one of the semi-frame ends – the auxiliary loading state. The bending moment diagrams from the two loading states are determined on the truss semi-frame bars, and, by using the Mohr – Maxwell relation, we get the flexibility δ which will serve in determining rigidity H [5.2]. The truss semi-frame rigidity is influenced, besides the bending stiffness of the truss frame bars, by the torsion rigidity of the flanges, which, because it is low, especially so in the case of the open sections, may be neglected. In doing the calculus we assume that the sectional characteristics of the truss semi-frame bars are known.

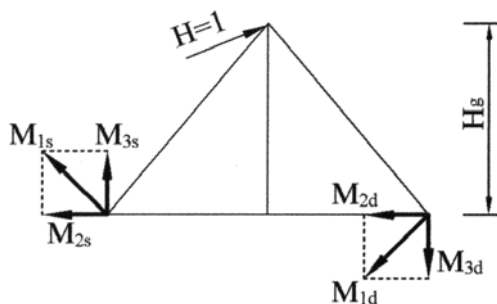


Fig. 3 Distribution of bending moment produced by $H = 1$

In order to determine the diagrams of the bending moments on the truss semi-frame structure, the bending moment produced by H or P is distributed over diagonals and stanchion in their fixed section of their in the lower flange, proportionally to their relative bending stiffness values, thus resulting in M_{1s} , M_{1c} , M_{1d} (Fig. 3). M_{1s} and M_{1d} divide themselves in the bending moments in vertical plane - M_{2s} and M_{2d} , respectively, and the bending moments in horizontal plane - M_{3s} and M_{3d} , respectively.

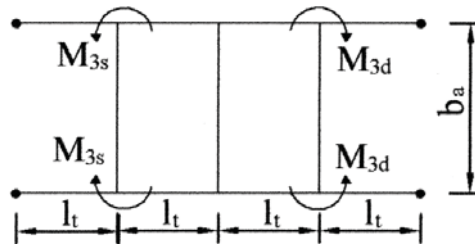


Fig. 4 Bending moments in the horizontal frame

The bending moments M_{2s} , M_{1c} , M_{2d} are transmitted to the cross girders (the effect of the flange torsion being neglected), and the moments M_{3s} and M_{3d} are distributed and transmitted by Cross method to the end of the bars that make the horizontal plane frame (Fig. 4), which is part of the truss semi-frame under investigation.

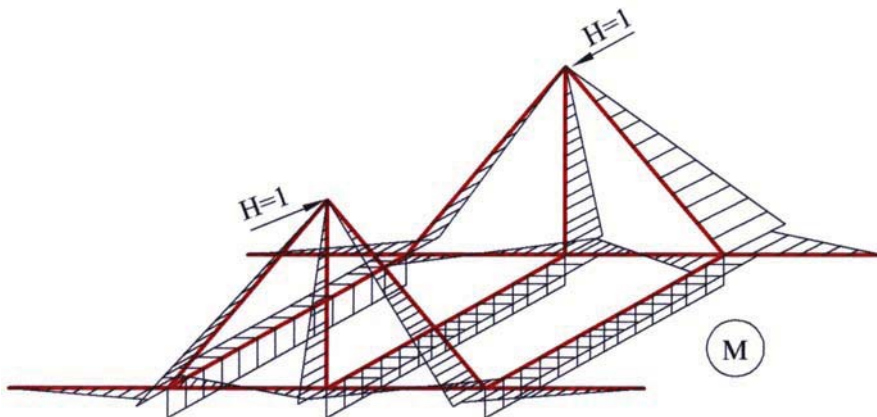


Fig. 5 Moment diagram from loading $H = 1$

The truss frame member in Fig. 4 may be calculated if it is considered to have fixed joints, having in view that the superstructure at the low flanges level is

always provided with vertical bracings that confer it a very high bending rigidity in horizontal plane and the lateral displacements of the nodes are insignificant.

The frame in fig. 4 was made up of 4 panels, although the rest of the deck panels could have been considered, as well, but the transmission of the bending moments to the other bars is insignificant, a calculus that was made taking into account that their contribution was not sensibly modified.

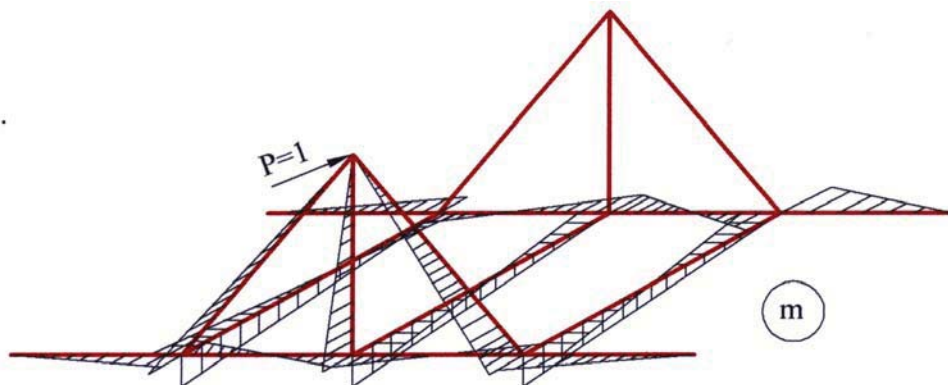


Fig. 6 Moment diagram from loading $P = 1$

In Figs 5 and 6 are presented the moment diagrams on the truss semi-frame under the actual and the auxiliary loading, with which, by using relation (3) we can obtain the flexibility of the truss semi-frame and then the rigidity.

$$\delta = \sum_{i=1}^n \int_0^{l_i} \frac{M_i \cdot m_i}{E \cdot I_i} ds \quad (3)$$

M_i, m_i – bending moment on bar i from diagrams M and m , respectively;

EI_i – bending stiffness of bar i ;

l_i – theoretical length of bar i .

3. CASE STUDY

For the three types of semi-frames and their variants (current and end ones) of one and the same truss, knowing the geometric (length) and sectional (axial inertia moments) characteristics of the bars, a numerical calculus was used to determine their rigidity, using the three calculus variants – SR 1911 – 98, EUROCODE 3 and the analysis made under subheading 2. The results are presented in Table 1.

Table 1. Numerical values of semi-frames rigidity

Crt. no.	Semi-frame position	Semi-frame type	Calculus method	Flexibility δ (cm/daN)	Rigidity H (daN/cm)
1	current	B	SR 1911-98	-	286
2		A_1	EURO-CODE 3	-	410
			Subheading 2	$1,98 \cdot 10^{-3}$	504
3		C_1	Subheading 2	$1,32 \cdot 10^{-3}$	759
4	end	B	SR 1911-98	-	345
5		A_2	EURO-CODE 3	-	509
			subheading 2	$1,57 \cdot 10^{-3}$	635
6		C_2	subheading 2	$1,23 \cdot 10^{-3}$	814

4. CONCLUSIONS

4.1. The resistance to lateral buckling of the compressed chord of the metal bottom-way truss bridges superstructure without vertical bracing depends on the magnitude of the rigidity to lateral displacement of the truss semi-frames, formed by truss members, cross girders and bottom chords which are elastic supports for the compressed flange.

4.2. The Romanian Code SR 1911 – 98 stipulates the value of the rigidity to lateral displacement of a semi-frame made of a cross girder and the corresponding stanchions (semi-frames no 1 and 4, Table 1), without taking into account the influence of the diagonals on rigidity.

4.3. The EUROCODE 3 stipulates the value of rigidity to lateral displacement of a semi-frame made as mentioned in 4.2, or made of cross girders and diagonals (semi-frames no 2 and 5, Table 1)

4.4. As none of the two codes is concerned about the value of semi-frame rigidity when the influence of both diagonals and stanchions is considered, the present paper has determined the rigidity of this type of semi-frame (semi-frames no. 3 and 6, Table 1), after having measured their flexibility by Mohr-Maxwell method.

4.5. The numerical calculus of rigidity for the three types of semi-frames of a superstructure with identical characteristics yields the following:

If the influence of diagonals on semi-frames rigidity is not considered, the rigidity undergoes a significant reduction, from 759 daN/cm to 286 daN/cm for a current semi-frame, and from 814 daN/cm to 345 daN/cm for an end semi-frame.

- If the influence of the stanchions on semi-frames rigidity is not considered, the parameter will undergo a slighter reduction as compared to the above-mentioned values, i.e. from 759 daN/cm to 410 daN/cm for a current semi-frame, and from 814 daN/cm to 509 daN/cm for an end semi-frame.

- If we compare the rigidity value of a semi-frame made of cross girders and diagonals (semi-frames no.2 and 5, Table 1), calculated with the relations from EUROCODE 3 and the method developed in the present paper, that is 410 daN/cm and 504 daN/cm for a current semi-frame and 509 daN/cm and 635 daN/cm for an end frame, there results an error of approx. 24% in both cases.

References

1. Timoshenko, Stephen P., Gere, James M. Teoria stabilității elastice (translated from English), București, Editura Tehnică, 1967.
2. Scarlat, A. Statica construcțiilor, II. București, Editura Didactică și Pedagogică, 1968.
3. Jantea, C. Poduri metalice. Iași, Editura Venus, 1996.
4. *** EN 1994, EUROCODE 3. Design of Steel structures.
5. *** SR 1911-98. Poduri metalice de cale ferată. Prescripții de proiectare.

Information flow for the determination in time of the bridge behaviour

Constantin Ionescu and Rodian Scînteie

“Gh. Asachi” Technical University of Iași, 700050, România

Summary

The paper represents an introduction to the information flow in the Bridge Engineering processes. A more detailed view is on the operational phase of the Bridge Engineering which refers to the bridge exploitation and maintenance.

There are also presented, according to the determination in time of bridge behaviour theory, more information systems such as: exploitation, current pursuit and special pursuit of the bridges.

It is given a definition for the information flow as the proportion between the information quantity and the time necessary to transmit it in the system. Also there is presented a logical scheme related to the transformation of data in information. The information through reasoning and experiments forms new knowledge necessary to the Bridge Engineering.

KEY WORDS: bridge, Bridge Engineering, system, information system, bridge exploitation, determination in time of bridge behaviour, current pursuit, special pursuit, information flow, data, information, knowledge.

1. INTRODUCTION. DETERMINATION IN TIME OF THE BRIDGE BEHAVIOUR

The pursuit in exploitation of the technical system behaviour is a systematic activity of selection, recording and exploitation of several data and information. The data and information result from the observation of phenomena and measurement of several parameters of the elements and the systems from the bridge area.

The main objective of the pursuit in exploitation of the bridge area behaviour refers to the bridge technical state evaluation on his entire life period.

The pursuit of the bridge area behaviour must give information which allows:

- The quick and objective appreciation of the bridge safety state;
- The prevention of the bridge disturbance state by the study of several phenomena;
- The confirmation of calculus hypothesis and the improvement of the bridge design knowledge;

- The beginning of the maintenance works processes for the bridges.

The pursuit in exploitation of the bridge area behaviour takes two forms: the current pursuit and the special pursuit.

The two categories are combined, so that the special pursuit doesn't stop the creation of the activities of the current pursuit.

The current pursuit of the determination in exploitation of the bridge behaviour applies to all the constructions in the bridge area and is realised in accordance with the instructions of current pursuit realised by designers or other experts in the field.

In the case of current pursuit of the constructions from the bridge area, when appear several deteriorations, which can interfere with the quality requests, the owner will ask for an extended inspection on the bridge area followed by a quality technical expertise.

The current pursuit in exploitation of a bridge is classified in: supervisions and inspections.

The special pursuit in exploitation of the bridge behaviour area contains the investigations necessary to create the objectives from the special pursuit projects. The pursuit has a permanent or temporary character and it's realised by specialised personnel with adequate technical means.

The special pursuit in exploitation of the bridge behaviour area is done by interpretation and adaptation of the obtained data by measurements, with measurement and control devices. It studies the time evolution of several phenomena and technical state parameters of the bridges.

2. INFORMATION SYSTEMS OF THE OPERATIONAL PHASE

The systemic approach of the bridge behaviour in time is determined by the fact that these are systems of great complexity [4]. The bridge has several subsystems, the system state vector exceeds a certain limit and the interaction structure between subsystems is under the uncertainty principle.

The behaviour in time of a system like this can be identified, according to The Systems Theory, by the determination of inputs and output of a bridge – system. There must be determined the conditions in which the bridges are being exploited and to determine their technical state. The state is being determined by the time evolution of the bridge parameters, of geometrical, physical – mechanical nature etc.

By monitoring the bridge behaviour, after a certain period of time, it's obtained a great volume of data and information. In order to reduce the uncertainty, the data and information will be processed by scientific methods.

All the elements – material and ideal – specific to a bridge are interacting, creating a whole. This way can be realized an information system specific to the Bridge Engineering. The information system will include the processes of collecting, adaptation and communication of the information necessary to the bridge management system leading process.

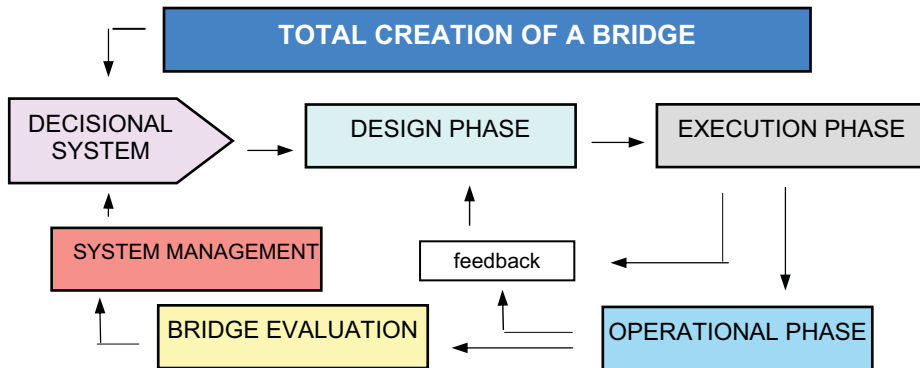


Fig.1. Information system – total creation of a bridge

In order to determine the Systems Engineering activity, the paper presents more information systems [2]. The first one, fig.1, contains: the bridge design phase subsystem, the bridge execution subsystem and the operational process subsystem and the evaluation subsystem (costs, technical performance).

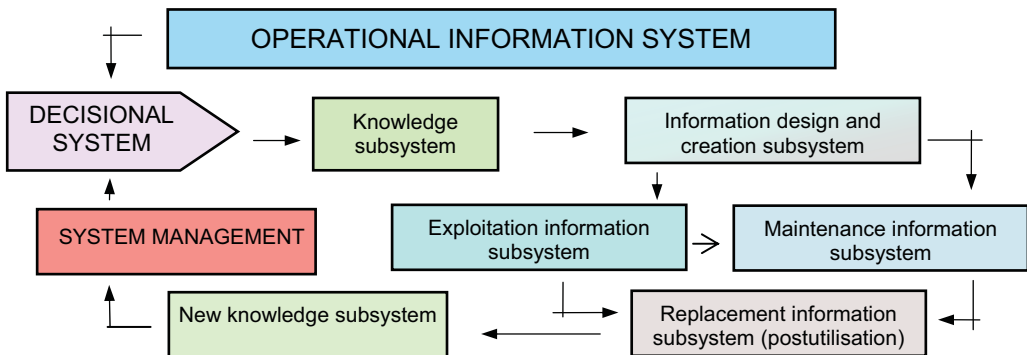


Fig.2. Operational information system of a bridge

The operational subsystem, fig.2, contains the exploitation subsystem and the maintenance subsystem. The collected data analysis and adaptation is realised by using the knowledge and information from the design and creation systems [3]. The knowledge subsystem is substituted to the inputs in the information system of the exploitation and/or maintenance. The knowledge subsystem contains the knowledge from the non-periodic publication (monograph, treaty, scientific

manifestation volumes, norms, standards) and periodicals (scientific and technical journals).

Another subsystem represents the new knowledge. It is determined by the adaptation of the information proper to the operational phase, for one or several bridges and it supplies the knowledge already possessed.

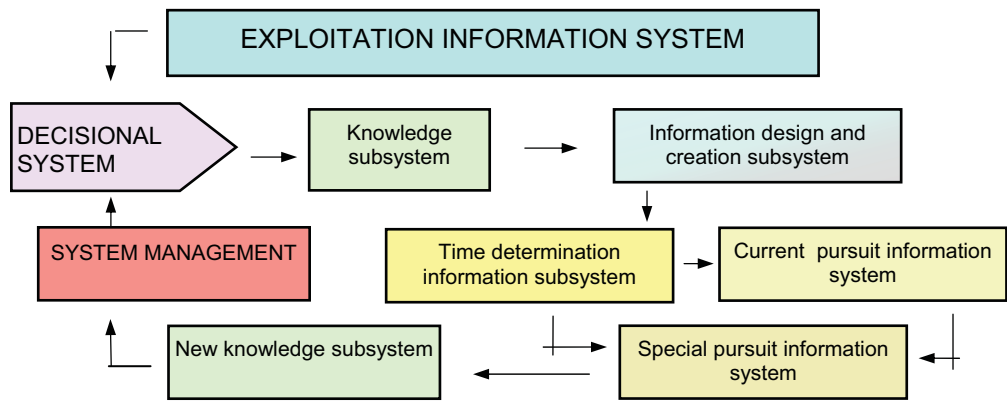


Fig.3. The bridge exploitation information system

The exploitation information subsystem is presented in fig.3. In the centre of this system is the bridge time determination pursuit subsystem with two main elements: current pursuit, fig.4. and special pursuit.

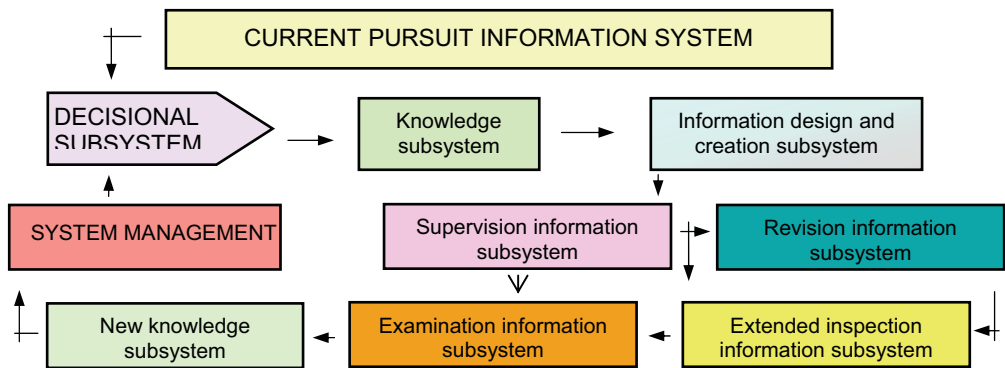


Fig.4. The bridge current pursuit information system

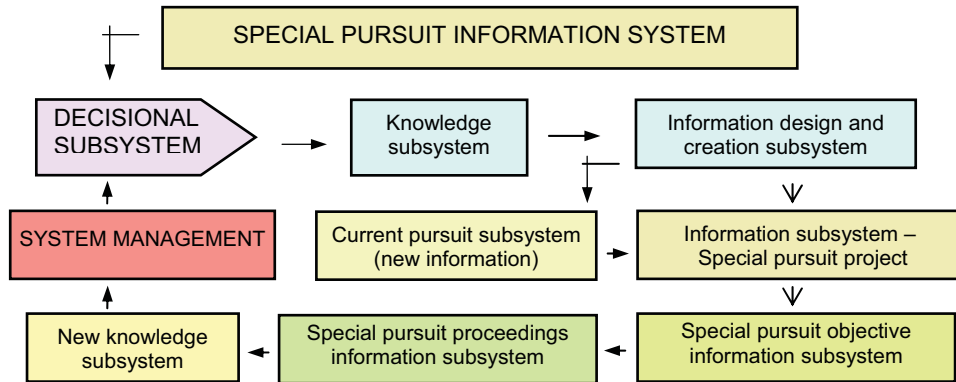


Fig.5. The bridge special pursuit information system

3. INFORMATION FLOW OF TIME PURSUIT PHASE OF THE BRIDGE BEHAVIOUR

In every information system, proper to the Bridge Engineering operation system, apply the collection, adaptation and communication of data and information necessary to the administration process. The information as the main resource of the Bridge Engineering has a special meaning for the bridge image, creation and exploitation.

The proportion between the information quantity, in the operational system, and the time used for communication defines the information flow.

It is known that the lack of information becomes an obstacle in the bridge operational system, while the abundance of information becomes non-information. Also, if the information doesn't circulate or it circulates uncontrolled, the global effect on the Bridge Engineering processes is the same [1]. The filtration – the evaluation considering the importance, the opportunity and purpose – and the information condensation represent two essential aspects of the information circulation.

The information filtration and condensation imposes the introduction of an information interface which allows the user to take the right measures in real time in the case of special situations.

The data, in Bridge Engineering, are formed from independent and unevaluated entities, presented as numerical values, perception and observations made by experienced experts in the field.

The information is the data interpretation result, compared with certain particular situations, considering the technical culture of the experts. The data adaptation fig.6, consists in the evaluation, selection and

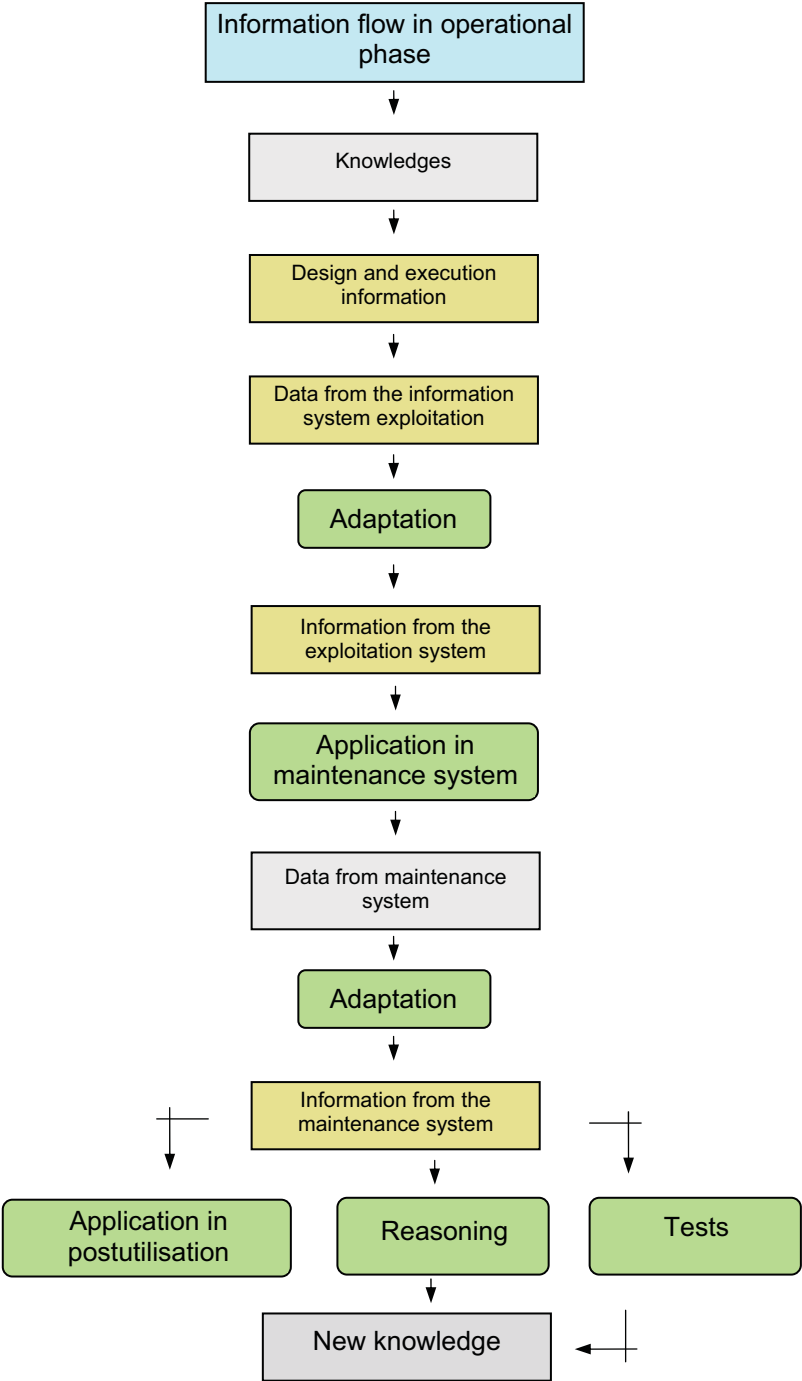


Fig. 6. Information Flow in Bridge Engineering

regulation in order to obtain certain information, which might lead to a better understanding of the events, situations or phenomena. The adaptation purpose is the uncertainty reduction.

The information, in the process of experimentation and reasoning, becomes knowledge. The knowledge is retained in monographs, treaties, norms, standards etc.

4. CONCLUSIONS:

- 4.1. The paper proposes a concept related to the operational information system creation (exploitation and maintenance) proper to the Bridge Engineering.
- 4.2. In accordance with the theories about the human society information, has been imagined an information flow for the transformation of data in information, and the information in knowledge, necessary to the Bridge Engineering processes understanding.
- 4.3. Are necessary studies for the proper definition of the data and information related to the Bridge Engineering and the determination of the selection and interpretation methodology.

References

1. Vasilescu, Petre, Discrepanța generațiilor în informatică, Editura Științifică și Enciclopedică, București, 1985 (in Romanian)
2. Păunescu, E., Badea – Dincă, N., Stăicuț, E., Informatizarea societății – un fenomen inevitabil?, Editura Științifică și Enciclopedică, București, 1985 (in Romanian)
3. Ionescu, C., Unele considerații privind informatizarea proiectării podurilor, Zilele Academice Timișene (Infrastructuri eficiente pentru transporturi), Editura Mirton, Timișoara, 1999. (in Romanian)
4. Stănciulescu, Fl., Modelarea sistemelor de mare complexitate, Editura Tehnică, București, 2003. (in Romanian)

Integral abutment bridges

Cristian Claudiu Comisu

“Gh. Asachi” Technical University of Iasi, 700050, Romania

Abstract

Integral abutment and jointless bridges are simple or multiple span bridges that have their superstructure cast integrally with their substructure. The jointless bridges cost less to construct and require less maintenance than equivalent bridges with expansion joints. This paper presents some of the important features of integral abutment and jointless bridge design and some guidelines to achieve improved design. The intent of this paper is to enhance the awareness among the engineering community to use integral abutment and jointless bridges in Romania.

KEYS WORDS: jointless bridges, integral abutment.

1. INTRODUCTION

A bridge should be designed such that it is safe, aesthetically pleasing, and economical. Prior to the 1960s, almost every bridge in the U.S., Canada and England was built with expansion joints. These expansion joints often did not perform as well as intended. They required considerable maintenance, which undermined the economical operation of the bridges. Accident and vehicle damage caused by defective expansion joints raised safety concerns. Starting in the early 1960s, the use of integral bridges for new bridge construction attracted widespread interest.

Integral abutment bridges are designed without any expansion joints in the bridge deck. They are generally designed with the stiffness and flexibilities spread throughout the structure/soil system so that all supports accommodate the thermal and braking loads. They are single or multiple span bridges having their superstructure cast integrally with their substructure.

Generally, these bridges include capped pile stub abutments. Piers for integral abutment bridges may be constructed either integrally with or independently of the superstructure. Semi-integral bridges are defined as single or multiple span continuous bridges with rigid, non-integral foundations and movement systems primarily composed of integral end diaphragms, compressible backfill, and movable bearings in a horizontal joint at the superstructure-abutment interface (fig. 1).

2. ADVANTAGES OF INTEGRAL BRIDGES

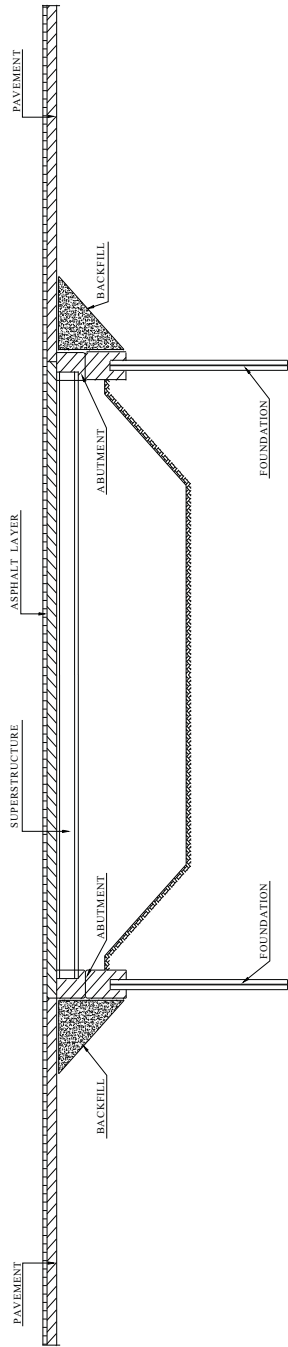
The principal advantages of integral abutment and jointless bridges include the following:

1. Lower construction costs and future maintenance costs. In conventional bridges, much of the cost of maintenance is related to repair of damage at joints. Fewer piles are required for foundation support. No battered piles are needed. Construction is simple and rapid. The integral abutment bridge acts as a whole unit.
2. Reduced removal of existing elements - Integral abutment bridges can be built around the existing foundations without requiring the complete removal of existing substructures.
3. Simplified widening and replacement - Integral bridges with straight capped-pile substructures are convenient to widen and easy to replace. Their piling can be recapped and reused, or if necessary, they can be withdrawn or left in place. There are no expansion joints to match and no difficult temperature setting to make. The smooth, uninterrupted deck of the integral bridge is aesthetically pleasing, and it improves vehicular riding quality.
4. Design efficiencies are achieved in substructure design. Longitudinal and transverse loads acting upon the superstructure may be distributed over more number of supports.
5. Integral abutments provide added redundancy and capacity for catastrophic events. Joints introduce a potential collapse mechanism into the overall bridge structure. Integral abutments eliminate the most common cause of damage to bridges in seismic events, loss of girder support. Integral abutments have consistently performed well in actual seismic events and significantly reduced or avoided problems such as back wall and bearing damage, associated with seat type jointed abutments. Jointless design is preferable for seismic regions.

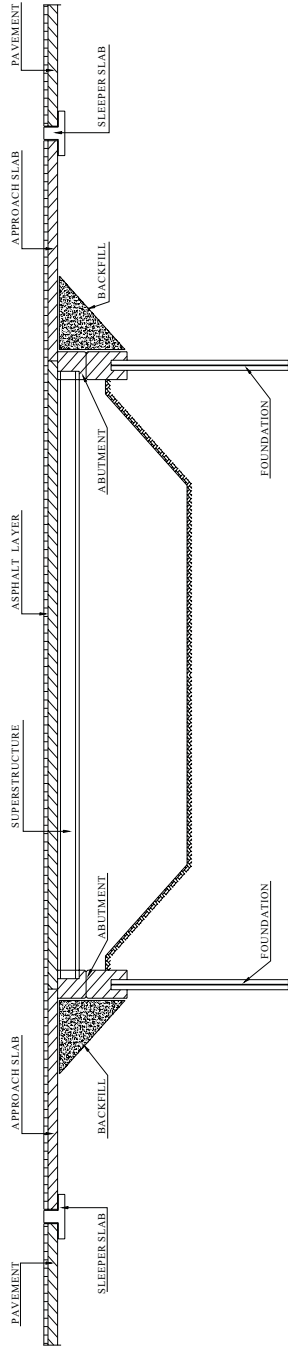
3. LIMITATIONS OF APPLICATION OF INTEGRAL BRIDGES

The application of integral bridge concept has limitations.

1. Integral bridges cannot be used with weak embankments or subsoil.
2. Integral bridges are suitable if the expected temperature-induced movement at each abutment is 51 mm or less, and somewhat larger movements may be tolerable.
3. The piles that support the abutments may be subjected to high stresses because of cyclic expansion and contraction of the bridge superstructure. These stresses can cause formation of plastic hinges in the piles, and may reduce their axial load capacities.



INTEGRAL BRIDGE WITHOUT AN APPROACH SLAB



INTEGRAL BRIDGE WITH AN APPROACH SLAB

Figure 1 - Geometry of integral abutment and jointless bridge

4. The bridge material (steel or concrete) and the geometry of the bridge (curved or skewed) are important factors that affect the displacement of integral bridges.
5. For composite concrete girder bridges with a total length of < 50 m integral abutments should normally be used. For steel girder bridges with a total length of < 40 m integral abutment should normally be used.

4. DESIGN OF INTEGRAL ABUTMENT

The integral abutment and jointless bridge concept is based on the theory that due to the flexibility of the piling, thermal stresses are transferred to the substructure by way of a rigid connection between the superstructure and substructure. The concrete abutment contains sufficient bulk to be considered a rigid mass. A positive connection with the ends of the beams or girders is provided by rigidly connecting the beams or girders and by encasing them in reinforced concrete. This provides for full transfer of temperature variation and live load rotational displacement to the abutment piling (fig. 2 and photo 1).

A semi-integral abutment design structure is one whose superstructure is not rigidly connected to its substructure. It may be a single or multiple span continuous structures whose integral characteristics include a jointless deck, integral end diaphragms, compressible backfill and movable bearings. In this concept, the transfer of displacement due to the piles is minimized.

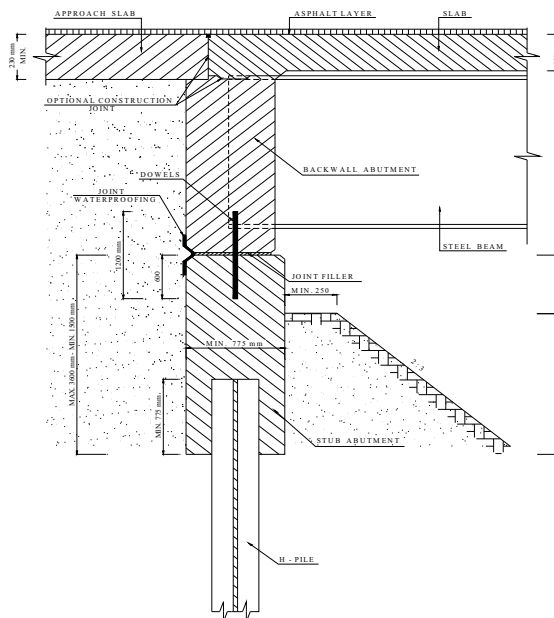


Fig. 2 - Integral and semi-integral bridge



Photo 1 - Integral and semi-integral bridge

5.1. Design of Superstructure

The superstructures of integral bridges are subject to both primary loads (loads acting on the conventional jointed bridges, i.e., dead and live loads, earthquake loads, etc.) and temperature induced secondary loads. Integral bridges must be able to withstand these loads. Because of the rigid connections between the bridge deck and the abutments, integral bridges have improved seismic resistance compared to jointed bridges.

5.2. Design of Piers

To design piers to accommodate potentially large superstructure movements, the following options are available:

- a) Flexible piers rigidly connected to the superstructure;
- b) Isolated rigid piers, connected to the superstructure by means of flexible bearings;

- c) Semi-rigid piers, connected to the superstructure with dowels and neoprene bearing pads;
- d) Hinged-base piers, connected to the superstructure with dowels and neoprene bearing pads.

5.2.1. Flexible Piers

A single row of piles, with a concrete cap that may be rigidly attached to the superstructure, provides a typical example of a flexible pier. This type of pier is assumed to provide vertical support only. The moments induced in the piles due to superstructure rotation or translation are small and may be ignored (fig. 2).

5.2.2. Isolated Rigid Piers

Rigid piers are defined as piers whose base is considered fixed against rotation and translation, either by large footings bearing on soil or rock, or by pile groups designed to resist moment. The connection to the superstructure is usually detailed in a way that allows free longitudinal movement of the superstructure, but restrains transverse movements. This type of detailing permits the superstructure to undergo thermal movements freely, yet allows the pier to participate in carrying transverse forces.

5.2.3. Semi-Rigid Piers

These piers are similar to rigid piers. Their bases are considered fixed by either large spread footings or pile groups; however, the connection of the piers to the superstructure differs significantly.

In utilizing prestressed concrete girders that bear on elastomeric pads, a diaphragm is placed between the ends of the girders. Dowels, perhaps combined with a shear key between girders, connect the diaphragm to the pier cap. Compressible materials are frequently introduced along the edges of the diaphragm, and, along with the elastomeric bearing pads, allow the girders to rotate freely under live load.

5.2.4. Hinged-Base Piers

This type of pier may be used to avoid the need for an expansion pier in a situation where semi-rigid piers have inadequate flexibility. A “hinge” is cast into the top of the footing to permit flexibility of the column.

Temporary construction shoring may be required, and additional detailing requirements at the top of the footing may increase cost; however, the designer should keep this alternate in mind under special circumstances where the other pier types are not feasible.

5.3. Design of the Abutment

To support the integral abutment, it is customary to use a single row of piles. The piles are driven vertically and none are battered. This arrangement of piles permits the abutment to move in a longitudinal direction under temperature effects.

The most desirable type abutment is the stub type. It will provide greater flexibility and will offer the least resistance to cyclic thermal movements.

In integral abutment bridges, the ends of the superstructure girders are fixed to the integral abutments. Expansion joints are thus eliminated at these supports. When the expansion joints are eliminated, forces that are induced by resistance to thermal movements must be proportioned among all substructure units. This must be considered in the design of integral abutments.

5.4. Design of Approach System

The approach system of an integral bridge consists of the backfill, the approach fill, and the foundation soil. An approach slab and a sleeper slab, if used, are also part of the approach system (fig. 1).

Approach slabs are used to provide a smooth transition and span the problematic area between road pavements and bridge decks and will always be required for integral abutment jointless bridges. Their lengths shall vary from a minimum of 3,0 m to a maximum that is based on the intercept of a 1 on 1,5 lines from the bottom of the abutment excavation to the top of the highway pavement. This length is to be measured along the centerline of roadway.

There are two main types of approach slabs. One type is tied to the abutment as in integral abutment bridges. The other type has an expansion joint between the bridge deck and the approach slab as in semi integral abutment bridges.

5.3. Semi-integral abutment design

1. A semi-integral abutment design structure is one whose superstructure is not rigidly connected to its substructure. It may be a single or multiple span continuous structure whose integral characteristics include a jointless deck, integral end diaphragms, compressible backfill and movable bearings. In this concept, the transfer of displacement due to the piles is minimized. The rotation is generally accomplished by use of a flexible bearing surface at a horizontal interface in the abutment. Horizontal displacements not eliminated in a semi-integral concept must still be considered in the design.

In lieu of conventional deck joint bridges, or where a full integral bridge is not desirable, semi-integral bridges may be considered. The foundations for this type structure shall be stable and fixed. A single row of piles should not be utilized. The foundation piles should be stiffened by inclusion of battered piles, or the foundation may be founded on bed rock.

2. The expansion and contraction movement of the superstructure should be accommodated at the roadway side of an approach slab. This type design shall only be used for symmetrical, straight beam structures. The geometry of the approach slab, design of the wingwalls and transition parapet, if any, must be compatible with the freedom required for the integral configuration (beams, deck, backwall and approach) to move longitudinally.

6. CONSTRUCTION PROCEDURES

The following sequence is recommended when constructing integral bridges. This will reduce the effects of thermal movements on fresh concrete and control moments induced into the supporting pile system.

1. Drive piling and pour the concrete to the required bridge seat elevation and install the rigid connection systems. Pour concrete for wingwalls concurrently.
2. Set the beams/girders and anchor to the abutment. Standard provides details for a welded plate rigid connection, for steel superstructures, to the substructure. As an alternate, slotted bolt holes in the bottom flanges may be used. The slotted holes will aid the girder placement. Anchor nuts should not be fully tightened at this time. Free play for further dead load rotations should be accounted for.
3. Pour the bridge deck in the sequence desired excluding the abutment backwall/diaphragm and the last portion of the bridge deck equal to the backwall/diaphragm width. In this manner, all dead load slab rotations will occur prior to lock-up, and no dead load moments will be transferred to the supporting piles.
4. If utilizing anchor bolts, tighten anchor nuts and pour the backwall/diaphragm full height. Since no backfilling has occurred to this point, the abutment is free to move without overcoming passive pressures against the backwall/diaphragm. The wing walls may also be poured concurrently.
5. Place back of wall drain system and backfill in 150 mm lifts until the desired subgrade elevation is reached. Place bond breaker on abutment surfaces in contact with approach pavement.
6. Pour the approach slab concrete starting at the end away from the abutment, progressing toward the backwall. If it can be so controlled, approach pavements should be poured in early morning so that the superstructure is expanding, and therefore not placing the slab in tension.
7. A construction joint should be located at a distance of 150 mm from the back of the backwall between the approach slab and bridge slab. This will provide a controlled crack location rather than allowing a random crack pattern to develop. Corrosion coated dowels shall pass through the joint and shall be located near the

bottom of the slab. This will keep the joint tight but still allow the approach slab to settle without causing tension cracking in the top of the slab.

8. The excavation for the approach slabs shall be carefully made after compacted abutment embankment material is in place. The slabs shall be founded on undisturbed compacted material. No loose backfill will be allowed.

9. To permit unhindered longitudinal movement of the approach slab, the surface of the subbase course must be accurately controlled to follow and be parallel to the roadway grade and cross slope.

10. A filter fabric or some type of bond breaker such as polyethylene sheets shall be placed on the finished subbase course the full width of the roadway prior to placement of approach slab reinforcement.

12. A lateral drainage system should be provided at the end of the approach slab adjacent to the sleeper slab.

7. BEST PRACTICE

The following best practice guideline was developed to provide guidance on when integral abutments should be used or considered.

7.1. For composite concrete girder bridges with a total length of < 50 m integral abutments should normally be used.

7.2. For steel girder bridges with a total length of < 40 m integral abutment should normally be used.

7.3. For longer bridge structures integral abutments should be considered, however, care must be taken to design proper details to accommodate cyclic thermal movements of the structure.

8. CONCLUSIONS

Based on the results of a literature review, field inspections, and a finite element analysis, the following conclusions are drawn concerning the behavior of integral abutment and jointless bridges.

1. Integral bridges perform well with fewer maintenance problems than conventional bridges. Without joints in the bridge deck, the usual damage to the girders and piers caused by water and contaminants from the roadway is not observed. Integral abutment and jointless bridges cost less to construct and require less maintenance than equivalent bridges with expansion joints.

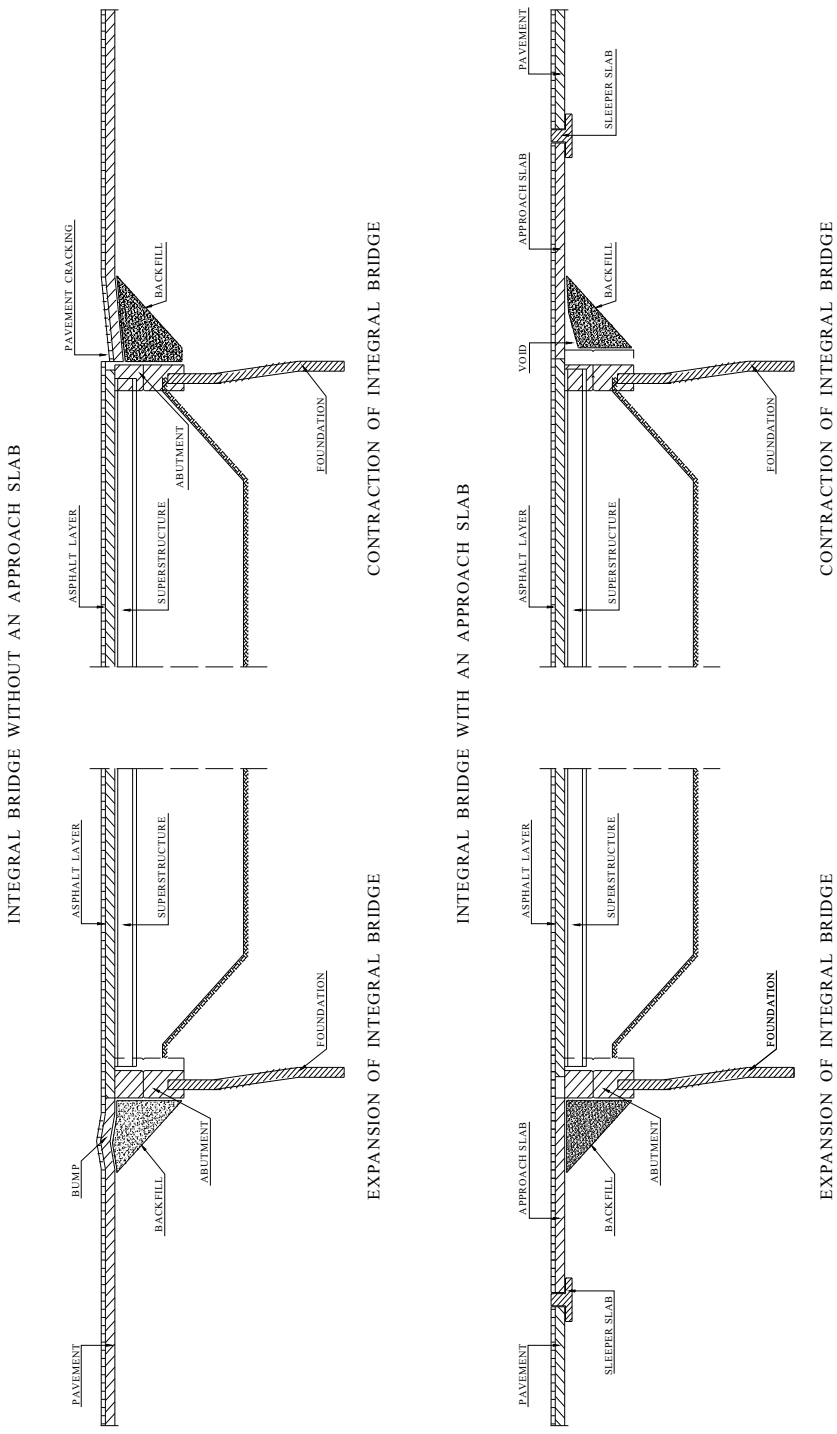


Figure 3. Interaction mechanism between abutment and approach fill

2. Simple Design - Where abutments and piers of a continuous bridges are each supported by a single row of piles attached to the superstructures, or where self-supporting piers are separated from the superstructure by movable bearings, an integral bridge may, for analysis and design purposes, be considered a continuous frame with a single horizontal member and two or more vertical members.
3. With jointless bridges, all of the movement due to temperature changes takes place at the abutments and this approach system area requires special attention to avoid development of a severe "bump at the end of the bridge." Finite element analyses show that the zone of surface deformation extends from the back of the abutment a distance equal to about three to four times the height of the abutment.
4. The movement of the abutment into the approach fill develops passive earth pressure that is displacement-dependent. Using full passive pressure regardless of displacement is not conservative because it reduces the flexural effects of dead and live load in the bridge girders.
5. The ground around the piles moves along with the movement of the abutment. The relative movement between the pile and ground is therefore reduced, resulting in relatively low shear forces at the top of the pile.
6. The total lateral movement of the top of the pile relative to the end embedded in the ground is important because it reduces the axial load capacity of the pile. This lateral movement is one of the key variables in assessing the maximum design length of integral abutment bridges. The cyclic nature of these movements raises concern about the vulnerability of piles to cyclic loading.
7. Settlement of the approach fill will occur with time. It can be mitigated by using a properly compacted well-drained backfill, but it cannot be eliminated.

References

1. AASHTO (1996). Standard Specifications for Highway Bridges, 16th edition, American Association of State Highway and Transportation Officials, Washington D.C., pp. 677.
2. Bennett, J.K., Siriwardane, H.J., and Spyrakos, C.C. (1996). Study of bridge approach behavior and recommendation on improving current practice - Phase I, WVDOT RP 106/CFC 95-214, West Virginia Dept. of Transportation, WVDOT, February 1996, pp. 191.
3. Briaud, Jean-Louis; James, R. W.; and Hoffman, S. B. (1997). Settlement of bridge approaches (The bump at the end of the bridge), National Academy Press, Washington, D.C., pp. 75.
4. Burke Jr., M.P. (1996). *The genesis of integral bridges in Ohio*, Concrete International, Vol. 18, July, pp. 48-51.
5. Burke, Martin P. Jr. (1996). *An introduction to the design and construction of integral bridges*, Workshop on Integral abutment bridges, November 13-15, 1996, Pittsburgh, PA, pp. 64.
6. Chang, Ming-Fang. (1997). *Lateral earth pressures behind rotating walls*, Canadian Geotechnical Journal, Vol. 34, August, pp. 498-509.
7. Chen, Yohchia. (1997). *Important considerations, guidelines, and practical details of integral bridges*, Journal of Engineering Technology, Vol. 14, Spring 1997, pp. 16-19.
7. GangaRao, H.; Thippeswamy, H.; Dickson, B.; and Franco, J. (1996). *Survey and design of integral abutment bridges*, Workshop on Integral abutment bridges, November 13-15, 1996, Pittsburgh, PA, pp. 129.

8. Hooper J. D.; Roeder, C. W.; Klemencic, R.; and Nordquist, K. (1999). *Best of both worlds*, Civil Engineering, ASCE, Vol. , No. , January, pp. 40-42.
9. Hoppe, E. J. and Gomez, J. P. (1996). Field study of an integral backwall bridge, Virginia Transportation Research Council, VTRC 97-R7, October 1996, 47 p.
10. Loveall, C. (1996). *Integral abutment bridges*, Workshop on Integral abutment bridges, November 13-15, 1996, Pittsburgh, PA, pp. 8.
11. Ng, Charles, Springman, S., and Norrish, A. (1998). *Soil-Structure interaction of spread-base integral bridge abutments*, Soils and Foundations, Vol. 38, No. 1, March 1998, pp. 145-162.
12. Oesterle, R. G.; Tabatabai, H.; Lawson, T. J.; Refai, T.M.; Volz, J. S.; and Scanlon, A. (1998). Jointless and integral abutment bridges summary report. CTL of Skokie, IL, to be published, under review by FHWA.

ROBOT MILLENIUM - Numerical methods involved in modal analysis

Octavian Roșca

“Gh. Asachi” Technical University of Iasi, 700050, Romania

Abstract

This paperwork deals with the numerical methods involved by the modal analysis. There are emphasized the most widely used, state-of-the-art solutions of the eigenvalue problem.

These methods are implemented in some of the most powerful programs dedicated to the structural analysis. However, the case-studies were carried out by the means of the ROBOT MILLENIUM Software, product of the Robobat Industries.

At the end some case studies are analyzed and some conclusions are drawn. The paperwork is thought as a slideshow, as it was presented during the conference.

MODAL ANALYSIS

ROBOT *Millennium*

NUMERICAL METHODS

Dr. Octavian, Roşca

Technical University “Gh. Asachi” of Iaşi, România

[next](#)



Contents:

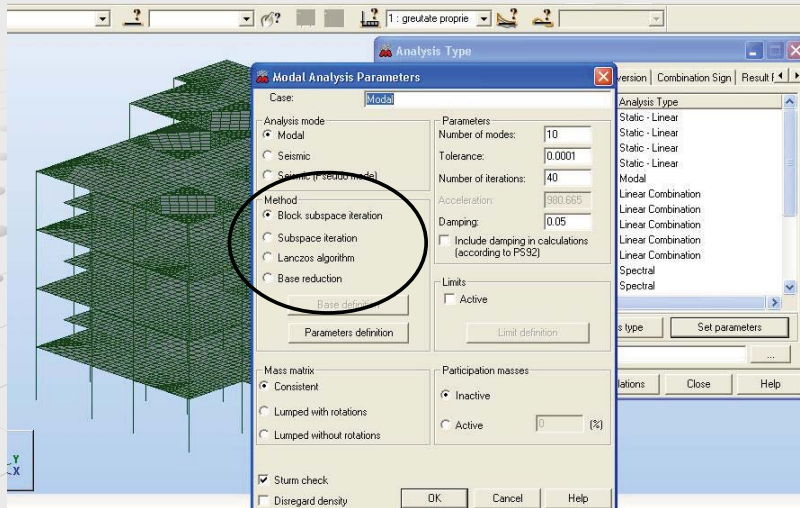
- Introduction
- Modal Analysis in Robot Millenium
 - types of analysis
 - computation parameters
 - mass modelling
 - types of inertia matrices
 - results
- Conclusions

[home](#)

[next](#)



Introduction


[home](#)
[back](#)
[next](#)

Modal Analysis

- Subspace iteration
- Block subspace iteration
- Lanczos algorithm
- Base vector reduction

The standard problem: $K x = \lambda x$ $K X = X \Lambda$

The generalized problem: $K x = \lambda M x$ $K X = X M \Lambda$

Solution:
$$\begin{cases} 0 \leq \lambda_1 \leq \lambda_2 \leq \dots \leq \lambda_{N-1} \leq \lambda_N \\ X = [x_1, x_2 \dots x_p] \end{cases}$$

[home](#)
[back](#)
[next](#)

The subspace iteration

(Klaus J. Bathe)

Iteration approaches

$$K x = \lambda M x$$

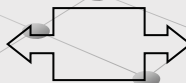
$$\lambda = 1$$

The choice of a start vector x_1

$$R_1 = (I) M x_1$$

$$K x_2 = R_1$$

Reverse iteration



Direct iteration

[home](#)

[back](#)

[next](#)



The reverse iteration:

$$K x = \lambda M x$$

Initial vector (start) z_1

for $k = 1, 2, \dots, L$:

$$K \bar{y}_{k+1} = z_k$$

$$\bar{z}_{k+1} = M \bar{y}_{k+1}$$

$$\rho(\bar{y}_{k+1}) = \frac{\bar{y}_{k+1}^T z_k}{\bar{y}_{k+1}^T \bar{z}_{k+1}}$$

$$z_{k+1} = \frac{\bar{z}_{k+1}}{(\bar{y}_{k+1}^T \bar{z}_{k+1})^{1/2}}$$

if $z_1^T \neq 0$, then for $k \rightarrow \infty$, $z_{k+1} \rightarrow M x_1$ și $\rho(\bar{y}_{k+1}) \rightarrow \lambda_1$

The convergence criterion: $\frac{|\lambda_1^{(k+1)} - \lambda_1^{(k)}|}{\lambda_1^{(k+1)}} \leq \varepsilon$

Solution: $\lambda_1 \cong \rho(\bar{y}_{L+1})$ $x_1 \cong \frac{\bar{y}_{L+1}}{(\bar{y}_{L+1}^T \bar{z}_{L+1})^{1/2}}$

[home](#)

[back](#)

[next](#)



The direct iteration:

$$K x = \lambda M x$$

The initial vector (start) y_1

$$z_1 = K y_1$$

for $k = 1, 2, \dots, L$:

$$M \bar{y}_{k+1} = z_k$$

$$\bar{z}_{k+1} = K \bar{y}_{k+1}$$

$$\rho(\bar{y}_{k+1}) = \frac{\bar{y}_{k+1}^T z_{k+1}}{\bar{y}_{k+1}^T \bar{z}_k}$$

$$z_{k+1} = \frac{\bar{z}_{k+1}}{(\bar{y}_{k+1}^T \bar{z}_k)^{1/2}}$$

if $x_n^T z_1^T \neq 0$, then for $k \rightarrow \infty, \rho(\bar{y}_{k+1}) \rightarrow \lambda_n$ şi $z_{k+1} \rightarrow K x_n$

The convergence criterion:

$$\frac{|\lambda_1^{(k+1)} - \lambda_1^{(k)}|}{\lambda_1^{(k+1)}} \leq \varepsilon$$

Solution: $\lambda_N \cong \rho(\bar{y}_{L+1})$

$$x_N \cong \frac{\bar{y}_{L+1}}{(\bar{y}_{L+1}^T \bar{z}_{L+1})^{1/2}}$$

[home](#)[back](#)[next](#)

The Gram-Schmidt orthogonalization:

By having stored the x_1, x_2, \dots, x_m vectors previously computed by reverse iteration:

Pre-multiply $x_i^T M \longrightarrow \tilde{y}_1 = y_1 - \sum_{i=1}^m \alpha_i \cdot x_i$

$$x_i^T M \tilde{y}_1 = 0, \quad x_i^T M x_j = \delta_{ij}, \quad i=1, \dots, m$$

$$\alpha_i = x_i^T M y_1, \quad i=1, \dots, m.$$

 \tilde{y}_1 - The start vector for the reverse iterationSolution: (λ_{m+1}, x_{m+1}) .[home](#)[back](#)[next](#)

The subspace iteration (SI)

$$K x = \lambda M x \quad K \Phi = M \Phi \Lambda \quad \Lambda = \text{diag}(\lambda_i) \quad \Phi = [x_1, \dots, x_p]$$

$$\text{Conditions for orthogonality: } \Phi^T K \Phi = \Lambda \quad \Phi^T M \Phi = I$$

$$K X_{k+1} = M X_k$$

$$\text{the Gram-Schmidt orthogonalization: } K \bar{X}_{k+1} = M X_k \quad X_{k+1} = \bar{X}_{k+1} R_{k+1}$$

where R_{k+1} is an upper triangular matrix such that

$$X_{k+1}^T M X_{k+1} = I$$

$$X_{k+1} \rightarrow \Phi \quad R_{k+1} \rightarrow \Lambda$$

$$E_k \rightarrow E_{k+1} \quad K \bar{X}_{k+1} = M X_k \quad K_{k+1} = \bar{X}_{k+1}^T K \bar{X}_{k+1} \quad M_{k+1} = \bar{X}_{k+1}^T M \bar{X}_{k+1}$$

$$K_{k+1} Q_{k+1} = M_{k+1} Q_{k+1} \Lambda_{k+1}$$

$$X_{k+1} = \bar{X}_{k+1} Q_{k+1}$$

$$\frac{\|K x_i^{(L+1)} - \lambda_i^{(L+1)} M x_i^{(L+1)}\|}{\|K x_i^{(L+1)}\|} \leq \varepsilon_{\text{adm}}$$

The convergence criterion:

$$\text{For } k \rightarrow \infty, \Lambda_{k+1} \rightarrow \Lambda \text{ si } X_{k+1} \rightarrow \Phi$$

[home](#)

[back](#)

[next](#)

(BLSI) - Block subspace iteration with shift application

The shifting in the vector iteration process $K x = \lambda M x$

- For $\lambda_1 < \lambda_2$, the eigenvector converges to x_1 depending on the λ_1 / λ_2 ratio

$$\eta_i = \lambda_i - \mu \quad i = 1, 2, \dots, N$$

$$K x = (\eta - \mu) M x$$

$$(K - \mu M) x = \eta M x$$

$$K_\sigma x = \eta M x \quad K_\sigma = K - \mu M$$

- The transform by using the base vectors: $x = X \cdot \psi$

- The equivalent problem: $(\Lambda - \mu I_N) \psi = \eta \psi$

$$Z_{L+1}^T = \begin{bmatrix} 1 & 1 & 1 \\ (\lambda_1 - \mu)^L & (\lambda_2 - \mu)^L & (\lambda_N - \mu)^L \end{bmatrix}$$

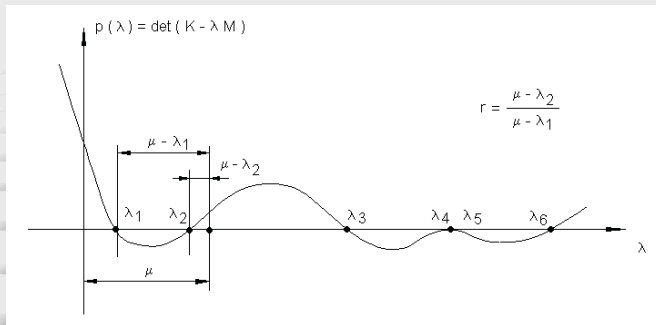
$$\bar{Z}_{L+1}^T = \begin{bmatrix} \left(\frac{\lambda_j - \mu}{\lambda_1 - \mu} \right)^L & \dots & \left(\frac{\lambda_j - \mu}{\lambda_{j-1} - \mu} \right)^L & 1 & \left(\frac{\lambda_j - \mu}{\lambda_{j+1} - \mu} \right)^L & \dots & \left(\frac{\lambda_j - \mu}{\lambda_N - \mu} \right)^L \end{bmatrix} \quad \bar{Z}_{L+1} \rightarrow e_j$$

[home](#)

[back](#)

[next](#)

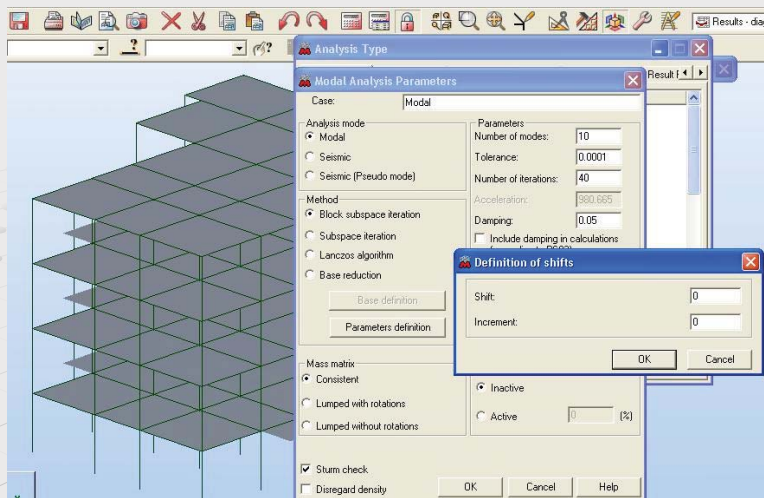
- The convergence rate: $r_1 = \frac{|\lambda_j - \mu|}{|\lambda_{j-1} - \mu|}$ sau $r_2 = \frac{|\lambda_j - \mu|}{|\lambda_{j+1} - \mu|}$



- The BLSI procedure consists of a simultaneously iteration of a vector in a subspace of "p" dimension
- Each convergent vector is eliminated and a new starting vector is selected
- Check the orthogonality at each step

The convergence criterion:

$$\frac{\|x_i^{(L+1)} - \lambda_i^{(L+1)} K^{-1} M x_i^{(L+1)}\|}{\|x_i^{(L+1)}\|} \leq \varepsilon_{adm}$$

[home](#)
[back](#)
[next](#)


Shift - μ	Increment = nr. iterații	Action
0	≥ 0	$\mu_{initial} = 0$
$\mu \geq 0$	0	$\mu = 0$
0	0	$K\sigma = K$ BLSI without shifting

[home](#)
[back](#)
[next](#)

The Lanczos Approach

$$A x = \lambda x$$

$$X^T X = I \quad A X = X T$$

$$A \cdot [x_1 \ x_2 \ \dots \ x_N] = [x_1 \ x_2 \ \dots \ x_N] \cdot \begin{bmatrix} \alpha_1 & \beta_2 & 0 & \dots & 0 & 0 & 0 \\ \beta_2 & \alpha_2 & \beta_3 & & 0 & 0 & 0 \\ \vdots & & & \ddots & \vdots & & \\ 0 & 0 & 0 & \dots & \beta_{N-1} & \alpha_{N-1} & \beta_N \\ 0 & 0 & 0 & & 0 & \beta_N & \alpha_N \end{bmatrix}$$

$$A x_1 = \alpha_1 x_1 + \beta_2 x_2$$

$$A x_2 = \beta_2 x_1 + \alpha_2 x_2 + \beta_3 x_3$$

$$A x_j = \beta_j x_{j-1} + \alpha_j x_j + \beta_{j+1} x_{j+1}$$

$$A x_N = \beta_N x_{N-1} + \alpha_N x_N$$

$$j = 1 \quad x_0 = 1$$

$$\beta_j = (\bar{x}_j^T \bar{x}_j)^{1/2} ; \quad x_j = \frac{\bar{x}_j}{\beta_j} ; \quad \alpha_j = x_j^T A x_j ; \quad \bar{x}_{j+1} = A x_j - \beta_j x_{j-1} - \alpha_j x_j$$

[home](#)

[back](#)

[next](#)



The Lanczos Approach

$$T_m = \begin{bmatrix} \alpha_1 & \beta_2 & 0 & \dots & 0 & 0 & 0 \\ \beta_2 & \alpha_2 & \beta_3 & & 0 & 0 & 0 \\ \vdots & & & \ddots & \vdots & & \\ 0 & 0 & 0 & \dots & \beta_{m-1} & \alpha_{m-1} & \beta_m \\ 0 & 0 & 0 & & 0 & \beta_m & \alpha_m \end{bmatrix}$$

For the computation of the T matrix eigenvalues - algorithm QR

$$\varepsilon_\lambda = |\beta_{m+1} \cdot x(m)|$$

$$X^T A X X^T x = \lambda X^T x$$

$$T \bar{x} = \lambda \bar{x}$$

$$\bar{x} = X^T x$$

$$T_{m-1} = \begin{bmatrix} \alpha_1 & \beta_2 & 0 & \dots & 0 & 0 & 0 \\ \beta_2 & \alpha_2 & \beta_3 & & 0 & 0 & 0 \\ \vdots & & & \ddots & \vdots & & \\ 0 & 0 & 0 & \dots & \beta_{m-2} & \alpha_{m-2} & \beta_{m-1} \\ 0 & 0 & 0 & & 0 & \beta_{m-1} & \alpha_{m-1} \end{bmatrix}$$

$$\hat{T}_2 = \begin{bmatrix} \alpha_2 & \beta_3 & 0 & \dots & 0 & 0 & 0 \\ \beta_3 & \alpha_3 & \beta_4 & & 0 & 0 & 0 \\ \vdots & & & \ddots & \vdots & & \\ 0 & 0 & 0 & \dots & \beta_{m-1} & \alpha_{m-1} & \beta_m \\ 0 & 0 & 0 & & 0 & \beta_m & \alpha_m \end{bmatrix}$$

$$K x = \lambda M x$$

$$T = X^T K^{-1} M X$$

$$\omega_j^2 = \frac{1}{\lambda_j}$$

[home](#)

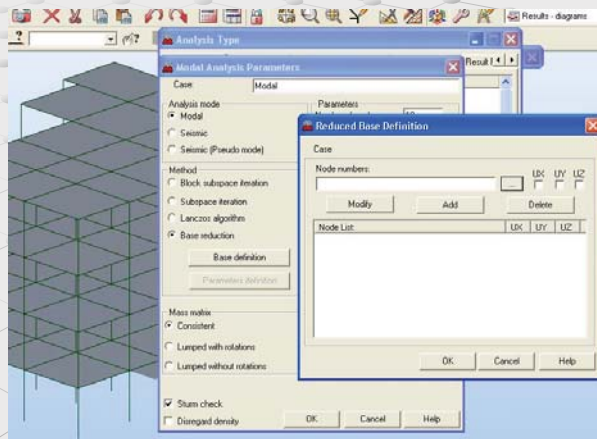
[back](#)

[next](#)



The Basis Reduction Method

- The approach is used for the approximately calculation of the "first" eigenpairs
- There are eliminated the disadvantages induced by the "accidental" eigenmodes
- The "master" joints must be declared, also the directions of the DOFs granted to these joints


[home](#)
[back](#)
[next](#)

The Basis Reduction Method

- The large scale problem

$$K \tilde{\Phi}_i - \omega_i^2 M \tilde{\Phi}_i$$

- The reduced model problem

$$[f] \{\alpha\} - \omega^2 [m_{\text{gen}}] \{\alpha\} = \{0\}$$

[f] – the influence matrix

[m_{gen}] – the generalized mass matrix

$$\{\alpha\} = \begin{Bmatrix} \alpha_1 \\ \alpha_2 \\ \dots \\ \alpha_n \end{Bmatrix}$$

$$\tilde{\Phi}_i \approx \sum_{j=1}^n \alpha_j X_j^*$$

- The solution of the large scale static system $K X_i^* = T_i \quad i = 1, 2, \dots, n$

T_i – the load vector produced by the unit forces

- The reduced problem is solved by Jacobi method $\Rightarrow (\omega_i, \tilde{\Phi}_i^*) \quad i = 1, 2, \dots, n$

[home](#)
[back](#)
[next](#)

The computation parameters implied in the modal analysis

The screenshot shows the 'Modal Analysis Parameters' dialog box. Callouts point to the following parameters:

- Frequency**: The limit period, Circular frequency
- Number of modes**: 10
- The calculus precision (digits)**: 0.0001
- No. of iterations per step**: 40
- Damping (%)**: 0.95
- The Sturm test**: Sturm check, Disregard density
- Consider Mass density = 0**: Disregard density
- The limit of the total participating mass (%) up to compute the modes**: 0

Buttons at the bottom: [home](#), [back](#), [next](#)

The Sturm Test

The procedure is very useful to check if the correct number of modal frequencies was computed, up to the limit specified by the user

$$\rho(v) = \frac{v^T K v}{v^T v} \quad \lambda_1 < \rho(v) < \lambda_N$$

$$K^{(m)} v^{(m)} = \lambda^{(m)} v^{(m)}$$

Using the notations $K^{(0)} = K, \lambda^{(0)} = \lambda, v^{(0)} = x$

the eigenvalues of the reduced problem by one order, denominated by $(N-m-1)$

$$K^{(m+1)} v^{(m+1)} = \lambda^{(m+1)} v^{(m+1)}$$

$$\lambda_1^{(m)} \leq \lambda_1^{(m+1)} \leq \lambda_2^{(m)} \leq \lambda_2^{(m+1)} \leq \dots \leq \lambda_{N-m-1}^{(m)} \leq \lambda_{N-m-1}^{(m+1)} \leq \lambda_{N-m}^{(m)} \quad \text{pentru } m = 0, 1, \dots, N-2$$

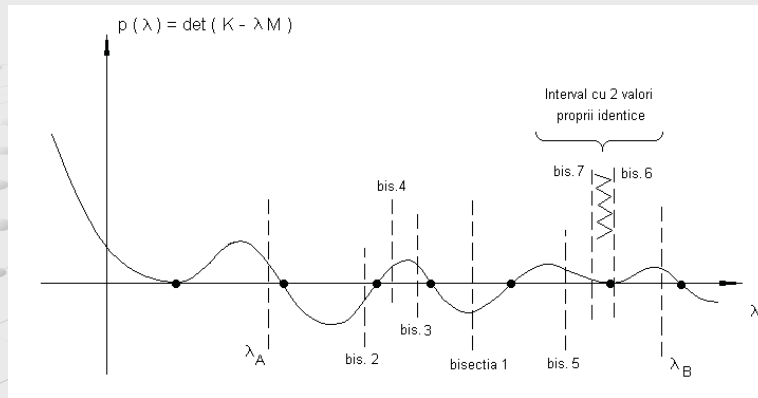
The characteristic polynomial

$$p^{(m)}(\lambda^{(m)}) = \det(K^{(m)} - \lambda^{(m)} I), m = 0, \dots, N-1$$

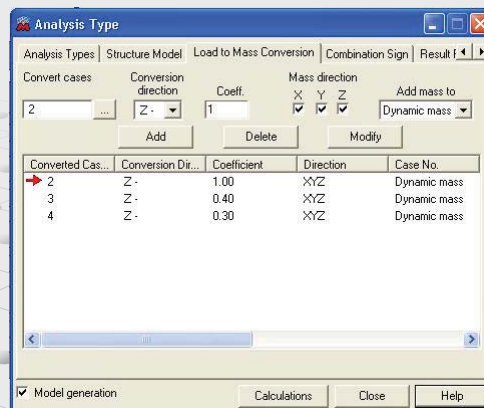
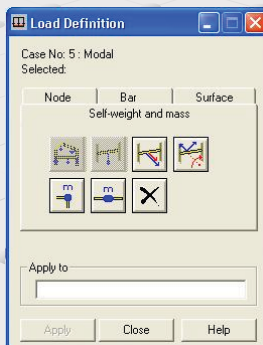
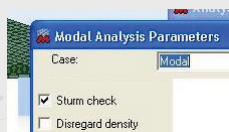
$$p^{(m)}(\lambda^{(m)}) = \det(K^{(m)} - \lambda^{(m)} M^{(m)}), m = 0, \dots, N-1$$

Buttons at the bottom: [home](#), [back](#), [next](#)

The Sturm Test


[home](#)
[back](#)
[next](#)

The mass modeling



The assemblage of the inertia matrix

Mass Matrix

Field for selecting the mass matrix type:

- consistent (consistent matrix - always with regard to the rotational degrees of freedom),
- lumped with rotations (diagonal matrix - with regard to rotational degrees of freedom),
- lumped without rotations (diagonal matrix without rotational degrees of freedom).

[home](#)
[back](#)
[next](#)

Results

- Modes of vibration – eigenpairs (frequencies, periods, circular frequencies; modal shapes)
- Modal participating masses on each direction (absolute / relative)

Robot Millennium - Project: BL_4_3_HEA_260_IPE200_final - Results (FEM): available - [Dynamic Analysis Results - Case: 5 (Modal) Active n

File Edit View Geometry Loads Analysis Results Format Tools Windows Help

1to82 85to124 127 2to21 23to27 29to3 5: Modal 1.10, SRSS

Case/Mode	Eigenvalue	Frequency (Hz)	Period (sec)	Pulsation (1/sec)	Cur.mas. UX (%)	Cur.mas. UY (%)	Cur.mas. UZ (%)	Rel.mas. UX (%)	Rel.mas. UY (%)	Rel.mas. UZ (%)	Total mass UX (kg)	Total mass UY (kg)	Total mass UZ (kg)
5/ 1	77.28	1.40	0.71	8.79	0.01	81.04	0.00	0.01	81.04	0.00	736464.15	736464.15	736464.15
5/ 2	79.59	1.42	0.70	8.92	78.80	0.01	0.00	78.81	81.05	0.00	736464.15	736464.15	736464.15
5/ 3	105.08	1.63	0.61	10.25	2.54	0.00	0.00	81.35	81.05	0.00	736464.15	736464.15	736464.15
5/ 4	739.95	4.33	0.23	27.20	0.01	10.85	0.00	81.36	91.90	0.00	736464.15	736464.15	736464.15
5/ 5	753.95	4.37	0.23	27.46	10.77	0.01	0.00	92.13	91.91	0.00	736464.15	736464.15	736464.15
5/ 6	893.44	5.02	0.20	31.52	0.17	0.00	0.00	92.30	91.91	0.00	736464.15	736464.15	736464.15
5/ 7	2359.18	7.73	0.13	48.57	0.00	4.83	0.00	92.30	96.74	0.00	736464.15	736464.15	736464.15
5/ 8	2361.69	7.77	0.13	48.80	4.82	0.00	0.00	97.12	96.74	0.00	736464.15	736464.15	736464.15
5/ 9	3425.08	9.31	0.11	58.52	0.07	0.00	0.00	97.20	96.74	0.00	736464.15	736464.15	736464.15
5/ 10	4008.69	10.08	0.10	63.31	0.00	0.01	10.68	97.20	96.75	10.69	736464.15	736464.15	736464.15
5/ SRSS	N/A	N/A	N/A	N/A	N/A	N/A	N/A	N/A	N/A	N/A	N/A	N/A	N/A

Validation of the analysis

- 2D - 3D Structures – The sum of the relative participating masses along the main directions $\geq 85\%$!

[home](#)

[back](#)

[next](#)

Results

Case-study: 2D frame – steel structure



5: Modal

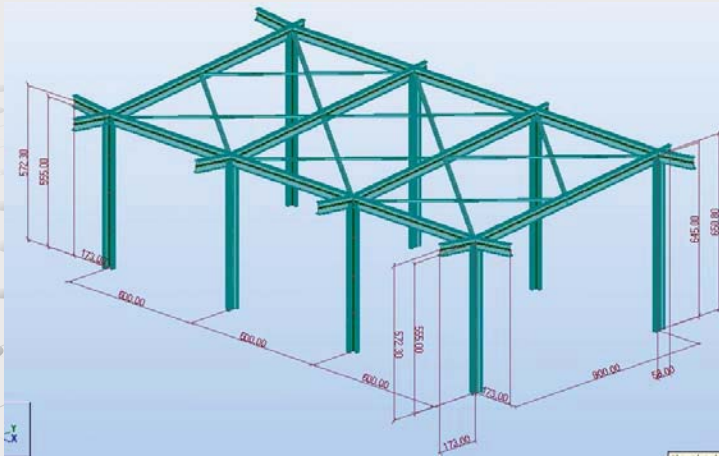
Case/Mode	Eigenvalue	Frequency (Hz)	Period (sec)	Pulsation (1/sec)	Cur.mas. UX (%)	Cur.mas. UY (%)	Rel.mas. UX (%)	Rel.mas. UY (%)
5/ 1	1112.79	5.31	0.19	33.36	87.39	0.00	87.39	0.00
5/ 2	2630.97	8.47	0.12	53.21	0.00	40.28	87.39	40.28
5/ 3	13893.94	18.76	0.05	117.87	7.20	0.00	94.58	40.28
5/ 4	44434.51	33.55	0.03	210.79	0.00	15.11	94.58	55.40
5/ 5	112201.73	53.31	0.02	334.97	0.60	0.00	95.19	55.40
5/ 6	130496.59	57.49	0.02	361.24	0.00	0.37	95.19	55.77
5/ 7	401923.48	100.90	0.01	633.97	0.25	0.00	95.43	55.77
5/ 8	509010.06	113.55	0.01	713.45	0.00	8.97	95.43	64.73
5/ 9	615816.74	124.90	0.01	784.74	0.42	0.00	95.85	64.73
5/ SRSS	N/A	N/A	N/A	N/A	N/A	N/A	N/A	N/A

[home](#)

[back](#)

[next](#)

Case-study: 3D frame – steel structure



next



Case-study: 3D frame – steel structure

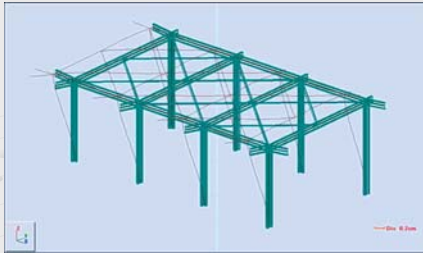
[illegible]

next

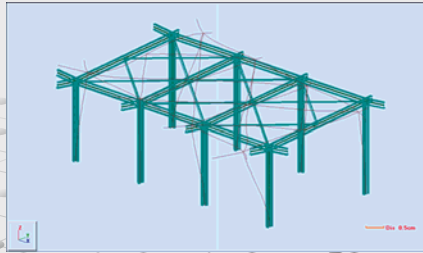


Results

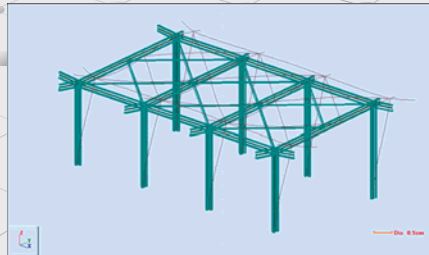
Case-study: 3D frame – steel structure



The first modal shape



The second modal shape



The third modal shape

[home](#)

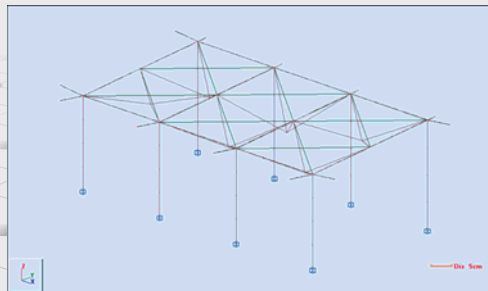
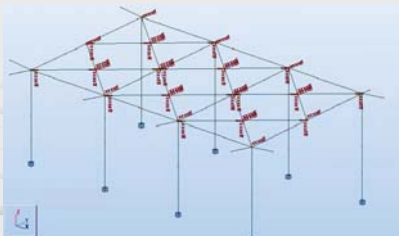
[back](#)

[next](#)



Results

Case-study: 3D frame – steel structure



The first modal shape

Case/Mode	Eigenvalue	Frequency (Hz)	Period (sec)	Pulsation (1/sec)	Cur.mas.UX (%)	Cur.mas.UY (%)	Cur.mas.UZ (%)	Rel.mas.UX (%)	Rel.mas.UY (%)	Rel.mas.UZ (%)
6/ 1	0.07	0.04	23.62	0.27	0.00	0.01	0.78	0.00	0.01	0.78
6/ 2	0.07	0.04	23.62	0.27	0.00	0.00	0.00	0.00	0.01	0.78
6/ 3	0.07	0.04	23.62	0.27	0.00	0.00	0.07	0.00	0.01	0.86
6/ 4	0.07	0.04	23.62	0.27	0.00	0.00	0.00	0.00	0.01	0.86
6/ 5	0.07	0.04	23.62	0.27	0.00	0.00	0.00	0.00	0.01	0.86
6/ 6	0.07	0.04	23.62	0.27	0.00	0.00	0.03	0.00	0.01	0.89
6/ 7	204.50	2.28	0.44	14.30	96.14	0.00	0.00	96.14	0.01	0.89
6/ SRSS	N/A	N/A	N/A	N/A	N/A	N/A	N/A	N/A	N/A	N/A

[home](#)

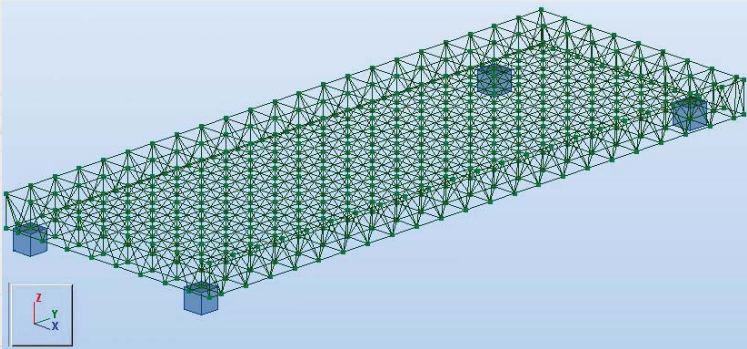
[back](#)

[next](#)



Results

Case-study: 3D truss – steel cover structure



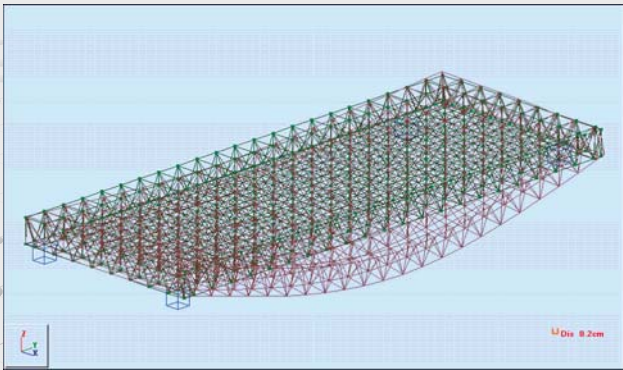
Case/Mode	Eigenvalue	Frequency (Hz)	Period (sec)	Pulsation (1/sec)	Cur.mas.UX (%)	Cur.mas.UY (%)	Cur.mas.UZ (%)	Rel.mas.UX (%)	Rel.mas.UY (%)	Rel.mas.UZ (%)
5/ 1	949.88	4.91	0.20	30.82	0.28	0.00	62.34	0.28	0.00	62.34
5/ 2	1544.29	6.25	0.16	39.30	0.15	0.07	2.7	0.43	0.07	70.11
5/ 3	3736.58	9.73	0.10	61.13	71.68	0.02	0.27	72.11	0.09	70.38
5/ 4	7870.09	14.12	0.07	88.71	0.01	10.51	0.05	72.12	10.60	70.43
5/ 5	12249.30	17.61	0.06	110.68	0.00	4.17	0.42	72.12	14.77	70.85
5/ 6	16375.98	20.37	0.05	127.97	0.01	0.01	0.05	72.13	14.78	70.90
5/ 7	23160.35	24.22	0.04	152.19	0.01	73.57	0.00	72.14	88.35	70.91
5/ 8	33715.93	29.22	0.03	183.62	3.16	0.01	7.92	75.30	88.36	78.83
5/ SRSS	N/A	N/A	N/A	N/A	N/A	N/A	N/A	N/A	N/A	N/A

[home](#) [back](#) [next](#)



Results

Case-study: 3D truss – steel cover structure



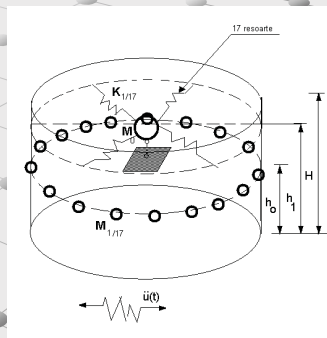
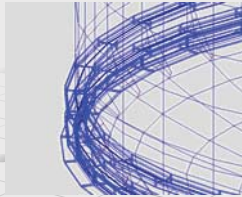
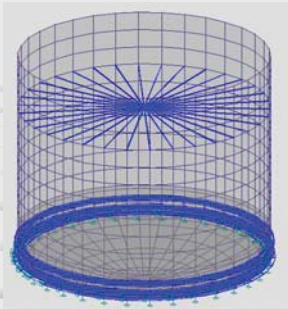
• The first (fundamental) shape (36 MPV computed)

[home](#) [back](#) [next](#)



Results

Case-study: steel water tank



The Housner dynamic model
(as stated in PE 737-92)

[home](#)

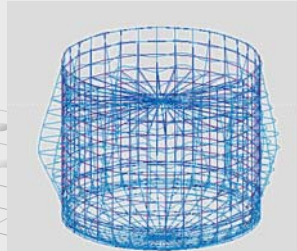
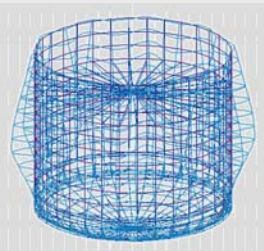
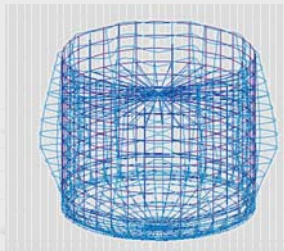
[back](#)

[next](#)



Results

Case-study: steel water tank



The first modal shape

The second modal shape

The third modal shape

Case/Mode	Eigenvalue	Frequency (Hz)	Period (sec)	Pulsation (1/sec)	Cur.mas.UX (%)	Cur.mas.UY (%)	Cur.mas.UZ (%)	Rel.mas.UX (%)	Rel.mas.UY (%)	Rel.mas.UZ (%)
4/ 1	2.74	0.26	3.80	1.65	0.00	23.10	0.00	0.00	23.10	0.00
4/ 2	2.74	0.26	3.80	1.65	23.10	0.00	0.00	23.10	23.10	0.00
4/ 3	274.82	2.64	0.38	16.58	0.00	0.00	0.00	23.10	23.10	0.00
4/ 33	2911.37	8.59	0.12	53.96	0.00	0.00	0.00	23.10	23.10	0.00
4/ 34	4786.95	11.01	0.09	69.19	25.32	25.50	0.00	48.42	48.60	0.00
4/ 35	4786.97	11.01	0.09	69.19	25.50	25.32	0.00	73.92	73.92	0.00
4/ 36	5910.18	12.24	0.08	76.88	0.00	0.00	0.03	73.92	73.92	0.03
4/ SRSS	N/A	N/A	N/A	N/A	N/A	N/A	N/A	N/A	N/A	N/A

[home](#)

[back](#)

[next](#)



Conclusions

- methods: BS, BLSI, Lanczos, BR
- the Sturm check
- the check of the modal participating masses

[home](#)
[back](#)
[next](#)

[home](#)
[back](#)
[next](#)


Manager systems for the topographic monitoring of bridges, during the execution and for monitoring the time behavior under the action of sunlight and wind

Gheorghe Mugurel T. Rădulescu¹ and Corina Rădulescu²

¹Mining Department, North University, Baia Mare, 430041, Romania

²Economic Department, North University, Baia Mare, 430041, Romania

Summary

The wind and the non-uniform sunlight determine oscillations and diurnal movements of the superstructure of bridges, and therefore knowing the characteristics (cause-effect relation, speed, acceleration, amplitude) is essential for preventing the deterioration or destruction of the building.

This paper is intended to present the current possibilities of topographic measurements of the oscillations under the action of wind or exploitation and of the slow diurnal movements under the action of non-uniform sunlight to designers and executants of bridges, and proposes some manager systems for monitoring these inherent phenomena concerning the behavior of real structures belonging to the category of bridges.

The main conclusion of the paper is that, without knowing the parameters of the actual behavior of a designed and executed structure, the validation of the design solution that was used is not possible, and even less its improvement.

KEYWORDS: GPS, classical or laser scanners, video systems, RTK-GPS systems, sensors, stamps, pendulums, laser levels, inclinometers, accelerometers.

1. INTRODUCTION

Monitoring the execution and time behavior of bridges is an activity of maximal importance that ensures respecting the project, validating the design solution and improving the design methods. The classical topographic methods are known: verifying the heights by means of middle geometric leveling, tracing and verifying in the plane by means of angular intersections or using the complete topographic station, which allows the precise measurement of distances, not only of angles. The main disadvantages are the need for the permanent presence of the operator loco-object, and especially the discontinuity of information.

Developing the modern, unconventional topographic methods was allowed exactly by their application to the construction of bridges with high pillars or suspended,

which needed knowing their behavior under the action of wind, non-uniform sunlight or traffic. The new methods have been applied then to the construction of high structures, dams or to the monitoring of railways.

A new chapter of topography was developed, which operates in continuous system, based especially on sensors: Kinematic surveying.

2. THE FRAME OF THE STUDY OBJECT OF KINEMETRIC SURVEYING

From among the applications of Topography in the area of special structures (fig. 1), the „dynamic” part refers to the study, recording and collecting of characteristic parameters of the external influences and of the geometry of the structures, under the action of some variations of some loads in a short period of time (at most 24 h).

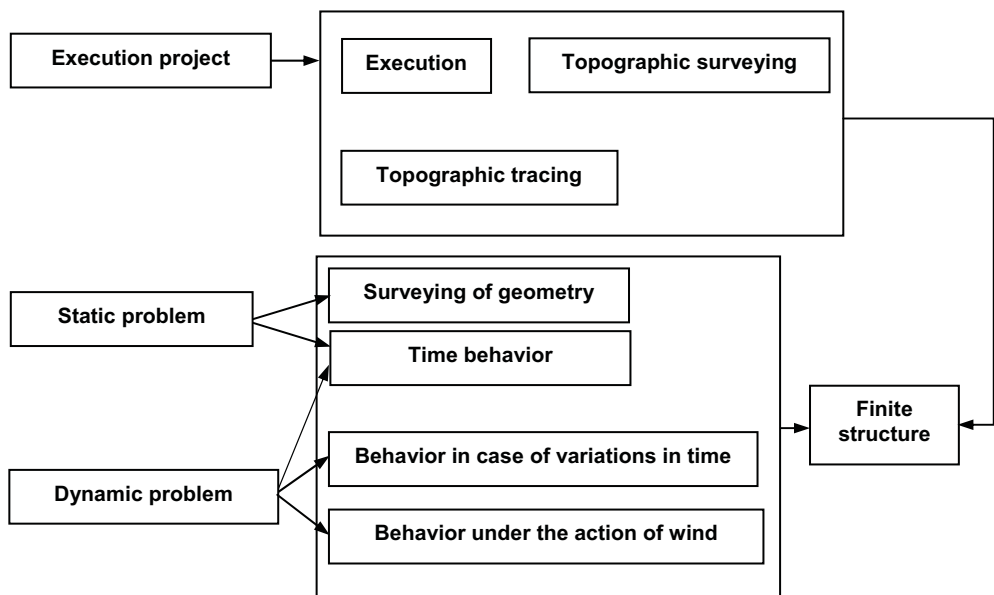


Figure 1. The static problem, the dynamic problem

3. NEW TECHNIQUES, DEVICES, MANAGER SYSTEMS FOR MONITORING THE STRUCTURES IN DYNAMIC REGIME

There have been created classical or laser scanners, video systems, RTK-GPS systems, sensors, stamps, pendulums, laser levels, inclinometers, accelerometers, in general, expert or manager systems for monitoring the structures, in order to

punctually, but mostly continuously, record the response of real structures to various stresses, especially wind, earthquake or diverse exploitation conditions.

Many are created by companies that produce geo-topographic equipment, especially Leica and Trimble, but there have appeared companies whose main activity area is represented by the monitoring of structures in continuous dynamic regime or which produce instruments for this activity.

3.1 Sensor systems

3.1.1. Typical New Sensors

Typical New Sensors systems which monitor the geometry and deformations of bridges is: linear variable displacement transducers (LVDT – a distance measuring device), vibrating wire strain gauges, foil strain gauges (set up in quarter, half, or full bridge strain configurations), inclinometers, crack and joint sensors, tilt sensors, piezoresistive accelerometers, piezoelectric accelerometers, capacitive accelerometers borehole accelerometers, servo force balance accelerometers and total stations.

The effort focuses on the design and development of a self-displacement measurement device and a wireless data communication system. The diagnosis techniques will include finite-element modeling of the suspension bridge, modeling and measurement of strong wind, earthquakes and traffic loadings, analysis of the ambient vibration data through the use of the technique to eliminate the use of an exciter, a global damage diagnosis technique to identify and characterize the damage, and selection of sensors and techniques to detect localized damage and defects.

The News concept of monitoring bridges combines on-site inspections of the building by static and/or dynamic measurements with Finite-Element calculations and remeasurements at specific times. Typically we conduct a detailed basic measurement to determine the modal parameters and static properties of the bridge. The optimization process is used to calibrate a FE- model representing the realistic dynamic behavior. These surveys show that it is already possible to evaluate the bridge condition and to calculate realistic reliability indices based on vibration measurements. In principle it is possible to operate bridge-monitoring systems on a periodic or continuous base:

- Periodical testing: measuring the vibration behavior is carried out in specific time intervals. Sensor location should be in accordance with the initial measurement.
- Continuous monitoring: sensors are installed permanently to the bridge, providing a continuous data concerning bridge condition.

3.1.2. Sensor Network

A significantly new research challenge is the need to integrate multiple sensor streams to develop local and global health-state indicator variables that need to be queried and monitored by the system. The indicators may be defined as user-specified aggregates (or other functions) over instantaneous values of several data streams, covering one or more sensors.

The sensor network may consist of a dense array of heterogeneous sensors (e.g., strain gages, accelerometers, cameras, potentiometers, ... etc.). In addition, the network must be easy to deploy, scalable – allowing for progressive deployment over time, and must allow for local processing and filtering of data, remote data collection, accessibility and control. Communicating with sensors has long been limited either to wired connections or to expensive, proprietary wireless communication protocols. Using a ubiquitous and inexpensive wireless communication technology to create Fixed Sensor Area Networks (FSANs) will accelerate the extensive deployment of sensor technology.

3.1.3. The Cambridge Monitoring System (CMS)

The Cambridge Monitoring System (CMS)(fig.2) is a new, ultrasonic-based monitoring system primarily for concrete structures but with possible application to structures made of other materials. Cambridge Ultrasonics has successfully developed an R&D prototype system that works well.



Figure 2. The Cambridge Monitoring System (CMS)

What CMS provides:

- * Regular, automated inspection of chosen locations on the structure at a frequency chosen by the operator (for a network of 100 sensors the inspection period could be as frequent as 50 times a day per sensor).
- * Uses injected ultrasound (not acoustic emission) with advanced pattern recognition signal processing to reject operational noise.

- * Uses advanced decision-making algorithms to decide if any change has happened at a test location.

- * Combines results from more than one test location to give a result for any part of the structure or the whole structure in the form of a probability of significant structural change.

- * Presents warnings in various forms: CAD representation of the structure showing locations of change, e-mail message or similar to a central control, audible warning, etc...

Benefits of using a CMS system:

- * Improves safety of operating concrete structures.

- * Helps make better use of repair budgets by directing inspection or repair to where most change is happening.

- * Extends working life of older structures - particularly beyond the normal working life.

- * Low annual running costs - automated system does not need a full-time operator.

- * Provides audit trail of any structural change in the event of litigation relating to integrity.

A network of intelligent, CMS sensors is attached to the structure to be monitored and connected by cable or radio back to an Archive PC. Each sensor injects a known pattern of waves into the part of the structure to which it is attached and each sensor collects echo-waves back from the interior of the structure. CMS is not an acoustic monitoring system, which is a passive monitoring system and which is potentially very sensitive to operational noise.

3.2. Trimble® GX™ 3D Scanner



Figure 3. Trimble® GX™ 3D Scanner

The Trimble® GX™ 3D Scanner is an advanced surveying instrument that uses high-speed laser and video to capture vast amounts of coordinate and image data. Trimble® RealWorks Survey™ office software is part of an integrated 3D scanning field and office software suite for surveyors and engineers. Taking advantage of the rich point cloud data provided by the Trimble GX,

RealWorks Survey manipulates and manages large scan files to produce dramatic and compelling 2D and 3D deliverables. The software also supports data collected using GPS and total station techniques, so you can coordinate and combine data from a surveying job in one project file for an Integrated Surveying™ solution.

Therefore, if benchmarks are assembled on the surveyed structure, these can be monitored in continuous regime, 24/7, recording the displacements of the bridge, under load or under the action of wind or non-uniform sunlight.

3.3. Digital & Electronic Levels



Figure 4. Electronic and digital level

Digital and electronic levels create a new standard for leveling on construction sites. They are easy to use, take measurements in double quick time and minimize human error, and the application programs on board further enhance leveling work.

One of the most precise methods for monitoring the time behavior of bridges is the middle geometric leveling, digital and electronic levels allowing the increase of the precision of recording the small displacements in time.

3.4. GeoMoS Monitoring Software

GeoMoS consists of a Monitor and Analyzer application. **Monitor** is the real-time application of GeoMoS responsible for data collection and online measurement control, limit checks, status messaging and measurement cycle control. **Analyzer** is

the analysis application of GeoMoS responsible for analyzing and reporting of the measured data plus editing and post-processing of data where required. Data and results can be viewed numerically or graphically and exported in various standard numerical and graphical formats.

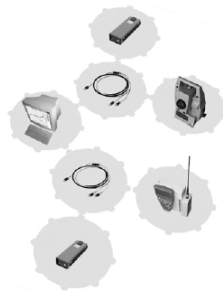


Figure 4. The equipment of the Geomos method

Connection of different sensors (e.g. TPS, GPS, meteorological sensors, geo-technical sensors) is handled by a LEICA Sensor Manager component, which also provides an interface for sensor configuration.

Sensor Connections: Total Stations, GPS Sensors: Leica GPS System, Connection to GPS Spider for advanced, Tilt Sensors, Meteorological sensors (e.g. temperature, pressure), Geo-technical sensors (e.g. extensometers), Sensors from other manufacturers

Software Features: Supports a project concept for periodic monitoring projects, System can be remotely accessed and configured, Scalable configurations from single station to multi-station configurations, Large database support with multi-user access (SQL-Server), Multiple number of measurement stations connected to the system, Parallel use of several sensors (TPS, GPS, meteorological and geo-technical sensors), Automatic data dispatching and synchronization using cable, radio link, LAN, WAN or Internet, Long distance measurement capability (up to 5 km), Meteorological network modeling over measurement area, Powerful Analyzer, Toolbox for visual and alphanumeric analysis, Editing and Post-processing throughout data history, Powerful status message management (e.g. limit exceeded, power failure, burglary), Status messages via E-mail or Digital I/O Interfaces, Import/Export to other systems (ASCII, DGN, WMF, standard Excel formats), Automatic Backup and Archive.

Applications: Deformation Measurements (e.g. dams, tunnels, volcanoes, bridges and high-rise buildings), Landslide and Settlement Detection (e.g. mining), Automated Surveys (e.g. continuous, automated measurements).

3.5. The Campbell system for monitoring bridges

A large number of bridges from Ireland, Australia, USA, and Canada have been monitored using the system presented in the sequel.

Campbell Scientific data acquisition systems' versatile capabilities make them ideal for structural and seismic monitoring. These data-loggers have been used in applications ranging from simple beam fatigue analysis, to structural mechanics research, to continuous monitoring of large, complex structures.

Highway overpasses, roads, buildings, retaining walls, bridges, and amusement park rides are the types of structures for which our systems provide remote, unattended, and portable monitoring. These data acquisition systems make reliable structural measurements, even in harsh environments.

System Benefits: Onboard, programmable, excitation is provided for ratiometric bridge measurements.

Systems provide triggered output with pre-trigger data capture capability.

Most sensors and communications options can be used, allowing systems to be customized to meet exact needs. Systems operate reliably in harsh environments.

Scan rates range from a few hours to 100,000 times per second. Systems can report conditions by calling out to pagers, radios, or phones. Systems support long-term, unattended data storage and transfer. Pick-and-click software facilitates programming.

Monitoring and Control: The versatility of systems allows them to be customized for each application. We offer a range of data-loggers from the most basic system with just a few channels, to expandable systems that measure hundreds of channels. Scan rates can be programmed from a few hours to 100,000 times per second, depending on the data-logger model. Measurement types, recording intervals, and processing algorithms, are also programmable. Data-loggers not only provide advanced measurement capabilities, but can also control external devices.

The configurable data-logger models, the CR9000X and CR9000XC, allow customizing a system with the channel types that best fit your application. The number and type of channels on most of our data-loggers are expandable using multiplexers and other measurement peripherals.

3.6. Using the GPS technology for monitoring bridges

It should be specified that the first use of GPSs in engineering was for monitoring bridges, in the '80, the development of professional GPSs was possible precisely because of these applications. The following applications were for monitoring very high-rise buildings, and the execution and monitoring the time behavior of the Petronas and Taipei 101 buildings was accomplished using this technology.

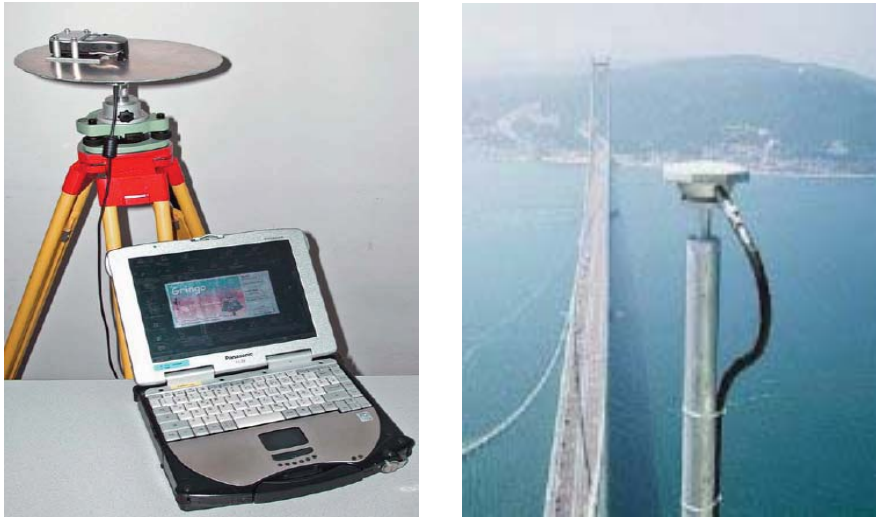


Figure 5. GPS technology, of geodesic rank can be used for monitoring bridges. A network of precise GPS reference stations, has been installed on the world's longest suspension bridge in Japan to monitor movements of the bridge's structure in real-time, with millimeter-level accuracy.

The Global Positioning System (GPS) is used for many purposes in surveying and geodesy like cadastral surveys, engineering surveys or intercontinental coordinate frames. The main characteristics of the GPS technology of geodesic class are: used signal code and phase in general 2 frequencies, accuracy 0,001 to 0,1 m, appr. costs 20-50000 €.

The technology is simple and easy to use. Therefore, the GPS antenna is assembled on the monitored structure, recording the position, in continuous regime, through coordinates in the WGS1984 worldwide system, then trans-calculating it in national system and then, for simplification, into a local system. The displacements, oscillations, displacement speed, hence, all the parameters that define the time behavior of the structure under the action of wind or exploitation, are established comparing the coordinates of the axis of the antenna, at various moments.

4. CONCLUSIONS

The monitoring of the execution of bridges is an activity of great importance, validating the adopted design solution and providing data for building the data-bank concerning the behavior of this kind of structures under the action of stresses. The classical solutions for monitoring the execution are still valid, can be used, and are used for small works. Modern, unconventional solutions have more advantages

that make them vital now, the continuity of recordings, the better quality of recordings, the increased precision, the independence of measurements of the weather conditions being the most important ones. The high cost of the unconventional technologies cannot represent a disadvantage, because the applications are performed for highly technical works, with very large values, the benefits of application couldn't be neglected.

References

1. Aziz .W., *Monitoring High-Rises Building Deformation using GPS*, Dept. of Geomatic Faculty, Univ. technology Malaysia,
2. Barber D, Mills J, Bryan P (2002) *Experiences of terrestrial laser scanning of close range structural recording*. Proc. CIPA WG 6, 30 Sept. 1-2, Corfu, Greece. Pp 121-126. 2000
3. Celebi M., *GPS monitoring of structures in real-time: Recent advances*, U.S. Geological Survey, Menlo Park, USA, 2000
4. Gordon, S. J., Lichti, D. D., Chandler, I., Stewart, M. P. and Franke, J. (2003b) *Precision Measurement of Structural Deformation using Terrestrial Laser Scanners*, Proceedings of Optical 3D Methods, Zurich, Switzerland, 22 - 25 September, pp. 322 - 329.
5. Jeffrey A., *Monitoring Structural Deformation at Pacoima Dam, California, Using Continuous GPS*, Unites States Geological Survey, 1999
6. Lichti, D. D., Gordon, S. J., Stewart, M. P., Franke, J. and Tsakiri, M. (2002) Comparison of Digital Photogrammetry and Laser Scanning, Proceedings of CIPA WG 6 International Workshop on Scanning Cultural Heritage Recording, Corfu, Greece, 1 - 2 September, pp. 39 - 44.
7. Nistor G., *Geodezie aplicată la studiul construcțiilor*, Editura Gh.Asachi, Iași, 1993
8. Roberts G.W. , col., *Real -time Deformation Monitoring of Structures Using GPS-Accelerometers*, Univesity of Nottingham, 1999
9. Sadek F., *Vibration Control of Tall Buildings Using Mega Subconfiguration*, Jurnal of Engeenering Mechanics Vol. 123, No. 6, VI-1997
10. * * *, *Prospecte de firmă Leica, Sokkia – Sokkisha, Zeiss, Nikon, Topcon, Zeiss, Ashtech, Trimble, Mercator*
11. * * *, *Motoarele de căutare Internet : Google, Yahoo, Alta Vista, Lycos, Excite, Webtop, Go, Hotbot*
12. * * *, *Colecția revistei topografilor americani* POBONLINE, 1995-2003
13. * * *, *SITE-urile Internet: kia-net, skyscraper.com, gi.geo-tu-dresden.de, lsg.polyu.edu.k, leica-geosystem.com, topcon.com, geotronics.se, lasertech.com, ashtech.com, sokkia.com, trimble.com, zeiss.com, nikonusa.com, mercator gps system.com.*
14. * * *, *Condor Earth Technologies, Real -time Monitoring Systems, USA, 2000*

Real and virtual in Bridge Engineering

Constantin Ionescu¹

¹“Gh. Asachi” Technical University of Iași, 700050, România

Summary

The paper presents from a logical point of view, two worlds specific to the bridge engineering: the real state and the virtual state.

A bridge real world is connected with two cycles of the bridge engineering more exactly the bridge construction and exploitation. The bridge real world analysis uses models and techniques with different abstractisation degrees. The final result for this world is the creation of several models and the modeling function is realized by observation, testing and reasoning.

The virtual world is defined by the ensemble of concepts, methods and models corresponding to a certain part of the real world. This ensemble organized under the form of a system interacts with a mechanism (a natural intelligence or an artificial intelligence) capable of creating the system image and to communicate with other intelligent systems in order to determine the image of the final system. The system image represents the virtual world of the bridge.

A first consequence of the real and virtual state interpretation is the possibility of simulation through different methods: system expert, artificial intelligence, neuronal networks. From the simulation can result a certain level of complexity and abstractisation in the creation of the real world.

The virtual world can be identified with the bridge design cycle and with the technical quality inspection of the project and the construction, including the project and bridge expertise.

KEY WORDS: bridge, real, virtual, modeling methods, inspection, expertise

1. INTRODUCTION. THE BRIDGE SYSTEM COMPLEXITY

The bridges are built in order to satisfy the users' necessities for a certain social order. The variety of the emplacements and the crossed obstacles imposed to the designers the creation of a bridge universe.

A bridge complexity can be analyzed from two essential points. The first one is determined by the bridge area complexity. This is defined by the interaction bridge

constructive system with the communication way which crosses the obstacle, with the crossed obstacle and the environment, fig. 1.

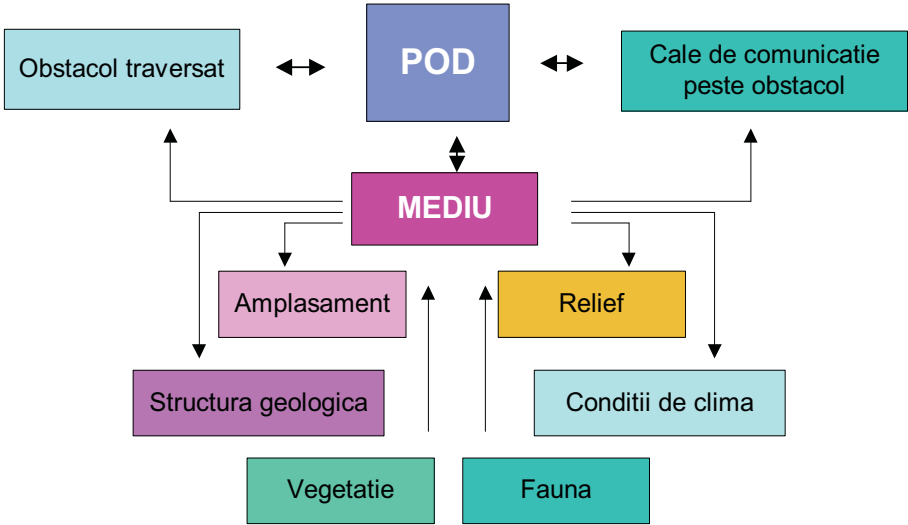


Fig.1. Interaction in the bridge area

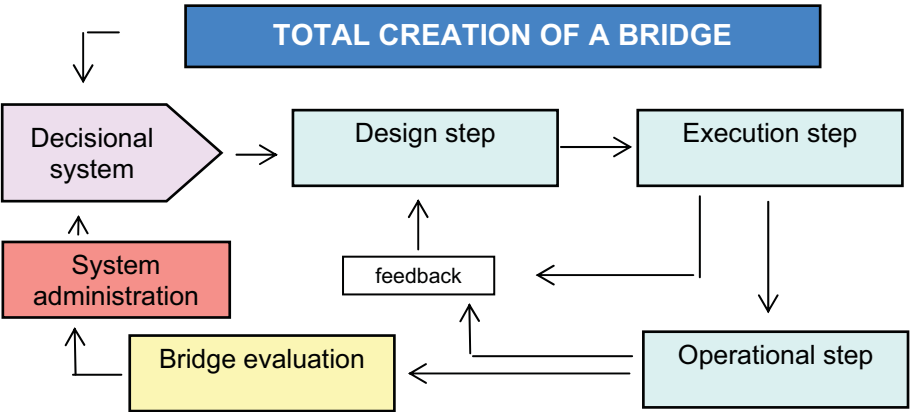


Fig.2. A bridge creation process cycle

The second proceeding refers to the bridge system. A bridge cycle starts with the social command till the design phase, followed by the construction step, the exploitation cycle and finally the bridge replacement moment, Fig. 2.

The big complexity systems which include also the bridges, subjected to the incertitude principle, need the development and application of specific methods of modeling, analysis, simulation and optimization of these systems.

The incertitude, for the bridges, is a structural type and has three sources:

- a. the big dimension of the system;
- b. the system complexity which determines the interaction between the bridge subsystems and between these and the environment;
- c. nonlinearity of the processes.

Big complexity system [1] is a system S , which has the following properties:

- a. Is formed by a multitude of systems S_i such as:

$$S_i = \{U_i, X_i, V_i, W_i, Y_i, \varphi_i, g_i, h_i, T\}; \quad (1)$$

- b. The system S dimension, expressed by the state vector dimension $x \in X$, overcomes a certain limit;
- c. The interaction structure between the S_i subsystems has an important degree of complexity;
- d. The processes involved in system S are nonlinear;
- e. The system S behavior is under the incertitude principle.

In the relation (1) the symbols U_i, X_i, V_i, W_i, Y_i represent the entrance, state, interaction, disturbance and exit; φ_i, g_i, h_i , means the transition function, interaction and exit and T is the time t variable multitude.

The incertitude principle is: „the state x_i of a subsystem of a big system, composed from n interconnected subsystems and their interaction, v_i , with the other $n-1$ subsystems can be simultaneous determined only to a certain accuracy degree”.

Regarding the incertitude concept is necessary to mention the opinion of several experts which consider that the incertitude in the system comes from inaccuracy, of the model, of the language etc., which comes from the lack of knowledge.

2. VIRTUAL IN THE BRIDGE ENGINEERING

The reality and the technical systems study, which are part of this reality, has as final result the real world modeling and its replacement with models. The reality modeling is based on theoretical and experimental research characterized by different complexity levels and different levels of abstraction.

The models, principles and concepts specific to a technical system and the intelligent techniques (natural and artificial), capable to realize the system image and interact with other intelligent systems, represents the virtual world of the technical systems.

The structure (configuration and architecture) of a technical system, such as bridges, can be determined in two ways:

- a. With the graph associated to the system, by which are determined the elements of the system (subsystems), the interactions between these, entry/exits, fig.1. The subsystems are in the graph node and the interactions between subsystems are represented by arches;
- b. By models associated to the system. These can be mathematical models, heuristical methods and their combination, mathematical – heuristical models.

Between the system and his model must be a perfect compatibility. The system structure depends on the researcher knowledge and it is obtained through a complicated operation.

Between the steps of a bridge creation, Fig.2., the design is part of the bridge engineering virtual world. The bridge designer uses analytical models for calculus, which were developed in time, by theoretical and experimental researches or by the study of the bridge behavior.

The design step models, principles and concepts are based on the knowledge from the theoretical mechanics, materials resistance, construction statistics etc. Among the principles are: the inertia principle, the forces interdependence principle, the equality of action and reaction principle, the virtual displacement principle etc.

For example, in order to express the equilibrium state for a certain system, subjected to a system of forces can be used the virtual displacement principle. This is: “in order for a system to be in equilibrium state it is necessary and sufficient like the sum of the virtual mechanical things adequate to all the forces which interact with the system to be zero for any virtual displacement compatible with the bonds”.

In order to apply this principle, a system must have one or several degrees of liberty and to be subjected to a system of forces action to be in equilibrium. Due to the equilibrium state, the forces action doesn't give to the system a real kinematic displacement. It can be imagined that independent on the exterior forces action, the system would have a very small displacement compatible with the bonds that might transfer it into a infinite next position. This displacement is called virtual displacement.

In order to apply the virtual displacement principle, a system must find itself into two different positions, a real one and another infinite, chosen by the system displacement from the real position. The new position is fictive, virtual.

In the above demonstration, the real and the virtual state are part of the virtual world, the system image created by the designer.

The bridge system, in the design phase, considering the virtual world concept, offers to the designer the objective premises of the future reality.

The designer work with analytical, heuristic and mathematical-heuristic models determines in the design phase several alternatives for the same system. Finally the solution choice is done by an optimization process.

The model concept saw a new evolution during the simulation technique with the PC. The simulation with hybrid models considers the existence of several interconnected models. At least one of them is a model of numerical simulation, a model of discrete events or a model based on knowledge.

In the virtual world of the bridges systems the researcher has limited degrees of liberty. The real world restrictions consider the bridge system structure and the incertitude which can be objective or subjective.

3. REAL IN BRIDGE ENGINEERING

A system transfer from the virtual world in the real world is done by the system construction and its exploitation.

At the limit between the virtual world and the real world is the bridge system project. The project in the final state is in the real world. The first operation proper to the real world is checking out the project quality, by the project verifier. The project quality is determined by the designers' team, in the virtual world, during the project. The neglect of the performance criteria, by the project, observed during the quality checking, implies the transfer from the real world in the virtual world in order to be recalibrated (revival of the mathematical and heuristic modeling).

The project materialization of what the designers imagined represents a main step of the real world. Once the bridge is done, the engineers realize the quality works.

The execution step ends with the construction reception and the construction technical book.

In the real world, after the bridge reception, follows the bridge exploitation cycle, where the main activities are determination of behavior in exploitation by direct examination of the bridge behavior or with observation and measurement. The bridge testing represents a process of the real world.

The conclusions of the activities done so far are the construction expertise, if is the case and the decision to interfere for the reconstruction, consolidation etc.

The virtual activities in the real world refer to stocking and data processing came from determination in time of the bridge behavior and expertise. The knowledge and information obtained from the data processing are used in the design cycle for

the project rehabilitation-consolidation, of the considered bridge, or for the future bridges design.

The technical state simulation is an activity of the virtual world. The simulation can be done by analytical and/or heuristic methods, based on the data and information from the determination in time of the bridge behavior.

4. CONCLUSION

4.1. The total realization of a bridge analysis from the point of view of the two worlds, real and virtual, opens a new frontier for interception, stocking and processing of new information and knowledge, fig.3.

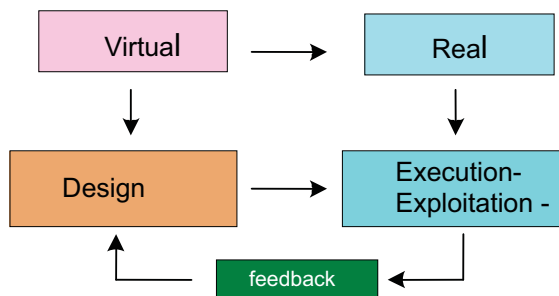


Fig.3. Dissociation between real world and virtual world

4.2. A consequence of the bridge real and virtual world concept is the possibility of applying the simulation in different methods: the expert system, artificial intelligence, neuronal networks etc.

4.3. The new concepts, methods and models available for a certain part of the real world, specific to the Bridge Engineering and their transfer in the virtual world of the bridges can lead in the future to the creation of bridges with superior technical characteristics.

References

1. Stănculescu, Fl., Modelarea sistemelor de mare complexitate, Ed. Tehnică, București, 2003. (in Romanian)
2. Ionescu, C., Simulation of the Technical Condition of Bridges in Design Stage by Real Behavior in Time Scenarios, The Second International Congress on the Behaviour of Damaged Structures, DAMSTRUC'2000. (in Romanian)
3. Barbu, Gh., Modele de simulare cu aplicații în Fiabilitate, Editura Tehnică, București, 1992. (in Romanian)

Considerations on the building of the bridges in Neamț historical area and the rivers Bistrița and Moldova

Raluca Popa and Constantin Ionescu

"Gh. Asachi" Technical University of Iași, 700050, România

Summary

The goal of this paper is to provide a review, based on chronicles, reference literature and on-site observations, of the most important bridges built in the historical area of Neamț and its surroundings, over Siret river and its most important affluents: Bistrița and Moldova.

The analysis pertains mainly to the bridge of "șeici" built in Tupilați, over Moldova River. This bridge exists since 1676, as documented in Mihail Sadoveanu's novel "Nicoară Potcoavă". During the past century an eleven-opening bridge on straight beams with cantilevers was built on the same location.

Other bridges presented herein are: the bridge built in 1952-1953 over Bistrița in Bicaz (with an opening of 85 m) and the bridge over Moldova in Timișești (reinforced at the end of last century and the beginning of this century). The bridges over Bistrița in Bacău and over Moldova in Roman are briefly discussed. Notably, the bridge in Roman (reinforced a few years ago) was doubled in the second part of the last century by a bridge with a solution of totally precast superstructure.

The paper also investigates the impact of the catastrophic floods recorded in the summer of 2005 on the exposed bridges.

KEY WORDS: bridge, constructive systems, history.

1. INTRODUCTION. NEAMȚ HISTORICAL AREA

Situated in the central – eastern part of Romania, on valleys of clear and fast waters (Bistrița, Siret, Moldova), guarded by the peaks of Bistrița mountains and Ceahlău massive, Neamț area is rich in historical connotations.

The first medieval urban settlements in Neamț area are documented around the time of Bogdan the First's coronation on Moldova's throne (1359-1365). These settlements evolved from some older rural structures placed at the crossing of commercial roads or on the stream of important rivers: (Crăciun's) Piatra on Bistrița, Roman at the confluence of Moldova and Siret rivers, and Neamț on the

river Ozana (also called river Neamț) - see fig.1. Recorded for the first time in the chronical “Story of the old times” or “Letopisețul Novgorodului”, the cities Neamț, Roman and Piatra are considered to be, at least from an archeological point of view, older.

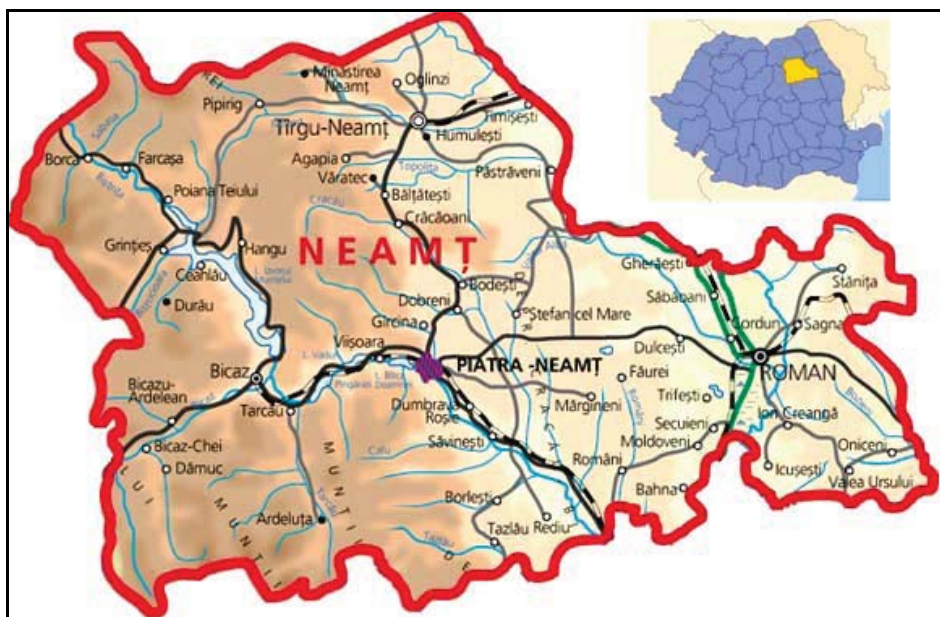


Fig.1. Historical area Neamț

The historical area Neamț is crossed by a dense hydrographic network. The most important rivers of the area, taking into account their discharges, are: Siret, Moldova and Bistrița.

2. HYDROGRAPHIC NETWORK IN NEAMȚ AREA

Siret river is the biggest of the Romanian interior rivers in terms of discharge (at river mouth 222 mc/s) - see tab.1. It outflows from the mountains Carpații Păduroși and enters the country near Siret city, crossing Sucevei Plateau and the corridor that bears its name between Subcarpații Moldovei and Bârladului Plateau. From Mărășești, it enters Câmpia Română and flows in Dunăre, west of Galați. The hydrographic basin of Siret is asymmetrical, having affluents on the right side that outflow from Carpații Orientali. Some of these affluents are: *Suceava*, with the affluent Putna, with Sucevița that outflows from Obcinele Bucovinei and *Moldova* with the affluent Moldovița, with Neamț (Ozana) that outflows also from Obcinele Bucovinei. Ozana (Neamț) river is a right affluent of Moldova.

Tab.1.1. The main streams in Neamț area

RIVER	AFFLUENT/RIVER	AFFLUENT/CREEK
1. Siret, right affluent of Dunărea river south of Galați, total length: 740 km., outflows from the mountains Carpații Păduroși	1.1. Moldova, right affluent of Siret river downstream of Roman, total length : 216 km., outflows from Obcina Sucina	1.1.1. Neamț , named Ozana in the superior course, l.t.:54 km., right affluent of Moldova river at Timișești, outflows from Stânișoarei Mountains
		1.1.2. Toplița , l.t.:54 km., right affluent of Moldova river at Păstrăveni, outflows from Stânișoarei Mountains
	1.2. Bistrița, right affluent of Siret river in Bacău, total length : 290 Km., outflows from Maramureșului Mountains	1.2.1. Cracău , l.t.:50 km., left affluent of Bistrița river at Roznov, outflows from Stânișoarei Mountains
		1.2.2. Bistricioara , l.t.:55 km., right affluent of Bistrița river at Ceahlău outflows from Călimani Mountains
		1.2.3. Tarcău , l.t.:? km., right affluent of Bistriței la Tarcău, outflows from Tarcăului Mountains
		1.2.4. Bicaz , l.t.:35 km., right affluent at Bicaz, outflows from Hășmașul Mare

Neamț river outflows from the mountain region of the carpathian flysch, from underneath Halauca peak and goes through Pipirig depression, then through Ozana-Topolița (Neamțului) depression from west to east, crosses Târgu Neamț city and flows into Moldova, downstream of Timișești, with a total length of 57,2 km. In the carpathian area it gathers affluents, mostly on the right side: Dolhesti, Domesnic and Secu. In the subcarpathian depression it gathers its most important affluent, Nemțisorul (that outflows from underneath Chitigaia peak), on the left side.

Another important affluent of Siret is **Bistrița** with its affluents: Dorna, Neagra, Bistricioara, Bicz, Tarcău and Cracău. Bistrița is the biggest affluent of Siret river. It outflows from Rodnei mountains (Lake Lala), goes through Dornelor depression and then through a sector of narrow passes at Toance between Giumalău and Bistriței mountains. At Hangu the valley widens having the appearance of a depression occupied by the anthropic lake Izvorul Muntelui (33 square kilometres). From Piatra Neamț until its flow into Siret near Bacău, it crosses Subcarpații Moldovei (Cracău – Bistrița depression). Since 1970 a „necklace” of seven microhydro-electric power plants was built on Bistrița river. Also the biggest artificial lake („Izvoru Muntelui”), with a retention volume at normal level of 1.130 mil. Mc, was created here.

3. ROAD NETWORK IN NEAMȚ AREA

Moldova has representative works in fields like road transportation, bridges and other works of art. Since 1862, within the Ministry of Agriculture, Commerce and Public Works twelve divisions were founded for roads and bridges maintenance works, most notably those located in Bacău (Roman, Bacău and Putna) and Iași (Suceava, Neamț and Iași). The current roads that provide access to Neamț historical area are built along the old passages towards the region. Examples of such road accesses are: București-Bacău-Roman-Piatra Neamț; Vaslui - Negrești – Roman; Iași - Târgu Frumos – Roman; Vatra Dornei - Poiana Teiului and Gheorgheni - Bicz and railroads: București – Bacău - Roman/Bicz and Suceava/Iași - Pașcani - Târgu Neamț.

Neamț historical area is now crossed by a relatively dense network of national roads (eight roads: DN2, DN12C, DN15, DN15B, C and D, DN17B and DN28), totalling a length of 407.228 km., district roads (44 roads: DJ207D, DJ207K, DJ208C, DJ208G, DJ209B etc.) totaling a length of 758.58 km. and communal roads (124 roads measuring 644.415 km.).

The most important localities (towns and cities) of Neamț area are crossed by the following national roads: DN15, going through Piatra Neamț and Bicz; DN15D, crossing Piatra Neamț and Roman; DN2, intersecting Roman; DN15B and C,

going through Târgul Neamț; and DN12C, superposed on some of the streets of Bicaz city.

Among the district roads we mention: DJ208C, with the direction Târgu Frumos - Hanul Ancuței – Girov; DJ207D, with the direction Sagna – Ion Creangă – Recea – Icușești – Bătrânești; DJ207K, with the direction Sagna – Buruienești – Rotunda – Doljești; DJ209B, with the direction Mălini – Stănișoara – Borca .

4. NOTES ON SELECTED BRIDGES IN NEAMȚ AREA

Among the first documented bridges in the region is the one in Tupilați, mentioned in Mihail Sadoveanu’s novel “Nicoară Potcoavă” [2]: “Haramin’s Inn was placed at a road crossing going towards Roman and Piatra, towards Baia, towards Valea Siretului and country’s capital. In Tuchilați, where there was also a bridge over Moldova’s water, a fair took place that day The very same day of Monday, before sundown, wandering travellers came to Siret’s bank for crossing, at a bridge that was Vercicani’s border line. It was an old and well-known bridge, spanning from one shore to the other, on *șeici*, tied with cable on both shores by huge oak trees.”



Fig.2. Bridge over Moldova in Tupilați

A bridge of reinforced concrete on Gerber girders with a total length of 304 m was built instead of the old bridge in Tupilați between 1911-1914. During the second world war, a portion of the bridge (220m in length) was destroyed and reconstructed afterwards - see Fig.2 .

The construction of definitive bridges flourished at the end of the XIXth century and the beginning of the XXth century. Many important constructions were built up until the First World War, predominantly from reinforced concrete and metal.

The most notable opening built in Moldova during this period is the bridge over Bistrița in Broșteni, with an opening of 78 m, built-in arches and overhead runway. The bridge was destroyed during the First World War and rebuilt using a different technical solution, continuous beam of reinforced concrete on three openings.

Bridges were built in other solutions too, generally beams with cantilevers on openings smaller than 24 m (for example, the bridges over Moldova at Tupilați and Mălini with eleven openings of 20,8 m each and two openings of 5,6 m) [3,4].

The war was followed by a period of reconstruction of the destroyed bridges, so no significant accomplishment can be reported in this respect. Immediately afterwards the construction of bridges in a wide variety of solutions began: vaults with overhead runways of reinforced concrete built on scaffoldings, falseworks with or without precasted elements, continuous beams and frameworks of reinforced concrete or metal beams with reinforced concrete plate -see tab.2.



Fig. 3. Poiana Teiului Viaduct

Some of the most representative works in Neamț historical area, constructed on vaults of reinforced concrete with overhead runways, are the bridge over Bistrița in Bicăz (with an opening of 85 m, constructed during 1952-1953) and Poiana Teiului viaduct (with a total length of 669m, built-on vaults of under-reinforced concrete with a maximum opening of 23 m, on direct foundations - see fig.3.). During the construction of the bridge over Bistrița in Bicăz metal profiles of 18-21m in length were used for the first time at the centering's execution.

Continuous beams of reinforced concrete were used for superstructures at the bridges over Bistrița, on Piatra Neamț - Bicăz sector, and the bridge over Moldova, in Timișești. The latter bridge (illustrated in fig.4) was consolidated around the end of the past century / the beginning of this century.

The Gerber girders with variable sections were used in the superstructures of the bridges over Bistrița in Bacău and over Moldova, in Roman. The latter bridge was plagued with problems in the joint area, requiring consolidations over time.

Tab.2. Bridges built in Neamț historical area

Road	Locality	River (obstacle)	Static structure	Openings (m)	Year of construction
DJ 207D	Sagna	Siret	bracing wired structure	2x58+1x85	1973
DN15	Gădiniți	Siret	Gerber girders	2x23.6+7x27.5	1966
D?	Ion Creangă	Siret	freely supported beam	2x17.5+9x31	1979
DN 2	Roman	Moldova	Gerber girders	2x17.7+9x22.3	1952
DN2	Roman	Moldova	freely supported beam	2x17.5+9x21.9	1983
DN15B	Timișești	Moldova	Gerber girders	2x19.6+9x25.65	1961
DN15C	Praxia	Moldova	Gerber girders	2x28+2x21	1960
DN15B	Pipirig	Neamț	freely supported beam	3x23.25	1974
DN15B	Vânători	Neamț (Ozana)	continuous beam	2x17.6+3x23.9	1969
DN15B	Humulești	Neamț (Ozana)	continuous beam	2x20.15+3x25.5	1989
DN15B	Humulești	Neamț (Ozana)	freely supported beam	2x20 +3x25.4	1989
DN15	Bicaz	Bistrița	braced arch	1x72.4+4x6	1953
DN15	Viișoara	Bistrița	continuous beam	2x31.45+2x33.45	1953

Tab.2 (continuation). Bridges built in Neamț historical area

Road	Locality	River (obstacle)	Static structure	Openings (m)	Year of construction
DN17B	Borca	Bistrița	freely supported beam	3x32.26	1974
DN17B	Frumoasa	Bistrița	freely supported beam	3x29.1	1975
DN17B	Savinești	Bistrița	freely supported beam	3x33.2	1974
DN15B	Girov	Cracău	freely supported beam	8x17.9	1968
DN15	Bradul	Bistricioara	freely supported beam	3x17.6	1974
DN15	Bradul	Bistricioara	freely supported beam	4x17.4	1970
DN12C	Bicaz	Bicaz	continuous beam	2x11+1x16	1968
DN12C	Bicaz	Bicaz	freely supported beam	6.5+18.5+14	1969
DN15	Bicaz	Bicaz	freely supported beam	2x10.6+1x40.5	1953
DN15	Lac de acumulare	Poiana Teiului	built-on vaults	27x23+1x29	1961
DN15	Canal de fugă	Straja	braced arch	2x11.5+ax23.0	1958



Fig. 4. Bridge over Moldova at Timișești

The solution of three-hinged vault of reinforced concrete was used in the designing of the bridge over Bicaz at Bicaz.

A similar solution was adopted at Ceahlău viaduct on DN15, where a flexible vault of 42 m opening, with rigid deck, made of a continuous beam on three openings, was also designed.

In the same category is the access viaduct on DN15 of the Bicaz dam, with an opening of 44 m in a curve with a 50 m radius. The particularity of this viaduct is the Potoci abutment, made of two bent concrete reinforcements with a 25 m height.

With the building of the first prestressed concrete bridges in the 1952-1954 period and the learning of the methods and the executing technologies, the usage of this material extended to the bridges in Neamț area. The main solutions belong to the bands-with-holes category, with the reinforcement of prestressed braids made on stands at industrial level and of straight beams with openings smaller than 40 m with prestressed cables made of small sections, big sections or whole beams [1].

The subsystems presented above were applied to many works of art, among which the bridges on DN17B at Săvinești and Borca, the bridge over Siret at Ion Creangă, (fig. 5.), and the passage in Piatra Neamț.

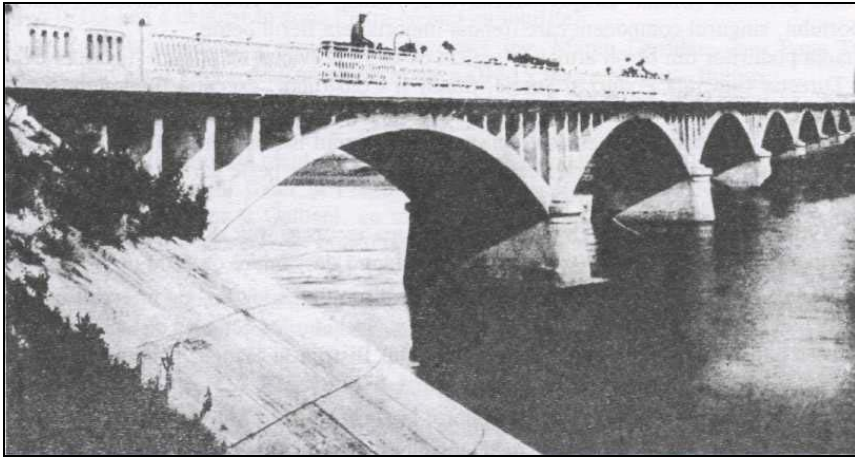


Fig.5. Bridge over Siret at Ion Creangă

In this category must be especially included the new bridge over Moldova at Roman, Fig.6., built near the old bridge, for which a solution with totally precast superstructure was adopted, the main beams being executed on site. The infrastructure's foundations were designed to be on open caissons.

Because the foundation height of the new infrastructures was 3,29 m lower then that of the existing bridge, endangering previous infrastructures, the designer stipulated a protection area made of metal sheet-piles around every infrastructure.



Fig.6. The new bridge in Roman

A special solution, of bracing wired structure made of prestressed concrete was applied to the bridge over Siret at Sagna. The bridge's superstructure is made of a continuous panel beam with a constant section on three openings, the main opening of 87 m, with bracing wires in the piles area and foundations on Benotto columns of 1,96 m in diameter. The bridge is in use but it needs repairs and support for maintaining the initial bearing capacity.

The roads infrastructure is greatly and rapidly affected by major meteorological phenomena like the ones in July – August 2005. Because of the floods recorded in this period many roads and bridges in Neamț area were severely damaged: DN 15 B – damaged on 100 m (in Pipirig village), DJ 157A – infrastructure damaged on 9 km (in Văleni village), DC Ivaneș – damaged on 2 km (Ivaneș creek overflow eroding 60 m of shore). Also, 4 tube bridges and 9 wooden bridges were destroyed, 2 tube bridges blocked, 4 concrete bridges and 34 decks destroyed – the list of casualties could go on and on.

Among the affected bridges we draw attention to the one in Roznov. The circulation on the bridge was discontinued because of the damages. The reconstructions were hindered by the successive floods; therefore an avoidance road was opened for traffic during the reconstruction –see fig. 7.



Fig.7. Avoidance road in Roznov

Also the bridge in Tupilați over Moldova was heavily damaged because of the undercutting and the damages in the protections of the bank. The consolidation and reconstruction works were made difficult because of the repeated rainfalls that settled the temporary piles, fig.8.

It may be worthwhile mentioning the alteration in the technical state of the bridge over Siret, at Ion Creangă, where undercutting and damages to the protections of the bank were reported. The circulation on the bridge was temporarily closed.



Fig. 8. Repairs at Tupilați bridge

CONCLUSIONS

1. Some of the most important bridges in Neamț area were reviewed above. The bridges with special/unique features received the due emphasis, being described in more detail.
2. The purpose of this preliminary analysis (meant to open trail for further research) was to point out the technical solutions adopted over time for the roads in Neamț historical area. The long-term objective to which this paper is subsumed envisions the development of these bridges in line with modern scientific research.

References

1. Avram, C., Reinforced concrete in România, Ed. Tehnică, 1987
2. Sadoveanu, M., Nicoară Potcoavă, Ed. Tineretului, 1952 (in Romanian)
3. Ionescu, I., Bridges, Polytechnic Society Bulletin, 1932
4. Ionescu, C., Bridges in history, literature and roads, Symposium, CNIT, Bacău, 25-26 may, 1989
5. Buzuloiu Gh., Can bridges become historical monuments?, Symposium, CNIT, Bacău, 25-26 may, 1989

Considerations regarding the evaluation of costs and resources specific to transport infrastructure

Alina Nicuță and Constantin Ionescu

“Gh. Asachi” Technical University of Iași, 700050, România

Summary

The study refers to the evaluation of costs and to resources specific to roads' infrastructure. Here are included national and territorial roads but also art construction. These are the main arteries of the roads traffic.

Even if the local roads network is very important for many people in our country, the development of this network is being blocked by the lack of financial resources but also because of a defective technical-economical organization.

The present paper wants to be a step in a systematic research in order to discover the components of the road infrastructure administration costs (initial, maintenance, rehabilitation etc.), users costs (vehicle usage, traffic delays) and exterior costs (accidents, noise decrease, air quality), considering as the final purpose the realization of a case study for a region.

An important role in this article have the financing methods for infrastructure development, from private budgetary funds and also from programs like: SAPARD, PHARE, ISPA etc.

KEY WORDS: road infrastructure, costs, resources.

1. INTRODUCTION

One of the main national priorities of our country refers to the infrastructure rehabilitation, more exactly the Romania's roads network and its development in accordance with the European Union standards. In order to complete this mission important amounts of money are being attached for roads infrastructure rehabilitation and maintenance.

Due to the fact that during the long time exploitation of the existing road network, there have not been taken measures for the modernization and adaptation of this network to the traffic intensity changes, together with the environment factors the roads network has been pretty much affected. Most of the times the reason for such situation is due to the lack of funds needed for repairs and maintenance works. The roads infrastructure development policy is based on several elements such as the

technical solutions adopted specific to the projection, execution, exploitation phases, direct costs, energy consumption, conservation of natural resources, traffic accidents, accessibility conditions etc.

In roads and bridges engineering the adopted solutions must be sustained by technical and economical efficiency. This efficiency mainly depends on factors like:

- a) The material used for the bridge construction. This element determines the cost and quality efficiency;
- b) The concept of general and detailed constructive organization. This factor is mainly determined by the professional level of the designers.
- c) The execution technology depends on the professional quality level of the workers and the technical equipments.
- d) The methods of static, dynamic and seismic analysis. There elements are important due to their scientific, theoretic and experimental level at the base of the official standards for the infrastructure engineering.

The optimization of the factors involved in the process of roads and bridges engineering refers to an approach on different levels. For example, a first level can be determined by the harmonization of the information owned by the research engineer, designer engineer, construction engineer, expert, economist and beneficiary. A second level of competence is that by which we can define the creation of the total transport infrastructure using the engineers cycles, fig.1.

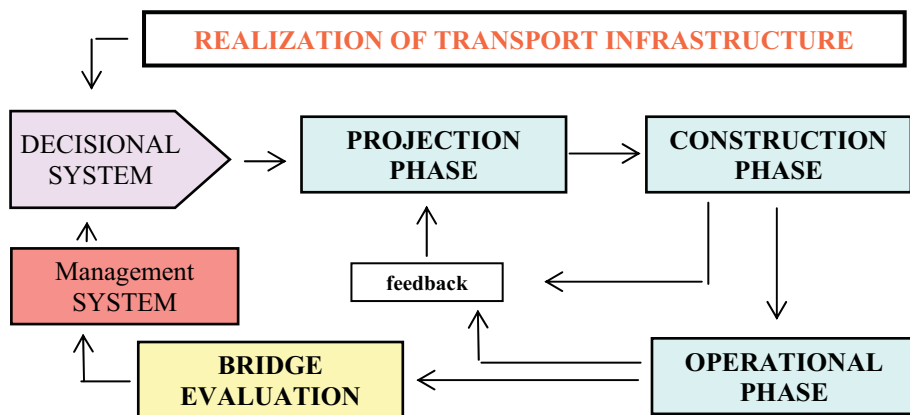


Fig.1. The construction realization cycle

If we consider the first cycle zone, more exactly that of the designer, we discover a few important factors that influence the researchers dreams in order to create modern and efficient constructions. We refer to the means by which we can develop this area and also through attracting an important number of researchers and by the creation of new efficient, technical and economical solutions. It is necessary to emphasize the utilization of several methodologies based on

simulations, optimization and creation of execution technologies useful for the works mechanization etc.

Another important factor is the improvement of the decision mechanism. The final solution must be always discovered through scientific negotiation of all technical-economical aspects, which may be presented in the process of total realization of transport infrastructure.

The information from the acquisition and transformation of the data specific to the bridge construction, operational and evaluation phases are mainly being used in the projection phase for the next bridges image.

A very important role has the phase of system-construction evaluation, which has the purpose to distinguish the bridge essential performances by the mean of technical characteristics and reliability indicators, maintenance and availability of the system general costs and the esthetic performances.

Starting with these elements and considering the present situation of the public roads network in our country the present paper will try a sensitization of the costs implied in the roads rehabilitation, as well as the available resources in order to realize these operations.

2. COSTS AND RESOURCES

In order to determine the costs evaluation and analysis for the development of roads infrastructure, considering the studies of different experts several of them being Americans, the paper proposes to determine a life cost cycle analysis.

This analysis has the purpose to offer to the owners, companies and engineers the possibility to evaluate and choose between different alternatives for infrastructure projects.

This analysis refers to the “total cost of creation, operation, custody and utilization of a construction” on a period of time.

The first element in the direct costs evaluation is the *initial investment costs*, fig. 2. These costs are implied for the construction edification, from the project till construction. Here we can mention for example buying the land, geotechnical study of the soil, technology, workers expenses and these are only a few of the costs involved in the process.

Operational costs are annual costs, excluding the construction rehabilitation and maintenance. Most of these costs imply the construction of utilities and services, and are more a function of the construction user. In order to understand better these elements we can mention as an example the electricity, water and sewerage system.

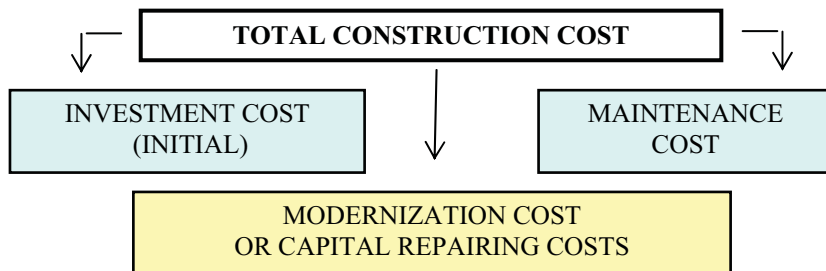


Fig. 2. The construction costs

Maintenance costs are programmed costs, associated with the suitable performance of the construction. They are a programmed element which has the purpose to maintain the construction in good performance. In order to give an example we can mention the soil improvement, infrastructure, superstructure, lateral protection system, reconstruction of road asphalt mixture etc.

Repairing costs are unanticipated outlays necessary to prolong the construction life without changing the system. The repairing costs are by definition unforeseen so it is impossible their anticipated evaluation.

Replacement costs are outlays of several major components of a construction which are necessary to maintain the system state of functionality.

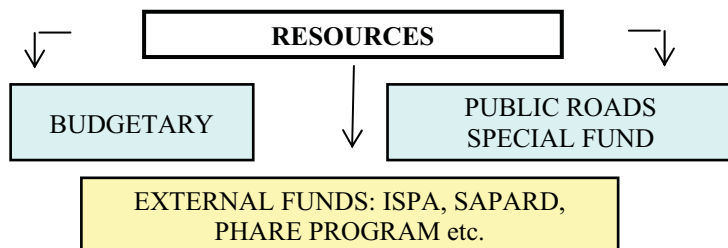


Fig.3. Transport infrastructure resources

The elements presented till now are the direct costs situated at the base of creation, performance and normal exploitation of a construction. If this type of costs is pretty easy to determine we also have to consider the indirect costs. These can be approached on two directions. One hand there are the costs determined by the relation between the construction and the social and natural environment, fig.3, issued from the road accidents consequences, air quality, phonic pollution etc, and on the other hand the costs determined by the construction users activity, influenced in the case of roads by the rolling surface characteristics, the works in progress and indirectly the costs of delay time and supplementary maintenance mechanisms, the discommode produced by covering certain areas; accidents that have several material and human damages etc.

In order to reduce the users' costs, it is necessary a good allocation of the state institution funds so that it can handle the whole national roads habitat.

Our country does not have enough funds to handle the qualitative changes of the transportation system. The investments, the legislation in the area of transports determine a temporary increase in the outlays for this area. The exacerbation of the economical conditions in the private sector determines a temporary reduction of the funds. In these conditions the financial support comes under the form of external loans (for example BERD) or un-repayable help (PHARE, ISPA, SAPARD), fig.4.

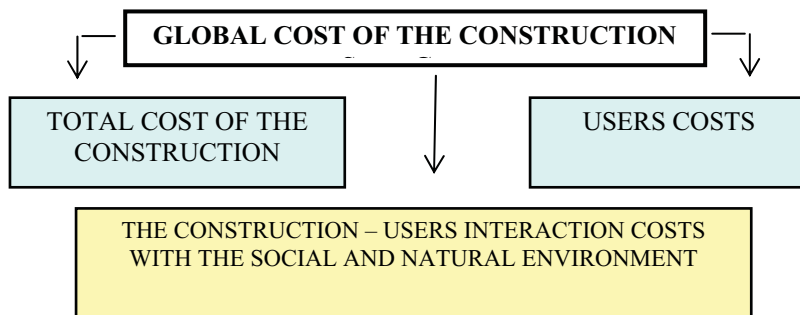


Fig 4: Global Cost of the Construction

Similar to other areas of economy , the transportation sector has allocated a value of 3,6% from the state budget to which joined starting from 1997 the Public Roads Special Fund which has its incomes from the introduction of a annual fixed sum compulsory for the owners of vehicles, but also ROVIGNETA, excise etc. This fund allocates 65% from the incomes for national roads and 35% for local roads. But still these sums are net inferior to the necessary so that the only solution is the external finances.

The BERD (European Bank for Reconstruction and Development) and BEI (European Bank for Investments) credits have the limit at 50% from a construction costs and are subject of governmental guarantee.

Complementary to those presented are the un-repayable finance programs. The financial help comes from the European Union co-financed with the national state. There are three communitarian programs specially created in order to help the countries with a disadvantageous infrastructure.

ISPA program (Instrument for structural policies of pre-adhering) finances equally important projects of infrastructure from transportation and environment area. The program beneficiaries are the local and central authorities that can sustain major infrastructure projects. The minimum value for infrastructure projects is 5 million euro. ISPA contribution is maximum 75% from the project value, rest of the money being allocated from the local budget, loans, donations etc.

SAPARD program sustains financially the area of agriculture and rural development. The projects may be realized by institutions but also by different individuals. The funds differ with the project but usually it is 50% from its value. Considering this there have been financed projects with a total eligible value between 30000 and 2 million euro. This type of finance was used for rehabilitation and construction of local road infrastructure system.

PHARE program is the financial instrument for the East-European countries pre-adhering strategy having as final purpose the integration in European Union structures. In the case of this program the projects are created by individuals but also by local and central administrations. The element that differs is the value of the financing which covers till 75% of the project costs.

3. CONCLUSIONS

The relation between the road infrastructure costs and resources allocated proves the necessity of a much deeper involvement in funds assessment for this area. The optimal mechanism of budget allocation is based on the real need of road infrastructure system. It is necessary the funds allocation process to consider the projects which are able to create a maximum benefit for road infrastructure users and for society.

The road network must be preserve to a level which can assure the users costs optimization and the maintenance costs, which is fundamental for the competitively simulation and assurance of roads efficient transports in ecological conditions.

References

1. Ionescu, C., Simulation of the Technical Condition of Bridges in Design Stage by Real Behavior in Time Scenarios, The Second International Congress on the Behaviour of Damaged Structures, DAMSTRUC'2000
2. Pachitac M, Dobre D, Schiau A.M, Georgescu D, Revista Drumuri si Poduri, nr. 28/2005, Aspecte privind analiza costului global al autostrazilor si drumurilor; (in Romanian)
3. Pachitac M, Dobre D, Schiau A.M Revista drumuri si poduri, nr. 29/2005, Stabilirea criteriilor de apreciere si a metodologiei de analizare tip Life Cycle Cost a solutiilor de realizare a cailor de rulare pentru vehicule pe pneuri; (in Romanian)
4. Mearing Tim, Nathan Coffee, Life Cycle Cost Analysis Handbook – State of Alaska – Department of Education & Early Development.

Transportation research and education in the new millennium

Radu Andrei

*Department of Transportation & Infrastructure Engineering, Technical University “Gh. Asachi” Iasi
43, Professor D. Mangeron Str., 700050 Romania*

Summary

This paper intends to present a comprehensive view of transportation research and education, as it exists today and can expects to evolve with the beginning of this new century, based on a various published papers by internationally recognized experts fully engaged in the progress of transportation engineering.

KEYWORDS: transportation, research, education, environment, intelligent transportation systems.

1. INTRODUCTION

To mark the beginning of this new millennium, the various transportation bodies and committees from the world (TRB,¹ ERC², AARB³, etc.) mounted a special effort to capture the current state of the art and practice and their perspectives on future directions in their respective areas of focus.

The results of that effort was a thoughtful and perceptive review, prepared by experts fully engaged in advancing the way the traveling public is served, providing a comprehensive view of transportation as it exists today and can be expected to evolve in this new century.

Various published papers [1],[2],[3],[4],[5],[6],[7],[8] present very useful information in gaining a better understanding of the current technologies, practices, and issues of interest to transportation professionals today, encouraging their readers to become major players as the new challenges are addressed by the transportation community.

In this context all over the world, the quality of education in general and transportation education in particular, continue to be a major factor in a nation's ability to succeed and excel.

¹ TRB-Transport Research Board (USA)

² ERC-European Road Conference

³ ARRB- Australian Road Research Board

2. TRANSPORTATION ENGINEERING AND EDUCATION

Undertaking a short insight into the current status of transportation education as an academic discipline and examining some significant areas that may challenge educators and administrators into the near future it was found out [1], that several recommendations to support future development in this academic area are necessary to be made.

Formal education programs and academic research efforts have not always been a determining factor in the development of transportation innovations. Nineteenth century innovations, such as steamboats and railroads, initially came from entrepreneurs' talents. In the 20th century, transportation issues became more complex. In the 1950s and 1960s, education endeavors in transportation were focused on the practical matters of building and maintaining road and rail networks. In the latter part of the 20th century, transportation education became a discipline in its own right. Development in the field now comes about because of continuing demands and commitments at several levels.

For the particular case of our country, from legislative point of view, it is necessary, at this stage to issue at the level of the Ministry of Education and Research (MEC) a document, through which government could support and encourage the development of all transportation organizations (government, private, etc.) and to mandate the existing university transportation centers, Bucharest, Timisoara Cluj and Iasi, to provide leadership in transportation education teaching and research. In this respect the government has to provide appropriate research programs and the necessary funding to achieve the commitment for teaching and research, as well as a technology transfer network to link transportation education needs. The outcome benefits of such undertaking will be not only for academics, but also for practitioners at various levels who wish to learn new skills or enhance their current knowledge base. In the new economical environment, it is also expected that beside the government sector, the private sector will provide also some education commitment, based on a research component capable to meet the specific needs of a developing product/service or to transform an existing transportation enterprise.

As the transportation education system grows, the focus is changing in several ways. From an academic standpoint, additional policy areas—as opposed to technical areas—become apparent. For example, students and professors will have to broaden their scope to examine communication between public and private interests, strategic management of human and capital resources, environmental impacts, as well as the impacts of computerization and technology. In this respect, more efficient management of existing infrastructure systems are envisaged now and this can be accomplished only through the use of enhanced management systems and intelligent transportation systems. At the same time, there is a growing realization that transportation education needs to broaden its focus beyond

academic offerings. To create future leaders in transportation careers, in the frame of the actual restructuring process, academic, elementary and secondary curricula have to be developed accordingly and revised. Some technology and transportation futures programs, capable to support lifelong learning endeavors and innovation at the elementary, secondary, college, and graduate levels have to be initiated.

At the other end of the learning spectrum, existing professionals, they themselves have to be engaging, in a lifelong learning process. Learning might also involve those who are informally interested in transportation issues. This perspective highlights the changing and evolving focus of the “transportation professional.”, because in order to meet the society’s demands it is no longer sufficient to have only a technical background or to view transportation education not just as a series of college courses but as a multidisciplinary and lifelong endeavor.

According this perception and in accordance with other specialist views, in this new century, some factors such as globalization, the progress of technology, changing demographics, and curriculum development will have a great impact on the educational process. In the frame of the actual globalization, defined as “seeing the whole world as nation less or borderless”, in the private-sector transportation organizations provide products, services, and research capabilities to a diverse world community that is becoming more competitive. In public-sector transportation endeavors, governments at various levels are responsible for the development, implementation, and maintenance of existing and evolving transportation infrastructures. In this context, transportation education may act as the catalyst to bind these forces together by supporting innovation. Globalization and the future entrance of our country into the European Community will significantly affect the changing academic environment. In a direct sense, it will have to face and to support the internationalization of resources, not only in the individual classroom, but also in the research facility that then extends out to the workplace environment. As global transportation education efforts support industrialization, the movement of goods and people, enhanced resources, better communication, and improvements in the quality of life for all countries, outcome shares learning innovations and the latest research and development endeavors that go beyond the academic setting. These globalization forces are also enhancing a very strong competition— thus providing a wonderful opportunity for education stakeholders to show leadership through innovative research projects, as well as by utilizing technology and communication to share resources and knowledge. Transportation innovations are expected to act as an “engine of growth” among the economic and environment drivers of the actual technology revolution involving major effects on transportation education. Within the teaching environment, the use of computers as a learning tool is revolutionizing how students study existing theoretical and practical problems. Within the learning environment, research methodologies and outcomes are bringing about continuing change, not only in tabulating and evaluating complex quantitative problems, but also in how

information is shared through web-site addresses and communication links. This revolution will extend beyond the formal classroom since it opens up distance learning opportunities to the academic and to the practitioner, even in remote locations. Technology will be used as information and learning tool to interest young students and those who wish to know more about the field. By combining technology and education endeavors, an opportunity is provided to build new technology, improve existing infrastructure, develop world-class facilities, enhance capital investments, create alternative energy sources, improve the environment, and make better communication alternatives.

At the same time, it can be used to create, test, implement, and monitor potential innovations before a financial, environmental, political, or research commitment is made. For transportation education to be relevant to society's needs, it must take into account the changing demographics in the workplace. For example, the traditional scope of jobs and careers is broadening to include women in key managerial and leadership positions, education being a key component in preparing and sustaining all individuals throughout their careers within the transportation hierarchy. To ensure broader interest and understanding for everyone, advantage should be taken of opportunities to extend the transportation learning process to the secondary and elementary levels.

At the other end of the spectrum, the older, established practitioners in the field will need to maintain and upgrade their existing knowledge and skills in the face of the massive technological and policy changes going on around them. As leaders in transportation they will have to prepare their students in such a way, that finally these students to be able to compete and demonstrate (a) leadership, to have (b) technical knowledge and skills, (c) analytical ability, (d) communication and intercultural skills, (e) technology/computerization skills, and (f) a variety of policy skills. At the same time, they need nontraditional skills, such as (g) ability to communicate between public and private interests, (h) talent to manage human and capital resources, and (i) ability to discern effects on the environment. All these objectives could be accomplished only if educators and administrators will succeed to meet changing demands through the courses of study that they offer and the research opportunities that their institutions provide. There must be a continuing commitment to broaden the focus beyond "traditional learning" to "students" of all ages. Also, there must be a commitment by numerous stakeholders to supply the tangible resources needed (e.g., funding, scholarships, grants, research opportunities, internships). Finally, educators must bridge the gap between the academic, the public, and the private sectors (e.g., by building public-private partnerships) and in a world of highly competitive resources, they need to market their success to academics and non-academics to build interest and support for their programs.

This complex approach is expected to have many benefits, by developing the next generation of transportation leadership and at the same time, building the field of

transportation education and creates the necessary innovation to meet known and unforeseen challenges. Finally, it will contribute significantly to the developing of a safe, efficient transportation system capable to meet not only.

3. TRANSPORTATION RESEARCH. CURRENT PRACTICE AND TRENDS

There has long been widespread recognition that transportation is the foundation of our society's economy and quality of life. The last century has brought major changes in the way we plan, coordinate, and conduct transportation research, primarily as a result of numerous trends in the transportation sector and in society as a whole. More recently, however, transportation agencies have begun to see their role as much more than simply providing infrastructure, their actual mission statements typically include enabling the movement of people and goods in an efficient, convenient, safe, and environmentally sustainable manner. In their new roles, transportation providers must interact and compete with other government departments and agencies, becoming more focused on making sound investments in transportation solutions that address strategic issues and needs.

This change requires an increased emphasis on the careful allocation of funds to achieve the maximum benefits and outcomes of the research programs, transportation research being expanded beyond traditional infrastructure concerns by including new areas such as policy, economics, sustainability, and the environment. Consequently, transportation engineers have to broaden their knowledge bases so that they will become prepared to deal with these new areas of concern and as program and project managers, to be effective at planning and delivering their products and meeting their customers' needs. Thus, in the field of road transportation, responding to an aging highway network the agencies is shifting their emphasis from building new roads to maintaining existing systems and optimizing their capacity. In addition, the construction, maintenance, and operation of transportation facilities, which traditionally was provided by government entities, are increasingly being delivered by private-sector firms and public-private partnerships.

The world's trading patterns and economies also have changed, and as communication networks continue to expand, additional change is inevitable. As economies expand from national systems to continental and global systems, new transportation issues and problems evolve in response and thus new research issues are emerging, challenging our professional ability to look beyond traditional borders for information, best practices, and potential partnerships. In this new environment, we must continue to imagine and to operate intermodal transportation systems that are efficient, safe, and environmentally sustainable. In this respect the envisaged research programs must demonstrate how they will support these goals

while remaining responsive to the transportation profession's current and future needs. It is this balance between supporting current programs and trends and anticipating the future that allows research programs to best serve their customers, even in times of shrinking budgets.

The recent advances in the fields of communication and information technology have had major impacts on research methods. Today, we have fast and convenient access to vast quantities of information. Electronic communication technologies have made the information available to transportation researchers, making the global knowledge more readily accessible. Improved communication tools and information resources, together with stronger partnerships with marketing and communications professionals, have contributed greatly to our ability to disseminate and implement the results of our research, these factors contributing to significant and benefic trends and changes in the conduct of transportation research such as financing and administration of transportation, information management, and implementation of research results.

Thus, to secure adequate research funding, transportation research organizations must closely reflect and support the strategic goals of society, most government transportation agencies now moving away from their old mission of solely providing and maintaining infrastructure, toward facilitating and enabling a broad range of integrated services, their research departments playing an important role in helping to achieve these new institutional objectives. Research programs with a strong policy and economic component will more likely be supported by their parent organizations, because they offer the resources and expertise that senior management needs to make wise strategic investment decisions, the research managers in transportation agencies being very often regarded as part of the strategic management process. It is envisaged that, in the context of global changes and increased demand for better use of limited resources, the research organizations that excel in the future will be those that pool their resources to work on common issues and problems. Transportation organizations must find new and innovative ways to finance their research. Cooperative partnerships are an important strategy for both maximizing the value of the research investment and reducing the duplication of effort. Cooperative research programs in the United States, in Europe and around the world are strongly supported, and all partners have a solid understanding of the value and benefits that result from sharing resources. Research collaboration, in various forms, has achieved a high level of prominence and partnerships between public, private, and academic institutions are common and are being used more frequently to leverage available funding for best results. The recently concluded Strategic Highway Research Program (SHRP) in US and the ongoing SHRP and RO-LTPP implementation programs are excellent examples of successful partnerships among governments, industry, and academia.

In Europe, by pooling funds and expertise, through various COST⁴ and SERP⁵ programs, and through various research bodies such as FEHRL⁶, ECREDI⁷, etc, the EC states are able to leverage their resources to study and develop solutions for a targeted list of problems over short (5-year) timeframes. In the foreseeable future, these arrangements will become even more common and will more often include multinational public and private sector partners. At the international level, the OCDE⁸ administers research programs using pooled voluntary resources contributed by the member countries.

To justify their programs, today's research managers must be able to measure and discuss the performance, quality, and value of their programs in terms that support the strategic goals of senior management. A significant example in this respect is the ongoing COST Action 345 “Performance Based Indicators for Road Pavements”, in which Romanian specialists are involved together with highway specialists from other ten European countries. Performance measures for research and development programs are currently a high priority among highway agencies. It is not enough to simply evaluate a program's performance, quality, and value. To develop and sustain support for a strong research program, researchers must proactively promote the value of research both within and outside the agency, by developing and perfecting their skills in marketing their programs and services. Today, transportation researchers also have better tools and training to carry out their work than their predecessors did. As the primary role of transportation agencies shifts from delivery of infrastructure to management of transportation services, research administrators need a broader set of management skills. Sustaining and improving the skills of the current research community and laying the groundwork for the next generation of highly trained and competent transportation researchers is a critical issue. Much work has been done to develop manuals, and courses that provide guidance and assistance in conducting research. The conduct of research will be treated in an even more systematic fashion in the future, and the emphasis on the application of superior research practices, scientific methods, networking, partnering, and marketing will likely increase.

Because organizations with sound fiscal management practices do not spend time or money duplicating research that has already been conducted and verified, comprehensive information on the state of the art and practice must be readily available. Information based on published reports and journals, research in progress, and human expertise can be found and retrieved by using a wide variety of manuals and electronic sources, which include bibliographic and statistical

⁴ COST-Cooperation Scientifique et Technique

⁵ SERP-Strategic European Research Program

⁶ FEHRL -Forum of European Highway Research Laboratories

⁷ ECREDI-European

⁸ OECD- Organization for Economic Cooperation and Development

databases, library catalogs, and web sites. The value of information and information services is gaining recognition among transportation researchers.

A recent study by FHWA⁹ found that the money spent on information services can yield benefit-to-cost ratios in excess of 10:1. The value of information can be measured in terms of reduced costs of agency research, technology development, and operations, quicker implementation of innovations, time savings, and more effective decision making at all levels of the agency. Transportation professionals from all over the world are becoming more aware of major transportation research resources such as the Transportation Research Information Service (TRIS) and the International Road Research Documentation (IRRD) database, as well as less focused sources. These resources provide access to the global network of research information and hence improve the quality of research and make more efficient use of resources. As the amount of information proliferates, the importance of the role of the information professional has become better understood and more prominent. Research librarians and information specialists—trained and skilled in the integration, analysis, and management of information—now are recognized as important members of the research team. Information professionals will play an important role in the organization and retrieval of web-based information systems in the future. Other information management initiatives have sprung up in recent years. For example, information clearinghouses are being developed that compile, organize, and disseminate information on high-priority topics such as those of intelligent transportation systems, work zone safety, and transportation demand management.

Concern for the timely reporting of current research is of growing interest. Information databases are only as useful as the information they contain, and research organizations are increasingly motivated to report new projects as they begin. New technologies are being developed and used to facilitate information gathering, making it easier for researchers to contribute information about their work to major international databases. So, information technology will continue to advance rapidly and significantly affect the way we exchange information, acquire new knowledge, and conduct transportation research. Issues involving the organization, storage, and retrieval of information present some of the greatest challenges that need to be addressed in the coming years. The preservation and archiving of printed transportation research documents (to ensure that documents are not lost as a result of age or deterioration) is another important concern. Finally, serious efforts must be taken to analyze and organize the volume of information being made available through web-based Internet sites, through either better design or integration of the sites as they are developed, or improved sophistication of tools that enable users to search for information across multiple web-sites.

⁹ FHWA- Federal Highway Administration , USA

The benefits of applied research will be realized only after the research products are implemented in the field. The information and communication tools described earlier can be used to help market innovative technologies and strategies for improving our transportation system. However, having the ability to quickly and efficiently access information about the latest research will not guarantee that the research products will be put into practice. Many barriers to the implementation of research results—resistance to change; the complexity of effective communications; and the cost and inconvenience of personal contact, which often is the most effective way to disseminate information about and learn to adopt new technologies—remain to be demolished.

The concepts behind technology transfer and its practice have received considerable attention from the transportation community during the past decade. Technology transfer generally refers to a strategy or process for bringing appropriate practices or technologies to the attention of the transportation practitioners who can benefit from them. Technology transfer has been described as a process that links research and implementation; however, it is more accurately described as an effective communication process that links information with the people who can benefit from it. Technology transfer involves packaging and communicating information in a manner most appropriate for its target audience. Technology transfer has a tremendous potential to optimize the operation of transportation systems cost-effectively, by reducing or eliminating duplicated effort and by facilitating the implementation of best practices and relevant technologies. Technology transfer in transportation will continue to expand, and the most effective practices for technology transfer will become more widely disseminated. Transportation agencies, seeking ways to hasten the implementation of research results, are increasingly encouraging or requiring researchers to develop implementation plans as part of the research process.

3. CONCLUSIONS

In the future, we will probably see even stronger ties between the research and implementation phases of innovation processes.

References

1. TRB Transportation in the New Millennium State of the Art and Future Directions.
2. Manning, P. *Transportation Education TRB/A1A04:Committee on Transportation Education and Training*
3. Hedges, C. Harrington-Hughes, C. Carrp, W. *Current Practice and a Look Forwar TRB/A5001: Committee on the Conduct of Research.*
4. Transportation Research

Romanian road infrastructure in the frame of sustainable development concept

Nicolae Tautu

Romanian Professional Associations for Roads and Bridges-APDP- Moldavian Branch

Summary

This article presents a brief but realistic evaluation of the present situation of the road infrastructure in Romania, in order to encourage the exchange of ideas about sustainable development in this important social and economical field. It presents the present technical state of the Romanian roads, the future requirements and the available resources to bring the road network at European standards.

KEYWORDS: road infrastructure, management system, transportation costs and resources, roads technical state.

1. INTRODUCTION

The Romanian road infrastructure constitutes a significant national asset, for which important human and financial resources are devoted. In the context of severe climatic and traffic conditions, specific to our country, a complex managerial strategy applied at national, regional and local levels is necessary to be conceived and implemented in order to preserve, modernize and extend the existing public road network .

Often, the absence of a correct strategy is justified by the permanent lack of funds and financial constraints, but in our opinion this is mainly caused by the lack of proper harmonization and adaptation of the general managerial principles to the specific social- economic development level attained by the respective countries.

At this crucial moment, when our country concentrates its efforts to enter into the European Union, and when the adhesion programs have to be developed in the context of the concept of sustainable development, the main objectives of the strategy adopted for the modernization of the road infrastructure have to be undertaken in a similar concept and to meet the European Commission requirements, proposed during 2001 year.

The following base principles involved in the sustainable development and specified by Clause 130 of the Maastricht Treaty has to be considered at the establishment of the programs of road works:

- the prevention against the serious and irreversible threats toward the environment;
- consideration of the environmental problems in defining and implementation of road policy;
- the participative principle, with the implication of the society in the process of taking major decisions;
- the obligation for the polluter agent to pay for the damages he is generating.

For our country, the implementation of this concept is rather complicated, considering the service level provided by the road infrastructure and its implications on the overall costs of the transportations system, taken as a whole.

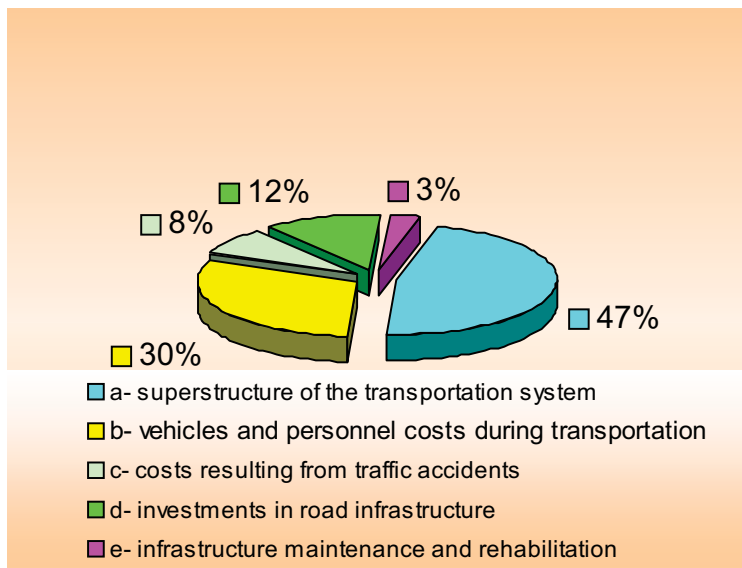


Figure 1: The structure of the costs in the transportation system

2. COSTS IN TRANSPORTATION SYSTEM

The technical state of the road infrastructure can influence decisively the transportation costs. The specialized literature in this field stresses the correlation that exists between the infrastructure and the superstructure of the transportation

system, represented in Figure 1. The percentages represent mean values, which may vary, depending on the country or region. A reduction of the transportation costs with only 5% may lead to double available funds for roads maintenance and, thereafter, a continuous reduction of the superstructure costs.

According to Japanese specialists (2), one less dollar in maintenance funds today is three more dollars in transportation costs tomorrow. Considering the presented structure of the costs, one can draw the conclusion that the necessary resources must be supplied by the user (the user is paying). This problem is complex and it is not the purpose of this article to analyze the worldwide used methods in this matter.

In the USA, a clearly defined principle governs the budgets of the all services (the road infrastructure representing also a service): there are no planned expenses without financing resources and also no taxes without a clear destination. In many other countries, there are cases when the money obtained from road infrastructure taxes are used in purposes other than road infrastructure works.

A very important study was done by C.E.S.T.R.I.N., analyzing the structure of taxes and tariffs applied to finance the road infrastructure works and it should be used as a strategic element for the roads management policy in our country (3).

3. TECHNICAL STATE OF THE PUBLIC ROADS IN ROMANIA

The public roads network in Romania, classified in national, departmental and rural roads, has a total length of 78658 km, according to Table 1. The evaluation of the technical state of this road network using a modern approach is practically impossible in our country. At least for the departmental and rural roads, measuring some technical parameters such as surface distress, irregularities, roughness can not be evaluated observing the current standards.

Therefore, from the data existing in each administrative department, it results the following:

For the national roads, from a total of 15166 km paved roads, 8025 km are in a good state, 3547 km are in a satisfying state and 3590 km in unsatisfying state. Also, there still are 269 km stone roads and 35 km earth roads. It must be stressed that, in between 1995 – 2004, on the national road network, an extensive rehabilitation program has been applied. It was developed in four stages and it continues now with works on E – class roads and main roads. The total length of roads in service by the end of 2004 was 2490 km, with a total value of the works undertaken of 1494790000 € (see Table 6).

For the local roads:

- departmental roads: their total length is of 35410 km, of which 5741 km are in good service conditions, 4840 km – satisfying and 7242 – unsatisfying service conditions. The length of the stone roads is 15985 km, and 1602 km are still earth roads.
- rural roads: the total length is 27781 km, of which 1187 km are in good service conditions, 1927 km – satisfying and 1558 – unsatisfying service conditions. The length of the stone roads is 16064 km, and 7045 km are earth roads.

For the national roads, but especially for the local roads, the situation is rather difficult because, in time, intervention actions were not performed regularly, which led to the fact that most roads have exceeded their service life, with the only exception of the rehabilitated roads.

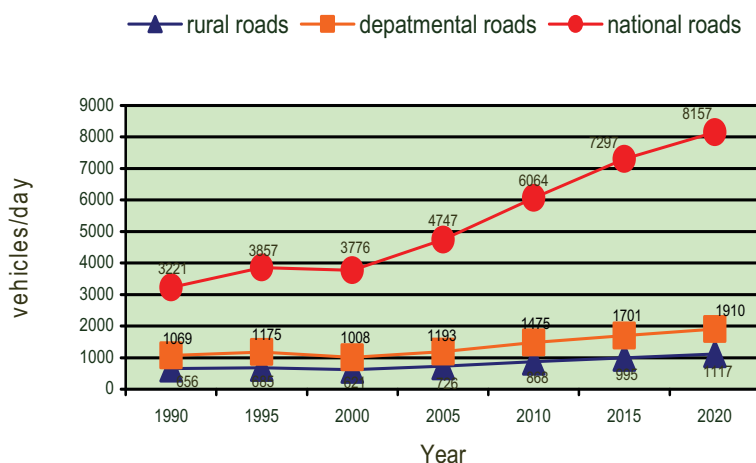


Figure 2: Traffic evolution on public roads, 1990 – 2000

The situation is even worse if we consider the predicted evolution of the traffic in the future. In Figure 2, presenting the traffic values for each category of public roads, it can be seen that, at the level of the reference year 2012, on the national roads the traffic is double compared to the year 2000, on departmental roads the increase is 60%, and on rural roads the traffic increase is 50%, this data being the maximal, optimistic ones.

4. ACTUAL RHYTHM OF IMPROVING ROAD NETWORK VIABILITY

If we consider the length of the public roads network, with various types of pavement systems – 37658 km – in between 2001 and 2004 there should have been

carried out, according to the present technical norms prescribing the rhythm of interventions, maintenance and rehabilitation works on 12552 km, which means an intervention every 12 years. However, in Table 2 it can be seen that the total length on which such works have been carried out is 4864 km.

The situation, for each road category, is as follows:

- national roads: total length: 15163 km; works done on 2473 km;
- departmental roads: total length: 17823 km; works done on 1906 km;
- rural roads: total length: 4200 km; works done on 176 km.

Concerning the bituminous surface treatments, the situation is also difficult. According to the standards, every 5 to 7 years, any flexible pavement must be rejuvenated. This means that, in four years, at least 75% (28244 km).

Globally, only 6875 km roads were treated: 2885 km national roads, 3862 departmental roads and 110 km rural roads. A better situation exists in the case of stone paving earth roads, but still insufficient: 3347 km done, from 11000 km existing earth roads in 2001. The total value of the funds used in 2001 – 2004, presented in Tables 3 and 6, is 1.627.687.721 €, from which 269.500.000 € were for rehabilitation works.

5. GLOBAL REQUIREMENTS FOR PUBLIC ROADS NETWORK FOR SATISFYING ECONOMICAL AND SOCIAL NEEDS

For determining these requirements, the delays of the maintenance programs have been taken into account, as well as the objective of bringing the roads and bridges network to satisfying service levels.

The structure of the costs involved is presented in Table 3.

The rehabilitation works for national roads have been estimated according to the strategy of the rehabilitation campaign, stating that at the end of this program (2012) the length of the European and main roads should be 6000km. For treatment works, the tasks were estimated according to the maintenance technical norms.

From Table 4, it results that the global cost is 10.407.830.689€: 4.343.565.324€ for national roads, 3.708.804.001€ for departmental roads and 2.355.465.364€ for rural roads.

Concerning the budget needed for bridges, the situation is presented in Table 5. The works considered were replacing provisory bridges, rehabilitation and maintenance. The total evaluated cost is 1.249.419.824 €. The global cost for finalizing this program is 11.657.250.513€.

6. AVAILABLE RESOURCES

After globally evaluating the required budget for improving the technical state of the road network, for the national, departmental and rural roads only, without considering the highways and village roads, an inventory of the possible resources to cover these needs is done.

6.1. Transfers government budget – this resource has been used continuously and many times exclusively. It could never withstand the real needs, being insufficient for the whole network, but especially for local roads.

6.2. Taxes and tariffs – this must be paid by those who use the road network, directly or indirectly. This resource is broadly used abroad, with various modalities of collecting and managing the funds. For our country, the system, only partially used now, must be reconsidered and adjusted to observe the European standards.

According to the norms of the European Union concerning taxes for roads users, the value of these taxes must reflect the wearing of the pavement due to the axle loads, the distance, the pollution due to carbon dioxide (CO₂) emissions. In this matter, The European Commission has published The White Book, referring to the taxes for using the road infrastructure.

The taxes and tariffs types, some of the also used in our country, are:

- taxes included in the price of the fuel, in most countries used for road maintenance works. Unfortunately, the management of these funds is done by the Ministry of Finance, which sometimes leads to the situation presented in Figure 3, where funds for roads works are allocated arbitrarily.
- transportation authorizations;
- custom taxes and excises for motorized vehicles imports;
- taxes and tariffs for transportation authorizations for high tonnage and special transportations ;
- taxes and tariffs for alien transporters, replaced more and more by transportation authorizations released on reciprocity bases.

Normally, the funds obtained from all these taxes, as well as others, such as those obtained from envelopes or vehicles selling, should be used for financing roads works.

The taxes for roads infrastructure from fuel purchase varies in every country, being in the range of 25% to 50% from the total price. Usually, these taxes decrease as the number of registered motorized vehicles increases.

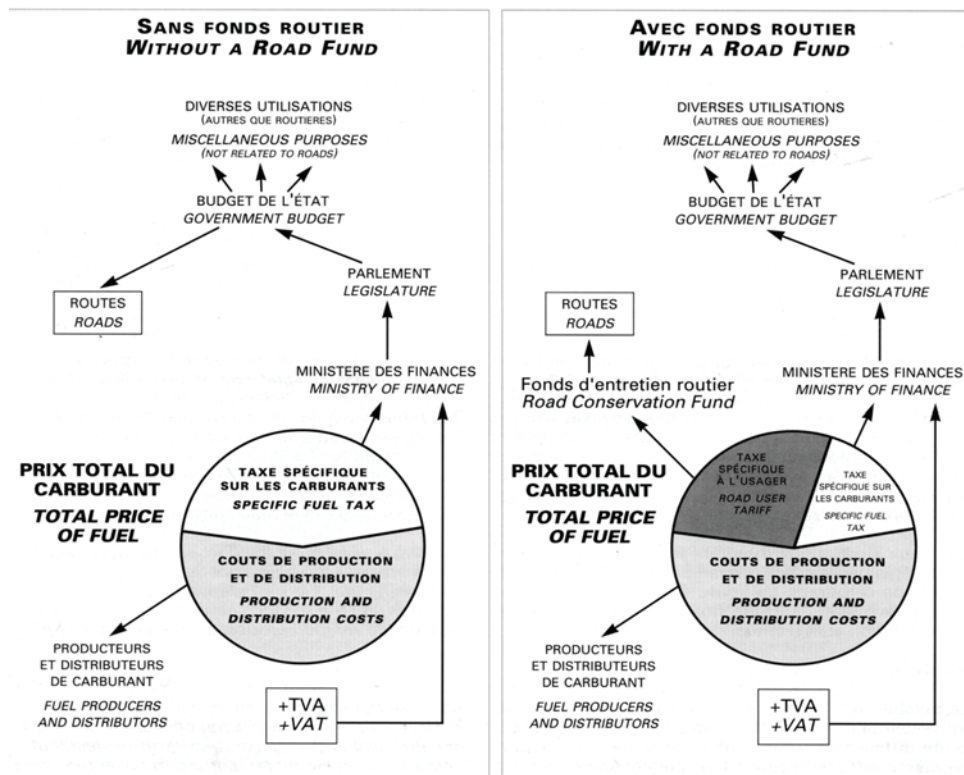


Figure 3: Use of money paid for purchase of fuel

6.3. A very important resource can be considered the savings due to good timing interventions for preventing the degradation of the road. This could dramatically decrease the maintenance costs, which increases exponentially with the delay of the intervention works. An example is the decision of withdrawing the technical agreement for bituminous treatments and recycling.

For Romania's situation, if a strategy to realize the objectives (7 years) is found, so that the repairing works amount is reduced every year, the saved funds could constitute real resources to cover the payments and the interest rates for the credits used in the program.

6.4. The volume of the works done by the Road Agency compared to those executed based on contracts also represents an important resource. In countries such as Sweden, Finland, Great Britain, important savings have been obtained by executing the current maintenance and winter works.

6.5. A resource difficult to evaluate, but extremely important to manage all categories of costs affecting the road infrastructure, is the quality of the specialists in this activity field and the quality of the management.

The training and the stability of the human resources in a pavement management system is a must. At this point, there exists a shortage for highly qualified personnel. The number of future graduates in this field must be reconsidered.

6.6. Early execution of studies and projects for road infrastructure development, done and supervised only by specialists. The cases when unfounded decisions were made were more than few, leading to increased costs or inefficiency. Preparation of consistent projects is even more important in the following period, as Romania will have access to important financing resources from European Community funds.

6.7. The structure of the works program may and must influence the costs on medium and long term. The works aiming for conserving the pavement systems must have top priority. As an example, it can not be allowed that an agency executes structural overlaying, but skips the surface treatments works (6).

Although the issues presented at points 6.3 – 6.7 can not be exactly evaluated, these aspects represent certain measures for reducing the maintenance costs as well as strategic elements in the frame of the national pavement management system.

7. CONCLUSIONS

This article presents a brief but realistic evaluation of the present situation of the road infrastructure in Romania, in order to encourage the exchange of ideas about sustainable development in this important social and economical field, and it is addressed to all the decision – makers, at all levels, with various responsibilities in initiating and promoting new development strategies for the Romanian road infrastructure.

The problem presented is very important also because it involves difficulties in assuring the necessary financial support. However, accomplishing the objectives of the proposed program for 2006 – 2012 could dramatically change the image of Romania.

Generally, a document such as this article presents at the end vast conclusions and program of measures. Still, we consider that a main conclusion, and measure to be taken, is of the most importance: the Romanian road infrastructure must be managed by a National Roads Program, elaborated by the National Roads Administration on legal basis. This program will eventually define a balance of requirements and resources, as well as the responsibilities of those who will carry out the objectives and who will assure the resources.

The National Roads Program, on medium and long term, will be approved by the Parliament and actualized by Governmental Ordinance. This objective is in accordance with the present Government Program. Chapter 17 – „Transportation policy”, point B – „Road infrastructure strategy”.

References:

1. Alain Couche – *Metodă de optimizare și apreciere a proiectelor rutiere potrivit principiilor de dezvoltare durabilă*, ROUTES nr. 317 – 2003.
2. Hiroshi Mitani – *Întreținerea și administrarea drumurilor în Japonia*, ROUTES nr. 310 – 2001
3. dr. ing. Stelea Laurențiu; dr. ing. Scînteie Rodian – *Considerații privind sursele de finanțare pentru lucrările de drumuri din diverse țări și România*
4. Indicativ A.N.D. NR.580-2002 – *Recensământul circulației din anul 2000*
5. Buletinul Tehnic Rutier nr. 9 2002
6. Andreas Schliessler și Alberto Bull – consultanți pentru comisia economica O.N.U. – *Finanțarea întreținerii drumurilor cu taxe și tarife plătite de utilizatori*, ROUTES nr. 280 – 1993
7. ing. Tăutu Neculai – *Infrastructura rutieră în România între nevoi și resurse*
8. Revista *Drumuri și Poduri* nr. 1 (70) - 2003
9. Susanne Kuschel (Centrul European pentru Studiul Infrastructurilor) – *Finanțarea privată a infrastructurilor de transport în Europa Centrală și orientală. Prea frumos pentru a fi adevărat*, ROUTES nr. 286 - 1995
10. Per Anders Ortendahl – *Administrația Drumurilor în Suedia. Obiective, metode și rezultatele reformelor în administrație*, ROUTES nr. 279 - 1993
11. Gustavo Marcelo Gentili și José Enrique Erbetto – *Experiența argentiniană în concesionarea lucrărilor de întreținere a drumurilor*, ROUTES nr. 280 – 1993
12. ing. Petru Ceguș – *Sisteme de evaluare: Gestiunea drumurilor*
13. Revista *Drumuri Poduri* nr.62 -2001

Considerations on the value of modulus of subgrade reaction

Horia Gh. Zarojanu, Radu Andrei

*Department of Transportation Infrastructure and Foundations, Faculty of Civil Engineering,
Technical University “Gh. Asachi” Iasi, Romania*

Summary

In structural design practice of rigid road pavements, the subgrade stiffness is generally represented by the modulus of subgrade reaction, now universally known as subgrade support or by the symbol K (K Value). As the in situ determination of the K value is laborious, a synthesis of correlations between K value and other deformability characteristics of the subgrade such a CBR and the dynamic elastic modulus E for which standardized values are available, is presented in this paper. Based on this synthesis, design values for the modulus of subgrade reaction have been adopted and proposed for the use in the frame of the actual structural method of design of rigid road pavements, elaborated by INCERSTRANS in collaboration with the Faculty of Civil Engineering of Iasi.

KEYWORDS: rigid pavements, structural design, modulus of subgrade reaction, deformability characteristics

1. INTRODUCTION

The modulus of subgrade reaction, universally known by the symbol K, is the number of pounds per square inch of subgrade reaction per inch of slab deflection, pounds per cubic inch or kN/m^3 . Usually this parameter, characterizing the subgrade stiffness is measured in situ), by applying a static load, on a 30-in diameter bearing block (plate).

According /6/, “no time rate of load application is included in the definition for modulus subgrade reaction, but the fact is that fast moving traffic loads are less severe in their slab-bending effect than static loads” and therefore it is assumed that static loads are significant loads for this purpose. As this process is quite laborious and costly, for preliminary design stages (pre-feasibility -SPF or feasibility-SF stages) and for construction objectives of minor importance such as local roads, parking or storage surfaces, K Values, obtained on the base of the following types of correlations are recommended to be used:

$$E_{\text{elasticitate dinamic}} - \text{CBR} \quad [\text{MPa} ; \%] \quad (1)$$

$$K - \text{CBR} \quad [\text{MN} / \text{m}^3 ; \%] \quad (2)$$

2. STUDIES OF VARIOUS CORRELATIONS

2.1. Studies undertaken for correlations of type (1)

For correlations of type (1) the following relations have been considered:

$$\text{LCPC Paris : } E = 5(\text{CBR}) \quad (3)$$

TRRL London: Table1

Table1. Correlations of type (1) recommended by TRL specifications

CBR [%]	1,5	2	5	15
E [MPa]	23	27	50	100

$$\text{C. Regis : } E = 8,5 (\text{CBR})^{0,825} \quad (4)$$

$$\text{G. Jeuffroy : } E = 6,5 (\text{CB R})^{0,65} \quad (5)$$

$$\text{Shell : } E = 10,0(\text{CBR}) \quad (6)$$

TEM / 1 / Table 2 :

Table 2. Correlations of type (1) recommended by TEM specifications:

CBR [%]	1,5	2	3	4	5	6	7	8
E [MPa]	14,5	20,0	26,5	32,0	37,5	42,0	46,0	50,0

For the correlations given in Table 1 and Table 2, the involved equations (Table 3) have been determined ; $x = \text{CBR}$; $y = E \text{ [MPa]}$:

Table3. The involved equations for the correlations given in Table1 & Table 2

Correlation	Equation	Coefficient of correlation	Standard deviation	Statistical residue
TRRL (table 1)	$y = \frac{a*b + c*x^d}{b + x^d}$	1,000	0,0	0,0
TEM	$Y = a+b*x+...+f*x^5$	0,999	0,047	< 0,03

The pairs: CBR –E values for those six correlations of type (1) are presented in Table 4:

Table 4. The pairs: CBR –E values, for those six correlations of type (1)

CBR [%]	E [MPa] for the correlations: :					
	(3)	(tab.1)	(4)	(5)	(6)	(tab.2)
1,5	7,5	23,0	12,0	8,5	15,0	14,5
2	10,0	27,0	15,0	10,0	20,0	20,0
3	15,0	35,0	21,0	13,5	30,0	26,5
4	20,0	42,5	26,5	16,0	40,0	32,0
5	25,0	50,0	32,0	18,5	50,0	37,5
6	30,0	56,5	37,5	21,0	60,0	42,0
7	35,0	63,0	42,5	23,0	70,0	46,0
8	40,0	69,0	47,5	25,0	80,0	50,0

In technical specifications for the structural design of rigid pavements/5/ the Shell correlation has been retained , as this correlation ensures a resonable correlation of the design values of the dynamic elastic modulus of subgrade for flexible/semirigid road pavement structures.

2.2. Studies undertaken for correlations of type (2)

For correlations of type (2): C.T.12 AIPCR /2/, TEM /1/ and PCA /3/, the results from Table 5 have been obtained:

Table 5. Correlations of type (2)

CBR [%]		10	9	8	7	6	5	4	3
K [MN/m ³]	CT 12	60	55	52	48	42	37	33	27
	TEM	55	51	48	46	41	37	33	27
	PCA	54	52	49	45	42	38	33	27
K _{mediu} [MN/m ³]		56	53	50	46	42	37	33	27

For K_{mediu} , the correlation (7): x= CBR; y=K, from below has been derived :

$$y = 8,74 + 6,75 * x - 0,202 * x^2 \quad (7)$$

this correlation having the following statistical parameters: R (the coefficient of correlation) =0,999; the standard error =0,323; statistical residue $< 0,50$.

The E [MPa] / CBR [%] / K [MN/m³] values, adopted according /5/, for the P_1 ... P_5 types of subgrade soils, for the climatic types I...III and for the hydrological conditions 1...2b, are presented in Table 6:

Table 6 The adopted values of E / CBR / K , for the various types of subgrade soils

Climatic Type	Hidrological conditions	The adopted values of E / CBR / K for the various types of subgrade soils					
		P ₁	P ₂	P ₃	P ₄	P ₅	
I	1	100/10/56	90/9/53	70/7/46	80/8/50	80/8/50	
	2a			65/6,5/44		75/7,5/48	
	2b				70/7/46	70/7/46	
II	1		80/8/50	60/6/42	80/8/50	80/8/50	
	2a				70/7/46	70/7/46	
	2b		90/9/53				
III	1		80/8/50	55/5,5/39	50/5/37	80/8/50	
	2a		65/6,5/44				
	2b						

The design value of the reaction modulus K_0 , at the superior level of subgrade is obtained function of the value of the subgrade reaction modulus K and the equivalent thickness (type AASHO Road Test), by using the diagram SBA /STBA Paris /4/.

3. CONCLUSIONS

In the frame of the Romanian method of structural design of rigid roads pavement structures/5/, the reaction subgrade modulus K [MN / m³] represents the stiffness characteristic of the subgrade.

The correlations between the value of the reaction subgrade modulus K and the E the dynamic elastic modulus –MPa) and CBR [%], for which laboratory or standard design values are available, permit the evaluation of the design values K , at least for the preliminary design stages, thus eliminating the in situ laborious and tedious studies.

References

1. *** *Pavements . Vol.II,TEM/TC/WP 137 71986*
2. . *** *C.T.12, AIPCR.Terrassements, Drenages.Projet 3, 1993*
3. *Huang Y, H, Pavement Analysis and Design, P.H. New Jersey,1993.*
4. *** *Dimensionnement des Chaussees, Vol.1, DGAC/SBA/STBA, Paris, 1988*
5. *** *Normativ de dimensionare a structurilor rutiere rigide, ind. NP 081-.2002 (in Romanian)*
6. Woods B. K., Berry S.D., Goetz H. W., *Highway Engineering Handbook, First Edition, page. 23-9, Mc GRAW –HILL BOOK COMPANY*

The average thickness of bituminous binder – criterion for the analysis of performance behavior of hot rolled road asphalt pavements

Horia Gh. Zarojanu, Radu Andrei

*Department of Transportation Infrastructure and Foundations, Faculty of Civil Engineering,
Technical University “Gh. Asachi” Iasi, Romania*

Summary

Although the average thickness of the bituminous binder does not represent a criterion for the design of the composition of the asphalt mixtures, it could be useful for the analysis of the premature distresses observed in the asphalt pavements. This paper intends to present the method of calculation of this parameter and suggests its correlation with the performance of the asphalt pavements, expressed in terms of type and extension in time of the specific distress phenomena. These correlations could be then recorded in a road data base, in order to be use, later on, for such analyses.

KEYWORDS: asphalt pavements, laboratory design, the average thickness of asphalt binder, road data base

1. INTRODUCTION

Although the average thickness of the bituminous binder does not represent a criterion for the design of the composition of the asphalt mixtures, it could be very useful for the analysis of the premature distresses observed in the asphalt pavements. If this thickness is too small, air will penetrate easier into the asphalt mix voids, thus leading to its faster oxidation, increased stiffness and cracking of the binder film.

This situation becomes more critical in case of using mineral aggregate susceptible to the action of water whose access at the surface of the aggregate will lead to the development of specific distresses.

This criterion is not applicable to the hot poured asphalt mixes, where the volume of binder exceeds the volume of voids in mineral aggregate.

2. USEFUL RELATIONS FOR THE CALCULATION OF THE AVERAGE THICKNESS OF THE BITUMINOUS BINDER

According to literature [1/2/3/], the average thickness of the bituminous binder (h_{bm}) in an asphalt mix is derived from the effective volume of the bituminous binder (V_{ef}), which represents the difference between the total volume of binder (V_t) and the volume of the binder absorbed by the natural aggregate (V_a), by using various usual relations.

2.1 The calculation of the average thickness of the bituminous binder

The average thickness of the bituminous binder (h_{bm}) is obtained by using the following relation:

$$h_{bm} = \frac{V_{ef}}{\sum_a M_a} \quad [m] \quad (1)$$

where: V_{ef} represents the effective volume of the binder [m^3]:

$$V_{ef} = V_t - V_a \quad (2)$$

Σ_a - the total surface of the mineral aggregate (m^2 / kg);

M_a – mass of mineral aggregate (kg).

2.2. The calculation of the total volume of binder:

The total volume of binder (V_t) is calculated with the relation (3):

$$V_t = \frac{M_m * p_b}{\rho_b} \quad [m^3] \quad (3)$$

where the involved parameters have the following significance:

M_m the mass of the asphalt mix (kg);

p_b - the percentage of binder (%);

ρ_b - the density of the bituminous binder [kg / m^3].

2.3 Calculation of the volume of the absorbed binder

The volume of the absorbed binder (V_a) by the mineral aggregate is obtained by using the relation (4):

$$V_a = \frac{p_{ba} * M_m * (1 - p_b)}{\rho_b} \quad [m^3] \quad (4)$$

where p_{ba} represents the percentage of the absorbed binder, determined with the relation (5) :

$$p_{ba} = 100 \frac{\rho_a - \rho_{aa}}{\rho_a * \rho_{aa}} \quad (5)$$

In relation (5), ρ_a represents the effective density of mineral aggregate , calculated with the relation(6):

$$\rho_a = \frac{100 - p_b}{(100 / \rho_m) - (p_b / \rho_b)} \quad [kg/m^3] , \quad (6)$$

The parameters involved in relation(6) have the following significance :

ρ_m -represents the maximum theoretical density of the asphalt mix , e.g. of the mix without voids [kg / m³];

ρ_{aa} - represents the apparent density of the mineral aggregate and is calculated with the relation (7) , [kg / m³] :

$$\rho_{aa} = \frac{\sum p_{ai}}{\sum (p_{ai} / \rho_{ai})} \quad [kg/m^3] \quad (7)$$

p_{ai} - the percentage of aggregate size “i”, having the apparent density ρ_{ai} .

2.3 Calculation of the total surface of the mineral aggregate

For the calculation of the surface aggregate Σ_a , in relation (1), the Duriez formula or the Asphalt Institute relation (8) can be used :

$$\Sigma_a = \sum a_i * p_i \quad (8)$$

where : a_i represents the surface factor for the material passing the sieve „i „, in percentage „, p_i ”, in accordance with the values given in Table 1 from below:

Table 1. The values of the surface factor a_i

Sieve	The maximum size*)	Sieve Number						
		4	8	16	30	50	100	200
Sieve size - mm-	Sieve size	4,75	2,36	1,18	0,60	0,30	0,15	0,75
Surface factor a_i	2	2	4	8	14	30	60	160

*)sieve through which 100% aggregate is passing

3. CONCLUSIONS

For the determination of the average thickness of the bituminous binder in an asphalt mix, there is no need for supplementary laboratory tests, the data obtained during the design stage of the asphalt mix are sufficient in this respect.

The determination of the average thickness of the effective film of binder and its correlation with the performance behaviour of the asphalt pavements, expressed in terms of the types of distresses and of the time of their observance, is fully justified for the creation of a specific road data bank by each Road Agency.

References:

1. *** Hot Mix Asphalt Materials, Mixture Design and Construction.N.C.A.T.,1994.
2. Asphalt Institute : *Mix design methods for asphalt concrete and other hot mix types*, Manual series No.2 (MS-2), USA, 1988
3. The Asphalt Institute : *The asphalt handbook*, , Manual series No.4 (MS-4), USA, 1970

The use of accelerated circular track for performance evaluation and validation of technical specifications for the asphalt mixes stabilized with various fibers, in Romania

Nicolae Vlad, Radu Andrei

*Department of Transportation & Infrastructure Engineering, Technical University “Gh. Asachi” Iasi
43, Professor D. Mangeron Str., 700050 Romania*

Summary

The research presented in this paper has been undertaken in the frame of Accelerated Load Testing (ALT -LIRA) facility at the technical University “Gh. Asachi” of Iassy, for performance evaluation and validation of national technical specifications for the asphalt mixes stabilized with various fibers, used for the construction of bituminous road pavements in the actual effort of road rehabilitation in Romania. The performance of five types of mixes involved in this research has been monitored and evaluated at various stages of the accelerated experiment before reaching the complete failure and compared between them and with the performance of a reference mix on a witness sector. Finally, specific failure criteria and valuable recommendations have been proposed for the use of practice industry, in this country.

KEYWORDS: stabilized asphalt mix, accelerated performance testing, permanent deformation, failure criteria.

1. INTRODUCTION

Since the year 1993, marking the beginning of a huge and resolute effort of National Administration of Roads, directed towards the rehabilitation the public road network, the Romanian specialists have been confronted with the difficult task of selection and implementation of new asphalt technologies, in order to replace the old and outdated ones, and to permit the design and construction of stronger and better flexible pavements.

These new pavements were seek to exhibit a better performance of the existing road network, to the severe traffic and climatic conditions, characterized by the sudden increase of the traffic volume, parallel with the adoption of the axle load of 115KN, and by huge temperature gradients between the hot and cold seasons.

A first and successful step realized in the frame of this strategy, was the research and implementation in the current road rehabilitation practice of the MASF16/8

type mixes [1], [2], stabilized with various fibers, customized to the specific technical properties of the Romanian aggregates and binders. The application of these superior mixes is now generalized on all road rehabilitation projects, in this country.

A second step was the adoption and implementation of the specific testing technology [3] for assessing the susceptibility of these mixes to rutting, in the conditions of very high temperatures reached in the asphalt pavement during the summers, for some regions, these temperatures over passing 65°C, according SHRP Algorithm [4].

A third and very important step was the undertaking of accelerated testing of these type of mixes, stabilized with indigenous or imported fibers, in order to assess and validate, in a short time, their behavior and performance under the specific new adopted axle load of 115 kN.

This paper describes the approach and presents the results of a two year research study undertaken in the frame of Accelerated Load Testing (ALT) facility at the Technical University “Gh. Asachi” of Iassy, for performance evaluation and validation of technical specifications for the asphalt mixes stabilized with various fibers, used for the construction of bituminous road pavements in the frame of the ongoing effort of road rehabilitation in Romania.

Five types of mix have been selected for this study. The performance of those five types of mixes involved in this research has been monitored and evaluated at various stages of this experiment, under loading on the accelerated circular track, before reaching the complete failure and compared between them and with the performance of classical reference mix, laid on a witness sector.

Finally the study was completed with the laboratory investigations on cores in order to assess the evolution of the asphalt mix properties under the total of $2,2 \times 10^6$ passes of the standard axle load of 115 kN.

2. THE ACCELERATED TESTING FACILITY

Full scale accelerated pavement is defined [5] as “the controlled application of a prototype wheel loading, at or above the appropriate standard (legal) load limit, to a particular structural pavement system, in order to determine the pavement response and performance under a controlled, accelerated, accumulation of damage in a compressed time period”.

The research facility of Technical University “Gh. Asachi” of Iassy is an experimental site, named LIRA (Laboratorul de Incercari Rutiere Accelerate) housing a full-scale accelerating circular testing track, its name and main technical parameters being described also in the related literature[6], among those 32

accelerated facilities developed all over the world after the 1962 year. In fact the first generation of this facility has been developed at the Iassy Technical University, since 1957 year, and the actual third generation is the only existing facility of this type in this country and also in the South-East European Region, now being actively involved in the EC research transport program: COST 347.[7]

The accelerated road research facility from Iassy University is one of those provided a circular track dedicated to the experimentation of various road pavement structures. The main modifications brought to the initial facility along the last 45 years, consisted mainly in the increase of the loading capacity and the extension of the length of running truck [8], [9].

Thus, with the first generation facility, which was functioned during the years 1957...1983, the length of the running arm was of 10 meter, and its mass of 4.6 tone transmitted to the investigated road structure a load of 23kN by two simple wheels, placed at the ends of the metal arm, the total length of the circular track being of 31.4 meter.

With the second generation, built on a new location and made functional since 1983 year, the new running installation had a total mass equal with that of the standard design vehicle: A13, and transmitted to the road structures a load of 45.5 kN by two groups of twin wheels. The length of the arm has been increased to 15 meter, so that the total length of the circular track have reached to 47.1m, thus becoming possible the simultaneous testing of many sectors with representative lengths, and with a greater number of measuring points, in order to get sufficient data for statistical interpretation.

The adoption in of the new standard axle load of 115 kN, in the 1997 year, led to the development of the third generation facility [10], [11], equipped with a new arm with a sufficient mass, capable to assure this new load. The running speed during the loading was maintained at 20 Km/h, from both security and technical reasons (the applied frequency of loads 4.25^{-1} sec, is quite sufficient).

3. INSTRUMENTATION

Even the instrumentation was not at the level of other similar accelerated facilities from abroad, the quantification of the main test parameters has been achieved, in order to get significant conclusions. These parameters, the instrumentation used and their precision and other useful information are given in Table 1.

Table 1. The main parameters investigated during the accelerated testing on the circular track

No	The investigated parameter	The instrumentation	Precision	Number of investigated points on the circumference	Position	The level from the pavement surface
1	Total deformation (wearing + permanent deformations)	The reference straightedge	0.01mm	40	Transverse profile	At the pavement surface
2	Elastic deformations (deflections)	Soiltest/ Benkelman beam or FWD	0.01mm	All	In the middle of the circulated strip	At the pavement surface
3	The radius of curvature	Device for measurement of the radius of curvature	0.01mm	All	In the middle of the circulated strip	At the pavement surface
4	The bearing capacity of the bearing structure	Loading plate	0.01mm for deformations	8	In the middle of the circulated strip	At the subgrade level and at the surface of each layer
5	The level of the underground water	Straightedge	5mm	4	At the inner circumference of the track	0.5....1.5m
6	The temperature	Thermocouple (copper/ constantan)	0.5°C	4	Any point	0.5....1.5m
7	Soil moisture content in subgrade	Normal soil sampling/ using standard methods/ drying)	0.1%	4...10	Any point	0.5....1.5m

4. PLANNING THE EXPERIMENT

Five sectors having an identical road pavement structures, each one equipped with a wearing course having the same thickness (4 cm) but realized from a specific mix; four of them has been equipped with asphalt mixes stabilized with indigenous or imported fibers, selected from those currently used in the road rehabilitation practice and the fifth one was equipped with a classical mix (asphalt concrete type BAR16) and considered as an witness, reference sector.

All five experimental sectors have been subjected to accelerate testing, on the circular track, under the repeated axle load identical with that of the standard vehicle. The adopted road pavement structure corresponded with that currently used in the ongoing road rehabilitation program, phase II, with a small reduction (20 cm instead of 23 cm) brought to the thickness of the foundation layer constructed from granular materials (ballast) stabilized with cement, as consequence of the reconsideration of the higher bearing capacity of the subgrade soil in the process of verification of the standard structural design. Finally, the following pavement structure has been adopted:

- subgrade layer (ballast): 25 cm;
- base course layer (natural aggregates stabilized with 5% cement): 20 cm;
- asphalt base course layer: 8cm;
- asphalt binder course: 4cm;
- asphalt wearing course: 4cm;

For the construction of the experimental sector on the circular track have been accepted and used only those materials proving to meet the quality conditions specified by the legal technical norms. As the objective of the research was the performance study of asphalt mixes with better resistance to the rutting phenomena induced by the heavy traffic, four types of asphalt mixes stabilized with various fibers, having compositions as shown in Table 2, have been selected.

Table 2. The asphalt mixes involved in the accelerated experiment

The component	Type of ix involved in the accelerated experiment				
	MASF 16 stabilized with imported cellulose fiber 1	MASF 16 stabilized with imported cellulose fiber 2	MASF 16 stabilized with indigenous textile fiber 3	MASF 16 stabilized with indigenous textile fiber 4	Classical asphalt concrete BAR 16
Chippings 8/16 (%)	41.8	41.9	37.5	37.5	42.5
Chippings 3/8 (%)	27.2	27.3	25.3	25.3	22.0
Quarry crashed send 03 (%)	16.1	16.2	24.4	24.4	22.8
Filler-lime stone (%)	8.3	8.4	6.6	6.6	7.6
Bitumen D60-80 (%)	6.5	6.2	6.2	6.2	5.1
Fibers (% from mix)	0.3	0.3	0.3	0.3	—

The imported (Germany) cellulose fibers used in the experiment have dimensions of the order of microns, whereas the indigenous textile fibers are obtained by whirling of individual threads, their length being of 15..30 mm and the diameter of over 1mm. Laboratory studies for establishing the mix composition has been undertaken for each type of mix, taking into consideration the provisions of the existing technical specifications (SR 174/97 for mixes and Technical Agreement for cellulose fibers), and seeking to obtain a volume of air voids in the compacted mix of around 3.5%.

Thus the bitumen content considered during the study was in the range of 6.2% to 7.2% for the MASF type mixes and in the range of 5.7% to 6.2% for the BAR16 mix. The percent of fiber was 0.3% from the mass of mix. At least three alternatives of bitumen content have been studied for each type of mix , the maximum limits (7.2% for the asphalt mixes stabilized with cellulose fibers and 7.2% for the mixes stabilized with textile fibers) being established in accordance with the requirements imposed by the Schellenberg Test (maximum 0.2%) [12].

The asphalt mixes have been prepared in a DS158 installation with a productivity of 40m³/h, the fibers being introduced directly in the mixer, the mixing time for the dry mix (aggregate + filler + fiber) being of 30 seconds, the mixing being continued after the adding of bitumen for another 30 seconds. The laying of the asphalt mix has been made manually, followed by compaction with the vibrating roller with a total mass of 1500Kg. The wearing layer, in those five alternatives has been laid accordingly, each sector having a total length of 9.5 m. The temperature conditions were carefully observed and recorded during al the process and the required compaction degree for each layer has been achieved. Samples taken from each mix during the laying process have been investigated in terms of composition and mechanical characteristics.

5. CONDUCTING THE EXPERIMENT

All five sectors have been subjected to the accelerated testing under the running installation having a total weight equal with that of the standard axle load (115kN), this load being transmitted to the pavement through a set of twin wheels placed at the end of the running installation. By the symmetric assembly of this installation, a circulated on strip o of 65 cm width, on which the wheels are passing two times with each complete rotation of the installation arm, with a frequency of load of 4.25 sec⁻¹ for the running speed of 20Km/h. The total number of 2,2x10⁶ have been achieved during a period of 22 months (January 2000...October 2001), this period including two hot and two cold seasons, the temperature recorded in the closed space of the accelerated facility being in the range of 10°C to 15°C during the cold season and of 35°C to 37°C during the hot one.

As it was mentioned before, one of the aims of the experiment was the testing of the capacity of the investigated asphalt mixes stabilized with fibers to resist the rutting trend and in this respect the main parameter monitored during the test was the permanent deformation of the pavement, measured at various stages of loading. Thus measurement of the surface level of the wearing course has been performed, with the precision of 0.1 mm, in a number of eight transverse profiles for each sector, the distance between the measured points on the same profile being of 20mm, as shown in Fig.1.

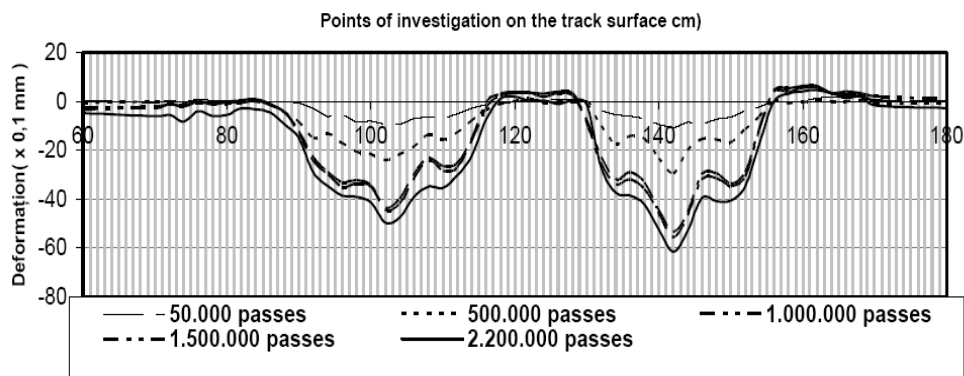


Fig. 1 Average permanent deformations - Sector 1, Asphalt mix with cellulose fiber 1

By making the difference from the initial recording, made just before submitting the pavement to the accelerated traffic, the value of permanent deformation recorded for each stage of loading has been obtained, the measurements being performed at the following loading stages: 10,000, 100,000 passes, and then at each additional 100×10^3 passes till the achievement of the final traffic of $2,2 \times 10^6$ passes of the standard axle load of 115kN.

Fig.1 presents the permanent deformations recorded during the test for the experimental sector equipped with an wearing course realized from asphalt mix type MASF16, stabilized with cellulose fiber type 1, after five significant stages (e.g. after 50,000, 500,000, 1,000,000, 1,500,000 and 2,200,000 passes). For the other investigated mixes have been recorded diagrams with similar shapes with different values. In relation with the Fig.1, one may observe that the main permanent sag deformations have been recorded on the strips corresponding to the wheel passes, whereas on the areas between the wheels and on the exterior of the circulated strips, rejection of material in the form of crests, specific to the rutting phenomena, have been recorded. The highest deformations observed on the right side of the diagram are corresponding to the inner wheel from the running assembly, this wheel being a motor one.

Further on, the evolution of the permanent deformations obtained by statistical processing of recorded data is presented in Fig.2, each of the five investigated mix being represented by distinct conventional signs:

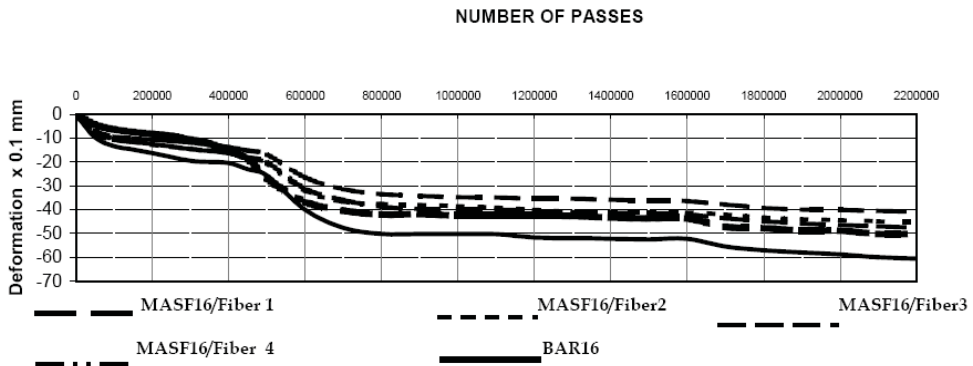


Fig. 2 Evolution of permanent deformations

From the analysis of this diagram one may observe the following:

- there is a significant difference between the behavior of the mixes stabilized with fibers and that of the witness mix (BAR16) which presents the highest permanent deformations;
- five distinct stages can be observed in the evolution of the permanent deformations, in accordance with the number of cumulated number of passes as follows:
 - stage I: with a traffic between 0 and 50,000 passes, representing the supplementary consolidation of the mix, under traffic, characterized by a significant rate of development of the permanent deformations;
 - stage II: with a traffic between 50,000 and 400,000 passes, realized during the cold season of the year 2000 (February...May), characterized by a reduced rate of permanent deformations;
 - stage III: with a traffic between 400,000 and 800,000 passes, realized during the hot season of the year 2000 (June ... September), characterized by a relative greater rate of the development of deformations;
 - stage IV: with a traffic between 0.8×10^6 and 1.7×10^6 passes, realized during the cold season (October 2000 ... May 2001), characterized by a very low rate (near zero) of development of permanent deformations;
 - stage V: with a traffic between 1.7×10^6 and 2.2×10^6 passes, realized during the a relative hot period (June...September 2001), characterized by a rate of deformation higher then the preceding one;

For the quantification of the rate of accumulation of the permanent deformations, for each stage the slope of the specific evolution curves (deformation/ number of passes) have been calculated, these slopes being shown in Table 3.

Table 3. The slopes of the evolution curve of the permanent deformations, on various stages of the experiment

The experimental sector	The type of mix in the experiment	The stage				
		I	II	III	IV	V
1	MASF16 with cellulose fiber 1	0.220	0.045	0.155	0.004	0.020
2	MASF16 with cellulose fiber 2	0.240	0.040	1.108	0.007	0.018
3	MASF16 with cellulose fiber 3	0.200	0.063	0.108	0.004	0.018
4	MASF16 with cellulose fiber 4	0.180	0.057	0.090	0.007	0.022
5	BAR16 (witness sector)	0.380	0.066	0.152	0.011	0.028

This evolution demonstrates the very strong influence of temperature reached in the asphalt layer on the development of the rutting phenomenon, this being also confirmed by similar experiments, conducted on the accelerated circular track at LCPC Nantes [14], where for the asphalt binder used in their experiment (penetration 50/70) a temperature level of 45°C, has been defined as a critical one for the initiation of the rutting phenomenon.

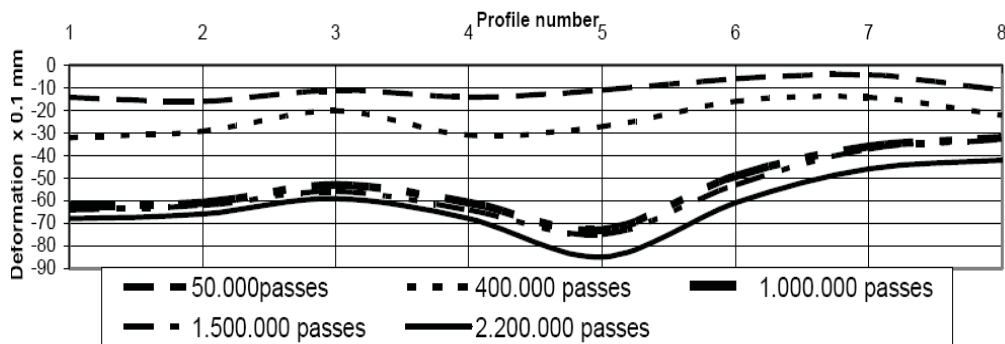


Fig.3. Average permanent deformations of the pavement, in longitudinal profile, recorded during the testing of the experimental sector 1

As the rutting distress was developed also along the circulated strips, longitudinal profiles have been performed along this direction, based on the maximum deformation values recorded during various stages of the experiment. Fig.3

presents the average permanent deformations of the pavement, in longitudinal profile, recorded during the testing on the experimental sector 1.

The maximum values of the depth of the rutting, recorded in longitudinal profile, at various stages of the experiment for each experimental sector and circulated strip are presented in Table 4. Table 5, presents the differences between the maximum a minimum depths of rutting, recorded in longitudinal profile on these sectors.

Table 4. The maximum values of the depth of the rutting, recorded in longitudinal profile, at various stages of the experiment for each experimental sector and circulated strip

The recorded traffic	The circulated strip	The experimental sector				
		1	2	3	4	5
50x10 ³ passes	Exterior	20	8	16	10	20
	Interior	16	16	20	18	19
2,2x10 ⁶ passes	Exterior	74	59	72	60	97
	Interior	85	66	79	68	85

Table 5. The differences between the maximum and minimum deformations recorded in longitudinal profile on each experimental sector

The recorded traffic	The circulated strip	The experimental sector				
		1	2	3	4	5
50x10 ³ passes	Exterior	20	8	16	10	20
	Interior	16	16	20	18	19
2,2x10 ⁶ passes	Exterior	74	59	72	60	97
	Interior	85	66	79	68	85

Finally the study was completed with the laboratory investigations on cores in order to assess the evolution of the asphalt mix properties under the total of 2,2x10⁶ passes of the standard axle load of 115 kN. A number of 36 cores have been taken from the experimental sectors and the mix susceptibility for rutting has been investigated at the Road Laboratory of the Romanian Center for Road Engineering Studies, by using the Wheel Tracking equipment, in accordance with the British procedures [16], adapted to the Romanian conditions [17]. These results [10] are fully confirming the main conclusions drawn from the measurements and investigations made on the wheel track, during the development of the experiment.

Based on the general results obtained during this experiment and on other specific literature data [18], specific failure criteria and valuable recommendations have been developed [2],[10],[14],[15], for the use in the planning of new accelerated experiments [19], [20], or for road practice industry, in this country ort abroad [7].

6. CONCLUSIONS. RECOMMENDATIONS FOR ROAD PRACTICE

The following conclusions and recommendations for practice have been derived from the results of this experiment:

1. The laboratory tests performed with the aim of the design of the various mix compositions, or for their quality control during the process of laying and compaction, are attesting slight improvement of the physic and mechanical characteristics of the asphalt mixes stabilized with various types of fibers in comparison with those of the classical mix BAR16. Marshall stability of the stabilized asphalt mixes is significantly improved, but this can not confirm a possible reinforcement effect in case of the use of the textile fibers;
2. The performance, under the repeated passes of the standard axle load of 115 kN appreciated in terms of the values of permanent deformation(depth of rutting) of the asphalt mixes stabilized with various types of fibers is significantly improved in comparison with that of the classical mix, without fibers. It was difficult to make a performance classification between those four types of mixes stabilized with fibers. But was evident that the behavior of the asphalt mixes stabilized with fibers types 1, 2 and 3 was much better than that of the asphalt mix stabilized with fiber type 4., and this conclusion was made known to the decision factors of the Road Agencies, in order to be considered at the selection of materials in the future rehabilitation works.
3. Related with the evolution of the permanent deformations, in time under repeated traffic, the following conclusions can be drawn:
 - the effect of the supplementary consolidation achieved during the first stage of experiment (50,000 passes) became very clear, despite the fact that the temperature was relatively lower;
 - the development of rutting phenomena is strongly influenced by the high temperatures, the most important values of the rutting depth have been recorded during the first hot season, even so the maximum temperature level recorded during the experiment did nit reached the critical temperature level obtained during the similar French experiments [14];
 - during the second hot period, a new trend for the increasing of the rutting depth has been recorded, but at a lower rate, due to the relative low values of the maximum temperatures and also to the existing consolidation;
4. The distress condition is characterized by both the shape and the depth of rutting in transverse profile and by its shape and evolution in longitudinal

direction, along each sector, where, function of the attained values on may reach the complete failure of the structure. Thus, in case of the witness sector, realized with classical mix BAR16, severe trends of corrugations, with an amplitude of over 5 mm, has been observed after a traffic of 2.2×10^6 passes of the standard axle load of 115kN, whereas on the other sectors this trend was very small (maximum 2..3 mm).

5. Based on the general results obtained during this experiment and on other literature data, specific failure criteria and valuable recommendations have been developed [2], [14], [15], for the use in the planning of new accelerated experiments [19], [20], or for road practice industry, in this country and abroad [7].

Acknowledgements

The authors would like to acknowledge the direct implication of the following administrative and research bodies involved in the positive development of the research study described in this paper:

- The Technical Council of National Administration of Roads for accepting and implementing the Technical specifications for the Asphalt Mixes stabilized with Cellulose Fibers used for the Construction of Bituminous Road Pavements;
- The Romanian Center for Road Engineering Studies and Informatics –CESTRIN, for the developing of NAR/ Specification No.539-98 (99)-2000 and for advance testing of asphalt pavement samples;
- The Research Center for Macromolecular Materials and Membranes from Bucharest, for providing various indigenous fibers for the experiment.

References

1. Andrei R., Oprea C. *Instructiuni tehnice pentru realizarea mixturilor bituminoase stabilizate cu fibre de celuloza, destinate executarii imbracamintilor rutiere*, AND 539-1997 (in Romanian)
2. Andrei R. Vasilescu M., Oprea C. Soalca L. *Normativ pentru realizarea mixturilor bituminoase stabilizate cu fibre de celuloza, destinate executarii imbracamintilor bituminoase rutiere*, AND539-2002, in Buletinul Tehnic Rutier, anul II, nr.18, iunie 2002, pag 86...87 (in Romanian)
3. Andrei R., Vasilescu M., Tanasescu M., Marian CONDILA *Consideratii privind evaluarea susceptibilitatii mixturilor si imbracamintilor rutiere la ornieraj, folosind echipamentul Wheel Tracking*, Al XI-le Congres national de Drumuri si Poduri din Romania, Timisoara/2002/Rapoarte nationale . pag49. (in Romanian)
4. Vlad N., & others *Stabilirea temperaturilor maxime si minime ale imbracamintilor rutiere pe baza metodologiei "SUPERPAVE"*, in Rapoarte Nationale, Al XI-lea Congres National de Drumuri si Poduri din Romania, Timisoara 11...14 septembrie 2002, TEMA T!- Tehnici rutiere, pag 5...52. (in Romanian)

5. Metcalf J.B. *The Application of Full Scale Accelerated Pavement Testing*, in the volume *40 ani de incercari accelerate, la scara naturala, in carol Universitatii Thence din Iasi*, Editure "Spiru Haret", 1997, pag 23...54.
6. Metcalf J. B. *Application of Full-Scale Accelerated Pavement Testing*, in NCHRP Synthesis 235, National Academy Press, Washington D.C., 1996.
7. COST347 *Improvements in Pavement Research with Accelerated Loading Testing*, output from Work group1, Final report, Appendix1- List of ALT facilities and contact persons,
8. ***Prof. D. Atanasiu *Pavement Research Center- The accelerated Pavement testing Facility(prospect)*
9. Vlad N., Zarojanu H., Cososchi B., Leon D., Nemescu M. *The Third Generation of Accelerated Road Testing Facility at the Technical University "Gh. Asachi" of Iassy*, the volume: *40 ani de incercari accelerate, la scara naturala, in cadrul Universitatii Tehnice din Iasi*, Editure "Spiru Haret", 1997, pag 7...23.
10. Vlad N. & other *Concluzii privind comportarea structurilor experimentale, prin incercare accelerate dupa 2.200 .000 treceri roata OS 115 kN*, research report no. 1046P/2000, AND/CESTRIN Bucuresti, 1997. (in Romanian)
11. *** A.T.005-07/008: *Agreement tehnic pentru utilizarea fibrelor celulozice ftip TEHNOCEL 1004 si TOPCEL*, AND/CESTRIN Bucuresti, 1997. (in Romanian)
12. Shultz S. *Celuloza ca o contributie la cresterea stabilitatii mixturilor asfaltice*, Simpozionul *Reabilitarea drumurilor si podurilor, realizari si perspective*, Cluj –Napoca, 1999. (in Romanian)
13. Bense P., Cousin St. *Diferite tipuri de anrobate cu fibre si utilizarile lor*, in *Revista Drumuri si Poduri*, nr. 51/1999. (in Romanian)
14. Corte.J, Brosseaud Y.,Keryeho J.P.,Spernot,A. *L'etude de l'ornierage des couches de roulement au manege d'essai du LCPC*, Bulletin LCPC nr. 217/1998. (in French)
15. Garsac G., Georgescu M., Popescu G., Stelea I., Stelea L., *Imbracaminti asfatice armate cu fibre*, Simpozionul *Reabilitarea drumurilor si podurilor. Realizari si perspective*, Cluj-Napoca, 1997. (in Romanian)
16. BS.598/ Part 110/1998 *Sampling and examination of bituminous materials for roads and pavement areas. Methods of test for the determination of wheel-tracking rate*
17. Vasilescu M, & others *Normativ privind detreminarea susceptibilitatii la formarea fagaselor, a mixturilor asfaltice preparate la cald, pentru imbracaminti bituminoase rutiere* AND 573-2002/CESTRIN, in "Buletinul rutier", Anul II,nr.18, June 2002. (in Romanian)
18. Powel W. D., Potter J.F., Nunn M.E. *The structural design of Bituminous Roads*, TRRL Report LR 1132
19. Kennedy C.K., Lister N.W., *Prediction of Pavement performance and the Design of Overlays*, TRRL Report LR 833
20. Vlad N., Zarojanu H., Andrei R. *COST347/WP4: "Pavement Condition Evaluation"*, Final Report 2003
21. Vlad N., Zarojanu H., Andrei R. *COST 347/WP4: "Recommendations for Experimental Design"*, Final Report 2003

The use of fly ash and volcanic tuff for the construction of the mixed road pavements

Vasile Boboc, Cristian Silviu Iriciuc, Andrei Boboc

Department of Transport Infrastructure and Foundation, Faculty of Civil Engineering, Technical University “ Gh. Asachi” Iasi ,700050, Romania

Summary

The paper presents the research results on the properties of the various sorts of fly ash and volcanic tuff, extracted from Eastern Carpathian Mountains, in order to be use for stabilization of local materials, at the construction of mixed road pavement structures. This research has been undertaken in the frame of the Department of Transport Infrastructures and Foundations from Technical University “Gh. Asachi” Iasi. The results obtained on experimental sectors equipped with such mixed road pavements, constructed on the Accelerated Loading Testing Facility “ Professor Dimitrie Atanasiu” and specific technical recommendations are also presented .

KEYWORDS: mixed road pavement structures, fly ash, volcanic tuff, alt-accelerated, loading testing.

1. INTRODUCTION

In the context of the actual economic and energetic crisis, it is necessary to apply new constructive solutions, capable to bring energy savings, reduction of deficient materials and to use, on a larger scale, of the local byproducts and materials. In the same time, the rational use of local materials involves the use, to a larger extent, of the stabilized aggregate mixes, as specific materials included in the composition of the mixed road pavements.

2. MATERIALS USED FOR THE STABILIZED MIXES

Romanian technical specifications [5] for the design and construction of road pavement layers stabilized with pozzolanic binders provide the use of natural aggregate (sand, ballast) and of the quarry aggregates including quarry byproducts. As binders, these specifications are recommending the use of various sorts of fly ash and of volcanic tuff.

3. POZZOLANIC BINDERS

The use of pozzolanic binders, of some industrial byproducts and of volcanic rocks such as tuffs, largely spread in many countries such as France, Belgium, USA, etc, has reached now, in our country, an operational status. Pozzolanic binders are siliceous and silico-aluminaceous materials containing chemical compounds which are able to combine with some additives like lime, so that, in the presence of water, at the usual temperature to be able to give birth for new formations, less soluble in water and manifesting binder properties.

3.1. The thermo industrial fly ash

Fly ash is an artificial pozzolanic binder which results as a byproduct at the burning in air suspension of the fine grinded carbon, at temperatures varying between 1200 to 1500 °C. The ash is obtained on dry procedure, by using specific separators and electro-filters, after which is stored in big deposits. The fly ash involved in our experiment has resulted from inferior carbon combustion and is looks like a gray color fine powder.

The grading curves of fly ash, produced in Iasi and Vaslui are presented in Fig.1. In relation with this figure, one may observe that the Vaslui ash is finer than that of Iasi (75% passing through sieve 0.071mm, in comparison with 57%)

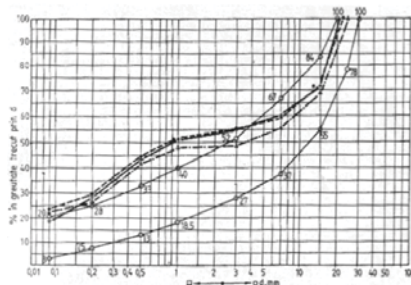


Fig.1. The grading of two sorts of fly ash

Physical characteristics of these two sorts of fly ash are presented in Table 1.

Table1. Physical characteristics of the investigated sorts of fly ash

		Fly ash from sources :		Grinded volcanic tuff
		Iasi	Vaslui	
Blaine specific surface, cm ² /g		3490	3800	3620
Apparent density, g/cm ³		2.209	2.349	2.289
Bulk apparent density	Loose state	0.735	0.819	0.785
	Compacted state	0.947	0.958	0.978

The chemical composition of the fly ash from those two sources and the technical conditions recommended by Romanian norms are presented in Table 2, from below:

Table 2. The chemical composition of the investigated sorts of fly ash

Chemical composition, %	MgO	2.20		2.10		3.40		Max 5.0
	PC	2.29		2.18				≤ 10
	K ₂ O							1.3
	Na ₂ O							1.3
	SO ₃	3.76		3.05		2.72		Max 3.0
	CaO	5.60		4.06		5.40		Min 5.0
	Fe ₂ O ₃	Σ = 90.05 %	7.58	Σ = 88.76 %	7.98	Σ = 89.70 %	5.48	SiO ₂ + Al ₂ O ₃ + Fe ₂ O ₃ ≥ 70 %
	Al ₂ O ₃		32.42		27.50		34.62	
	SiO ₂		50.05		53.28		49.20	
Name and source of the investigated binder		Fly ash from Iasi (lignit)		Fly ash from Vaslui (lignit)		Grinded volcanic tuff Harghita		Technical conditions according Romanian specifications

3.2. Grinded volcanic tuff

Tuff is a volcanic-sedimentary rock resulted from deposition and cementation of the volcanic ash. The main source from Eastern Charpatian Mountains is the Santdominic quarry. The raw material is presented under the form of a quarry aggregate, size 8-20mm.

This aggregate is then grinded to obtain finer material, with a grading, similar to that shown in Fig.2. the grinding fineness, being of 67%. The chemical composition of the grinded volcanic tuff is given in Table 2. In relation with Table two, one may observe that this composition meets the technical conditions specified in the Romanian norms [4].

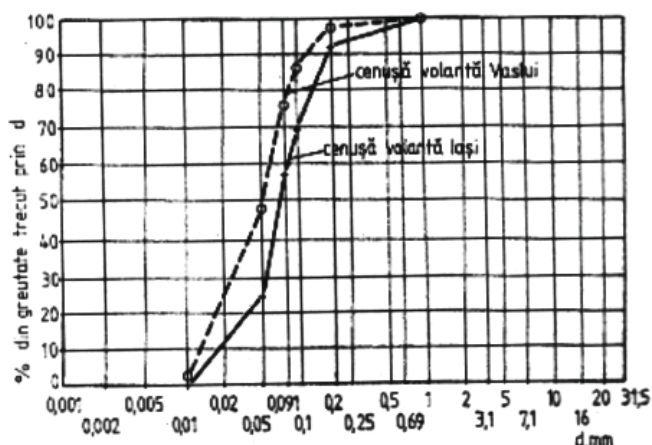


Fig.2. Grading of the grinded volcanic tuff

3.3. The hydraulic lime

The hydrated lime, furnished by the Bicaz factory, under the form of a fine powder has a content of calcium oxide (CaO) of 60,7% and a grading with a rest of 12,3% on the 0,09 sieve.

4. EVALUATION OF THE POZZOLANIC ACTIVITY

4.1.,[4]/ The modified ASTM Method

In accordance with this method the resistance to compression is determined on specimens realized from a mix of calcium hydroxide (one part) and uniform sand (two parts), compacted in cylinder molds having 5 cm diameter and 10 cm height, after curing in water at the temperature of 23 °C for 24 hrs and then at the temperature of 55 °C for six days.

The compression resistance, determined on cylinders, in these conditions, at the age of seven days, must be at least 0,55 N/mm, in order the ash to be considered as an active one. The laboratory positive results obtained by testing these three types of pozzolanic binder investigated are presented in Table 3:

Table 3 the mechanical characteristics of the investigated pozzolanic binders

The type of the pozzolanic binder	R_c 7 at 7 days, N/mm ²
Fly ash / Iasi	0.96
Fly ash /Vaslui	0.90
Volcanic tuff/Harghita	0.67

5. A PROPOSED METHOD FOR EVALUATION OF THE ACTIVITY OF POZZOLANIC BINDERS

This method consist in determining the compression resistance at 28 days on specimens stored in wet atmosphere and at seven days for specimens stored one day in wet atmosphere and then on accelerated dry at 55 0C for the rest of 6 days. Test specimens are realized from mixes of 90% pozzolanic binder and 10% hydrated lime, brought at the optimum moisture content established according AASHTO (modified) Proctor procedure, on cylinders having the same dimensions as in the ASTM method. In both cases, according ASTM recommendations the resistance value has to be of at least 0.55 N/mm. The results obtained on these tests are presented in Table 4:

Table 4. Compression resistance for the investigated specimens

The type of mix	Curing conditions		
	normal	thermo-accelerated	
	R _c (N/mm ²)		
	Age , in days		
	7	28	7
Fly ash/ Iasi (90%) + hydrated lime (10%)	0.37	0.58	0.55
Fly ash/ Vaslui (90%) + hydrated lime (10%)	0.37	0.55	0.54
Volcanic tuff Sindominic (90%) + hydrated lime (10%)	0.26	0.61	0.57

6. NATURAL AGGREGATES

Natural aggregates of ballast type extracted from the Pascani quarry and quarry byproducts from Santdominic, Suseni and Chileni sources, complying with the Romanian technical conditions [5] have been used in the experiment.

7. THE STABILIZED MIXES

Four types of stabilized mixes have been used, as follows:

- Ballsat/ Siret stabilized with 25% Iasi/ flying ash
- ballast /Siret stabilized with 25% Vaslui/flying ash
- quarry byproduct/Sandominic stabilized with 8% volcanic tuff
- quarry byproduct/ Suseni-Chleni stabilized with 8% volcanic tuff

Grading curves of these mixes are presented in Fig. 2 the Proctor compaction characteristics are presented in Table 5 from below:

Table 5 . The Proctor compaction characteristics obtained for the four types of stabilized mixes

The type of mix	γ_d (g/cm ³) ^{max}	W _{opt} , (%)
Siret ballast + 25% Iasi fly ashe	1.89	9.5
Siret ballast + 25% Vaslui fly ashe	1.863	9.5
Sindominc quarry by product + 8% volcanic tuff	2.345	8.5
Suseni - Chileni quarry byproduct + 8% volcanic tuf	2.283	9.98

The results obtained on compression tests, performed on cylinders prepared from these mixes and tested at 14, 28, 60, 90, 180 and 360 days are given in Table 6.

Table 6. Results obtained on compression tests, performed on cylinders prepared from these mixes and tested at 14, 28, 60, 90, 180 and 360 days

Technical conditions	R _{tg} N/mm ²	-	-	-	-	-	-	-
	R _c N/mm ²	Base course	1.3	2.2	-	-	-	-
		Foundation course	0.7	1.2	-	-	-	-
Suseni - Chileni quarry byproduct + 8% volcanic tuff		R _c N/mm ²	0.2	0.3	0.34	0.40	0.50	0.80
		R _c N/mm ²	2.3	2.5	3.5	3.9	4.2	6
Sindominc quarry by product + 8% volcanic tuff		R _c N/mm ²	0.2	0.3	0.35	0.4	0.7	0.75
		R _c N/mm ²	2	2.5	3.3	4	4.6	5.9
Siret ballast + 25% Vaslui fly ash		R _c N/mm ²	0.2	0.25	0.3	0.4	0.45	0.5
		R _c N/mm ²	1.6	2.2	2.75	3.2	3.7	5
Siret ballast + 25% Iasi flay ash		R _c N/mm ²	0.2	0.3	0.4	0.5	0.6	0.75
		R _c N/mm ²	1.4	2.2	3.2	3.3	3.8	6.2
Age in days			14	28	60	90	180	360

8. RESULTS OBTAINED ON ALT PILOT TESTS

Three types of road pavement structures has been conceived by using Siret ballast stabilized with 25%Valsui fly ash and used for the construction of thre experimental ALT sectors as follows:

-sector 1: foundation layer /20 cm ballast; base layer / 10 cm stabilized ballast; wearing course: 5 cm rough asphalt concrete ;

-sector 2: foundation layer /20 cm ballast; base layer / 15 cm stabilized ballast; wearing course: 5 cm rough asphalt concrete ;

-sector 3: foundation layer /20 cm ballast; base layer / 20cm stabilized ballast; wearing course: 5 cm rough asphalt concrete.

These sectors were exposed to the accelerated traffic after a period of 60 dyes necessary for the curing of the stabilized mixes with fly ashes.

Permanent deformations under ALT tests have been recorded at various stages and the results are presented in Fig. 3.

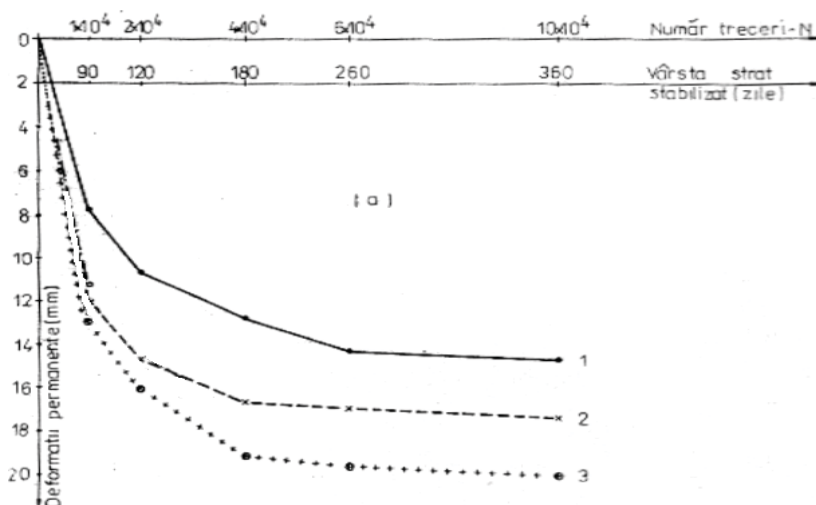


Fig.3 Permanent deformations under ALT tests, recorded at various stages of the experiment

In relation with Fig.3, one may observe that the more rapid accumulation of the deformation in the initial loading period till reaching the number of 4×10^6 passes of the standard axle load (11.5 kN), this limit corresponding with the age of 60...180 days , necessary for the complete curing of the stabilized mixes.

8. CONCLUSIONS

- The fly ashes from sources Iasi and Vaslui used for the stabilization of the Siret ballast may be an alternative solution for the construction and rehabilitation of roads in this region of Romania;
- The grinded volcanic tuffs from eastern Carpathian Mountains (Harghita county) is also a good alternative for the realization of the stabilized mixes for stabilization of the quarry byproducts from sandominic and Suseni-Chileni, in order to be used for the construction of road pavement structures in the region ;
- The mixed road pavement structures realized with Siret ballast stabilized with Vaslui fly ashes have a satisfactory behavior under accelerated traffic , and thus they could be used for the modernization of the roads subjected to low and medium traffic.

References

1. V. Boboc – Teza de doctorat: “ Contributii privind dimensionarea sistemelor rutiere semirigide” U.T. “ Gh. Asachi”Iasi -1995 (in Romanian)
2. Gh. Gugiuman – “Suprastructura drumurilor” – Ed. Tehnica “Universitate Tehnica a Moldovei”, Chisinau -1996 (in Romanian)
3. H. Zarojanu – “Drumuri - Suprastructura” – Tipar Rotaprint- I.P.Iasi - 1976 (in Romanian)
4. N.I. Voina – “ Teoria si practica utilizarii cenuselor de la centralele termoelectrice” –Ed. Tehnica - 1981 (in Romanian)
5. * * * * * - “ instructiuni tehnice departamentale de proiectare si de executie a straturilor rutiere din aggregate naturale stabilizate cu lianti puzzolanici” Indicativ CD 127-85 (in Romanian)

The Research Centre for Geotechnics, Foundations and Modern Transportation Engineering Infrastructure «Dimitrie Atanasiu» - CCGEOFIMIT

Radu Andrei

*Department of Transportation & Infrastructure Engineering, Technical University “Gh. Asachi” Iasi
43, Professor D. Mangeron Str., 700050 Romania*

1. MISSION STATEMENT

The primary mission of the Center is to conceive develop and implement advanced modern technologies and/or computer simulation for building longer lasting airfield pavements and other infrastructures and intermodal transport facilities (roads, railways, viaducts, bridges etc), including monitoring and preserving the existing national transportation infrastructure.



Research Center Type C/ Certificate CNCIS No. 84/2005

The center will conduct research to find reliable and cost-effective solutions to the stated mission which has a vital importance for the development of the national economy. The center will accomplish the mission primarily by conducting research on projects of national significance in the areas of transportation infrastructure using advanced accelerated road pavement testing facility (ALT), parallel with

computer simulation projects focused on building reliable and longer lasting airfields, highways and intermodal facilities.

Other projects will develop innovative applications for long lasting, durable road and airfield pavements, and remote sensing technologies for extending the life and for preserving the health of the nation's transportation infrastructure assets. Also, through its Virtual Consulting Group on SUPERPAVE and Long Lasting Pavements (website: <http://www.tuiasi.ro/~ccgfimit#>) the Center will be able to provide, at national and regional levels (especially for the Central and South-East Regions of Europe), the necessary expertise in the field of assimilation and implementation of the modern technologies for the field and laboratory assessment of asphalt binders and mixes, based on performance criteria and also for the conception and structural design of long lasting - durable road pavements

2. RESEARCH AREAS:

Accelerated Road Pavement Testing, Soil and Material Advanced Testing and evaluation, Soil Mechanics and prevention of land slides, Nondestructive Evaluation and Dynamic Analysis of Bridges, Pavement and Bridge Management Systems, Mechanistic Pavement Analysis and Design, High Performance Pavement Materials (Superpave), Infrastructure Asset Management, Remote Sensing Applications in Transportation, Road Safety and Security Studies, Intelligent Transportation Systems, Transportation Planning, Highway Safety and computer /digital Crash Simulation, Advanced Finite Element Modeling and Simulation of Transportation Structures.

For inquiries contact:

- Paulica RAILEANU, Ph.D., P.E., Professor of Civil Engineering, Head of Department of Transportation Infrastructures and Foundations, email address: raileanu@ce.tuiasi.ro
- Radu ANDREI, Ph.D., Professor of Civil Engineering, Director of CCGEOFIMIT, Email address: andreir@yahoo.com, web site: <http://www.tuiasi.ro/~randrei>.

Visit our web site at: <http://www.ce.tuiasi.ro/~ccgfimit>.

How to build on difficult foundation soils in Iasi County area

Ancuța Rotaru, Paulică Răileanu and Petru Rotaru

*Department of Transportation Infrastructures and Foundation, Faculty of Civil Engineering,
"Gh. Asachi" Technical University of Iasi, 700050, Romania*

Summary

Romania is a medium-sized country (23.83 millions ha), located in the south-eastern part of Europe. Geographically, plains and tablelands occupy 49.3 percent of the country area, hills occupy 30.2 percent, and mountains 20.5 percent.

Being the second largest city of Romania by number of inhabitants (after Bucharest), through its numerous historical, cultural and economic sites, also called "the museum-city", but also as an educational and business centre, Iași is the city of "Gh. Asachi" Technical University, we come from.

During the past decade, damage due to swelling action of swell-shrinking clays from Iași area, Romania, has been observed more clearly in some parts of Iași where rapid expansion of the city led to the construction of various kinds of structures.

In this study, a research program has been conducted to investigate the effect of remoulding and desiccation on the swelling behaviour of swell-shrinking clay and its swelling anisotropy, to estimate depth of active zone, to develop a simple technique in determining the magnitude of swelling based on water content of the soaked specimen after 24 and 72 h, and to produce predictive models which could be used to estimate the swelling potential of swell-shrinking clays from its mineralogical and simply measured engineering characteristics. A laboratory testing program was carried out using both undisturbed, and remoulded and desiccated samples selected from different locations.

KEYWORDS: difficult foundation soils, building.

1. INTRODUCTION

The relief of Romania varies from high mountains to low plains: these categories are represented by the Carpathian Mountains, the lower basin of the River Danube and the Western coast of the Black Sea with the most important wetland of Europe – the Danube Delta. Various natural resources and a large agricultural potential characterize the territory of Romania. After the Second World War and particularly under the communist government, the economic and industrial development of the

country took place without any concern for environmental protection and sustainable use of mineral and human resources. Consequently, Romania faces at present numerous difficult environmental problems, which require urgent actions for rehabilitating the quality of the environment and for improving the quality of life. Solving or mitigating these problems is a large scientific and technological endeavour, which needs up-to-date know-how. Such efforts are surpassing the national capacity of Romania and thus can only be achieved by an efficient international co-operative programme.

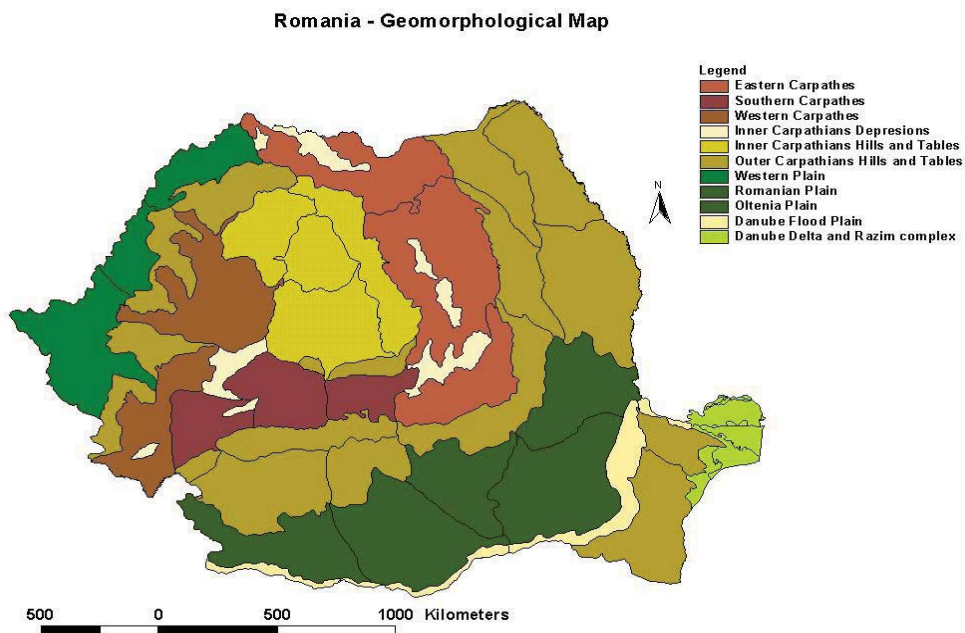


Fig.1 – Map of Romania and geomorphological map of Romania

Iași is placed in north-eastern Romania, more exactly where the $47^{\circ} 10' N$ parallel meets the $27^{\circ} 35' E$ meridian. Seated on seven hillock covering 3770 ha, its altitude varies between 40 m in the Bahlui Meadow, and 407 m in Păun Hill. It is the capital of Iași County, with a total area of 5,470 square kilometres, and an average altitude of less than 250 meters. On the eastern side, Iași County is neighbouring the Republic of Moldova.

From the point of view of the relief, the area of the town of Iași lies at the contact of two big geographical sub-units of the Moldavian Plateau: The Moldavian Plain and the Central Moldavian Plateau.

The landscape is dominated by plains, with very good agricultural potential, and by low hills, whose elevation increase going west, where they are to meet the Eastern

Carpathians mountain chain. Generally, the vegetation and wild animals are quite typical to those of Central Europe.

The county is especially rich in building materials (sand, gravel, and limestone), pottery clay, as well as mineral waters well-known for their medical properties.

The capital city is crossed by Bahlui River, one of the county's four main rivers.

The general climate is temperate continental, with hot summers and freezing winters. Here are some characteristic values:

- ☐ Annual absolute maximum: 37 Celsius degrees
- ☐ Annual absolute minimum: -19.5 Celsius degrees
- ☐ Rainfall: is about 600 millimetres per year

The analyzed area is characterized by preponderance of two categories of difficult soils: contractive soils and macroporous soils. These two categories of soils complicate the selection of the locations and also complicate the design, the execution and the exploitation of all the buildings of the zone.

2. THE GENESIS AND STRUCTURE OF ALLUVIAL DEPOSITS FROM IAȘI AND CLIMATE FACTORS

To the geologic formation of the studied area take place deposits from Quaternary, Miocene, Cretacic, Silurian and crystalline beds. The zone's relief belongs to the category of fluvial and deluvial deposits of accumulation of Quaternary age.

Climatologically, Iași City and its surroundings belong to the temperate – continental climate. Atmosphere's dynamic is characterized by the preponderance of the influence of Europe's north – west and north air – masses, with abundant precipitations, those from south – east and east creating dryness weather and great differences between winter's and summer's temperatures. The thickness of the snow - bed is different every year and the storms and hailstones are constant meteorological phenomena in the area of Iași City, especially in July and August months.

3. PHYSICAL AND MECHANICAL PROPERTIES OF BAHLUI CLAYS

The observations made in the open holes of the studied zone in the summer time indicate that foundation soil is structured from brown plastic clay with thin zones of bluish and yellow colour. Until -1.10m depth the plastic clay is stiff and it can be digged. From this level to -1.90m the colour become darker, with ferruginous

zones, with concretions of limestone, the clay is very stiff and is digged hard. This section allows the influence of the compressive process, realised by repeated drying and wetting tests of a clay soil. Between -1.90 and -2.40 meters the colour gets brown – black with ferruginous and bluish zones. Between -2.40 and -3.20 meters the water content of the soil keeps almost constant, the plastic clay has plastic consistency, is stiff and the colour is yellow with bluish – ferruginous zones. The natural water content varies from 28% to 43%. The results of the classification in function of geotechnical index are presented in Table 1.

Table 1 – Geotechnical index

Bore	Sample	Level m	W_{net} %	Plasticity			Grain-size				γ_s		Physical index				
				Wf	Ip	Wc	2 μ	5 μ	1 mm	2 mm	Pic	Gr	γ_g	γ_u	n	e	S
				%			%				g/cm ³		g/cm ³		%		
S1	1	1.0	28.0	23.8	59.7	83.5	45	21	32	-	2.75	2.69	1.69	1.31	52.4	1.10	0.701
	2	1.5	30.0	27.0	46.8	73.6	3	18	33	-	2.72	2.69	1.74	1.40	51.1	1.04	0.783
	3	2.0	40.0	36.4	52.5	88.9	41	21	30	-	2.83	2.69	1.74	1.24	56.3	1.29	0.880
	4	2.5	35.4	26.5	55.5	82.0	46	23	30	-	2.76	2.69	1.76	1.30	52.7	1.11	0.875
	5	3.0	36.4	30.4	53.4	83.8	56	13	29	-	2.74	2.69	1.89	1.23	55.2	1.23	0.810
S2	1	1.0	40.7	29.7	55.2	84.9	54	18	24	-	2.74	2.70	1.76	1.25	54.4	1.19	0.936
	2	1.5	36.6	26.3	59.1	85.4	49	18	30	-	2.76	2.70	1.82	1.33	51.8	1.07	0.937
	3	2.0	36.7	25.8	58.0	83.8	44	22	31	-	2.77	2.70	1.82	1.35	51.4	1.05	0.962
	4	2.5	35.9	24.4	65.7	90.1	46	24	27	-	2.79	2.70	1.82	1.33	52.5	1.10	0.912
	5	3.0	33.7	22.5	59.5	82.0	47	22	30	-	2.81	2.70	1.87	1.40	50.3	1.01	0.936
S3	1	1.0	42.9	34.3	61.6	95.9	46	26	25	-	2.83	2.70	1.77	1.25	55.9	1.27	0.959
	2	1.5	42.3	31.5	74.7	106	55	22	20	-	2.80	2.70	1.78	1.26	54.6	1.20	0.984
	3	2.0	43.0	32.6	60.5	93.1	44	23	29	-	2.76	2.70	1.75	1.23	55.6	1.25	0.948
	4	2.5	39.8	26.2	76.3	103	40	24	30	-	2.74	2.70	1.78	1.27	53.4	1.15	0.949
	5	3.0	38.8	31.7	60.0	91.7	46	22	29	-	2.77	2.70	1.82	1.33	52.0	1.09	0.982

Taking into account the plasticity (Cassagrande line A), the Iași clay is in the category of inorganic clay soils with high plasticity.

The grain - size composition and distribution classifies the soil in plastic clay, the clay fraction being between 61% and 82%. This classification is also verified by the ternary diagram, which places it in the zone of plastic clays.

Natural unit weight is $1.67 \text{ g/cm}^3 - 1.69 \text{ g/cm}^3$;

Dry unit weight is $1.23 \text{ g/cm}^3 - 1.35 \text{ g/cm}^3$;

Porosity, n, has a great variation: $50.3\% - 56.3\%$:

Degree of saturation is 0.701 – 0.984.

Swelling processes being a consequence of wetting processes, the water absorbed by the hydrophilic swelling body is followed by heat of absorption. Taking into account the amounts of the heat of wetting used as index for the recognition of the very active clays (which presents volume changes at water content changes) the soil activity may be classified.

Thus, for heats of wetting of more then 7 cal/g the soils are considered active and very active.

Knowing the amounts of the total heat of swelling, we calculated the water content which corresponds to the adsorbed water. We also calculated the amount of specific surface, which is between 343mp/g and 270.5 mp/g. Experimentally testing the total heat of wetting as geotechnical index, we drew up the conclusion that the clays from Bahlui Plain are placed in the very active soils category and from the point of view of shrinkage and swelling in the category of very swell – shrinking soils.

4. THE STUDY OF SWELL – SHRINKING SOILS

4.1. The study of shrinkage phenomena

Many researchers analyzed the shrinkage and swelling behaviour of the clay soils. The number of joints or cracks per volume and their dimensions increase accordingly to the proximity of the soil's upper surface. Therefore, the most adequate geotechnical index, which characterise the properties of these clays are the shrinkage coefficients. There are three shrinkage coefficients: α_l , α_s , α_v . The graph water content versus geometrical dimensions before and after drying (dimensions of length, surface and volume) marks some straight lines which slope is precisely the shrinkage coefficient (fig.2, fig.3 and fig.4). The montmorillonitcal clay of Iași we obtained the following values: $\alpha_l = 0.52$, $\alpha_s = 1.17$, $\alpha_v = 2.03$.

4.2. The study of swelling phenomena

In certain conditions, absorbing water, the shrinkage clays present volume expansions. If the volume expansions are limited, they produce remarkable swelling pressures. The experimental tests realised on undisturbed clays draw curves like those shown in fig.2, fig.3 and fig.4 which represent the line between pressure p, water content w and volume V. These curves propose a variable moisture index depending on water content.

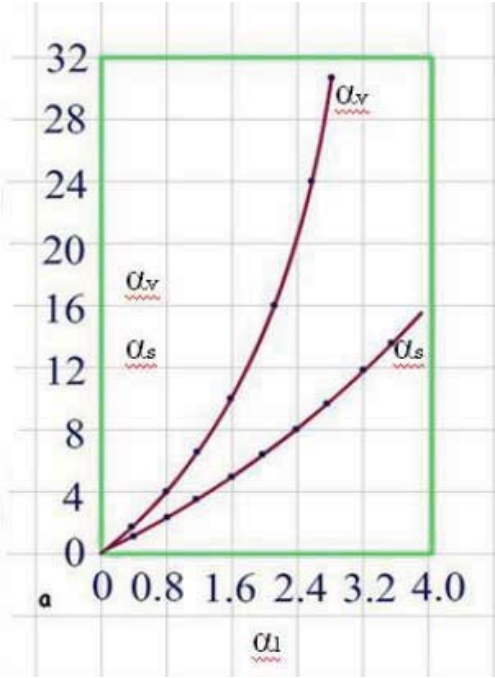


Fig.2 – The influence between shrinkage indexes

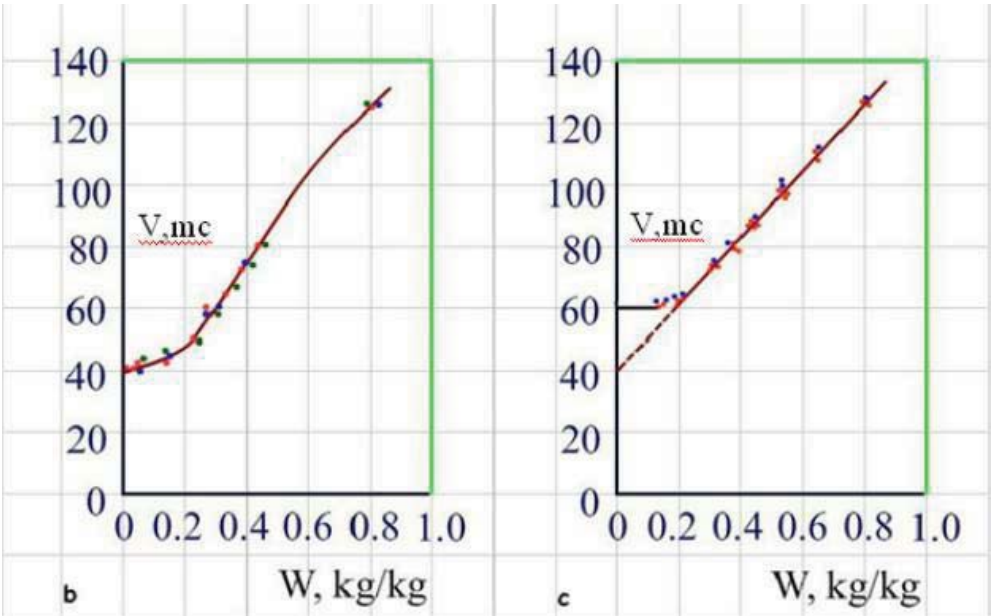


Fig.3 and 4 – Volume variation in function of water content, at continuous drying and at repeated dryings.

Experimental tests for establishing the swelling pressure are made in triaxial apparatus or in special adapted odometers. Like in the study of shrinkage, the swelling at higher water content must be a preoccupation of those who place structures on such soils. Experimental results and the observations made indicate that the clay from this area produces volume changes, movements of the ground, respectively, which are in connection with the transmitted pressure and with water content.

In conclusion, on Bahlui clays we can admit:

- The plasticity index, the grain – size composition and analysis, consistency index, activity index place these soils in the category of active and very active soils.
- The chemical – mineralogical study of foundation course from the plain Bahlui River, colour's reactions, the studies on electron microscope and the thermodynamics analysis led to the conclusion that most clay minerals are from the groups of montmorillonite and hydrated mica.
- The heat of wetting places the clay in the category of the swell – shrinking soils.
- The experimental research allows an improvement of the method for establishing the shrinkage coefficient. The elimination of the water content must be done slowly because the water content must be uniformity distributed in the sample. The increase of water content leads to important increases of the volume. The swelling depends on water content and pressure.
- The use of remolded and desiccated specimens seems to be a better approach in swelling tests for achieving more reliable swelling parameters. The swell pressures obtained from the remoulded samples showed better correlations with mineralogical, index and physical properties when compared to swelling percent and swell indices, such as free swell and modified free swell index.
- On this basis and considering its use in design, it can be concluded that the swell pressure is a better parameter for quantifying the swell potential.
- On the basis of the experimental results, we compute the swelling volumetric coefficient. In the field of $1 - 20 \text{ daN/cm}^2$ the values of the volumetric coefficient vary between -0.2 and 1.0 .

A hazard map showing the area distribution of high and very high expansive soils for the city of Iași is considered to be a very important tool. It is hoped that this map will be a useful tool for planners and engineers in their efforts to achieve better land use planning and to decide necessary remedial measures. Preparation of such a map based on swelling pressure or swelling percent, which are determined

through expensive laboratory tests, takes long time. Therefore, the use of the predicted models seems to be more practical tools for this purpose. A study by the authors for the preparation of a map of swell potential for Iași City by considering the predictive models is in progress.

4.3. Recommendations regarding foundation execution

- The depth of foundation must be established in order that the variations of the water content have no influence upon the swell – shrinking phenomena. Thus, in the area of Bahlui Meadow this depth of foundation must be at least 2m.
- The execution of tree – plantations and the public utility equipment in the areas with shrinking soils must be realized taking into account the amplitude of ground movements caused by water content variations.
- When the depth of foundation of 2m cannot be respected, for the swell – shrinking soils of the area we must study the transmission to the ground of the effective pressure, in function of foundation pressure.

5. THE STUDY OF MACROPOROUS SOILS (LOESSOIDAL SOILS)

5.1. Conditions of loessoidal soils

Iași City is at contact of two areas, different from geomorphologic point of view – The Jijia Depression, The Bahlui Depression and The Moldavian Plateau. Iași City develops and extends on the cliffs and on the Valley of Bahlui River. The loessoidal deposits are on the upper cliff and on the medium cliff, which include areas of Copou Hill, Șorogari Hill and Ciric Hill.

The loess deposits from Iași area have the follow stratification: the surface is formed by a vegetable layer with fill here and there. It follows passing beds to the form bed of the deposit, with sand layers and transition silty clay between Quaternary and Sarmatian. The loessoidal underlay is sarmatian's clay marl.

The plasticity of the loess of Iași is medium with yield limit between 30 and 50. The thickness of loess layer varies between 8 m and 11 m, with a peak value of 24 m in the north – west of the city.

The level of underground water presents variations: 11 – 16 m in the upper cliffs and 5 - 12 m in the medium cliffs with low rate flow. The loesses from Iași area and from the basin Jijia – Bahlui are alluviums transported and deposited in Pleistocene over the clay marls from Sarmatian.

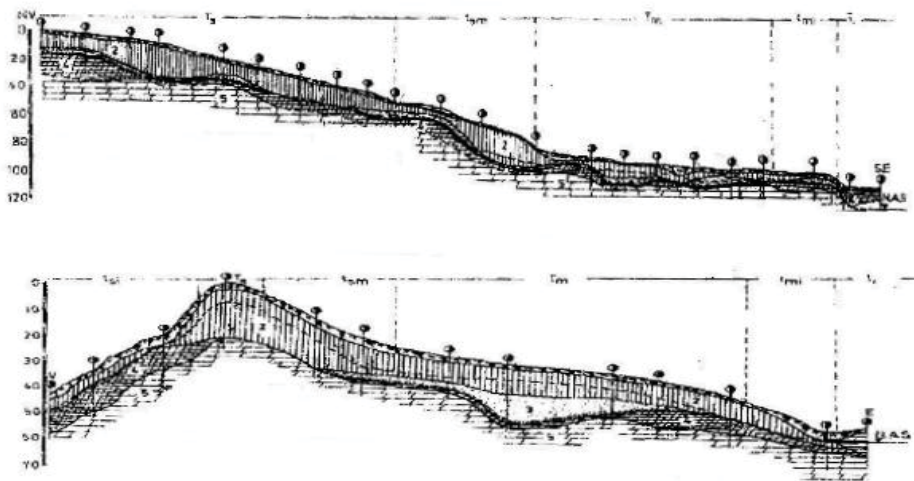


Fig.5: Extension of macroporous soils from Iași area

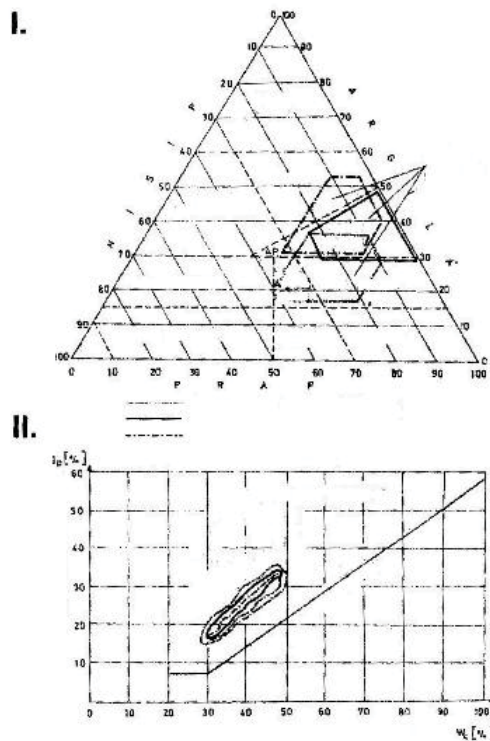


Fig.6 From the grain – size point of view the loess of Iași is represented in the ternary diagram

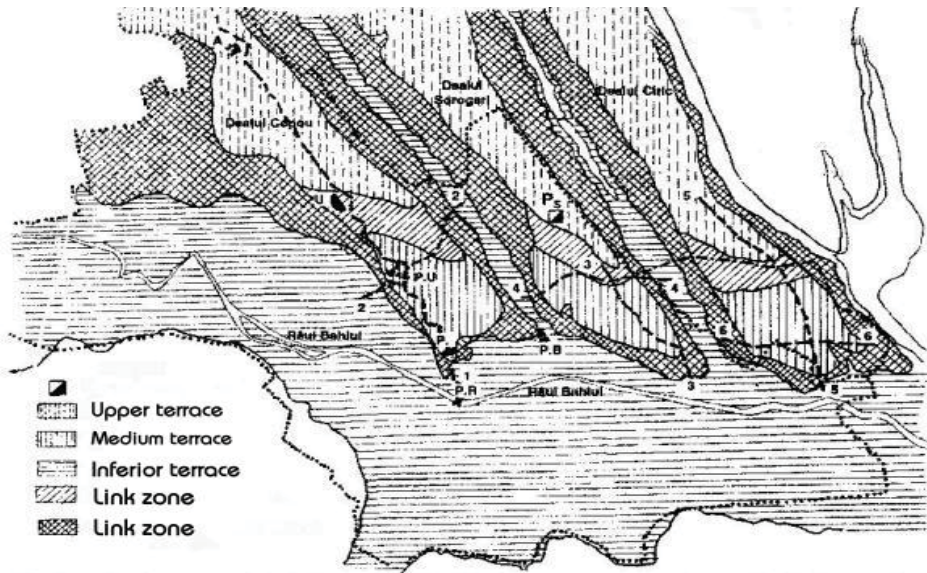


Fig.7: The loess of Iași presents more amounts of clay in the zone of Copou Hill

The specific properties of loessoidal rocks (high porosity, flocculated structure, accumulations of calcium carbonate, yellow – brown colour) formed due to a specific process of macroporous soils.

5.2. Foundation conditions

- The necessity of improvement of the macroporous soils.
- The compulsory check of constructions built on these soils at the effects of the complementary loads induced by the non – homogeneous settlements.
- The diminution of the length of the constructions built on these soils (settlement joints) especially for the soils capable of important total settlements.
- The checking of the systems of soils consolidation taking into account the analysis of relative bending and the analysis of average settlement.
- The limitation of non – homogeneous settlements taking into account the structure's configuration.
- The utilization of computational methods to establish the soil's deformations, different from the structure's deformation.

- The ensuring of the stiffness and of the solidity of the substructure allowing the computations of the unequal settlements.

Building on locations with difficult foundation soils requires a distinct attention (in design, execution and exploitation) in order to choose the right structure and foundation and to pursue and keep in time these buildings.

Analyzing the geologic column from different locations we observe the nature and the properties of the layers and the expected sliding or some others geologic phenomena which would lead to the building's collapse.

Analyzing the different methods used in order to know the depth of active zone, we must grant a distinct attention to the macroporous soils, to the shrinking soils, to laboratory and in situ tests, in order to elaborate accurate solutions for foundations and for the co – operation soil – foundation – structure.

For these soils we must do more complex studies, in order to establish some properties which may influence the strength, the stability and the costs of the building (compressibility, swelling pressures, shrinking pressures, flood settlement).

The costs of the analysis of the soil's properties may lead to the decrease of the properties of these soils.

References:

1. Ciornei Al., Raileanu P. – *Cum dominam pamanturile macroporice sensibile la umezire* – Editura Junimea, Iasi, 2000 (in Romanian)
2. Boti N. – *Contributii la studiul pamanturilor contractile ale stratului de fundare din zona orasului Iasi* – Teza dedoctorat – 1975 (in Romanian)
3. Ciornei Al. – *Contributii la studiul pamanturilor loessoide din zona municipiului Iasi* – *Teza de doctorat* – 1978. (in Romanian)

ISBN 973-7962-76-1



MANIFESTARI STIINTIFICE